

Dissertation der Fakultät für Biologie
der Ludwig-Maximilians-Universität München

advanced gonadal channelome:

Transient Receptor Potential Vanilloid 2

a new player in the gonadal channelome

München, 2022

Katja Eubler



Die vorliegende Dissertation wurde unter der Leitung von
Prof. Dr. med. Artur Mayerhofer und PD Dr. Lars Kunz
im Bereich Zellbiologie - Anatomie III
des Biomedizinischen Centrums
der Ludwig-Maximilians-Universität München angefertigt.

Erstgutachter:	PD Dr. Lars Kunz
Zweitgutachter:	Prof. Dr. Wolfgang Enard
Datum der Abgabe:	05.04.2022
Datum der Prüfung:	19.07.2022

Eidesstaatliche Erklärung

Ich versichere hiermit an Eides statt, dass meine Dissertation selbständig und ohne unerlaubte Hilfsmittel angefertigt worden ist. Die vorliegende Dissertation wurde weder ganz, noch teilweise bei einer anderen Prüfungskommission vorgelegt. Ich habe noch zu keinem früheren Zeitpunkt versucht, eine Dissertation einzureichen oder an einer Doktorprüfung teilzunehmen.

München, den 05.04.2022

Katja Eubler

Directory	
List of Abbreviations	V
List of Figures	VII
Publications and Contributions	VIII
Summary	XI
Zusammenfassung	XIII
1 Introduction	1
1.1 Membrane Proteins an their Functional Scope	2
i. Ion Channels & Channelome - worth a closer Look	3
1.2 Incomplete Channelome of Testis & Ovary	5
i. The Human Gonadal Tissues - still Terra incognita	5
a. The Testis	5
b. The Ovary	7
ii. Infertility & Social Aspect	9
iii. Unravelling the Human Testicular Channelome	11
iv. Expanding the Channelome of the Human Ovary	12
1.3 TRPV2 - a yet unknown Player in the Human Gonadal Channelome	14
i. The TRP Superfamily	14
ii. Vanilloid TRPs & the ‘mysterious’ TRPV2	17
iii. TRPV2- Implications in Inflammation & Immunology	20
2 Aims of the thesis	21
3 Results	23
3.1 Publication I (Eubler et al., 2018)	23
3.2 Publication II (Eubler et al., 2021)	37
Supplements - Publication II	58
3.3 Publication III (Beschta & Eubler et al., 2021)	62
4 Discussion	72
4.1 TRPV2 - a new Player within the Gonadal Channelome	72
4.2 Gonadal TRPV2 - strong Evidence for Immunological Importance	74
i. Somatic Cells	74
ii. Immune Cells	76
4.2 Gonadal TRPV2 - Potential Impact on other Gonadal Channels	77
4.3 TRP Channels in the Human Gonads	79
4.4 Mouse is not Human - Species matters	80
4.5 Hunt for Physiological Activation Mechanism of Gonadal TRPV2	81

5	Outlook & Future Perspectives	83
6	References	85
	Acknowledgements	i
	Additional Publications	iv
	Scientific Posters & Talks	v
	Curriculum Vitae	vi

List of Abbreviations

Abbreviation	Full name	Abbreviation	Full name
2-AG	2-Arachidonylglycerol	i.e.	id est / that is
2-APB	2-aminoethoxydiphenyl borate	IGF-1	Insulin-like growth factor-1
AEA	Anandamide	IK	intermediate conductance Ca ²⁺ -activated K ⁺ channel
BK _{Ca}	Large conductance Ca ²⁺ -activated K ⁺ channel	IL	Interleukin
Ca ²⁺	Calcium	IVF	In Vitro Fertilization
Ca _v	Voltage-dependent Ca ²⁺ channel	K ⁺	Potassium
CatSper	Cation channel of sperm	K _v	Voltage-dependent K ⁺ channel
CB	Cannabinoid receptor	LPC	Lyso-phosphatidylcholine
CBD	Cannabidiol	LPI	Lyso-phosphatidylinositole
CBN	Cannabinol	LPS	Lipopolysaccharide
CD206	Cluster of Differentiation 206	MCP-1	Monocyte chemoattractant protein-1
ChT	Chloramine-T	Mg ²⁺	Magnesium
CLIC	Chloride intracellular channel	MHC II	Major histocompatibility complex class II
Cs ⁺	Caesium	Na ⁺	Sodium
DPBA	Diphenylboronic anhydride	Na _v	Voltage-dependent Na ⁺ channel
ECM	Extracellular matrix	NF-κB	Nuclear factor kappa-B
ECS	Endocannabinoid system	NK	Natural Killer
e.g.	exempli gratia / for example	PDGF	Platelet-derived growth factor
ER	Endoplasmic reticulum	PI3K	Phosphatidylinositol 3-kinase
fMLP	Formyl Met-Leu-Phe	PLC	Phospholipase C
Gd ³⁺	Gadolinium	RNA	Ribonucleic acid
GRC	Growth-factor regulated channel	ROS	Reactive Oxygen Species
H ₂ O ₂	Hydrogen peroxide	siRNA	Small interfering RNA
hGCs	IVF-derived primary human granulosa cells	SK	Small conductance Ca ²⁺ -activated K ⁺ channel
HTPCs	Human testicular peritubular cells		

Abbreviation	Full name	Abbreviation	Full name
THC	Trans- Δ^9 -tetrahydrocannabinol	TRPC	TRP canonical
THCV	Δ^9 -tetrahydrocannabivarin	TRPM	TRP melastatin
TNF- α	Tumor necrosis factor alpha	TRPML	TRP mucolipin
TRP	Transient Receptor Potential	TRPP	TRP polycystin
TRPA	TRP Ankyrin	TRPV	TRP vanilloid

List of Figures

Figure 1. Trinity of the components of a biological membrane	1
Figure 2. Testicular compartments with dedicated components	6
Figure 3. Ovarian compartments with dedicated components	8
Figure 4. Testicular <i>TRPV2</i> expression	12
Figure 5. Ovarian <i>TRPV2</i> expression	13
Figure 6. Phylogenetic tree of the mammalian TRP superfamily	15
Figure 7. <i>TRPV2</i> pharmacology & translocation	19

Publications and Contributions

Publication I

Ca²⁺ signaling and IL-8 Secretion in Human Testicular Peritubular Cells involve the Cation Channel TRPV2.

Katja Eubler, Carola Herrmann, Astrid Tiefenbacher, Frank M. Köhn, J. Ullrich Schwarzer, Lars Kunz & Artur Mayerhofer

A. Mayerhofer and K. **Eubler** conceived of the study. F.M. Köhn and J.U. Schwarzer provided the human testicular tissue samples. A. Tiefenbacher performed the immunohistochemical stainings. With technical and experimental support of C. Herrmann, **K. Eubler** performed the majority of the cellular experiments, including the live-cell imaging experiments, RNA and protein extraction, qPCR, Western Blot studies, cytokine profiler and siRNA transfections and did all the downstream analysis. **K. Eubler** together with A. Mayerhofer and L. Kunz wrote and revised the manuscript. All authors contributed and approved the final manuscript.

published in *International Journal of Molecular Sciences*,
September 2018, 19 (9): 2829
doi: 10.3390/ijms19092829

We hereby confirm the above stated contributions to the mentioned publication.

Katja Eubler

Prof. Dr. Artur Mayerhofer

PD Dr. Lars Kunz

Publication II

Exploring the ion channel TRPV2 and testicular macrophages in mouse testis.

Katja Eubler, Pia Rantakari, Heidi Gerke, Carola Herrmann, Annika Missel, Nina Schmid, Lena Walenta, Shibojyoti Lahiri, Axel Imhof, Leena Strauss, Matti Poutanen & Artur Mayerhofer

A. Mayerhofer, P. Rantakari, L. Strauss, M. Poutanen and **K. Eubler** conceived of the study. L. Strauss, M. Poutanen and P. Rantakari gave access to the animals and provided laboratories, equipment, instrumentation, analysis tools, reagents and materials for the experiments performed at the University of Turku, Finland. P. Rantakari performed and analyzed the cell sorting experiments. S. Lahiri and A. Imhof performed and analyzed the mass spectrometry measurements. H. Gerke, A. Missel, N. Schmid, L. Walenta and **K. Eubler** collected murine tissue samples. A. Missel and **K. Eubler** performed the tissue incubation experiments. Supported by C. Herrmann, **K. Eubler** performed the majority of experiments including *in situ* hybridization, microscopical imaging, RNA and protein extraction, qPCR, Western Blot and cytokine profiler and did the corresponding analysis and interpretation. The manuscript was written by **K. Eubler** and A. Mayerhofer and corrected by P. Rantakari, L. Strauss and M. Poutanen. All authors helped to revise the manuscript and approved the final version for submission.

published in *International Journal of Molecular Sciences*,

April 2021, 22(9): 4727

doi: 10.3390/ijms22094727

We hereby confirm the above stated contributions to the mentioned publication.

Katja Eubler

Prof. Dr. Artur Mayerhofer

PD Dr. Lars Kunz

Publication III

A rapid and robust method for the cryopreservation of human granulosa cells.

Sarah Beschta*, **Katja Eubler***, Nancy Bohne, Ignasi Forné, Dieter Berg, Ulrike Berg & Artur Mayerhofer

* joint first authors

A. Mayerhofer, S. Beschta and **K. Eubler** conceived of the study. D. Berg and U. Berg provided the human follicular fluids. S. Beschta and **K. Eubler** isolated the cells and performed the cellular experiments including cultivation, microscopical imaging, RNA isolation, protein extraction and qPCR and did all the downstream analysis. N. Bohne performed the progesterone measurements. I. Forné conducted the mass spectrometry measurements and S. Beschta analyzed the results. A. Mayerhofer together with S. Beschta and **K. Eubler** wrote and revised the manuscript. All authors contributed and approved the final version for submission.

published in *Histochemistry and Cell Biology*,

July 2021

doi: 10.1007/s00418-021-02019-3

We hereby confirm the above stated contributions to the mentioned publication.

Sarah Beschta

Katja Eubler

Prof. Dr. Artur Mayerhofer

PD Dr. Lars Kunz

Summary

Membrane proteins are encoded by roughly one third of the human genome whereof more than 400 genes code for ion channels. The repertoire of ion channels is referred to as channelome. Knowledge of its composition cannot only help to understand the behaviour of cells in an environmental and interactive context, but also enables one to identify novel therapeutic options. In the last decade, a multitude of transcriptomic and proteomic studies were conducted and provided a glimpse of the channelome. With respect to the human gonads, ion channels have not been all too much in focus of research endeavours yet. Nevertheless, the emerging results shed a new light on these still quite unknown organ systems and their channelome.

The focus of this work is the cation channel transient receptor potential vanilloid 2, TRPV2, which was found to be highly abundant in several cell types of both, the testis and the ovary. However, functional investigations of this channel in a gonadal tissue-specific context had not been performed yet. TRPV2, although first described in the late 90s, is still one of the most mysterious and least characterized members of the TRP ion channel superfamily. This non-selective cation channel is linked to thermal and mechanical sensation and its expression was found in the nervous system of developing and adult organisms, in the pancreas, in smooth muscle and endothelial cells, in a broad set of immune cells including mast cells and macrophages, but also in some cancer types. The studies indicate that its functionality appears to depend strongly upon the examined tissue and species.

In the human testis, TRPV2 transcripts and channel protein were found in some interstitial cells and in the wall-forming (myoid) peritubular cells of seminiferous tubules. Generally, the access to human testicular tissue is restricted and the *in vitro* cultivation of specific testicular cell types is limited. However, peritubular cells are available for cellular studies of TRPV2 functionality. In these cells, which fulfil a much broader functional scope than generating pulsatile waves along the seminiferous tubules to transport immotile sperm, the pharmacological activation of TRPV2 elicited transient Ca^{2+} currents that were missing in a Ca^{2+} -free environment. In addition, prolonged activation induced inflammatory responses evidenced by increased secretion of several cytokines.

On one hand, these findings argue for a participation of TRPV2 in immunological processes in the immune-privileged male gonad, and on the other hand, it could imply involvement of TRPV2 in sterile inflammation that is often associated with disturbed spermatogenesis and impaired fertility in men.

Inflammation in human male infertility may also involve testicular macrophages, yet there is a lack of an adequate human cell culture model. However, with transgenic AROM⁺ mice a model for male infertility and testicular inflammation exists. Due to the expression of the human aromatase enzyme, these animals exhibit imbalanced androgen levels, are infertile and feature high macrophage infiltration into the undescended testes. Besides increased levels of a number of inflammatory factors, TRPV2 is expressed by testicular macrophages and expression significantly accelerates in an age-dependent manner in these animals. TRPV2 could be localized to an unusual macrophage population arising in these animals. In the corresponding wild-type animals, TRPV2 was mainly localized to interstitial macrophages with constant expression levels with independent of age. This indicates a specific role in testicular inflammation, but not in aging.

TRPV2 is also expressed in the female gonad in follicular granulosa cells (GCs) and several types of immune cells. Yet, investigation of human ovarian cells is hampered since experimental access to human cells is restricted to IVF patient-derived primary GCs, which represent cells from the peri-ovulatory window. In addition, these cells are available only in small quantities and are heterogeneous due to medical history, lifestyle and age of the individual patients. To improve this situation, a freeze/thawing method was established and its consequences on viability, morphology, gene and protein expression and functionality of GCs from individual patients were evaluated. Comparison between fresh and frozen/thawed cells revealed that this method had only very little to no effect on the cells and hence proved to be a reliable base of future *in vitro* cellular studies addressing also TRPV2 and its roles in the human ovary.

The insights gained so far implicate TRPV2 as a player in the concert of the regulators of human gonads, whose role(s) however must be further elucidated. Its involvement in inflammatory events in the testis suggests that it may be a potential target for treatment.

Zusammenfassung

Membranproteine werden von etwa einem Drittel des menschlichen Genoms kodiert, wovon mehr als 400 Gene für Ionenkanäle kodieren. Das Repertoire an Ionenkanälen bezeichnet man als „Channelom“. Dessen Kenntnis kann nicht nur dabei helfen, das Verhalten von Zellen in Zusammenhang mit ihrer Umgebung und dem Zusammenspiel mit anderen Faktoren zu verstehen, sondern ermöglicht es auch, neue Behandlungsmöglichkeiten zu identifizieren. In den letzten Jahrzehnten wurde eine Vielzahl an Studien durchgeführt, die sich mit dem Transkriptom und dem Proteom verschiedener Gewebe beschäftigt haben und es erlauben einen Blick auf das Channelom zu erhaschen. Das trifft auch auf die menschlichen Gonaden zu, in denen Ionenkanäle bisher nicht allzu sehr im Fokus der Forschung standen. Die erzielten Ergebnisse werfen ein neues Licht auf diese nach wie vor recht unbekanntes Organsysteme und deren Channelom.

Im Mittelpunkt dieser Arbeit steht der Kationenkanal Transient Receptor Potential Channel Vanilloid 2, TRPV2, der in hoher Dichte in mehreren Zelltypen des Hodens und des Ovars nachgewiesen werden konnte. Bisher wurden jedoch keinerlei funktionelle Untersuchungen dieses Kanals in den menschlichen Gonaden unternommen. Obwohl TRPV2 bereits in den späten 90er Jahren erstmals beschrieben wurde, gilt er nach wie vor als eines der geheimnisvollsten und am wenigsten charakterisierten Mitglieder der TRP-Superfamilie. Dieser nichtselektive Kationenkanal wurde im Zusammenhang mit der Empfindung von Wärme und Druck beschrieben und konnte im Nervensystem, im Pankreas, in glatten Muskelzellen, in Endothelzellen, sowie in einem breiten Spektrum von Immunzellen, darunter Mastzellen und Makrophagen, nachgewiesen werden. Außerdem wurde TRPV2 bei einigen Krebsarten nachgewiesen. Die Studien lassen erkennen, dass die Funktionalität von TRPV2 sehr stark vom untersuchten Gewebe und der Spezies abhängt.

Im menschlichen Hoden wurden TRPV2-Transkripte und -Protein in einigen interstitiellen Zellen und in den wandbildenden (myoiden) peritubulären Zellen der Samenkanälchen gefunden. Grundsätzlich ist der Zugang zu Gewebe des menschlichen Hodens schwierig und die *in vitro* Kultivierung von bestimmten Zelltypen ist nur begrenzt möglich.

Peritubulären Zellen sind jedoch für zelluläre Studien verfügbar und erlauben es funktionelle Aspekte von TRPV2 zu untersuchen. In diesen Zellen, die ein weitaus größeres funktionelles Spektrum erfüllen als lediglich rhythmische Kontraktionen entlang der Tubuli seminiferi zu generieren und damit die noch unbeweglichen Spermien zu transportieren, führt die pharmakologische Aktivierung von TRPV2 zu transienten Ca^{2+} -Strömen, die in einer Ca^{2+} -freien Umgebung ausbleiben. Eine anhaltende Aktivierung des Kanals führt zudem zu Entzündungsreaktionen, die sich mit einer erhöhten Sekretion verschiedener Zytokine nachweisen lassen. Diese Ergebnisse sprechen einerseits dafür, dass TRPV2 an immunologischen Prozessen beteiligt ist, die für den immunologisch privilegierten Hoden und dessen Funktionalität von grundlegender Bedeutung sind. Andererseits könnte es darauf hinweisen, dass dieser Kanal an der sterilen Entzündung des Hodens beteiligt ist, die häufig mit einer gestörten Spermatogenese und einer Beeinträchtigung der männlichen Fruchtbarkeit einhergeht.

Bei Entzündungsvorgängen im Rahmen humaner männlicher Unfruchtbarkeit sind möglicherweise auch testikuläre Makrophagen beteiligt, für die jedoch kein adäquates kultivierbares Zellmodell zur Verfügung steht. Im Hoden der Maus kommen Makrophagen vergleichsweise häufig vor und zudem existiert ein etabliertes Modell für männliche Infertilität und sterile Entzündung des Hodens, die transgene AROM⁺-Maus. Die Expression des menschlichen Aromatase-Enzyms führt in diesen Tieren zu unausgeglichene Androgenspiegeln, die in männlichen Tieren zu Hodenhochstand, Infertilität und starker testikulärer Makrophageninfiltration führen. Neben erhöhter Spiegel von zahlreichen Entzündungsfaktoren, lässt sich in diesen Tieren die Expression von TRPV2 in einer ungewöhnlichen Population testikulärer Makrophagen nachweisen und weist einen signifikanten Anstieg mit dem Alter auf. In den entsprechenden Wildtyp-Tieren ist TRPV2 in interstitiellen Makrophagen anzutreffen, die Expression unterliegt hier jedoch keinen altersbedingten Änderungen. Diese Beobachtungen sprechen dafür, dass TRPV2 eher in testikulären Entzündungsprozessen beteiligt zu sein scheint, als an der testikulären Alterung. Ungeachtet dessen bedarf es einer vollständigen funktionellen Untersuchung dieses mysteriösen Kanals, sowohl für Wildtyp- als auch für AROM⁺-Tiere.

Die Expression von TRPV2 wurde auch für die weiblichen Gonaden gezeigt, hier in den folliculären Granulosazellen und mehreren Immunzelltypen. Die experimentelle Untersuchung von humanen ovariellen Zellen ist jedoch erschwert und hauptsächlich auf Granulosazellen beschränkt, die von IVF-Patientinnen stammen. Diese Zellen spiegeln den peri-ovulatorischen Zustand eines Follikels wider. Zudem stehen die Zellen meist nur in kleinen Mengen zur Verfügung und sind außerdem aufgrund der medizinischen Vorgeschichte, des Lebensstils und des Alters der Patientinnen heterogen. Um diese Situation zu verbessern, wurde eine Methode zum Einfrieren und Auftauen von human Granulosazellen individueller Patientinnen etabliert und dabei der Einfluss auf die Viabilität, die Morphologie, die Gen- und Proteinexpression, sowie die Funktionalität dieser primären Zellen untersucht. Der Vergleich zwischen frischen und eingefroren/aufgetauten Zellen zeigte, dass die angewandte Methode kaum bis keinen Einfluss auf die Zellen hat und somit als zuverlässige Basis für zukünftige zelluläre Studien dienen kann und damit auch die weitere Untersuchung von TRPV2 und seinen Funktionen im menschlichen Ovar möglich macht.

Die bisherigen Erkenntnisse weisen darauf hin, dass TRPV2 ein wichtiger Akteur in den menschlichen Gonaden ist, seine Rolle(n) jedoch noch genauer aufgeklärt werden muss (müssen). Seine Beteiligung an entzündlichen Prozessen im Hoden deutet auf die Möglichkeit als potentiell Ziel für Behandlungen hin.

1 Introduction

Roughly 4 billion years ago the earliest forms of life, microorganisms, appeared on earth (Oparin, 1938; Peretó, 2005; Dodd et al., 2017; Djokic et al., 2017; Betts et al., 2018). The so-called origin of life is highly complex, yet not fully explored, nor understood. As one important step, it includes the formation of a biological membrane and thereby the establishment of an enclosed compartment, the cell (Witzany, 2016; Tirard, 2014). This biological membrane allows for realization and maintenance of the internal milieu of every living cell, irrespective of the pro- or eukaryotic nature. It is likewise essential for a cell's protection and thus pictorially resembles an unbreachable barrier. At the same time, a biological membrane offers some recognition features and gateways to permit communication with the outside world. This trinity of membranous properties is realized by the membrane's individual components, i.e. lipids, carbohydrates and membrane proteins (**Figure 1**). Lipids, in shape of phospholipids, glycolipids or sterols, are the fundamental structural elements building up the unbreachable barrier and give rise to the membranous bilayer (Lodish et al., 2000). The cellular recognition features are realized by carbohydrates, either glycoproteins or glycolipids. As a whole, they sum up to the glycocalyx with the main functions allotted to protection of the cell surface, cell-adhesion, recognition and interaction (McKinley & O'Loughlin, 2012; Saladin, 2010). Membrane proteins realize the gateways within the unbreachable barrier and as such establish its specific functions, thus embodying the bridging elements between different worlds (Cooper, 2000).

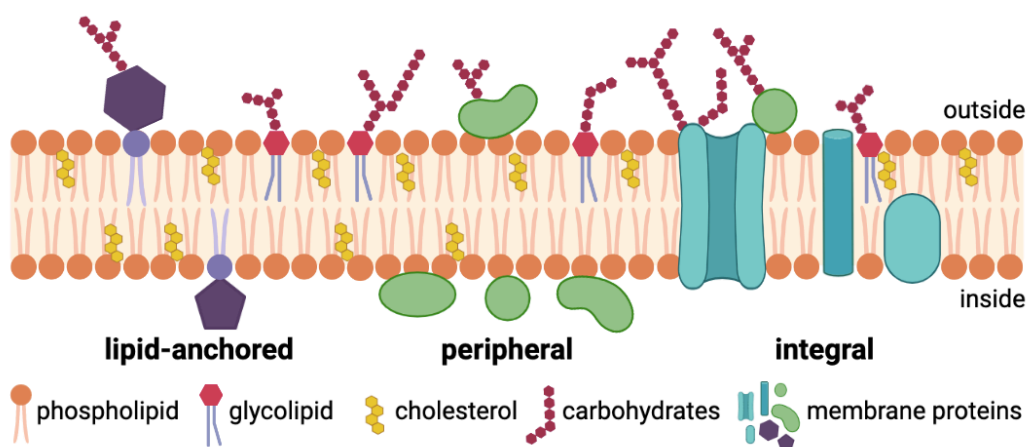


Figure 1. Trinity of the components of a biological membrane. The membranous bilayer is made up of two leaflets consisting of phospholipids, glycolipids and cholesterol. The outside is covered by the glycocalyx composed of glycoproteins and glycolipids. With respect to their localization, membrane proteins can be defined either as lipid-anchored (purple), peripheral (green) or integral (petrol). Created with BioRender.com.

1.1 Membrane Proteins and their Functional Scope

Providing half of a membrane's weight, membrane proteins amount to approximately one third of the whole human proteome, emphasizing the importance of these proteins as gateways for controlled passage of molecules and information over the cell membrane (Krogh et al., 2001; Lander et al., 2001; Ahram et al., 2006; Clamp et al., 2007; Almén et al., 2009; Gould, 2018; Martin & Sawyer, 2019). At the same time, membrane proteins are irreplaceable targets for modern medical drugs with about 50-60 % of such compounds operating at this site. Thereby they offer treatment options for common human diseases such as cystic fibrosis, diabetes, obesity, multiple sclerosis, Alzheimer's disease, heart and neurological diseases, but also cancer (Martin & Sawyer., 2019; Hauser et al., 2017; Du & Xie, 2012; Bar-Shavit et al., 2016; Lappano & Maggioloni, 2011; Overington et al., 2006). Generally, membrane proteins can be divided into three main categories with regard to their individual localization within or in relation to the lipid-bilayer as lipid-anchored, peripheral or integral membrane proteins and as such hold different functions (Singer & Nicholson, 1972; Cooper, 2000).

Lipid-anchored proteins (**Figure 1**, purple) are covalently attached to one or more lipids within the bilayer and can be found on both sides of the membrane (Casey & Seabra, 1996; Karp, 2009; Voet et al., 2011). G proteins, for instance, are amongst this category of membrane proteins and generally function as signal transducers from the outside to the inside of a cell (Alberts et al., 2002; Syrovatkina et al., 2016). Peripheral membrane proteins (**Figure 1**, green) are temporally and reversibly bound to the cell membrane and can be localized both on the cytosolic side of the cell membrane, such as actin, but also on the extracellular face, such as fibronectin (Takida & Wedegaertner, 2004). The individual localization of these peripheral proteins goes along with their distinct function in terms of the organization of the cytoskeleton or the extracellular matrix, respectively. They also play important roles as part of transmembrane complexes, for instance as enzymes or carriers (Nelson et al., 2008; Lodish et al., 2008; McMahon et al., 2011).

Integral proteins, in contrast to peripheral ones, are embedded into to the phospholipid bilayer of the cell membrane due to their amphipathic nature (**Figure 1**, petrol). They can either be attached to only one of the two leaflets of the bilayer as monotopic

proteins, such as cyclooxygenase I (Fowler et al., 2006), or span the whole width of the membrane as transmembrane or polytopic proteins, such as integrins (Nelson et al., 2008; Wallin & von Heijne, 1998). Transmembrane proteins can consist of single or multiple transmembrane elements, i.e. α -helices, β -sheets or a combination of both. Furthermore, they can span the membrane only once or several times, respectively, and can be divided into six categories depending on their orientation and organization within the phospholipid bilayer (Wallin & von Heijne, 1998; von Heijne, 2006; Karp, 2009). Their hydrophilic domains on both sides of the biological membrane allow for interaction with molecules from both the extracellular and the cytosolic side giving rise to ion channels, protein pumps and G protein-coupled receptors. Of note, these proteins hold an essential role for the realization and the maintenance of the electrochemical gradient of every living cell and accomplish the selective semi-permeability of each individual cell.

i. Ion Channels & the Channelome - worth a closer Look

Although usually associated with the nervous system, there being irreplaceable for the neuronal membrane potential and the electrical and synaptic transmission, ion channels are ubiquitously expressed by every cell and are essential for its proper functionality (Abdul et al., 2018; Alexander et al., 2011; Hille, 2001). In fact, more than 400 genes encode for ion channels summing up to roughly 1.5 % of the whole human genome. Additionally, multiple splice variants and the generally possible assembly of several individual proteins either from the same (homomeric) or different subtypes (heteromeric) increase ion channel numbers and give rise to new channel properties (Gotti et al., 2007; Collins et al., 2009). The human inner ear, for instance, houses more than 300 different types of ion channels (Gabashvili et al., 2007).

The individual subunits, typically four of them, organize circularly within the membranous bilayer building a water-filled pore equipped with a highly selective filter. This so-called selectivity filter was first described by Hille and Armstrong in the late 1960s and determines which kind of ions can pass through (Hille, 1971, 1973 & 1975; Bezanilla & Armstrong, 1972). The channel-based ion flow generally happens without consumption of any metabolic energy and with a very high rate of more than 10^6 ions per second (Alexander et al., 2011; Hille, 2001).

Ion channel classification is based on the gating mechanism, the type of ions they let pass, and the cellular localization (Hille, 2001; Purves et al., 2001; Zhang et al., 2018a). The mechanism of gating refers to the stimulus that opens or closes a distinct channel. Typically, it is a change in the voltage across a membrane (voltage-gated), binding of an extracellular ligand (ligand-gated), a lipid (lipid-gated) or an intracellular second messenger, but can also include stimuli like light, membrane stretch, pressure, shear stress or temperature. The type of ion that can pass through an ion channel strictly depends on its selectivity filter, which can either be exclusively permeable for only one ion type or for several but equally charged ions giving rise to non-selective anion or cation channels (Hille, 1971 & 2001). In terms of cellular localization, ion channels can either be incorporated into the plasma membrane or into intracellular membranes, i.e. of the endoplasmic reticulum, the Golgi apparatus or the two mitochondrial leaflets. However, the cellular localization is not a fixed state, since ion channels are, in principle, able to traffic between membranous pools. An adequate stimulus, such as growth factors, can involve channel incorporation into the plasma membrane. In case of missing demand, ion channels can also be withdrawn from the cellular surface and be re-integrated into the intracellular reservoir (Kavalali, 2002; Moss & Henley, 2002; Royle & Murrel-Lagnado, 2002; Hong & Shaw, 2016).

The study on ion channels is referred to as channelomics. This scientific branch employs techniques such as immunohistochemistry, electrophysiology, crystallography and pharmacology to unravel the channelome, i.e. the whole set of ion channels expressed by a biological tissue or organism (Doyle et al., 1998; Barrett-Jolley et al., 2010; Lehmann-Horn & Jurkat-Rott, 2003; Camerino et al., 2007). In addition, this discipline also includes the evaluation of structural alterations that potentially lead to malfunction or loss of ion channel function, referred to as channelopathies. For instance, malfunctioning ion channels have an impact on and cause diseases such as blindness, respiratory dysfunction, epileptic, ataxia or pain syndromes (Kass et al., 2005; Ashcroft et al., 2006).

In this context, screening for pharmacological treatment targets takes place. With currently only 5 % of all medical drugs on the market targeting ion channels, there might be a big and yet undiscovered potential for new and hopefully effective compounds (Camerino et al., 2007; Lehmann-Horn & Jurkat-Rott, 2003; Imbrici et al., 2016).

1.2 Incomplete Channelome of Testis & Ovary

In general, knowledge about human channelomes still seems to be limited or maybe is simply beyond the scope of most scientific questions, a fact also true for the human gonads. From 1980 until 2021, just about 40 studies were published with the title keywords “testis/testicular” and “channel”, whereas the search for “ovary/ovarian” and “channel” on PubMed.gov led to almost 80 results, regardless of the species investigated. Although, there is some knowledge about the channel repertoire in the human and murine gonadal tissues, these numbers appear to be insignificant in comparison to the roughly 2000 works already published on the brain since 1870, dealing with both physiological and pathological channel function. Nevertheless and now even more, the channelome of the human gonadal system could be of special interest in regard to a better fundamental understanding of these organs. In terms of increasing infertility or other reproductive issues these days, it also appears worthwhile to keep channelopathies in mind.

i. The Human Gonadal Tissues - still Terra incognita

The almost 4,000 publications about the testis only in 2020 and 6,000 publications in the same year dealing with the ovary, respectively, indicate that new insights are still accumulating about both systems and emphasize how little is really understood yet. What is known, however, are the two essential and fundamental functions of the human gonadal tissues. First, the production of sex hormones to develop and maintain the corresponding sex phenotype, and second, the generation of germ cells to ensure continuity of the individual genetic pool. The following section will shortly summarize the anatomical organization of the gonads with regard to their distinct functions.

a. The Testis

The testis is surrounded by a capsule of tight connective tissue, the *tunica albuginea*, and is composed of two major compartments, i.e. the interstitial and the tubular space. These two compartments are separated by the basal lamina and several layers of the wall-forming peritubular myoid cells, that together can be recapitulated as a third, peritubular

compartment. The production of the primary male sex hormone, testosterone, is mainly localized to the interstitial space (**Figure 2**, light purple), where Leydig cells are situated. These cells are controlled indirectly by the hypothalamus via gonadotropin-releasing hormone and directly by the pituitary gland and its glandotropic product, i.e. luteinizing hormone. Within the loose connective tissue of the interstitial space, mast cells and macrophages are frequently present, but also blood and lymphatic vessels and elements of the extracellular matrix (ECM) and of the nervous system can be found (Weinbauer et al., 2009; Aumüller et al., 2017).

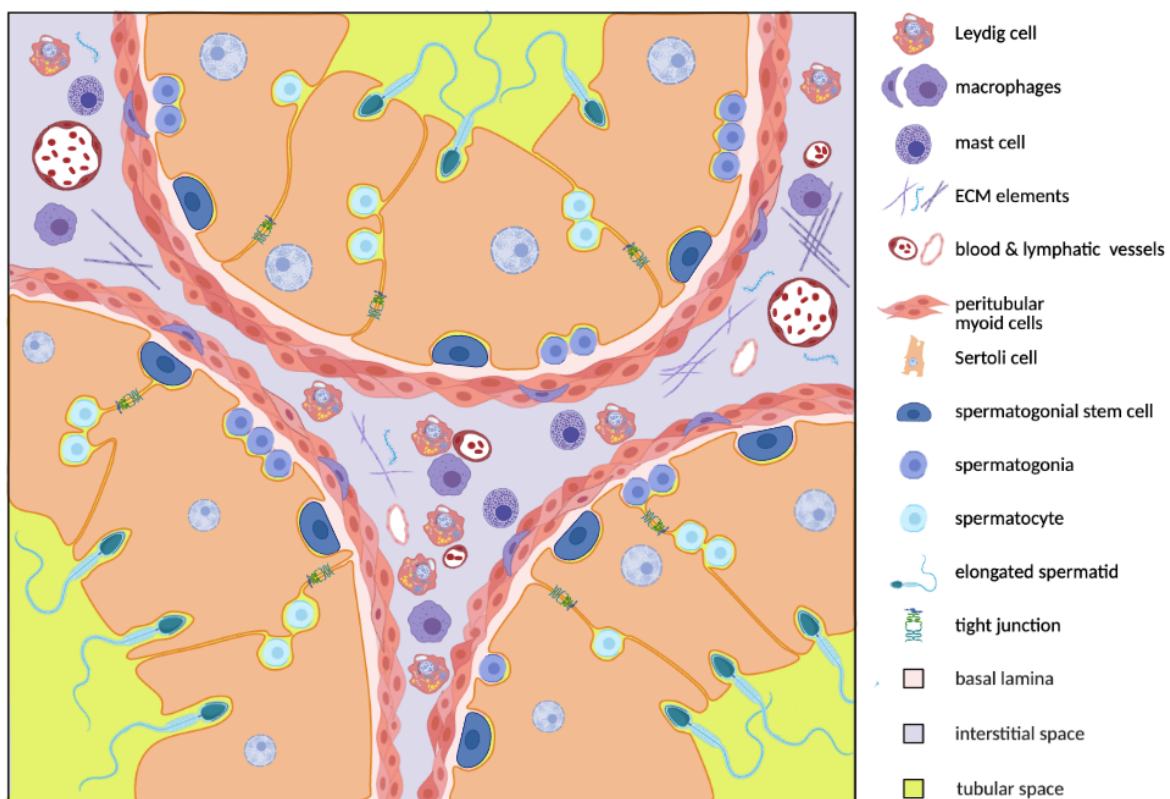


Figure 2. Testicular compartments with dedicated components. Schematic drawing of the two major testicular compartments, the interstitial and the tubular space. The loose connective tissue of the interstitial space (light purple) is interspersed with extracellular matrix (ECM), blood and lymphatic vessels, androgen producing Leydig cells, macrophages and mast cells. Several layers of myoid cells surround the basal lamina and thereby build the tubular wall that separates the two compartments and can be recapitulated as third, peritubular compartment. Within the tubular space (yellow), Sertoli cells, the spermatogonial stem cells and spermatogonia are located at the basal site, whereat the different developmental states of the germ cells, i.e., spermatocytes and elongated spermatids, are situated behind the blood-testis-barrier realized by tight junctions between neighboring mature Sertoli cells. Created with [BioRender.com](https://www.biorender.com).

The generation of mature male germ cells, i.e. spermatogenesis, takes place within the tubular space of the testis (**Figure 2**, yellow). This compartment harbors the somatic Sertoli cells and the spermatogonial stem cells. They give rise to the individual developmental states

of germ cells, i.e. spermatogonia, primary and secondary spermatocytes, round and elongated spermatids, and structurally mature sperm (Clermont, 1966; Miller & Auchus, 2011). Upon the establishment of the blood-testis-barrier by mature Sertoli cells during puberty, spermatogenesis starts and continues throughout life. The individual processes of spermatogenesis and the preservation of the spermatogonial stem cell niche strongly depend on the presence and actions of testosterone on peritubular, Sertoli and Leydig cells. Furthermore, testosterone is essential for the maintenance of the blood-testis-barrier formed between neighboring Sertoli cells in order to shield the maturing germ cells from the immune system (Welsh et al., 2009 & 2012; Smith & Walker, 2014; O'Donnell et al., 2017).

b. The Ovary

The ovary is enclosed by the *tunica albuginea* and can be divided into a marrow and a cortical region. The marrow region (**Figure 3**, light orange) is characterized by loose connective tissue interspersed with nervous elements, androgen producing hilus cells, blood and lymphatic vessels. The cortical region (**Figure 3**, light pink) harbors the ovarian-specific spinocellular connective tissue with a large portion of fibrocytes, the germ cells and the dedicated somatic cells, theca and granulosa cells. The latter play an important role in both steroidogenesis and folliculogenesis, but are also significantly involved in protection of the follicular reserve pool (Hoffmann & Williams, 2012; Brown & Russell, 2014; Aumüller et al., 2017).

In striking contrast to the testis and male germ cells, the number of female germ cells is limited in number and temporal availability. The germ cell pool of primary oocytes is established during embryonic development and reaches its peak of roughly seven million cells around embryonic week 20. All oocytes then start meiosis I and are arrested in the dictyotene. Once formed, the germ cell pool is subjected to an ongoing decline due to cell death. Already at birth, only 1-2 million primary oocytes are left and upon puberty merely 300-500,000 primary oocytes are still present. Finally, at around 50 years of age, the germ cell pool is depleted and women enter menopause, emphasizing the limited female reproductive window (Gilbert, 2000; Takahashi & Johnson, 2015).

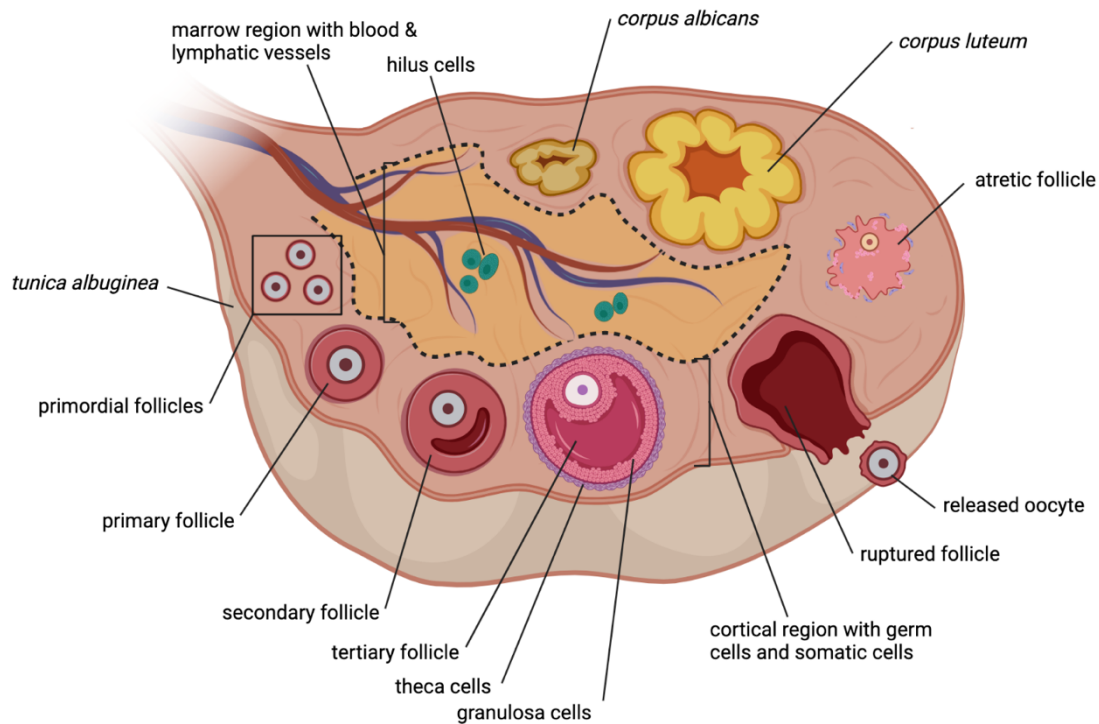


Figure 3. Ovarian compartments with dedicated components. Schematic drawing of the human ovary, enclosed by the tight connective tissue of the *tunica albuginea*, and its two compartments, the marrow and the cortical region. The marrow region (light orange) is composed of loose connective tissue with blood and lymphatic vessels, and androgen producing hilus cells. The germ cells with their dedicated somatic cells, i.e. the surrounding granulosa cells and later also the theca cells, and the different follicle states (primordial, primary, secondary, tertiary, ruptured, atretic) are embedded within the spinocellular connective tissue of the cortical region (light pink). After release of the oocyte, the somatic cells of the ruptured follicle left behind transform into the steroidogenic active *corpus luteum* and later regress into the *corpus albicans*. Adapted from “Ovary (oogenesis)”, by [BioRender.com](https://www.biorender.com) (2020).

During this reproductive period of life, every menstrual cycle a number of primary oocytes completes the first meiotic division giving rise to haploid secondary oocytes, a process occurring at ovulation (Pinkerton et al., 1961; Lobo, 2003; Wallace & Kelsey, 2010). The second meiotic division will only be completed upon fertilization, transforming the secondary oocyte into an ovum. Parallel to the maturation of the oocyte, the surrounding granulosa and theca cells develop and change their morphological and endocrine steroidogenic phenotype. Together with the growing oocyte they represent the different stages of folliculogenesis, i.e. primordial, primary, (antral) secondary, antral tertiary and preovulatory follicles. The dominant antral follicle, the Graafian follicle, ruptures and thereby releases the oocyte. The somatic cells are left behind and give rise to the steroidogenic active *corpus luteum*, that later degenerates and forms the *corpus albicans*. Much more likely however, the fate of follicles is cell death by atresia (Hsueh et al., 1994; Kaipia & Hsueh, 1997; Rolaki et al., 2005).

All things considered, merely ~400 oocytes equivalent to only 0.1 % of all formed follicles will reach ovulation, whereas the major fraction will die and never complete folliculogenesis (Faddy, 2000). Numerous of the above-mentioned processes, especially degradation of atretic follicles and remodeling of the ovarian tissue, require the presence of macrophages, a cell type that can be found frequently in the ovary (Bulmer, 1964; Fukumatsu et al., 1992; Nishimura et al., 1995; Tamura et al., 1998; Wu et al., 2004).

Many of the underlying regulatory processes and consequences for the testis and the ovary, respectively, are poorly understood. It is conceivable that these cell-specific functions, their impact upon the whole system and distinct malfunctions could play a role in fertility or even lead to infertility.

ii. Infertility & Social Aspects

According to the World Health Organization estimative 15 % of all couples at the reproductive age and 186 million individuals worldwide are affected by infertility (Rutstein & Shah, 2004; Boivin et al., 2007; Mascarenhas et al., 2012), described as *“a disease of the male or female reproductive system defined by the failure to achieve a pregnancy after 12 months or more of regular unprotected sexual intercourse”* (Zegers-Hochschild et al., 2009; World Health Organization, 2018). Childlessness might originate from known male or female factors, a combination of both or frequently from unknown reasons. Generally, environmental factors, for instance exposure to pollutants or toxins, and the individual lifestyle including, for example, smoking, obesity or excessive alcohol intake may have an impact upon fertility (Gore et al., 2015; Segal & Giudice, 2019). For both sexes, personal and social consequences of infertility are dramatic. Infertile couples often get divorced and infertile individuals being unable to fulfil the stereotypical ideals of man/womanhood experience feelings like inadequacy and unworthiness, and tend to develop depressions and suicidal thoughts. In addition, such individuals are often confronted with social stigmata such as emasculation, mental distress, social exclusion and shaming (Whiteford & Gonzalez, 1995; Gerrits, 1997; Araoye, 2003; McQuillian et al., 2003; Inhorn, 2004; Inhorn & Wentzell, 2011; Serour, 2008; Smith et al., 2009).

Male infertility, the disability to impregnate a fertile female (Leslie et al., 2020), occurs in 7-9 % of all men (Lotti & Maggi, 2015) and is the basis of 40-50 % of infertility cases (Hirsh, 2003; Brugh & Lipschultz, 2004; Cui, 2010; Pandruvada et al., 2021). The known causes of male infertility are manifold, including immunological dysfunctions, genetic abnormalities, formation of varicoceles, disturbances in the hypothalamic-pituitary-testicular axis, sperm deficiencies, abnormalities in the ductal system, and erectile dysfunctions (Jarow et al., 1989; Arai et al., 1998; Cooke & Saunders, 2002; Montague et al., 2005; Cavallini, 2006; Ferlin et al., 2006; Restrepo & Cardona-Maya, 2013; Rao, 2013; Wosnitzer, 2014; Kupis et al., 2015; Leslie et al., 2020). Starting in the 80s, many researchers from different countries uttered their concerns about the declining quality of sperm. In India for instance, as little as one decade was sufficient to reduce sperm counts by 30.3 %, motility by 22.9 % and morphology by 51 %, respectively (Menkveld et al., 1986; Murature et al., 1987; Carlsen et al., 1992; Mukhopadhyay et al., 2010; Sengupta, 2012). Based on a systematic meta-regression analysis, a significant decline in sperm counts by 52.4 % between the years 1973 and 2011 could also be demonstrated for western men (Levine et al., 2017).

For female infertility there is no clear definition, but according to the World Health Organization it "*can be described as the inability to become pregnant, maintain pregnancy, or carry a pregnancy to life birth*" (Rutstein & Shah, 2004; World Health Organization, 2018). In the United States, 10 % of women at the reproductive age between 15 and 44 years are affected by infertility (CDC, 2013 & 2018) and in a global view the highest rates of female infertility are reported in Eastern Europe, the Middle East, North Africa, Oceania and Sub-Saharan Africa (Mascarenhas et al., 2012). Female infertility can result from several factors including genetic abnormalities, anatomical disorders of the tubal, uterine or ovarian tissue and hormonal imbalances due to an impaired hypothalamic-pituitary-ovarian axis (Alexander & Cotanch, 1980; Raga et al., 1997; Bodri et al., 2006; Guven et al., 2007; Kovacs & Norman, 2007; Gleicher et al., 2009; Nelson, 2009; Bulletti et al., 2010; Fauser et al., 2011; Wang et al., 2014; Qin et al., 2015; Zondervan et al., 2020).

iii. Unraveling the Human Testicular Channelome

In 2001, the family of cation channels of sperm, CatSper, was first described to be essential for the hyperactivation of sperm via calcium (Ca^{2+}) entry while traveling through the female reproductive tract and thus for male fertility. It is an excellent example for the growing interest in the human testicular channelome. There are some individual cases of infertility, in which the dysfunction or loss of one member of this ion channel family leads to decreased sperm motility and the loss of the ability to fertilize healthy oocytes (Ren et al., 2001; Quill et al., 2001; Carlson et al., 2003; Loblely et al., 2003; Qi et al. 2007; Hildebrand et al., 2010; Sun et al., 2017). However, in these patients spermatogenesis seems to be unaffected, since testicular histology, sperm morphology and counts are found to be normal (Chung et al., 2011; Park et al., 2014).

In 2014, Flenkenthaler and colleagues performed a proteome analysis of the wall-forming myoid human testicular peritubular cells (HTPCs), providing among others a first impression of a part of the testicular channelome (Flenkenthaler et al., 2014). Three groups of ion channel proteins were detected in HTPCs. First, the voltage-dependent anion-selective channel 1 and 2 (VDAC1 and 2) being part of the mitochondrial porin family (Blachly-Dyson & Forte, 2001; De Pinto et al., 2010). Second, the chloride intracellular channel 1 and 4 (CLIC1 and 4), both being important for the stabilization of the membrane potential and the intracellular pH but also for trans epithelial transport and cell volume regulation (Valenzuela et al., 1997; Suginta et al., 2001). Third and of special interest, the transient receptor potential cation channel vanilloid 2 (TRPV2), a non-selective cation channel with increasing controversies about its function and activation, also in terms of species and cell type (Caterina et al., 1999; Perálvarez-Marín et al., 2013; Shibasaki, 2016). Expression of this 'mysterious' and fascinating ion channel could also be shown for other testicular cells, as Guo and colleagues extended the insight into the testicular channelome in 2018 by unravelling the transcriptome of the whole testis of young adult men (Guo et al., 2018). In this study, five different somatic cell types, i.e. macrophages, Leydig, Sertoli, myoid and endothelial cells, and five developmental different spermatogonial states were identified and their distinct transcriptional repertoire revealed. Here, abundance of TRPV2 was most pronounced in macrophages, endothelial and myoid cells, but also in early primary spermatocytes (**Figure 4**).

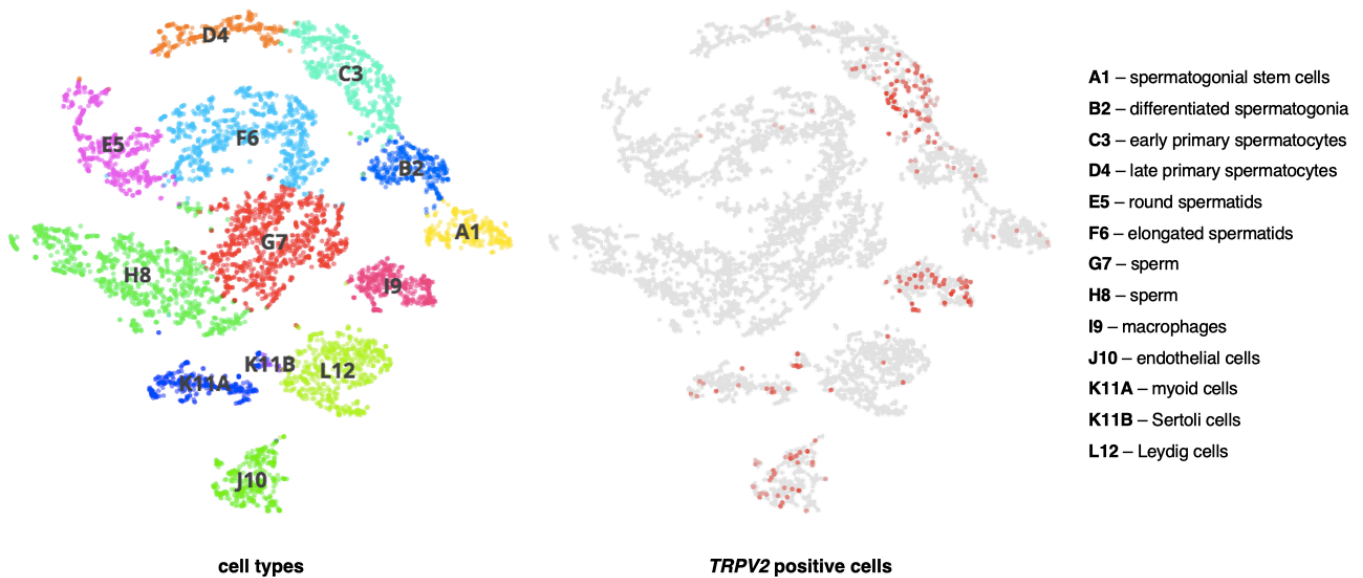


Figure 4. Testicular *TRPV2* expression. RNA-sequencing based single cell transcriptional *TRPV2* expression in the human testis from three young men revealed high abundance in myoid and endothelial cells, in macrophages and early primary spermatocytes. *TRPV2* positive cells are depicted in red. Data adapted from [Guo et al., 2018](#). See webpage: <https://humantestisatlas.shinyapps.io/humantestisatlas1/>

iv. Expanding the Channelome of the Human Ovary

Using cultured in vitro fertilization (IVF) patient-derived primary human granulosa cells (hGCs) as a cellular model, Kunz and colleagues demonstrated functional expression of voltage-dependent Ca^{2+} ($\text{Ca}_v1.2$ and $\text{Ca}_v3.2$), potassium (K^+ ; $\text{K}_v4.2$) and sodium (Na^+) channels ($\text{Na}_v1.7$), and of Ca^{2+} -activated potassium (K^+) channels of small (SK), intermediate (IK), and big conductance (BK_{Ca}), by human granulosa cells (Bulling et al., 2000; Kunz et al., 2002 & 2006; Agoston et al., 2004; Mayerhofer & Kunz, 2006; Traut et al., 2009). In these cells, BK_{Ca} , amongst others, is crucial for human chorionic gonadotropin-induced ovarian steroidogenesis (Kunz et al., 2002). Already one year later, Doheny and colleagues showed that BK_{Ca} is the main potassium channel in the murine and human myometrium with a modulatory role for myometrial function (Doheny et al., 2003). Although channelopathies of BK_{Ca} are related to neurological disorders and impaired smooth muscle function in diabetes type 2 patients (Miller et al., 2021; Nieves-Cintrón et al., 2017), it is conceivable that functional impairment or loss of this channel might result in consequences for the female reproductive tract, as well.

In the years 2018 and 2019, the ovarian transcriptome and proteome were studied and a more detailed insight into the female gonad was obtained. Zhang and colleagues

focused on the human ovarian transcriptional landscape of oocytes and granulosa cells derived from primordial, primary, secondary and antral follicles (Zhang et al., 2018b). One year later, Bagnjuk and colleagues performed a proteomic study with cultured hGCs and, in addition, the knowledge about the ovarian transcriptome was broadened by Fan and colleagues who studied granulosa, theca, stroma, endothelial, immune and smooth muscle cells (Bagnjuk et al., 2019; Fan et al., 2019).

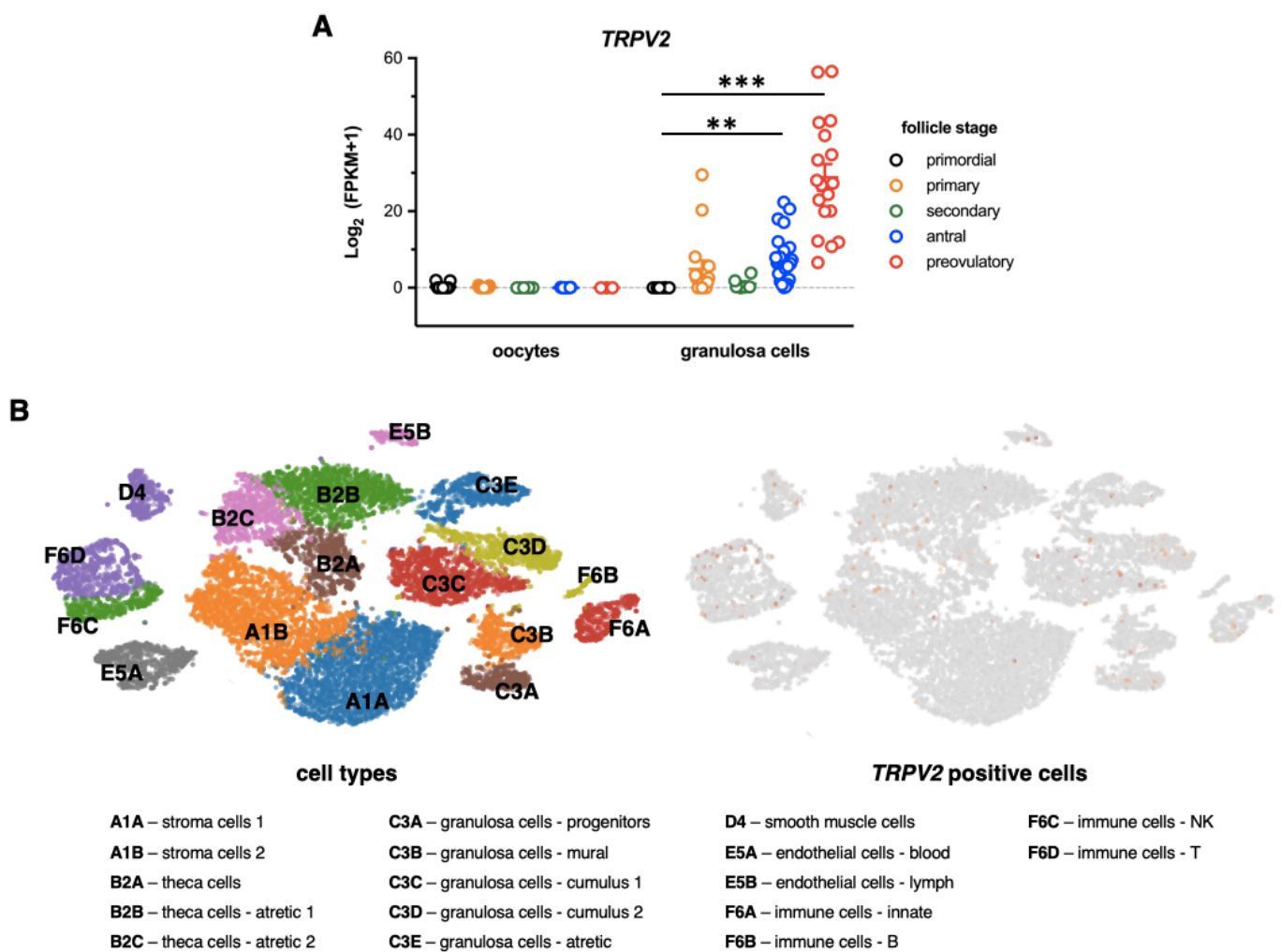


Figure 5. Ovarian *TRPV2* expression. RNA-sequencing based single cell transcriptional *TRPV2* expression in the human ovary. **A** *TRPV2* expression in oocytes and granulosa cells from different developmental follicle stages obtained from seven female individuals. *TRPV2* is absent in oocytes independent from the developmental follicle stage, but increases significantly with folliculogenesis in granulosa cells. Nonparametric Kruskal-Wallis test, $\alpha = 0.05$, ** - $\alpha < 0.01$, *** - $\alpha < 0.001$. Data adapted from Zhang et al., 2018b. **B** *TRPV2* expression in ovarian tissue from five adult women revealed abundance in granulosa, theca and several immune cells. *TRPV2* positive cells are depicted in red. Data adapted from Fan et al., 2019. See webpage: <http://ovogrowth.net/ovary-expression>

The transcriptional expression of *TRPV2* channel appears to be insignificant for oocytes, independent from the distinct follicle stage. However, expression of *TRPV2* by granulosa cells could be shown both on the transcriptional and translational level and the abundance of *TRPV2* shows a developmental increase from the primordial to the preovulatory follicle (**Figure 5A**). Moreover, also theca cells and a broad spectrum of immune cells, especially innate, natural killer (NK) and T cells, were found to possess *TRPV2* (**Figure 5B**). *¹

1.3 *TRPV2* - a yet unknown Player in the Human Gonadal Channelome

Until recently, expression of *TRPV2* by the human gonadal tissues was unknown. When reviewing the literature, this quite 'mysterious' channel gathers a lot of controversies in terms of expression, activation mechanism and function also with regard to the investigated species. In addition, *TRPV2* provides some interesting immunological features, also being of special importance for the gonadal tissues where controlled immunological processes are fundamental for proper organ function.

i. The TRP Superfamily

TRPV2 is part of the transient receptor potential (TRP) superfamily of voltage-gated ion channels, whose first member was discovered in a *Drosophila melanogaster* mutant in the late 1960s by Cosens and Manning. By the current state of scientific knowledge the TRP superfamily comprises 28 members in mammals (Cosens & Manning, 1969; Minke et al., 1975; Montell & Rubin, 1989; Hardie & Minke, 1992). Unusual for ion channel classification that is normally settled on a common ligand, function or selectivity, these 28 TRP channels are separated into six subfamilies solely based on sequence homology (**Figure 6**), i.e. canonical (TRPCs), vanilloid (TRPVs), melastatin (TRPMs), mucolipins (TRPMLs), polycystins (TRPPs), and ankyrin (TRPA).

*¹ For completeness, *VDAC1* and *2* and *CLIC4*, respectively, are also expressed by both oocytes and granulosa cells, though without clear regulation between the developmental stages. Of note, *CLIC1* could only be identified in granulosa cells but was absent in oocytes (Zhang et al., 2018b; Bagnjuk et al., 2019). Screening the data published by Fan and colleagues, *VDAC1* and *2* feature a ubiquitous expression with highest abundance in granulosa, stroma and theca cells, whereat *CLIC4* transcriptional expression is rather weak (Fan et al., 2019).

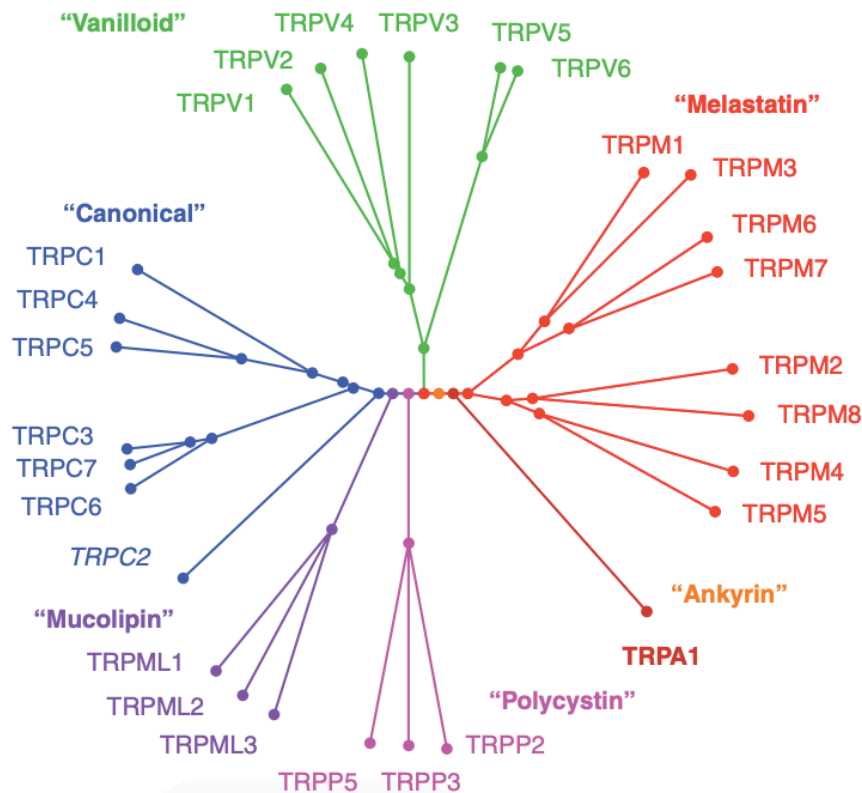


Figure 6. Phylogenetic tree of the mammalian TRP superfamily. Classified by homology, the 28 mammalian TRP channels cluster into 6 subfamilies, i.e. canonical (TRPCs), vanilloid (TRPVs), melastatin (TRPMs), mucolipins (TRPMLs), polycystins (TRPPs), and ankyrin (TRPA). Data adapted from [Gees et al., 2010](#).

The difference between these individual subfamilies bears on the structural and functional elements of the cytosolic N- and C-terminal regions (Clapham, 2003; Clapham et al., 2005; Gees et al., 2010; Wu et al., 2010; Nilius & Owsianki, 2011). They can either be localized to organellar membranes or to the cell membrane, where four subunits consisting of six transmembrane domains assemble to a functional homo- or heteromeric ion channel (Ramsey et al., 2006; Venkatachalam & Montell, 2007; Blair et al., 2019). A common feature of all TRPs is the permeability for mono- and divalent cations and their *“function as cellular sensors responding to a broad range of stimuli”* (Blair et al., 2019).

The spectrum of activating or modulating stimuli for TRP channels is extremely broad and one channel typically responds to multiple stimuli. The list of stimuli acting on TRP channels is composed of physical and chemical stimuli and of receptor coupled signaling pathways. Sensitivity to changes in temperature and mechanical forces is a feature of one-third of the TRP family, including TRPV1-4, TRPC5, TRPM3, TRPM5, TRPM8, TRPA1 and TRPP1.

However, in spite of lacking physiological evidence and relevance, this does not necessarily make them sensors for heat/cold or mechanical stimuli (Feng, 2014; Plant, 2014). Considering chemical stimuli acting on TRP channels, there is a trench between *in vitro* and *in vivo* results and also the specificity of the modulating compounds seems to be limited. Known molecules activating TRPs include inorganic ions like Ca^{2+} (directly or indirectly via calmodulin) and Mg^{2+} , bioactive lipids, natural compounds like capsaicin, tetrahydrocannabinol and menthol, but also some synthesized agents. Comparably, potent and selective blockers are also merely conditionally available, aggravating a targeted exploration of TRPs (Caterina et al., 1997 & 2000; Ramsey et al., 2006; Wu et al., 2010).

With respect to physiological functions, only a few members have been thoroughly characterized. As an example, TRPV1 has been demonstrated to be irreplaceable in primary afferent nociceptors responding to noxious heat, pain or capsaicin, and participate in the development of the post-inflammatory thermal hyperalgesia (Caterina et al., 1997 & 2000). Besides sensory functions, TRPs generally participate in Ca^{2+} homeostasis, contribute to immunological and inflammatory processes and are present in the nervous system, as well as in the endocrine, the renal and the cardiovascular system (Montell et al., 2002; Blair et al., 2019). Of special note, some channels have been linked to human inherited diseases with the most frequent pathogenic mutations in the genes of TRPV4 (50 mutations leading to skeletal dysplasia and peripheral neuropathies), TRPM6 (35 mutations linked to autosomal recessive hypomagnesemia with secondary hypocalcemia 1) and TRPP1 (278 mutations implicated in autosomal polycystic kidney disease). However, mechanistic knowledge about how channel dysfunction leads to the observed pathogenesis is sparse (Nilius et al., 2005 & 2007; Nishimura et al., 2012; Nilius & Voets, 2013; Lainez et al., 2014; Ong & Harris, 2015). Generally, due to their strong contribution in Ca^{2+} signaling, an abnormal activity might impact other Ca^{2+} -dependent cellular processes and thereby lead to a Ca^{2+} overload (Nilius & Owsianik, 2010; Nilius & Voets & 2013; Tóth & Nilius, 2015). Furthermore, changes in TRP channel expression and function rather than mutations have been reported to be especially important in some cancer types with regard to processes like proliferation, differentiation, cell death, migration and angiogenesis, all of them depending on Ca^{2+} signaling (Monteith et al., 2007; Shapovalov et al., 2011; Kondratskyi & Prevarskaya, 2015).

ii. Vanilloid TRPs & the ‘mysterious’ TRPV2

The vanilloid subfamily of TRP ion channels was first described in the late 90s with the discovery of the osmotic avoidance abnormal family member 9 (OSM-9) in *Caenorhabditis elegans*, there being involved in olfaction and mechanosensation (Colbert et al., 1997), and was later extended by four more members (Xiao & Xu, 2011). The mammalian TRPV subfamily consists of six members with TRPV1-4 being allotted to thermal sensation, although yet only reliably proven for TRPV1. TRPV5 and 6 are solely Ca^{2+} -selective channels involved in general Ca^{2+} homeostasis (Hellwig et al., 2005; Montell, 2005; Clapham, 2007a; Caterina et al., 2000).

The first mammalian vanilloid TRP channel, vanilloid receptor 1 (VR1) and later TRPV1, was described by Caterina and colleagues as a non-selective cation channel that shows sensitivity to capsaicin and is essential for thermal pain perception (Caterina et al., 1997). Merely two years later, another structurally related member of this subfamily was identified, holding 50 % sequence homology to TRPV1. In contrast, this channel was not sensitive to capsaicin or moderate heat but was responsive to noxious temperatures above $\sim 52^\circ\text{C}$ and hence was named vanilloid receptor-like 1 (VRL-1). Expression was found in medium- to large-diameter sensory neurons suggesting participation in heat perception, but it was also present in other cell types indicating a broader functional scope (Caterina et al., 1999). In the same year, the identical ion channel was independently identified by the Kojima lab to translocate from intracellular pools like the endoplasmic reticulum (ER) to the plasma membrane upon insulin-like growth factor-1 (IGF-1) stimulation. Therefore, the term growth-factor-regulated channel (GRC) was established (Kanzaki et al., 1999; Kojima & Nagasawa, 2007). Translocation of this channel, later called TRPV2, also occurs upon exposure to the chemotactic peptide formyl Met-Leu-Phe (fMLP) and upon stimulation of phospholipase C (PLC), phosphatidylinositol 3-kinase (PI3K) and other kinase signaling pathways, and can be inhibited by the PI3K inhibitor LY294002 or pertussis toxin (Nagasawa et al., 2007; Penna et al., 2006; Rohacs & Nilius, 2007; Rohacs et al., 2008).

Once integrated, TRPV2 mediates a non-selective cation flux with a slightly higher permeability for divalent ions ($\text{Ca}^{2+} > \text{Mg}^{2+} > \text{Na}^+ \sim \text{Cs}^+ \sim \text{K}^+$, $P_{\text{Ca}^{2+}}/P_{\text{Na}^+} = 2.94$; Venkatachalam & Montell, 2007).

From a physiological and pharmacological perspective, specific functional examination of TRPV2 is aggravated since most stimuli and compounds do not exclusively affect TRPV2 and, additionally, show strong species-dependencies (Ramsey et al., 2006; Vriens et al., 2009; Perálvarez-Marín et al., 2013). Thus, results should generally be viewed with caution.

Besides high temperatures, physiological channel activation and gating occurs upon exposure to red light (Zhang et al., 2012) or upon membrane stretch, for instance due to osmotic cell swelling (Shibasaki et al., 2010; McGohan et al., 2016; Sugio et al., 2017). Hu and colleagues introduced 2-aminoethoxydiphenyl borate (2-APB) as activator for TRPV1-3, which could not be confirmed by other groups for human TRPV2 (Hu et al., 2004; Juvin et al., 2007). Diphenylboronic anhydride (DPBA) turned out to elicit transient currents in TRPV2 transfected rodent cells, but was unable to activate human TRPV2 (Juvin et al., 2007; Nepper et al., 2007). Further, the oxidant chloramine-T (ChT), the reactive oxygen species (ROS) hydrogen peroxide (H₂O₂), lyso-phosphatidylcholine (LPC), lyso-phosphatidylinositol (LPI) and lipopolysaccharide (LPS) can induce cationic currents via TRPV2 (Monet et al., 2009; Harada et al., 2017; Fricke et al., 2019).

In many cases, derivatives of *Cannabis sativa* emerged as potent TRPV2 activators with trans- Δ^9 -tetrahydrocannabinol (THC), cannabidiol (CBD) and Δ^9 -tetrahydrocannabivarin (THCV) being the most potent ones (Qin et al., 2008; De Petrocellis et al., 2011). Additionally, growth factors like platelet-derived growth factor (PDGF) and IGF-1 activate TRPV2, as does the uricosuric agent probenecid (Kanzaki et al., 1999; Bang et al., 2007; Robbins et al., 2012; Siveen et al., 2020).

Pharmacological blocking is difficult due to lacking specificity of the general Ca²⁺ channel blocker ruthenium red, amiloride, SKF96365, citral and trivalent cations (like gadolinium). For tranilast, the underlying blocking mechanism is incompletely validated (Nie et al., 1997; Caterina et al., 1999; Leffler et al., 2007; Stotz et al., 2008; Reichhart et al., 2015; McGohan et al., 2016). Recently, SET2 was proposed as promising TRPV2-specific inhibitor, but still awaits scientific approval (Chai et al., 2019).

Recently, Fricke and colleagues demonstrated that TRPV2 features redox sensitivity, like the other temperature-sensitive TRP ion channels, leading to channel sensitization and gating. This redox sensitivity is caused by oxidation of methionine residues, most likely in the positions M528 and M607, via endogenous ROS (such as H₂O₂) and oxidants (like chT), and leads to channel sensitization and gating. In addition, TRPV2 is sensitized upon exposure to ultraviolet light A (UVA), that is known to trigger the intracellular generation of ROS (Fricke et al., 2019). However, the oxidation-induced channel sensitization only accounts for heat and chemical stimuli, but not for mechanical activation (Oda et al., 2021).

Known physiological stimuli and pharmacological compounds that affect TRPV2, either activating, inhibiting or sensitizing, or that are involved in the translocation of TRPV2, are summarized in **Figure 7**.

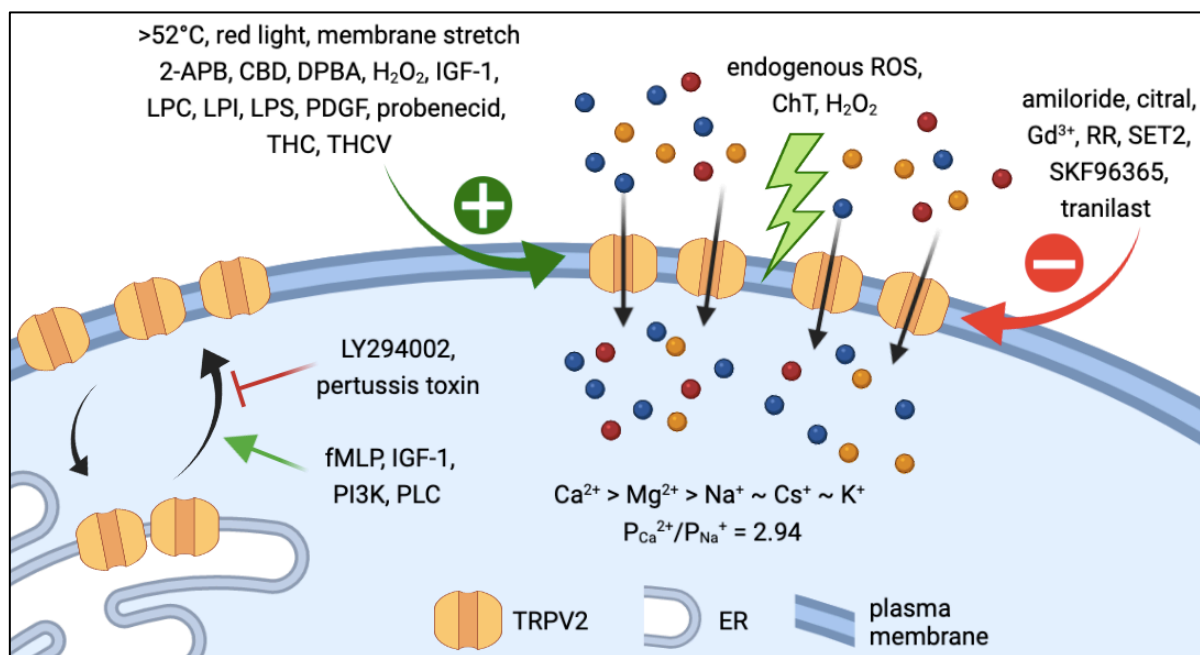


Figure 7. TRPV2 pharmacology & translocation. Known stimuli and compounds acting on TRPV2 **I)** activating (green arrow & plus): temperatures >52 °C, red light, membrane stretch, 2-Aminoethoxydiphenyl borate (2-ABP), cannabidiol (CBD), chloramine-T (ChT), diphenylboronic anhydride (DPBA), hydrogen peroxide (H₂O₂), insulin-like growth factor 1 (IGF-1), lyso-phosphatidylcholine (LPC), lysophosphatidylinositol (LPI), lipopolysaccharide (LPS), platelet-derived growth factor (PDGF), probenecid, tetrahydrocannabinol (THC), tetrahydrocannabivarin (THCV); **II)** blocking (red arrow & minus): amiloride, citral, gadolinium (Gd³⁺), ruthenium red (RR), SET2, SKF96365, tranilast; **III)** sensitizing (lightning bolt): endogenous ROS, ChT, H₂O₂. Compounds involved in translocation of TRPV2 (black arrows) between the the endoplasmic reticulum (ER) and the plasma membrane, **IV)** promotional (green arrow): chemotactic peptide formyl Met-Leu-Phe (fMLP), IGF-1, phospho-inositide 3-kinases (PI3K), phospholipase C (PLC); **V)** repressive (red inhibition): PI3K inhibitor (LY294002), pertussis toxin. Generally, each stimulus or compound lacks exclusive specificity for TRPV2 or needs further approval and shows species-dependency. Created with [BioRender.com](https://www.biorender.com).

iii. TRPV2 - Implications in Inflammation & Immunology

The controversies around TRPV2 also include the aspect of its physiological roles. Initially described as noxious heat sensor, TRPV2 was later considered to function as mechano- and/or osmo-sensor (Iwata et al., 2003; Muraki et al., 2003; Nagasawa & Kojima, 2015). However, based on results obtained from knockout mice, TRPV2 has only little to do with thermal and mechanical sensation, since these animals display normal responses to the respective stimuli. However and of special note, animals lacking functional TRPV2 feature reduced embryonic and adult body weight, higher perinatal lethality, accelerated general mortality and higher bacterial load (Caterina et al., 1999; Link et al., 2010; Park et al., 2011a). These observations might be the consequences of impaired function of macrophages, for which TRPV2 was shown to be the sole TRPV member (Yamashiro et al., 2010). In these cells, TRPV2 plays an essential and irreplaceable role in particle binding, phagocytosis, production of the cytokines tumor necrosis factor- α (TNF- α) and interleukin-6 (IL-6), chemoattractant-evoked motility and migration (Link et al., 2010; Yamashiro et al., 2010; Santoni et al., 2013). TRPV2 is also expressed in hematopoietic stem cells, in innate immune cells (granulocytes, mast cells, NK cells, dendritic cells, neutrophils and monocytes), and in adaptive immune cells (T- and B-lymphocyte). This expression profile emphasizes its participation in both innate and adaptive immunological processes (Heiner et al., 2003; Nagasawa et al., 2007; Yamashiro et al., 2010; Park et al., 2011b; Zhang et al., 2012; Santoni et al., 2013). In mast cells, for instance, activation of TRPV2 leads to degranulation in a kinase A-dependent signaling pathway and a subsequent Ca^{2+} entry (Stokes et al., 2004; Freichel et al., 2012; Zhang et al., 2012). However, the physiological function of TRPV2 in each individual cell type is partially still not known yet and has only started to be unraveled.

In the end, TRPV2 is claimed to be “*one of the least characterized members [...]*” with its “*physiological role [...] probably one of the most unsettled and controversial among TRP channels*” (Perálvarez-Marín, et al., 2013) and “*still, very little is known about the biological functions of this channel [...]*” (Link et al., 2010). This general lack of knowledge and the absence of studies in gonadal tissues, make this distinct TRP channel even more attractive and fascinating for a detailed examination in the gonads of human and mouse.

2 Aims of the Thesis

Several transcriptomic and proteomic studies have recently identified the non-selective transient receptor potential cation channel vanilloid 2, TRPV2, in numerous cell types of the human gonads, both in the testis and the ovary. The high abundance of this mysterious ion channel in some cell types implies involvement in gonadal functions. This study aimed at gaining new insights in these functional roles of TRPV2 in a tissue-specific context and thereby at expanding the knowledge about the gonadal channelome.

1. While expression of TRPV2 in the human testis was recently uncovered, the roles of this cation channel were unknown. The human male gonad is not readily accessible, but examination of TRPV2 functionality and role in the wall-forming cells of the seminiferous tubules, i.e. myoid human testicular peritubular cell (HTPCs) is possible. Studies on isolated HTPCs from men with obstructive azoospermia and normal spermatogenesis were performed. The functional examination included short-term monitoring of intracellular Ca^{2+} levels during pharmacological activation by the known agonist cannabidiol (CBD) and blocking via ruthenium red (RR) or tranilast (TRA). In addition, consequences of prolonged pharmacological activation upon the transcriptome and the secretome were investigated. Finally, specificity of the used compound was tested after transfection of the cells with small interfering RNA (siRNA) aligned with TRPV2.
2. There are no studies that focus on TRPV2 in murine testis so far. Therefore this gap was filled by the examination of testes from wild-type and AROM⁺ animals, i.e. an established model for human sterile inflammation and infertility that features high macrophage infiltration. Histological investigation of testicular sections in parallel to analysis of the transcriptional and translational expression of whole tissue were performed in an age-dependent manner, since the AROM⁺ phenotype is known to aggravate with age.

As TRPV2 was mainly found in testicular macrophages from both wild-type and AROM⁺ mice, testicular cells were subjected to cytometrical analysis to characterize the nature of TRPV2⁺ testicular macrophages. To examine the reasons of the observed changes, AROM⁺ animals crossed with mice lacking the estrogen α receptor, ERKO, were also investigated.

- 3.** TRPV2 expression by human ovarian granulosa cells (GCs), i.e. the major somatic cell type of the ovarian follicle, was reported. However, similar to the male gonad, the human ovary is not readily accessible. Access to GCs is depending on and limited to IVF patients-derived material, a fact resulting in availability of small cellular quantities that are in addition generally heterogeneous due to medical history, lifestyle and age of the individual patients. Cryopreservation could improve this situation, but the existing methods for bovine and human GCs yielded rather low survival rates. In addition, the impact of these methods upon cellular and functional aspects are not fully examined. Hence, a robust and reliable method for cryopreservation was established to set the stage for meaningful studies on human GCs minimally affected regarding cell viability, morphology, transcriptome, proteome and functionality.

3 Results

3.1 Publication I

Ca²⁺ Signaling and IL-8 Secretion in Human Testicular Peritubular Cells Involve the Cation Channel TRPV2.

Katja Eubler, Carola Herrmann, Astrid Tiefenbacher, Frank M. Köhn, J. Ullrich Schwarzer, Lars Kunz & Artur Mayerhofer

International Journal of Molecular Sciences, September 2018, 19 (9): 2829

doi: 10.3390/ijms19092829

Peritubular cells are part of the wall of seminiferous tubules in the human testis and their contractile abilities are important for sperm transport. In addition, they have immunological roles. A proteomic analysis of isolated human testicular peritubular cells (HTPCs) revealed expression of the transient receptor potential channel subfamily V member 2 (TRPV2). This cation channel is linked to mechano-sensation and to immunological processes and inflammation in other organs. We verified expression of TRPV2 in peritubular cells in human sections by immunohistochemistry. It was also found in other testicular cells, including Sertoli cells and interstitial cells. In cultured HTPCs, application of cannabidiol (CBD), a known TRPV2 agonist, acutely induced a transient increase in intracellular Ca²⁺ levels. These Ca²⁺ transients could be blocked both by ruthenium red, an unspecific Ca²⁺ channel blocker, and tranilast (TRA), an antagonist of TRPV2, and were also abolished when extracellular Ca²⁺ was removed. Taken together this indicates functional TRPV2 channels in peritubular cells. When applied for 24 to 48 h, CBD induced expression of proinflammatory factors. In particular, mRNA and secreted protein levels of the proinflammatory chemokine interleukin-8 (IL-8/CXCL8) were elevated. Via its known roles as a major mediator of the inflammatory response and as an angiogenic factor, this chemokine may play a role in testicular physiology and pathology.



Article

Ca²⁺ Signaling and IL-8 Secretion in Human Testicular Peritubular Cells Involve the Cation Channel TRPV2

Katja Eubler ¹, Carola Herrmann ¹, Astrid Tiefenbacher ¹, Frank-Michael Köhn ²,
J. Ullrich Schwarzer ³, Lars Kunz ⁴ and Artur Mayerhofer ^{1,*}

¹ Biomedical Center Munich (BMC), Cell Biology, Anatomy III, Ludwig-Maximilian-University (LMU), D-82152 Planegg-Martinsried, Germany; katja.eubler@lrz.uni-muenchen.de (K.E.); carola.herrmann@lrz.uni-muenchen.de (C.H.); tiefenbacher@lrz.uni-muenchen.de (A.T.)

² Andrologicum Munich, D-80331 Munich, Germany; info@andrologicum.com

³ Andrology-Center-Munich, D-81241 Munich, Germany; J.U.Schwarzer@gmx.de

⁴ Division of Neurobiology, Department of Biology II, Ludwig-Maximilian-University (LMU), D-82152 Planegg-Martinsried, Germany; lars.kunz@biologie.uni-muenchen.de

* Correspondence: mayerhofer@lrz.uni-muenchen.de; Tel.: +49-89-2180-75859

Received: 3 August 2018; Accepted: 14 September 2018; Published: 19 September 2018



Abstract: Peritubular cells are part of the wall of seminiferous tubules in the human testis and their contractile abilities are important for sperm transport. In addition, they have immunological roles. A proteomic analysis of isolated human testicular peritubular cells (HTPCs) revealed expression of the transient receptor potential channel subfamily V member 2 (TRPV2). This cation channel is linked to mechano-sensation and to immunological processes and inflammation in other organs. We verified expression of TRPV2 in peritubular cells in human sections by immunohistochemistry. It was also found in other testicular cells, including Sertoli cells and interstitial cells. In cultured HTPCs, application of cannabidiol (CBD), a known TRPV2 agonist, acutely induced a transient increase in intracellular Ca²⁺ levels. These Ca²⁺ transients could be blocked both by ruthenium red, an unspecific Ca²⁺ channel blocker, and tranilast (TRA), an antagonist of TRPV2, and were also abolished when extracellular Ca²⁺ was removed. Taken together this indicates functional TRPV2 channels in peritubular cells. When applied for 24 to 48 h, CBD induced expression of proinflammatory factors. In particular, mRNA and secreted protein levels of the proinflammatory chemokine interleukin-8 (IL-8/CXCL8) were elevated. Via its known roles as a major mediator of the inflammatory response and as an angiogenic factor, this chemokine may play a role in testicular physiology and pathology.

Keywords: Ca²⁺ signaling; interleukin-8; TRPV2; human testis

1. Introduction

Peritubular cells of human testis are cellular components of the wall of seminiferous tubules. They form several layers and, due to their contractile abilities, they are responsible for the transport of immotile sperm [1,2]. Besides these crucial functions for male fertility, newer studies imply that these cells possess a much broader spectrum of functions [3,4]. For instance, they are involved in paracrine signaling in the male gonad [5] and their participation in regulation of spermatogonial stem cells was shown for mice and men [6–8]. In addition, it became clear that in the human, peritubular cells can produce proinflammatory factors, express Toll-like receptors and have a say in the immune surveillance of the testis [9–12]. They may thus be players in sterile inflammation and male infertility [11,12].

A previous proteomic study of isolated human testicular peritubular cells (HTPCs) revealed, among others, expression of transient receptor potential cation channel subfamily V member 2

(TRPV2) [8]. While TRPV2 expression in organs such as brain, spleen and lung was described before [13], its expression in the testis is, to the best of our knowledge, not reported.

TRPV2 is activated by mechanical stimuli [14,15], temperatures above 52 °C [16] or by chemicals such as 2-Aminoethyl diphenylborinate and cannabidiol [17,18]. Controversial results concerning activation and function are reported and may be due to species-related differences [19]. However, it is generally accepted that activation leads to an influx of cations and it has been shown, that channel permeability covers classical cations such as Ca²⁺ and Na⁺ with a ratio 2.9/1 [16,20]. Very recently the structural basis for permeation of not only metal ions but also large organic cations was provided [21,22]. Several studies reported that TRPV2 is involved in a wide range of physiological and pathological cellular processes. For instance, this non-selective cation channel was found to be pivotal for macrophage function [23], involved in innate and adaptive immune response [24], in promoting H₂O₂ cytotoxicity [25] and expression and secretion of cytokines [26].

The lack of information on TRPV2 in the human testis and its possible involvement in immune responses prompted us to study TRPV2 in human testis and in HTPCs.

2. Results

2.1. TRPV2 Expression in Cultured HTPCs and Human Testis

An immunocytochemical study confirmed the presence of TRPV2 in cultured HTPCs (Figure 1A). Using the same antibody for Western blotting, TRPV2 was readily detected in cultured HTPCs derived from three individual patients as a single band of the expected size (Figure 1B, upper panel). RT-PCR and sequencing further confirmed expression of *TRPV2* in cultured HTPCs (Figure 1B, lower panel).

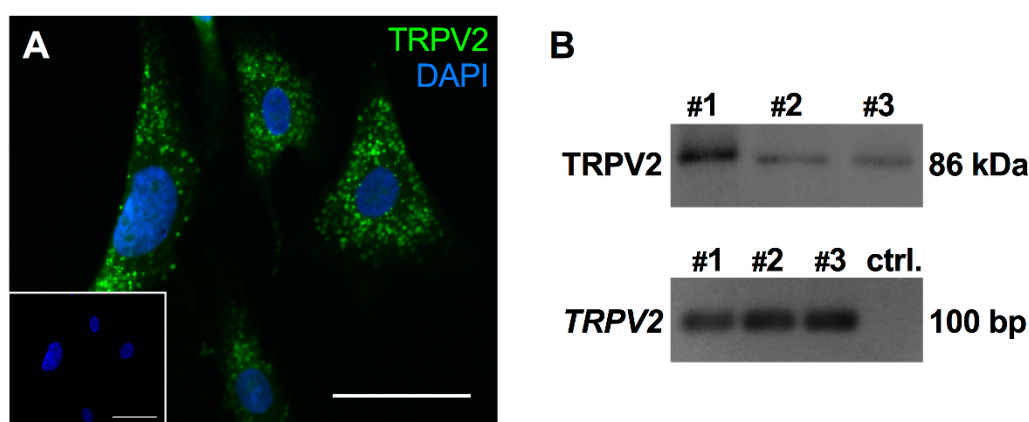


Figure 1. TRPV2 expression was confirmed in cultured HTPCs. (A) On the cellular level, TRPV2 exhibited a scattered expression pattern. Scale bar 10 μm. (B) In cultured HTPCs, expression of TRPV2 was detected by Western blot with a single band of the expected size (86 kDa) and RT-PCR showed clear bands at ~100 bp. Sequencing of the PCR-product validated expression of *TRPV2*. Bands obtained from three individual patients (#1–3) and negative control without cDNA in the RT-PCR reaction (ctrl.).

In addition, immunohistochemical investigation of human testicular slices revealed expression of TRPV2 in several testicular cells, including peritubular cells, but also Sertoli and interstitial cells (including presumable Leydig cells) (Figure 2A). Control slices, where the TRPV2 antibody was pre-adsorbed or omitted, were negative (Figure 2B,C). These results indicate a widespread distribution of TRPV2 in the human testis. *TRPV2* expression levels in cultured HTPCs did not change when dihydrotestosterone (DHT; 10 μM) was added to the culture medium for 24 h or for 7 day ($n = 5$ and $n = 3$, respectively), implying that androgens do not play a role in the regulation of this channel.

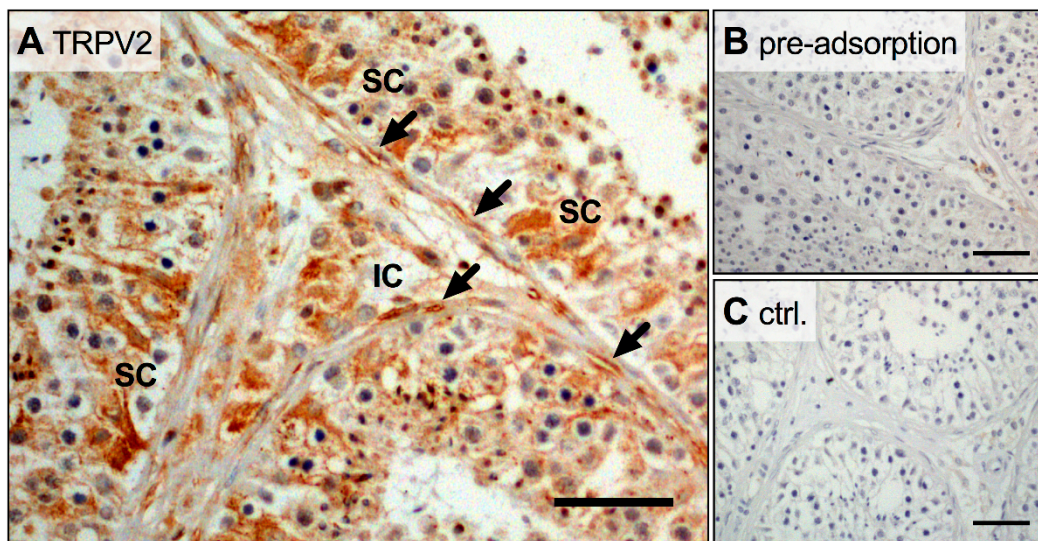


Figure 2. Broad expression of TRPV2 in human testis. (A–C) In human testicular slices, immunohistochemistry showed TRPV2 signals in Sertoli (SC), interstitial (IC) and in peritubular cells (arrows). In both controls, pre-adsorption with TRPV2 peptide (B) and omission of the primary antibody (C), no TRPV2 signal could be detected. Scale bar 100 μm .

2.2. Functionality of TRPV2 in HTPCs

Being a non-selective cation channel permeable for Ca^{2+} , functionality of TRPV2 in cultured HTPCs was examined by monitoring intracellular Ca^{2+} levels upon application of the known activator CBD and two blockers, ruthenium red (RR) and tranilast (TRA). Specificity of CBD to TRPV2 was ensured by the extracellular solution continuously containing the cannabinoid receptor 1 (CB1)-, and 2 (CB2)-blocker AM251 (80 nM) and AM630 (800 nM), respectively. With 1 mM Ca^{2+} in the extracellular solution (Figures 3A and 4A), acute application of CBD (10 μM) led to a rapid and strong transient increase of intracellular Ca^{2+} level in most analyzed cells (responder rate $88.6 \pm 5.5\%$, $n = 121$ cells from 5 patients). RR (10 μM), a non-selective Ca^{2+} channel blocker, did not affect intracellular Ca^{2+} levels (responder rate 0%, $n = 11$ cells), but blocked the CBD induced transients in nearly all cells (responder rate 9%, $n = 11$ cells; Fisher's exact test, $p < 0.0001$; Figure 3A,C, left part). TRA (10 μM), recently described as TRPV2 blocker [27,28], reduced the number of responding cells (responder rate 16%, $n = 25$ cells) and led to a decrease in fluorescence change of $69.4 \pm 3.1\%$ compared to the initial CBD application (Figure 4). CBD-induced changes in intracellular Ca^{2+} levels were not seen when Ca^{2+} was omitted from the extracellular solution (responder rate 0%, $n = 11$ cells); however, the combined acute application of CBD and Ca^{2+} (1 mM) in this Ca^{2+} free environment elicited an increase of intracellular Ca^{2+} levels in 82% of the analyzed cells ($n = 11$ cells; Fisher's exact test, $p < 0.0001$; Figure 3B,C (right part)), revealing an extracellular source of the transients.

Also, the striking nuclear Ca^{2+} influx upon CBD application (Figure 3A(b)) observed in all sets of experiment must be noted although it was not investigated in detail. Furthermore, application of CBD did not evoke any notable changes in cell size or shape.

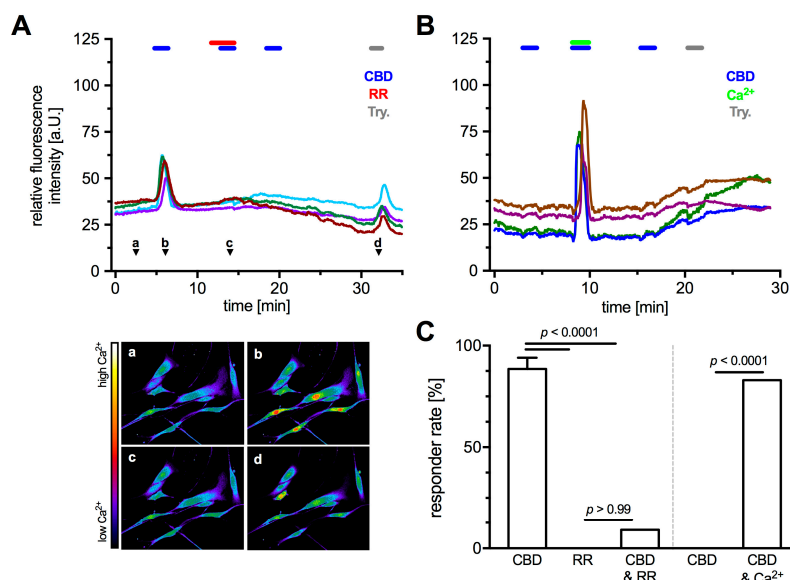


Figure 3. TRPV2 functionality as a Ca^{2+} -channel in HTPCs was studied by applying the agonist CBD and the unspecific antagonists RR, in presence of CB1 and 2 blockers (AM251 and AM630), during Ca^{2+} imaging. **(A)** Application of TRPV2 activator CBD (10 μM) in presence of 1 mM extracellular Ca^{2+} led to a transient increase in intracellular Ca^{2+} that could be blocked completely by RR (10 μM). **(a–d)** Relative Ca^{2+} concentrations at the indicated time points (**A**, arrow heads) as pseudo color images (red = high Ca^{2+} ; purple = low Ca^{2+}). **(B)** In absence of extracellular Ca^{2+} (0 mM), CBD alone did not induce any transients, whereas the combined application with Ca^{2+} (1 mM) resulted in Ca^{2+} transients, most likely due to Ca^{2+} influx. Each graph shows original traces of four representative cells from different donors (in total 5). In all experiments, trypsin (1%) served as positive control. **(C)** The total rate of responding cells upon CBD application was $88.6 \pm 5.5\%$ (121 cells from 5 donors). No reaction occurred upon RR application (0%), but combined application with CBD led to transients in 9.1% of the analyzed cells (11 cells from 2 donors). In absence of any extracellular Ca^{2+} , cells did not show reactions to CBD application (0%), whereas combined application with extracellular Ca^{2+} (1 mM) led to a responder rate of 83% (11 cells from 2 donors). The data were analyzed using Fisher's exact test.

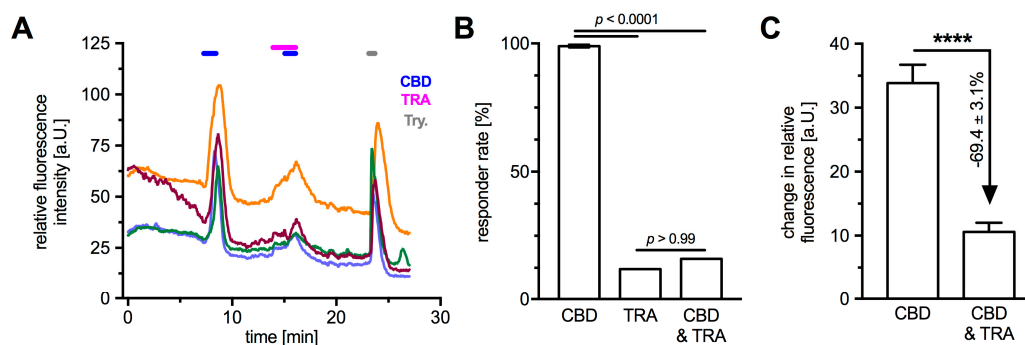


Figure 4. Application of the TRPV2-blocker TRA provided further evidence for functionality of TRPV2 in HTPCs during Ca^{2+} imaging. **(A)** In presence of CB1 and CB2 blockers (AM251 and AM630), application of TRPV2 activator CBD (10 μM) led to a transient increase in intracellular Ca^{2+} that could partially be blocked by TRA (10 μM). Graph shows original traces of four representative cells; three individual donors were analyzed. In all experiments, trypsin (1%) served as positive control. **(B)** The total rate of responding cells upon CBD application was $99.0 \pm 0.6\%$ (25 cells from 3 donors). TRA application elicited transients in 12% of the analyzed cells and combination with CBD led to a responder rate of 16% (25 cells from 3 donors). The data were analyzed using Fisher's exact test. **(C)** Application of TRA significantly reduced the measured changes in fluorescence intensity compared to the initial CBD-induced Ca^{2+} transients (**** $p < 0.0001$; 25 cells from 3 donors).

2.3. TRPV2 Activation Induced Expression and Secretion of Cytokines in HTPCs

Based on several publications, which linked TRPV2 to inflammatory processes, a screening experiment was performed employing a commercial cytokine proteome profiler assay. With CB1 and 2 blocked, CBD treatment (10 μ M) for 48 h increased the medium levels of Interleukin-8 (IL-8; 7.1-fold), Monocyte Chemoattractant Protein-1 (MCP-1; 3.4-fold) and Osteopontin (OPN; 3.2-fold) (Figure 5A; $n = 1$).

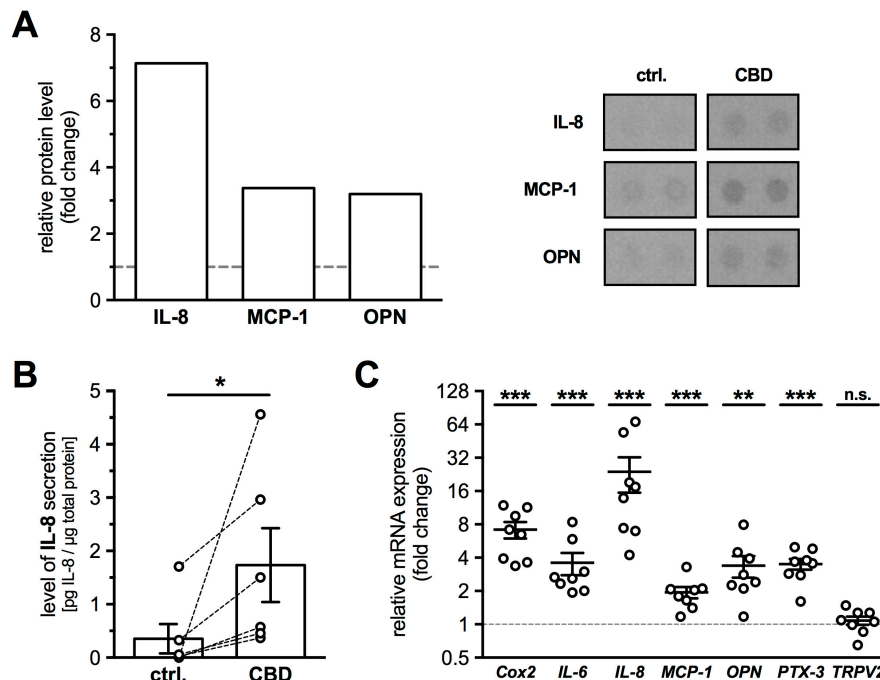


Figure 5. Activation of TRPV2 induced secretion of cytokines, especially of IL-8. (A) HTPCs preincubated with AM251 (80 nM) and AM630 (800 nM), and treated for 48 h with 10 μ M CBD, exhibited increased secretion of IL-8 (7.1-fold), MCP-1 (3.4-fold) and OPN (3.2-fold) compared to untreated cells ($n = 1$), demonstrated by a Human Proteome Profiler. Right panel shows corresponding membrane spots of untreated control and CBD (10 μ M) treated HTPCs revealing an increase of signal intensity of IL-8, MCP-1 and OPN. (B) Using an immunoassay, significantly increased IL-8 levels could be detected in culture media of HTPCs from six individual patients treated for 24 h with 10 μ M CBD in the presence of CB1 and CB2 blockers (1.74 ± 0.69 pg/ μ g total protein), compared to the corresponding control condition (0.35 ± 0.28 pg/ μ g total protein). Results were normalized to total protein amount and statistically analyzed using Wilcoxon test (two-tailed, paired test: $p = 0.0312$; $n = 6$). (C) Quantitative PCR revealed significantly increased mRNA expression levels of *Cox2*, *IL-6*, *IL-8*, *MCP-1*, *OPN* and *PTX-3* in HTPCs after 24 h stimulation with 10 μ M CBD and CB1 and 2 blockers. mRNA levels of *TRPV2* did not show any significant changes (1.08 ± 0.09 -fold; $p = 0.5905$). $n = 8$; * $p \leq 0.05$, ** $p \leq 0.01$, *** $p \leq 0.001$ vs. control cells.

In addition, several other factors were found to be slightly elevated in the culture medium (>2-fold change: Insulin-like growth factor-binding protein-3, Interleukin-17A, Urokinase receptor). As IL-8 secretion showed the strongest increase upon CBD treatment, HTPCs from 6 more patients were investigated using an immunoassay. CBD treatment (24 h, 10 μ M) resulted in significantly increased IL-8 levels in the culture media (Figure 5B), with 0.35 ± 0.28 pg/ μ g in supernatants from untreated and 1.74 ± 0.69 pg/ μ g in those from treated cells (Wilcoxon test, $p = 0.0312$; $n = 6$). Also, at the mRNA level, expression of *IL-8* (23.91 ± 7.88 -fold, $p < 0.0001$), *MCP-1* (1.94 ± 0.21 -fold, $p = 0.0008$) and *OPN* (3.38 ± 0.70 -fold, $p = 0.0012$) were significantly increased in CBD treated cells ($n = 8$). Additionally, the mRNA levels of *Cox2* (8.34 ± 1.78 -fold, $p < 0.0001$), *IL-6* (3.62 ± 0.78 -fold, $p = 0.0005$) and *PTX-3*

(3.24 ± 0.42 -fold, $p = 0.0002$) showed significant increases. However, *TRPV2* itself did not show any changes (1.08 ± 0.09 -fold, $p = 0.5905$) in expression level upon 24 h activation (Figure 5C; $n = 8$).

To further test the specificity of CBD to activate *TRPV2*, cells from two donors were transfected with siRNA targeting *TRPV2* or scrambled non-targeting control siRNA and then treated with CBD for 24 h (Figure 6). The transfection led to a reduction in *TRPV2* protein amount ($47.03 \pm 16.94\%$; $n = 2$) and resulted in a slight decrease of *TRPV2* in cells transfected with the siRNA (siTRPV2-ctrl. 0.55 ± 0.03 -fold, siTRPV2-CBD 0.67 ± 0.02 -fold; $n = 2$ each), whereas the non-targeting control siRNA showed no effects on mRNA expression levels of *TRPV2* (Scr-CBD 0.99 ± 0.25 -fold; $n = 2$). In control cells, CBD increased mRNA levels of *IL-8* (4.84 ± 0.08 -fold; $n = 2$), whereas no changes in *IL-8* could be observed in the silenced cells (siTRPV2-ctrl. 1.11 ± 0.10 -fold, siTRPV2-CBD 1.10 ± 0.14 -fold; $n = 2$ each).

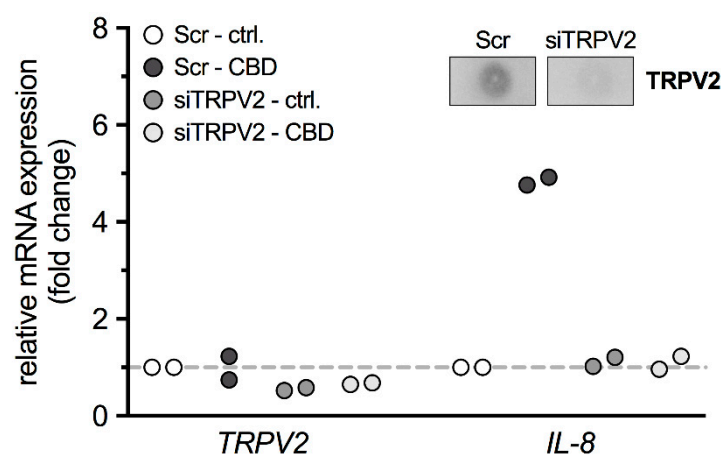


Figure 6. Transfection of HTPCs with a *TRPV2* siRNA abolished the observed effects upon *IL-8*. Quantitative PCR data from HTPCs transfected with scrambled (Scr) non-targeting control siRNA or *TRPV2* siRNA (siTRPV2) and treated with CBD (10 μ M; Scr-CBD and siTRPV2-CBD) or equal volume of EtOH (Scr-ctrl. and siTRPV2-ctrl.) for 24 h. Upper panel shows a representative *TRPV2* dot blot from HTPCs transfected with scrambled (Scr) non-targeting control siRNA and *TRPV2* siRNA (siTRPV2), emphasizing the efficiency of the transfection.

3. Discussion

To our knowledge *TRPV2* has not been described in human testis before, yet a proteome analysis of HTPCs had indicated its presence in this testicular cell type [8]. The present study confirms expression in HTPCs and their in situ counterparts, but also reveals an unexpected widespread expression of *TRPV2* in the human testis. Results obtained in HTPCs implicate *TRPV2* function in the release of *IL-8*.

Immunohistochemistry showed *TRPV2* not only in peritubular cells but also in Sertoli cells, and interstitial cells, including presumably Leydig cells and immune cells of the human testis. We did not attempt to analyze their nature but rather focused on peritubular cells, because in contrast to other testicular cells, they can be isolated and studied in vitro.

Peritubular cells are smooth muscle-like cells and are thought to be pivotal for the transport of immotile sperm. Recent results obtained in HTPCs showed that they also contribute to the spermatogonial stem cell niche [6,29] and that they have immunological properties [11,12]. Peritubular cells possess androgen receptors, yet expression levels of *TRPV2* in these cells was not affected by DHT, a potent androgen, added to the culture medium for up to 7 days. Such a treatment led to an increased expression of a growth factor (*PEDF*) in HTPCs [29], as well as smooth muscle markers and androgen receptors [30].

To investigate the role of *TRPV2*, the known pharmacological activator CBD was used [17]. Since at least CB1 expression was shown in HTPCs, CBD in combination with the CB1 and 2 blockers, AM251 and AM630, respectively, were employed as done before [18]. Application of

CBD during Ca^{2+} imaging experiments resulted in transient increases of intracellular Ca^{2+} levels. Specificity of CBD, acting on TRPV2, was demonstrated by the application of the Ca^{2+} channel blocker RR and the TRPV2 antagonist TRA, resulting in significant reduction or even absence of any transients. Additionally, the external source of these transients was shown by omission of any transients during CBD application in absence of extracellular Ca^{2+} . The measurements support functionally active TRPV2 in HTPCs.

Expression of TRPV2 is reported in dendritic cells, granulocytes, lymphocytes, monocytes, and macrophages [24,31], i.e., cells where the concentration of intracellular Ca^{2+} is crucial for their proper functionality. In HTPCs, we did not observe obvious changes in cell size or any other hints of contractions associated with increases of intracellular Ca^{2+} levels. Such changes in HTPCs were previously seen, for example, upon addition of angiotensin II [10]. Hence CBD-induced activation of TRPV2 may not be linked to the regulation of contractility of HTPCs. This point remains to be further investigated as it was suggested to occur in retinal arterioles [14].

Several reports have linked TRPV2 to inflammation e.g., in rheumatic diseases [32], experimental colitis [33] and oral inflammation [26], rather than to thermal sensation as described earlier [16]. Furthermore, TRPV2 was found to be enriched in several cancer types such as bladder and prostate cancer [34,35]. It was shown that activation of TRPV2 led to elevated levels of IL-6 and IL-8 in human periodontal ligament cells, and that deficiency of TRPV2 resulted in reduced macrophage infiltration and impaired phagocytosis [23]. As HTPCs are sources for cytokines [11,12], we explored consequences of TRPV2 activation. Despite expected heterogeneity between the samples stemming from individual patients [11,36], a proinflammatory influence of CBD became apparent with robustly increased levels of IL-8 in different experimental approaches. We focused on IL-8.

IL-8 is a known chemotactic and inflammatory cytokine being involved in recruitment of neutrophils, macrophages and mast cells into inflammatory sites and their activation [37–39]. The expression of the corresponding receptors for IL-8, i.e., CXCR1 and 2, was demonstrated also in human phagocytes, lymphocytes, and endothelial cells [40,41]. IL-8 has been reported in the male genital tract, especially in prostate and seminal plasma in health and disease [42,43]. In contrast, a role of IL-8 in normal testicular function remains to be determined [44] as testicular expression of the corresponding receptors for IL-8, CXCRs, was reported to be low or even absent. Yet, in cases of male infertility, which is associated with signs of sterile inflammation, it seems possible that IL-8 may have a say [11,12,45,46]. IL-8 is also involved in regulation of angiogenesis [47,48] with proangiogenic properties such as promoting proliferation, migration and tube-forming ability shown for human umbilical vein endothelial cells [49] and human aortic endothelial cells [50]. Promotion of proliferation and angiogenesis was also shown for colorectal cancer cells [51] revealing a link to cancer biology [52]. As the microvessel network contributes to the spermatogonial stem cell niche of the testis and because HTPCs produce pro- and anti-angiogenic factors [53], IL-8 may be a further factor involved.

In summary, our study describes testicular TRPV2 and identified a role in the regulation of proinflammatory factors, especially IL-8, in HTPCs. Beside peritubular cells, other testicular cells also possess TRPV2 and its specific involvement in the regulation of these cells is unknown. Furthermore, the physiological mechanisms leading to TRPV2 activation in the testis are not known. It is tempting to speculate that mechanical stimuli could be involved.

4. Materials and Methods

4.1. Isolation and Cell Culture of HTPCs

HTPCs stem from small samples of testicular tissue from vasectomized men from 36–55 years of age ($n = 11$) with obstructive azoospermia but normal spermatogenesis, as described [3,9]. The local Ethics Committee (Ethikkommission, Technische Universität München, Fakultät für Medizin, München, project number 5158/11, 18 October 2011; and project 309/14; 28 August 2014) has approved the study. The scientific use of the cells was permitted by written informed consent from all patients.

The experiments were carried out in accordance with the relevant guidelines and regulations. Dulbecco's Modified Eagle Medium high glucose (DMEM; Gibco, Paisley, UK) with 10% fetal calf serum (FCS; Capricorn Scientific, Ebsdorfergrund, Germany) and 1% penicillin/streptomycin (P/S; BioChrom, Berlin, Germany) was used for cell culture (37 °C, 5% CO₂, 95% humidity). For experiments, HTPCs from passages 8–13 were used.

4.2. Immunohistochemistry and Immunofluorescence

Slices from human testicular sections of patients with normal spermatogenesis were used for immunohistochemical (IHC) and cultured HTPCs for immunocytochemical (ICC) staining as described before [3,54]. A polyclonal TRPV2 antibody (1:200; HPA044993, Atlas Antibodies, Stockholm, Sweden) was used for both methods. For IHC, a biotinylated α -rabbit secondary antibody (1:2500; Vector Laboratories, Inc., Burlingame, CA, USA), an avidin-biotin complex peroxidase (ABC, Vector Laboratories, Inc., Burlingame, CA, USA) and DAB (Sigma Aldrich, St. Louis, MO, USA) were used, followed by slight counterstaining with hematoxylin. For ICC, a fluorescence tagged secondary antibody (1:800; goat α -rabbit Alexa 488, life technologies, Carlsbad, CA, USA) and DAPI were used. Omission of primary antibody and pre-adsorption (1:100; APrEST83822, Atlas Antibodies, Stockholm, Sweden) served as negative controls.

4.3. RT-PCR and qPCR

Total RNA was extracted with the RNeasy Micro Kit (Qiagen, Hilden, Germany) and subjected to reverse transcription followed by real time PCR (LightCycler 96[®] System, Roche Diagnostics, Penzberg, Germany) using the QuantiFast SYBR Green PCR Kit (Qiagen, Hilden, Germany) as described [10]. Changes in gene expression were normalized to the geometric mean of mRNA levels of *Peptidylprolyl isomerase A (PPIA)* and *ribosomal protein L19 (L19)* as internal controls and analyzed according to the $2^{-\Delta\Delta Cq}$ method, as described elsewhere [55]. Information on primers are given in Table 1. PCR products were visualized using a Midori Green Advance DNA stain (Nippon Genetics Europe, Dürren, Germany) in a 2% agarose gel and sequenced to verify identity (GATC, Konstanz, Germany).

Table 1. Oligonucleotide primer sequences and corresponding amplicon size.

Gene	Reference ID	Nucleotide Sequence	Amplicon Size
<i>L-19</i>	NM_000981.3	5'-AGG CAC ATG GGC ATA GGT AA-3' 5'-CCA TGA GAA TCC GCT TGT TT-3'	199 bp
<i>PPIA</i>	NM_021130.4	5'-AGA CAA GGT CCC AAA GAC-3' 5'-ACC ACC CTG ACA CAT AAA-3'	118 bp
<i>Cox2</i>	NM_000963.3	5'-CTT ACC CAC TTC AAG GGA-3' 5'-GCC ATA GTC AGC ATT GTA AG-3'	132 bp
<i>IL-6</i>	NM_000600.4	5'-AAC CTG AAC CTT CCA AAG ATG G-3' 5'-TCT GGC TTG TTC CTC ACT ACT-3'	159 bp
<i>IL-8</i>	NM_000584.3	5'-TCT TGG CAG CCT TCC TGA-3' 5'-GAA TTC TCA GCC CTC TTC-3'	190 bp
<i>MCP-1</i>	NM_002982.3	5'-AGG TGA CTG GGG CAT TGA T-3' 5'-GAA GTG ATG GGT ATC CGG TC-3'	109 bp
<i>OPN</i>	NM_001040058.1	5'-TTT TCA CTC CAG TTG TCC CC-3' 5'-TAC TGG ATG TCA GGT CTG CG-3'	109 bp
<i>PTX-3</i>	NM_002852.3	5'-TAG TGT TTG TGG TGG GTG GA-3' 5'-TGT GAG CCC TTC CTC TGA AT-3'	110 bp
<i>TRPV2</i>	NM_016113.4	5'-CCA GCA AGT ACC TCA CCG AC-3' 5'-CAG GCA TTG ACT CCG TCC TT-3'	100 bp

4.4. Immunoblotting

Immunoblotting was performed with HTPC whole cell lysates, as described elsewhere [56] employing the same antibody as used for IHC and ICC (polyclonal TRPV2 antibody; HPA044993, Atlas Antibodies, Stockholm, Sweden). Western blot or dot blot bands were detected using a corresponding HRP-conjugated secondary antibody and chemiluminescent solutions (SuperSignal® West Femto Maximum Sensitivity Substrate; Thermo Fisher Scientific, Rockford, IL, USA).

4.5. Reagents

Dihydrotestosterone (DHT; Sigma Aldrich, St. Louis, MO, USA) was used to evaluate potential hormonal regulation of *TRPV2* expression. Channel functionality was examined by application of cannabidiol (CBD), as reported elsewhere [3]. CBD is known to also activate cannabinoid receptors and at least presence of cannabinoid receptor 1 (CB1) was detected. Therefore, experiments were carried out in presence of CB1 and CB2 blockers, AM251 and AM630, respectively [3]. In addition, the unspecific Ca^{2+} channel blocker ruthenium red (RR) and the recently described TRPV2 blocker tranelast (TRA) were used [13,57]. CBD, AM251, AM630 and RR were purchased from Tocris Bioscience (Bristol, UK), TRA was from Cayman (Ann Arbor, MI, USA). Stock solutions were dissolved in EtOH, DMSO or H_2O , respectively. Application of equal concentrations of the corresponding solvent was used as control.

4.6. Ca^{2+} Imaging

For Ca^{2+} imaging experiments, HTPCs were loaded with the Ca^{2+} sensitive fluorescent dye Fluoorte® Reagent (5 μM , Enzo Life Sciences, Lörrach, Germany) for 30 min at 37 °C and 5% CO_2 . Standard extracellular solution was composed of (in mM) 140 NaCl, 3 KCl, 10 HEPES, 10 glucose (pH 7.4 with NaOH), additionally AM251 (80 nM) and AM630 (800 nM) were added. The free extracellular Ca^{2+} concentration was set to 1 or 0 mM and that of CBD, RR and TRA to 10 μM . Trypsin (0.1 %, BioChrom, Berlin, Germany) served as a positive control at the end of every experiment. With excitation and emission wavelengths of 488 nm and 520 nm, fluorescence intensity was monitored using a confocal microscope (Axiovert 200M; Carl Zeiss Microscopy, Jena, Germany) equipped with a laser module (LSM 5, Carl Zeiss, Jena, Germany) and the software AIM 4.2 (Carl Zeiss MicroImaging, Jena, Germany). Data are expressed as relative fluorescence intensity based on a pseudo color scale from black/purple (low Ca^{2+}) to white/red (high Ca^{2+}) in arbitrary units (a.U.).

4.7. Treatment of Cells

For treatment, cells were serum starved 24 h prior to application of any drug. All stimulations were performed in FCS-free medium. For investigation of hormonal *TRPV2* regulation, cells were stimulated with DHT (10 μM) for 24 h or 7 d. For functional analysis of TRPV2, cells were preincubated for 1 h with AM251 (80 nM) and AM630 (800 nM) and then stimulated with CBD (10 μM) for 24 h for qPCR experiments and for 48 h for Human XL cytokine array.

4.8. Supernatant Protein Profiling

For the Proteome Profiler Human XL Cytokine Array (R&D Systems, Minneapolis, MN, USA), HTPCs were treated as described above and supernatants were collected. A total amount of 500 μL of supernatant was applied on the membranes according to the manufacturer's instructions. Quantitative analysis was performed using Fiji software [58]. For each membrane, average spot signal density was determined by densitometry, followed by background subtraction and normalization to the respective protein concentrations.

4.9. IL-8 Immunoassay

Following the manufacturer's instructions, the level of IL-8 in the supernatant after 24 h incubation with CBD (10 μ M) was determined using an IL-8 ELISA (Human IL-8/NAP-1 Platinum ELISA; affymetrix eBioscience, Santa Clara, CA, USA). The lowest detectable IL-8 concentration was 2.0 pg/mL and the inter-assay coefficient of variance was less than 5.3%. Samples from 6 different patients were analyzed and the levels of IL-8 were expressed in pg/ μ g total protein amount.

4.10. siRNA Transfection

As both RR and TRA are not well suited for 24 h stimulation due to described side effects [59], cells were transfected with TRPV2 siRNA to block the observed effects. At ~80% confluency, cells were transfected for 6 h with Lipofectamine[®] 2000 Transfection Reagent (Invitrogen, Carlsbad, CA, USA) dissolved in DMEM (Gibco Paisley, UK) according to the manufacturer's protocol. A control non-silencing siRNA (negative control siRNA, 5 nM, #1022076; Qiagen, Hilden, Germany) and a TRPV2 siRNA (TRPV2 Silencer[®] Pre-designed siRNA, 40 nM, #AM16708; life technologies, Carlsbad, CA, USA) were used. Cells were starved on DMEM containing 2% FCS and 1% P/S for further 18 h, preincubated with AM251 and AM630 for 1 h and then treated for 24 h with CBD and EtOH as solvent control, as described above. Efficiency of silencing was verified by a dot blot using 5 μ g of total protein, the above listed TRPV2 antibody and β -actin as housekeeping control (monoclonal β -actin antibody, 1:10,000; A5441, Sigma Aldrich, St. Louis, MO, USA). The experiment was performed twice with similar results.

4.11. Data Analysis and Statistics

Data analyses were performed using GraphPad Prism 7.0 (GraphPad Software Inc., San Diego, CA, USA). For statistical analysis of qPCR data and changes in fluorescence intensity, two-tailed one-sample t-test based on given Gaussian distribution (Shapiro-Wilk normality test) was used and the level of significance was set to 5%. For the responder rate, the Fisher's exact test was used, and significance was set to 5%. Immunoassay data of control condition did not achieve normal distribution (Shapiro-Wilk normality test: $p = 0.0009$) and therefore data were analyzed using Wilcoxon test. Data are presented individually for each patient and, for qPCR and ELISA data, also as mean \pm SEM.

Author Contributions: K.E. and A.M. conceived and designed the experiments; K.E. and C.H. performed the experiments; A.T. performed the immunohistochemistry experiments; K.E. analyzed the data; F.-M.K., J.U.S. and A.M. contributed reagents/materials/analysis tools; K.E., L.K. and A.M. wrote the paper.

Funding: This study was supported in parts by grants from Deutsche Forschungsgemeinschaft (DFG) especially MA1080/27-1.

Conflicts of Interest: The authors declare no conflict of interest. The funding sponsors had no role in the design of the study; in the collection, analyses, or interpretation of data; in the writing of the manuscript, and in the decision to publish the results. This work was done in partial fulfilment of the requirements for a Dr. rer. nat degree at LMU (KE).

References

1. Holstein, A.F.; Maekawa, M.; Nagano, T.; Davidoff, M.S. Myofibroblasts in the lamina propria of human semi-niferous tubules are dynamic structures of heterogeneous phenotype. *Arch Histol. Cytol.* **1996**, *59*, 109–125. [[CrossRef](#)] [[PubMed](#)]
2. Middendorff, R.; Muller, D.; Mewe, M.; Mukhopadhyay, A.K.; Holstein, A.F.; Davidoff, M.S. The tunica albuginea of the human testis is characterized by complex contraction and relaxation activities regulated by cyclic GMP. *J. Clin. Endocrinol. Metab.* **2002**, *87*, 3486–3499. [[CrossRef](#)] [[PubMed](#)]
3. Albrecht, M. Insights into the nature of human testicular peritubular cells. *Ann. Anat.* **2009**, *191*, 532–540. [[CrossRef](#)] [[PubMed](#)]
4. Mayerhofer, A. Human testicular peritubular cells: More than meets the eye. *Reproduction* **2013**, *145*, R107–R116. [[CrossRef](#)] [[PubMed](#)]

5. Maekawa, M.; Kamimura, K.; Nagano, T. Peritubular myoid cells in the testis: Their structure and function. *Arch. Histol. Cytol.* **1996**, *59*, 1–13. [[CrossRef](#)] [[PubMed](#)]
6. Spinnler, K.; Kohn, F.M.; Schwarzer, U.; Mayerhofer, A. Glial cell line-derived neurotrophic factor is constitutively produced by human testicular peritubular cells and may contribute to the spermatogonial stem cell niche in man. *Hum. Reprod.* **2010**, *25*, 2181–2187. [[CrossRef](#)] [[PubMed](#)]
7. Chen, L.Y.; Brown, P.R.; Willis, W.B.; Eddy, E.M. Peritubular myoid cells participate in male mouse spermatogonial stem cell maintenance. *Endocrinology* **2014**, *155*, 4964–4974. [[CrossRef](#)] [[PubMed](#)]
8. Flenkenthaler, F.; Windschuttl, S.; Frohlich, T.; Schwarzer, J.U.; Mayerhofer, A.; Arnold, G.J. Secretome analysis of testicular peritubular cells: A window into the human testicular microenvironment and the spermatogonial stem cell niche in man. *J. Proteome. Res.* **2014**, *13*, 1259–1269. [[CrossRef](#)] [[PubMed](#)]
9. Schell, C.; Albrecht, M.; Mayer, C.; Schwarzer, J.U.; Frungieri, M.B.; Mayerhofer, A. Exploring human testicular peritubular cells: Identification of secretory products and regulation by tumor necrosis factor- α . *Endocrinology* **2008**, *149*, 1678–1686. [[CrossRef](#)] [[PubMed](#)]
10. Welter, H.; Huber, A.; Lauf, S.; Einwang, D.; Mayer, C.; Schwarzer, J.U.; Kohn, F.M.; Mayerhofer, A. Angiotensin II regulates testicular peritubular cell function via AT1 receptor: A specific situation in male infertility. *Mol. Cell. Endocrinol.* **2014**, *393*, 171–178. [[CrossRef](#)] [[PubMed](#)]
11. Mayer, C.; Adam, M.; Glashauser, L.; Dietrich, K.; Schwarzer, J.U.; Kohn, F.M.; Strauss, L.; Welter, H.; Poutanen, M.; Mayerhofer, A. Sterile inflammation as a factor in human male infertility: Involvement of Toll like receptor 2, biglycan and peritubular cells. *Sci. Rep.* **2016**, *6*, 37128. [[CrossRef](#)] [[PubMed](#)]
12. Walenta, L.; Fleck, D.; Frohlich, T.; von Eysmond, H.; Arnold, G.J.; Spehr, J.; Schwarzer, J.U.; Kohn, F.M.; Spehr, M.; Mayerhofer, A. ATP-mediated Events in Peritubular Cells Contribute to Sterile Testicular Inflammation. *Sci. Rep.* **2018**, *8*, 1431. [[CrossRef](#)] [[PubMed](#)]
13. Peralvarez-Marin, A.; Donate-Macian, P.; Gaudet, R. What do we know about the transient receptor potential vanilloid 2 (TRPV2) ion channel? *FEBS J.* **2013**, *280*, 5471–5487. [[CrossRef](#)] [[PubMed](#)]
14. McGahon, M.K.; Fernandez, J.A.; Dash, D.P.; McKee, J.; Simpson, D.A.; Zholos, A.V.; McGeown, J.G.; Curtis, T.M. TRPV2 Channels Contribute to Stretch-Activated Cation Currents and Myogenic Constriction in Retinal Arterioles. *Investig. Ophthalmol. Vis. Sci.* **2016**, *57*, 5637–5647. [[CrossRef](#)] [[PubMed](#)]
15. Sugio, S.; Nagasawa, M.; Kojima, I.; Ishizaki, Y.; Shibasaki, K. Transient receptor potential vanilloid 2 activation by focal mechanical stimulation requires interaction with the actin cytoskeleton and enhances growth cone motility. *FASEB J.* **2017**, *31*, 1368–1381. [[CrossRef](#)] [[PubMed](#)]
16. Caterina, M.J.; Rosen, T.A.; Tominaga, M.; Brake, A.J.; Julius, D. A capsaicin-receptor homologue with a high threshold for noxious heat. *Nature* **1999**, *398*, 436–441. [[CrossRef](#)] [[PubMed](#)]
17. Qin, N.; Neeper, M.P.; Liu, Y.; Hutchinson, T.L.; Lubin, M.L.; Flores, C.M. TRPV2 is activated by cannabidiol and mediates CGRP release in cultured rat dorsal root ganglion neurons. *J. Neurosci.* **2008**, *28*, 6231–6238. [[CrossRef](#)] [[PubMed](#)]
18. De Clercq, K.; Held, K.; Van Bree, R.; Meuleman, C.; Peeraer, K.; Tomassetti, C.; Voets, T.; D’Hooghe, T.; Vriens, J. Functional expression of transient receptor potential channels in human endometrial stromal cells during the luteal phase of the menstrual cycle. *Hum. Reprod.* **2015**, *30*, 1421–1436. [[CrossRef](#)] [[PubMed](#)]
19. Neeper, M.P.; Liu, Y.; Hutchinson, T.L.; Wang, Y.; Flores, C.M.; Qin, N. Activation properties of heterologously expressed mammalian TRPV2: Evidence for species dependence. *J. Biol. Chem.* **2007**, *282*, 15894–15902. [[CrossRef](#)] [[PubMed](#)]
20. Tykocki, N.R.; Boerman, E.M.; Jackson, W.F. Smooth Muscle Ion Channels and Regulation of Vascular Tone in Resistance Arteries and Arterioles. *Compr. Physiol.* **2017**, *7*, 485–581. [[PubMed](#)]
21. Zubcevic, L.; Le, S.; Yang, H.; Lee, S.Y. Conformational plasticity in the selectivity filter of the TRPV2 ion channel. *Nat. Struct. Mol. Biol.* **2018**, *25*, 405–415. [[CrossRef](#)] [[PubMed](#)]
22. Nabissi, M.; Morelli, M.B.; Santoni, M.; Santoni, G. Triggering of the TRPV2 channel by cannabidiol sensitizes glioblastoma cells to cytotoxic chemotherapeutic agents. *Carcinogenesis* **2013**, *34*, 48–57. [[CrossRef](#)] [[PubMed](#)]
23. Link, T.M.; Park, U.; Vonakis, B.M.; Raben, D.M.; Soloski, M.J.; Caterina, M.J. TRPV2 has a pivotal role in macrophage particle binding and phagocytosis. *Nat. Immunol.* **2010**, *11*, 232–239. [[CrossRef](#)] [[PubMed](#)]
24. Santoni, G.; Farfariello, V.; Liberati, S.; Morelli, M.B.; Nabissi, M.; Santoni, M.; Amantini, C. The role of transient receptor potential vanilloid type-2 ion channels in innate and adaptive immune responses. *Front. Immunol.* **2013**, *4*, 34. [[CrossRef](#)] [[PubMed](#)]

25. Ma, W.; Li, C.; Yin, S.; Liu, J.; Gao, C.; Lin, Z.; Huang, R.; Huang, J.; Li, Z. Novel role of TRPV2 in promoting the cytotoxicity of H₂O₂-mediated oxidative stress in human hepatoma cells. *Free Radic. Biol. Med.* **2015**, *89*, 1003–1013. [[CrossRef](#)] [[PubMed](#)]
26. Son, G.Y.; Hong, J.H.; Chang, I.; Shin, D.M. Induction of IL-6 and IL-8 by activation of thermosensitive TRP channels in human PDL cells. *Arch. Oral Biol.* **2015**, *60*, 526–532. [[CrossRef](#)] [[PubMed](#)]
27. Nie, L.; Oishi, Y.; Doi, I.; Shibata, H.; Kojima, I. Inhibition of proliferation of MCF-7 breast cancer cells by a blocker of Ca(2+)-permeable channel. *Cell. Calcium* **1997**, *22*, 75–82. [[CrossRef](#)]
28. Zhang, D.; Spielmann, A.; Wang, L.; Ding, G.; Huang, F.; Gu, Q.; Schwarz, W. Mast-cell degranulation induced by physical stimuli involves the activation of transient-receptor-potential channel TRPV2. *Physiol. Res.* **2012**, *61*, 113–124. [[PubMed](#)]
29. Windschuttl, S.; Nettersheim, D.; Schlatt, S.; Huber, A.; Welter, H.; Schwarzer, J.U.; Kohn, F.M.; Schorle, H.; Mayerhofer, A. Are testicular mast cells involved in the regulation of germ cells in man? *Andrology* **2014**, *2*, 615–622. [[CrossRef](#)] [[PubMed](#)]
30. Mayer, C.; Adam, M.; Walenta, L.; Schmid, N.; Heikela, H.; Schubert, K.; Flenkenthaler, F.; Dietrich, K.G.; Gruschka, S.; Arnold, G.J.; et al. Insights into the role of androgen receptor in human testicular peritubular cells. *Andrology* **2018**. [[CrossRef](#)] [[PubMed](#)]
31. Parenti, A.; De Logu, F.; Geppetti, P.; Benemei, S. What is the evidence for the role of TRP channels in inflammatory and immune cells? *Br. J. Pharmacol.* **2016**, *173*, 953–969. [[CrossRef](#)] [[PubMed](#)]
32. Laragione, T.; Cheng, K.F.; Tanner, M.R.; He, M.; Beeton, C.; Al-Abed, Y.; Gulko, P.S. The cation channel Trpv2 is a new suppressor of arthritis severity, joint damage, and synovial fibroblast invasion. *Clin. Immunol.* **2015**, *158*, 183–192. [[CrossRef](#)] [[PubMed](#)]
33. Issa, C.M.; Hambly, B.D.; Wang, Y.; Maleki, S.; Wang, W.; Fei, J.; Bao, S. TRPV2 in the development of experimental colitis. *Scand. J. Immunol.* **2014**, *80*, 307–312. [[CrossRef](#)] [[PubMed](#)]
34. Caprodossi, S.; Lucciarini, R.; Amantini, C.; Nabissi, M.; Canesin, G.; Ballarini, P.; Di Spilimbergo, A.; Cardarelli, M.A.; Servi, L.; Mammana, G.; et al. Transient receptor potential vanilloid type 2 (TRPV2) expression in normal urothelium and in urothelial carcinoma of human bladder: Correlation with the pathologic stage. *Eur. Urol.* **2008**, *54*, 612–620. [[CrossRef](#)] [[PubMed](#)]
35. Monet, M.; Lehen'kyi, V.; Gackiere, F.; Firllej, V.; Vandenberghe, M.; Roudbaraki, M.; Gkika, D.; Pourtier, A.; Bidaux, G.; Slomianny, C.; et al. Role of cationic channel TRPV2 in promoting prostate cancer migration and progression to androgen resistance. *Cancer Res.* **2010**, *70*, 1225–1235. [[CrossRef](#)] [[PubMed](#)]
36. Landreh, L.; Spinnler, K.; Schubert, K.; Hakkinen, M.R.; Auriola, S.; Poutanen, M.; Soder, O.; Svechnikov, K.; Mayerhofer, A. Human testicular peritubular cells host putative stem Leydig cells with steroidogenic capacity. *J. Clin. Endocrinol. Metab.* **2014**, *99*, E1227–E1235. [[CrossRef](#)] [[PubMed](#)]
37. Baggiolini, M.; Walz, A.; Kunkel, S.L. Neutrophil-activating peptide-1/interleukin 8, a novel cytokine that activates neutrophils. *J. Clin. Investig.* **1989**, *84*, 1045–1049. [[CrossRef](#)] [[PubMed](#)]
38. Baggiolini, M.; Clark-Lewis, I. Interleukin-8, a chemotactic and inflammatory cytokine. *FEBS Lett.* **1992**, *307*, 97–101. [[CrossRef](#)]
39. Kobayashi, Y. The role of chemokines in neutrophil biology. *Front. Biosci.* **2008**, *13*, 2400–2407. [[CrossRef](#)] [[PubMed](#)]
40. Moser, B.; Schumacher, C.; von Tscharnner, V.; Clark-Lewis, I.; Baggiolini, M. Neutrophil-activating peptide 2 and gro/melanoma growth-stimulatory activity interact with neutrophil-activating peptide 1/interleukin 8 receptors on human neutrophils. *J. Biol. Chem.* **1991**, *266*, 10666–10671. [[PubMed](#)]
41. Moser, B.; Barella, L.; Mattei, S.; Schumacher, C.; Boulay, F.; Colombo, M.P.; Baggiolini, M. Expression of transcripts for two interleukin 8 receptors in human phagocytes, lymphocytes and melanoma cells. *Biochem. J.* **1993**, *294 Pt 1*, 285–292. [[CrossRef](#)]
42. Castro, P.; Xia, C.; Gomez, L.; Lamb, D.J.; Ittmann, M. Interleukin-8 expression is increased in senescent prostatic epithelial cells and promotes the development of benign prostatic hyperplasia. *Prostate* **2004**, *60*, 153–159. [[CrossRef](#)] [[PubMed](#)]
43. Khadra, A.; Fletcher, P.; Luzzi, G.; Shattock, R.; Hay, P. Interleukin-8 levels in seminal plasma in chronic prostatitis/chronic pelvic pain syndrome and nonspecific urethritis. *BJU Int.* **2006**, *97*, 1043–1046. [[CrossRef](#)] [[PubMed](#)]
44. Lotti, F.; Maggi, M. Interleukin 8 and the male genital tract. *J. Reprod. Immunol.* **2013**, *100*, 54–65. [[CrossRef](#)] [[PubMed](#)]

45. Meineke, V.; Frungieri, M.B.; Jessberger, B.; Vogt, H.; Mayerhofer, A. Human testicular mast cells contain tryptase: Increased mast cell number and altered distribution in the testes of infertile men. *Fertil. Steril.* **2000**, *74*, 239–244. [[CrossRef](#)]
46. Frungieri, M.B.; Calandra, R.S.; Lustig, L.; Meineke, V.; Kohn, F.M.; Vogt, H.J.; Mayerhofer, A. Number, distribution pattern, and identification of macrophages in the testes of infertile men. *Fertil. Steril.* **2002**, *78*, 298–306. [[CrossRef](#)]
47. Li, A.; Dubey, S.; Varney, M.L.; Dave, B.J.; Singh, R.K. IL-8 directly enhanced endothelial cell survival, proliferation, and matrix metalloproteinases production and regulated angiogenesis. *J. Immunol.* **2003**, *170*, 3369–3376. [[CrossRef](#)] [[PubMed](#)]
48. Brat, D.J.; Bellail, A.C.; Van Meir, E.G. The role of interleukin-8 and its receptors in gliomagenesis and tumoral angiogenesis. *Neuro. Oncol.* **2005**, *7*, 122–133. [[CrossRef](#)] [[PubMed](#)]
49. Koch, A.E.; Polverini, P.J.; Kunkel, S.L.; Harlow, L.A.; DiPietro, L.A.; Elner, V.M.; Elner, S.G.; Strieter, R.M. Interleukin-8 as a macrophage-derived mediator of angiogenesis. *Science* **1992**, *258*, 1798–1801. [[CrossRef](#)] [[PubMed](#)]
50. Szekanecz, Z.; Shah, M.R.; Harlow, L.A.; Pearce, W.H.; Koch, A.E. Interleukin-8 and tumor necrosis factor- α are involved in human aortic endothelial cell migration. The possible role of these cytokines in human aortic aneurysmal blood vessel growth. *Pathobiology* **1994**, *62*, 134–139. [[CrossRef](#)] [[PubMed](#)]
51. Wang, J.; Wang, Y.; Wang, S.; Cai, J.; Shi, J.; Sui, X.; Cao, Y.; Huang, W.; Chen, X.; Cai, Z.; et al. Bone marrow-derived mesenchymal stem cell-secreted IL-8 promotes the angiogenesis and growth of colorectal cancer. *Oncotarget* **2015**, *6*, 42825–42837. [[CrossRef](#)] [[PubMed](#)]
52. Xie, K. Interleukin-8 and human cancer biology. *Cytokine Growth Factor Rev.* **2001**, *12*, 375–391. [[CrossRef](#)]
53. Windschuttl, S.; Kampfner, C.; Mayer, C.; Flenkenthaler, F.; Frohlich, T.; Schwarzer, J.U.; Kohn, F.M.; Urbanski, H.; Arnold, G.J.; Mayerhofer, A. Human testicular peritubular cells secrete pigment epithelium-derived factor (PEDF), which may be responsible for the avascularity of the seminiferous tubules. *Sci. Rep.* **2015**, *5*, 12820. [[CrossRef](#)] [[PubMed](#)]
54. Lucke, C.; Siebert, S.; Mayr, D.; Mayerhofer, A. Connexin expression by human granulosa cell tumors: Identification of connexin 32 as a tumor signature. *Cancer Biomark. Sect. Dis. Mark.* **2010**, *8*, 137–144. [[CrossRef](#)] [[PubMed](#)]
55. Pfaffl, M.W. A new mathematical model for relative quantification in real-time RT-PCR. *Nucleic Acids Res.* **2001**, *29*, e45. [[CrossRef](#)] [[PubMed](#)]
56. Rossi, S.P.; Windschuttl, S.; Matzkin, M.E.; Rey-Ares, V.; Terradas, C.; Ponzio, R.; Puigdomenech, E.; Levalle, O.; Calandra, R.S.; Mayerhofer, A.; et al. Reactive oxygen species (ROS) production triggered by prostaglandin D2 (PGD2) regulates lactate dehydrogenase (LDH) expression/activity in TM4 Sertoli cells. *Mol. Cell. Endocrinol.* **2016**, *434*, 154–165. [[CrossRef](#)] [[PubMed](#)]
57. Leffler, A.; Linte, R.M.; Nau, C.; Reeh, P.; Babes, A. A high-threshold heat-activated channel in cultured rat dorsal root ganglion neurons resembles TRPV2 and is blocked by gadolinium. *Eur. J. Neurosci.* **2007**, *26*, 12–22. [[CrossRef](#)] [[PubMed](#)]
58. Schindelin, J.; Arganda-Carreras, I.; Frise, E.; Kaynig, V.; Longair, M.; Pietzsch, T.; Preibisch, S.; Rueden, C.; Saalfeld, S.; Schmid, B.; et al. Fiji: an open-source platform for biological-image analysis. *Nat. Methods* **2012**, *9*, 676–682. [[CrossRef](#)] [[PubMed](#)]
59. Huang, Y.; Jiang, H.; Chen, Y.; Wang, X.; Yang, Y.; Tao, J.; Deng, X.; Liang, G.; Zhang, H.; Jiang, W.; et al. Tranilast directly targets NLRP3 to treat inflammasome-driven diseases. *EMBO Mol. Med.* **2018**, *10*. [[CrossRef](#)] [[PubMed](#)]



3.2 Publication II

Exploring the Ion Channel TRPV2 and Testicular Macrophages in Mouse Testis.

Katja Eubler, Pia Rantakari, Heidi Gerke, Carola Herrmann, Annika Missel, Nina Schmid, Lena Walenta, Shibojyoti Lahiri, Axel Imhof, Leena Strauss, Matti Poutanen & Artur Mayerhofer

International Journal of Molecular Sciences, April 2021, 22 (9): 4727

doi: 10.3390/ijms22094727

The cation channel TRPV2 is known to be expressed by murine macrophages and is crucially involved in their functionality. Macrophages are frequent cells of the mouse testis, an immune-privileged and steroid-producing organ. TRPV2 expression by testicular macrophages and possible changes associated with age or inflammation have not been investigated yet. Therefore, we studied testes of young adult and old wild-type (WT) and AROM⁺ mice, i.e., transgenic mice overexpressing aromatase. In these animals, inflammatory changes are described in the testis, involving active macrophages, which increase with age. This is associated with impaired spermatogenesis and therefore AROM⁺ mice are a model for male infertility associated with sterile inflammation. In WT animals, testicular TRPV2 expression was mapped to interstitial CD206⁺ and peritubular MHC II⁺ macrophages, with higher levels in CD206⁺ cells. Expression levels of TRPV2 and most macrophage markers did not increase significantly in old mice, with the exception of CD206. As the amount of TRPV2⁺ testicular macrophages was relatively small, their possible involvement in testicular functions and in aging in WT mice remains to be further studied. In AROM⁺ testis, TRPV2 was readily detected and levels increased significantly with age, together with macrophage markers and TNF- α . TRPV2 co-localized with F4/80 in macrophages and further studies showed that TRPV2 is mainly expressed by unusual CD206⁺ MHC II⁺ macrophages, arising in the testis of these animals. Rescue experiments (aromatase inhibitor treatment and crossing with ER α KO mice) restored the testicular phenotype and also abolished the elevated expression of TRPV2, macrophage and inflammation markers. This suggests that TRPV2⁺ macrophages of the testis are part of an inflammatory cascade initiated by an altered sex hormone balance in AROM⁺ mice.

The changes in testes are distinct from the described alterations in other organs of AROM⁺, such as prostate and spleen. When we monitored TRPV2 levels in another immune-privileged organ, namely the brain, we found that levels of TRPV2 were not elevated in AROM⁺ and remained stable during aging. In the adrenal, which similar to the testis produces steroids, we found slight, albeit not significant increases in TRPV2 in both AROM⁺ and WT mice, which were associated with age. Thus, the changes in the testis are specific for this organ.



Article

Exploring the Ion Channel TRPV2 and Testicular Macrophages in Mouse Testis

Katja Eubler ¹, Pia Rantakari ², Heidi Gerke ², Carola Herrmann ¹, Annika Missel ¹, Nina Schmid ¹, Lena Walenta ¹, Shibojyoti Lahiri ³ , Axel Imhof ³, Leena Strauss ^{4,5}, Matti Poutanen ^{4,5} and Artur Mayerhofer ^{1,*}

¹ Cell Biology-Anatomy III, Biomedical Center Munich (BMC), Faculty of Medicine, Ludwig-Maximilian-University (LMU), D-82152 Planegg-Martinsried, Germany; katja.eubler@bmc.med.lmu.de (K.E.); carola.herrmann@bmc.med.lmu.de (C.H.); annika.missel@bmc.med.lmu.de (A.M.); nina.schmid@bmc.med.lmu.de (N.S.); lena.walenta@gmail.com (L.W.)

² Turku Bioscience Center, University of Turku and Åbo Akademi University, FI-20300 Turku, Finland; piaranta@utu.fi (P.R.); hmsulo@utu.fi (H.G.)

³ Protein Analysis Unit, Biomedical Center Munich (BMC), Faculty of Medicine, Ludwig-Maximilian-University (LMU), D-82152 Planegg-Martinsried, Germany; Shibojyoti.Lahiri@med.uni-muenchen.de (S.L.); aimhof@med.uni-muenchen.de (A.I.)

⁴ Research Center for Integrative Physiology and Pharmacology, Institute of Biomedicine, University of Turku, FI-20300 Turku, Finland; leesal@utu.fi (L.S.); matpou@utu.fi (M.P.)

⁵ Turku Center for Disease Modeling, Institute of Biomedicine, University of Turku, FI-20300 Turku, Finland

* Correspondence: mayerhofer@bmc.med.lmu.de; Tel.: +49-89-218075859



Citation: Eubler, K.; Rantakari, P.; Gerke, H.; Herrmann, C.; Missel, A.; Schmid, N.; Walenta, L.; Lahiri, S.; Imhof, A.; Strauss, L.; et al. Exploring the Ion Channel TRPV2 and Testicular Macrophages in Mouse Testis. *Int. J. Mol. Sci.* **2021**, *22*, 4727. <https://doi.org/10.3390/ijms22094727>

Academic Editor: Karel Talavera

Received: 8 April 2021

Accepted: 26 April 2021

Published: 29 April 2021

Publisher's Note: MDPI stays neutral with regard to jurisdictional claims in published maps and institutional affiliations.



Copyright: © 2021 by the authors. Licensee MDPI, Basel, Switzerland. This article is an open access article distributed under the terms and conditions of the Creative Commons Attribution (CC BY) license (<https://creativecommons.org/licenses/by/4.0/>).

Abstract: The cation channel TRPV2 is known to be expressed by murine macrophages and is crucially involved in their functionality. Macrophages are frequent cells of the mouse testis, an immune-privileged and steroid-producing organ. TRPV2 expression by testicular macrophages and possible changes associated with age or inflammation have not been investigated yet. Therefore, we studied testes of young adult and old wild-type (WT) and AROM⁺ mice, i.e., transgenic mice overexpressing aromatase. In these animals, inflammatory changes are described in the testis, involving active macrophages, which increase with age. This is associated with impaired spermatogenesis and therefore AROM⁺ mice are a model for male infertility associated with sterile inflammation. In WT animals, testicular TRPV2 expression was mapped to interstitial CD206⁺ and peritubular MHC II⁺ macrophages, with higher levels in CD206⁺ cells. Expression levels of TRPV2 and most macrophage markers did not increase significantly in old mice, with the exception of CD206. As the number of TRPV2⁺ testicular macrophages was relatively small, their possible involvement in testicular functions and in aging in WT mice remains to be further studied. In AROM⁺ testis, TRPV2 was readily detected and levels increased significantly with age, together with macrophage markers and TNF- α . TRPV2 co-localized with F4/80 in macrophages and further studies showed that TRPV2 is mainly expressed by unusual CD206⁺MHC II⁺ macrophages, arising in the testis of these animals. Rescue experiments (aromatase inhibitor treatment and crossing with ER α KO mice) restored the testicular phenotype and also abolished the elevated expression of TRPV2, macrophage and inflammation markers. This suggests that TRPV2⁺ macrophages of the testis are part of an inflammatory cascade initiated by an altered sex hormone balance in AROM⁺ mice. The changes in testis are distinct from the described alterations in other organs of AROM⁺, such as prostate and spleen. When we monitored TRPV2 levels in another immune-privileged organ, namely the brain, we found that levels of TRPV2 were not elevated in AROM⁺ and remained stable during aging. In the adrenal, which similar to the testis produces steroids, we found slight, albeit not significant increases in TRPV2 in both AROM⁺ and WT mice, which were associated with age. Thus, the changes in the testis are specific for this organ.

Keywords: TRPV2; testis; macrophages; aging; inflammation; AROM⁺; infertility

1. Introduction

Transgenic mice overexpressing aromatase (AROM⁺) have been studied for many years [1–3]. The hormonal imbalance in these animals causes immunological changes and, in some organs, inflammation. A recent paper described higher plasma immunoglobulin levels, mainly IgE, in AROM⁺ mice and distinct changes in the enlarged spleen [4]. The analysis of splenocytes revealed changes in the ratio of mature/immature B cells and increased IgE synthesis after IgE class-switching. Inflammatory changes in two organs were described, namely in the prostate and testis. In prostate, inflammation (prostatitis) and pre-malignant changes were found and occurred in an age-dependent manner [5]. In the inflammatory lesions several immune cell types, including mast cells, neutrophils, T-lymphocytes, and F4/80⁺ macrophages were present. In testis of AROM⁺, the most striking observations were the age-dependent increase in testicular macrophages positive for CD68, elevated TNF- α levels, and the parallel decline in spermatogenesis [1,2,6,7]. The changes became detectable at about 2 months of age and further increased with age. Of note, in many cases of human idiopathic male infertility due to impaired spermatogenesis, massive increases in testicular macrophage numbers, defined by the expression of CD68, occur, as well [8]. This and other similar changes led to the assumption that AROM⁺ mice are a model for human male infertility associated with sterile inflammation [9].

Tissue-resident macrophages of the testis have mainly been studied in rodents, and these studies indicated that macrophages normally participate in a broad spectrum of testis-specific functions, i.e., regulation of vascularization and morphogenesis [10], support of Leydig cell function [11], differentiation of spermatogonia [12], and maintenance of the immune privilege [13,14]. Macrophages are typically classified into inflammatory-activated (M1) and alternatively activated immunosuppressive macrophages (M2). M1 macrophages secrete proinflammatory mediators including large amounts of the proinflammatory cytokine TNF- α . M2 macrophages are essential for tissue homeostasis, immune surveillance, and inflammation resolution and secrete low amounts of TNF- α [15]. For rodent testicular macrophages a polarization towards the immunoregulatory and immunotolerant M2 phenotype is typical. However, it is becoming clear that this state is not fixed and that the local environment governs the polarization of testicular macrophages [16]. Such regulatory influences play a role in inflammation and possibly also in aging of the testis. The last-mentioned point is not well known, but changes in testicular macrophage numbers during aging have been reported in rodents [17].

From a developmental point of view, the murine testis normally contains two different populations of macrophages, which have their origin predominantly in the fetal liver, as just very recently demonstrated [18]. Already at birth, a testicular compartment, i.e., the interstitial space is occupied by CD206⁺MHC II⁻ macrophages, whereas CD206⁻MHC II⁺ ones surround the seminiferous tubules. Furthermore, a new study showed that after radiation or during infection, bone marrow-derived circulating monocytes are recruited to the testis and give rise to inflammatory macrophages which then promote tissue damage [19]. Hence, testicular macrophages can be heterogeneous.

The family of transient receptor potential (TRP) channels consists of a large group of rather ubiquitously expressed ion channels with a broad spectrum of functions and activating stimuli and is further divided into nine subfamilies (TRPA, TRPC, TRPM, TRPML, TRPN, TRPP, TRPS, TRPV, TRPVL), each comprising members with structural homology. All these channels have in common a relatively non-selective permeability for cations and all are regarded to act as molecular sensors. Among these channels, the transient receptor potential channel subfamily V member 2 (TRPV2) remains one of the least known channels [20]. It was considered as a thermal sensor for noxious heat > 50 °C [21] for a long time, however, TRPV2 has a much more complex physiology and properties, as demonstrated by knock-out mice [22]. Furthermore, the properties strongly depend on the species and cell type [23]. The known modulators include, in addition to noxious heat, Δ^9 -tetrahydrocannabinol (THC), cannabidiol (CBD), and 2-amino-ethoxydiphenyl borat (2-APB), acting as activators [24,25], and tranilast and ruthenium red, which represent

antagonists [26,27], respectively. Yet all of these modulators lack specificity for TRPV2. Only very recently, it could be demonstrated that oxidation of a methionine residue within the structure of TRPV2 by reactive oxygen species (ROS), such as H₂O₂, or ultraviolet A light leads to activation and sensitization of TRPV2 [28], giving rise to endogenous regulatory mechanisms.

TRPV2 is reported to be expressed in different organs, including the brain [29], pancreas [30], muscle [31], spleen [21], and other immune-related tissues [32]. In the last decades, TRPV2 has been described to be crucially involved in innate and adaptive immunity and has been found in several cell types of the immune system in both human and mouse, i.e., in macrophages and osteoclasts, mast cells, granulocytes, monocytes, and also in T-lymphocytes [33–36]. In most of these cells, TRPV2 is essential for migration and it appears to be irreplaceable for differentiation of osteoclasts [37] or degranulation of mast cells [33,36].

In macrophages, TRPV2 is essential for phagocytosis and chemotaxis [34,35,38]. TRPV2-deficient mice exhibit a higher bacterial load and increased mortality [22]. TRPV2 expression in macrophages was mainly demonstrated for resident populations, e.g., of brain, liver, skin, lung, and bone [39,40]. While a sizable number of organs and their respective macrophages were analyzed, the testis and in particular testicular macrophages have not been studied.

This paucity of information led us to perform this study. We examined, whether TRPV2 is expressed by mouse testicular macrophages, attempted to define the macrophage subtype by flow cytometry and studied, whether levels may change in old animals. Since TRPV2 is associated with inflammation we specifically focused on the testis of AROM⁺ mice [1,2]. Additionally, the testicular tissue from known successful rescue experiments, i.e., treatment with an aromatase inhibitor [6] and crossbreeding with ER α KO animals [41,42], were included in this study to gain insights into the regulation of TRPV2. Finally, we explored the expression of TRPV2 in the murine adrenal, i.e., an organ of steroid production, similar to the testis, and TRPV2 levels in the brain, which is similar to the testis, an immune-privileged organ.

2. Results

2.1. Testicular Expression of TRPV2, Macrophage and Inflammation Markers in Young and Old WT Mice

Whole testes lysates of young (2–3 months, $n = 21$) and old WT mice (6–8 months, $n = 9$) were subjected to a detailed analysis employing quantitative RT-PCR and Western blotting. Next to TRPV2 and NOX2, we examined macrophage and inflammation markers. Testicular sections were further investigated by means of TRPV2 in situ hybridization and immunohistochemistry. In addition, we incubated the testicular tissue with cannabidiol (CBD), known to activate TRPV2, and screened for consequences of activation of TRPV2.

TRPV2 was detected at the mRNA level in young and old mice, and a slight, although not statistically significant increase of TRPV2 levels was found in old animals (Figure 1A). Immunoblotting did not reveal changes in TRPV2 level with increasing age (Figure 1B). Levels of the ROS generating enzyme NOX2 were slightly but not significantly higher in older animals (Figure 1A).

When testicular sections of both young (2 months, Figure S1A) and even older, 10 month-old, WT animals were examined by TRPV2 in situ hybridization (Figure 1C), we observed a distinct localization in the interstitial space (arrows) and within or in close proximity to the peritubular wall of seminiferous tubules (arrow heads).

Based on a detailed quantitative RT-PCR analysis, levels of all investigated macrophage markers, i.e., CD54, CD68, CD74, and CD206, remained unchanged in old WT animals (Figure 1D), as well as the examined markers for inflammation, i.e., CXCL-1, TIMP-1, and TNF- α (Figure 1E).

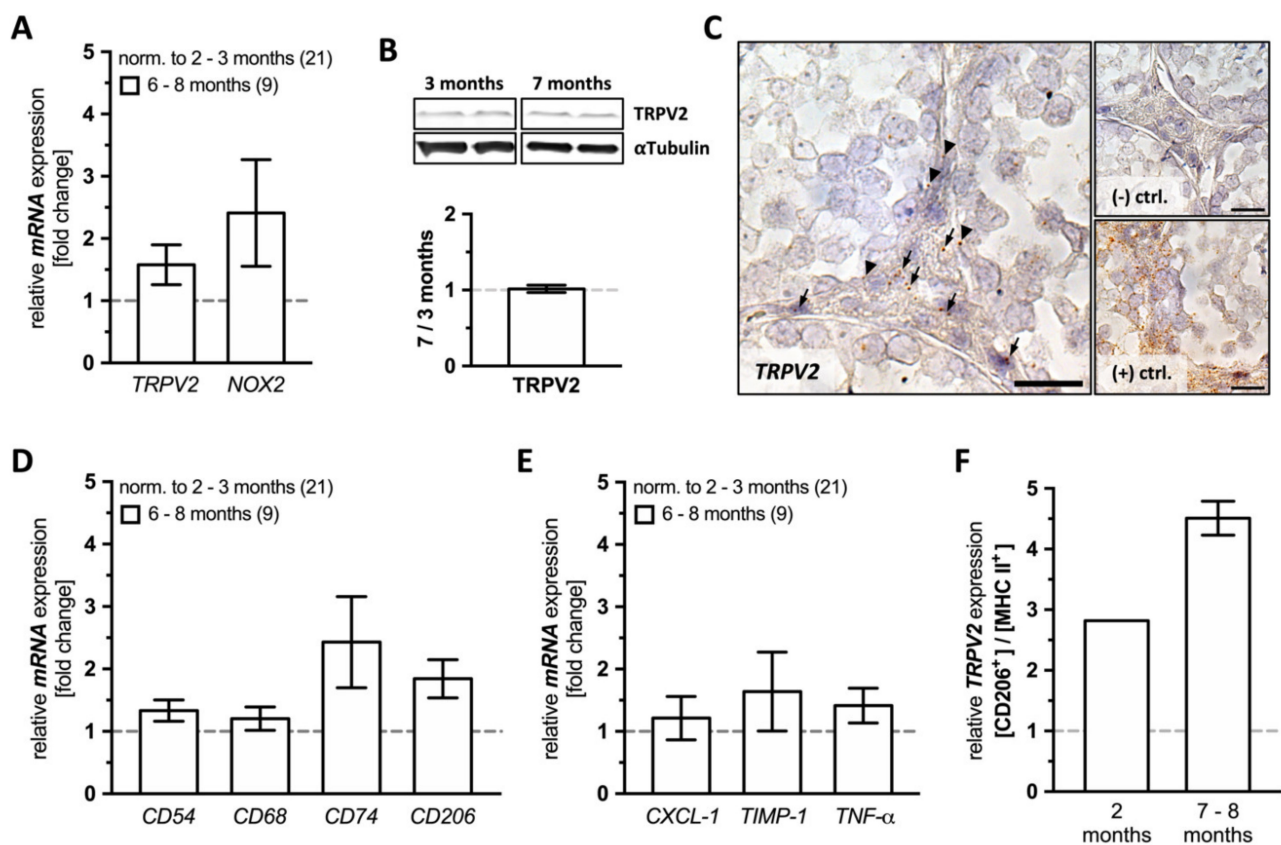


Figure 1. Expression profile of *TRPV2*, *NOX2*, macrophage and inflammation markers in WT testes. (A) Relative mRNA expression levels of *TRPV2* and *NOX2* in whole testes of old WT mice, normalized to young animals. Levels were not significantly different (*TRPV2*: 1.578 ± 0.319 , $p = 0.3505$; *NOX2*: 2.412 ± 0.856 , $p = 0.2802$). (B) *TRPV2* immunoblotting of young (3 months, $n = 2$) and old WT testes (7 months, $n = 2$) showed weak bands (~ 63 kDa) for both ages and quantification revealed a mean expression level in old WT testis of 1.016 ± 0.049 , compared to young ones. Staining for α Tubulin was used as a loading control. (C) Testicular sections of 10 month-old WT mice subjected to *TRPV2* in situ hybridization showed punctuated staining mainly in the interstitial space (arrows) with few spots at the peritubular walls (arrow heads; left panel). The negative control (upper right panel, (-) ctrl.) showed no signals, but the positive control (lower right panel, (+) ctrl.) did. Scale bar is $50 \mu\text{M}$. (D,E) Relative mRNA expression levels of (D) macrophage markers (*CD54*: 1.332 ± 0.172 , $p = 0.1157$; *CD68*: 1.205 ± 0.188 , $p = 0.8506$; *CD74*: 2.430 ± 0.732 , $p = 0.2402$; *CD206*: 1.843 ± 0.305 , $p = 0.0589$) and (E) inflammation markers (*CXCL-1*: 1.214 ± 0.348 , $p = 0.6767$; *TIMP-1*: 1.638 ± 0.633 , $p = 0.7160$; *TNF-α*: 1.416 ± 0.279 , $p = 0.5198$) in whole testes of old WT mice normalized to young animals. (A,D,E) The graphs represent mean \pm SEM of old WT mice (6–8 months, $n = 9$) normalized to young animals (2–3 months, $n = 21$); unpaired two-tailed *t*-test, $\alpha = 0.05$. (F) Testicular macrophages from young (2 months, $n = 1$, pool of three animals) and old WT mice (7–8 months, $n = 2$, pool of three animals each) sorted for their CD206 and MHC II expression by FACS were subjected to mRNA extraction and quantitative RT-PCR for *TRPV2* expression. The graphs represent mean \pm SEM.

To further characterize the macrophage subpopulation(s) expressing *TRPV2*, testicular macrophages were isolated and subjected to FACS for expression of CD206 and MHC II and then scanned for *TRPV2* expression by quantitative RT-PCR (Figure 1F). In both young and old WT animals, CD206⁺ macrophages showed numerically higher *TRPV2* expression levels compared to MHC II⁺ ones (young: 2.820; old: 4.510 ± 0.280). This result suggests that predominantly interstitial macrophages express *TRPV2*, at least at the mRNA level (Figure 1C,F).

Since there was no change in *TRPV2* expression in older animals, consequences of *TRPV2* activation were explored in an organotypic incubation with testicular tissue from young WT mice (2–3 months, $n = 6$). The testicular tissue was pre-incubated with cannabinoid receptor 1 (CB1) and 2 (CB2) blockers, AM351 (80 nM) and AM630 (800 nM), respectively, for 1 h and then exposed to CBD (30 μM) for 6 h.

Using a proteome profiler, a 2.596-fold higher CXCL-1 level could be detected in the supernatant of CBD treated tissue (4031.422 signal density/ μg RNA) compared to the control tissue (1553.138 signal density/ μg RNA) and an albeit weak signal for IFN- γ was found exclusively in the CBD-treated tissue supernatant (128.919 signal density/ μg RNA; Figure S1B, upper panel).

A detailed quantitative RT-PCR analysis performed with mRNA isolated from the individual tissue pieces revealed significantly higher levels of CXCL-1 (1.767 ± 0.326 , $p = 0.0493$), CXCL-2 (1.807 ± 0.334 , $p = 0.0180$), and IL-6 (1.697 ± 0.174 , $p = 0.0066$) upon exposure to 30 μM CBD, whereas CD54, COX2, IL-1 β , MCP-1, TIMP-1, TNF- α , and TRPV2 remained unchanged (Figure S1B, lower panel).

2.2. TRPV2, Macrophage and Inflammation Markers in Testes from Young and Old AROM⁺ Mice

In the testes of AROM⁺ animals, TRPV2 was readily detected already in young adults, as shown by several methods. Testicular sections of both young (2 months, Figure S2) and old AROM⁺ mice (10 months) were subjected to TRPV2 in situ hybridization. The results showed strong punctuated staining in the interstitial space, indicating that TRPV2 is present in large cells (Figure 2A). Immunohistochemistry using antibodies against the murine macrophage marker F4/80 (left panel) and TRPV2 (right panel) was also performed on consecutive sections from old AROM⁺ animals (10 months). Immunoreactive signals indicate the co-localization of the two proteins and support the fact that testicular macrophages express TRPV2 in AROM⁺ mice (Figure 2B).

Protein extracted from whole testis lysates of both young (3 months, $n = 2$) and old AROM⁺ animals (7 months, $n = 2$) further confirmed the increase in TRPV2 amount (1.987 ± 0.378 ; Figure 2C).

Comparing young (2–3 months, $n = 21$) and old AROM⁺ mice testes (6–8 months, $n = 15$) by means of quantitative RT-PCR showed that levels of both TRPV2 (3.375 ± 0.257 , $p \leq 0.0001$) and NOX2 (6.283 ± 1.114 , $p \leq 0.0001$) presented highly significant increases with age (Figure 2D).

Moreover, we found a highly significant increase for all investigated macrophage markers (CD54: 2.521 ± 0.415 , $p = 0.0010$; CD68: 6.318 ± 1.580 , $p \leq 0.0001$; CD74: 9.838 ± 2.292 , $p \leq 0.0001$; CD206: 3.377 ± 0.669 , $p = 0.0002$; Figure 2E), and, as expected, also TNF- α (5.341 ± 1.158 , $p \leq 0.0001$) and TIMP-1 (4.307 ± 1.205 , $p = 0.0292$) were significantly increased. However, CXCL-1 was not changed (Figure 2F).

2.3. TRPV2, Macrophage and Inflammation Markers in a Genotypic Comparison

For a better appreciation of the differences between the observed findings in testes from young and old WT and AROM⁺ mice, on the one hand, quantitative RT-PCR datasets were re-analyzed comparing coeval animals of both genotypes (Figure S3) and on the other hand, datasets of proteomes from both WT and AROM⁺ testes of 11 month-old animals subjected to mass spectrometry were re-analyzed and screened for macrophage and inflammation markers, TRPV2 and ROS generating enzymes (Figure 3).

In testes from young AROM⁺ animals, TRPV2 mRNA expression levels were found to be significantly higher compared to coeval WT mice (2.464 ± 0.365 , $p = 0.0029$), and the difference between the two genotypes was further strongly augmented with the increasing age (5.217 ± 0.397 , $p \leq 0.0001$). In terms of testicular NOX2, there were significantly higher levels of the ROS producing enzyme in AROM⁺ mice compared to coeval WT mice (Figure S3A), both in young (3.049 ± 0.602 , $p = 0.0210$) and old animals (8.604 ± 1.526 , $p \leq 0.0001$).

Comparison of macrophage marker expression levels in testes from young WT and AROM⁺ animals revealed significantly higher levels of CD54 (2.772 ± 0.431 , $p \leq 0.0001$) and CD68 (3.441 ± 0.304 , $p \leq 0.0001$), but not of CD74 and CD206. However, in old animals all analyzed macrophage markers showed significantly higher expression levels in AROM⁺ animals compared to coeval WT mice (CD54: 4.062 ± 0.539 , $p \leq 0.0001$; CD68:

$18.610 \pm 4.654, p \leq 0.0001$; $CD74: 6.488 \pm 1.511, p = 0.0022$; $CD206: 2.399 \pm 0.475, p = 0.0176$; Figure S3B).

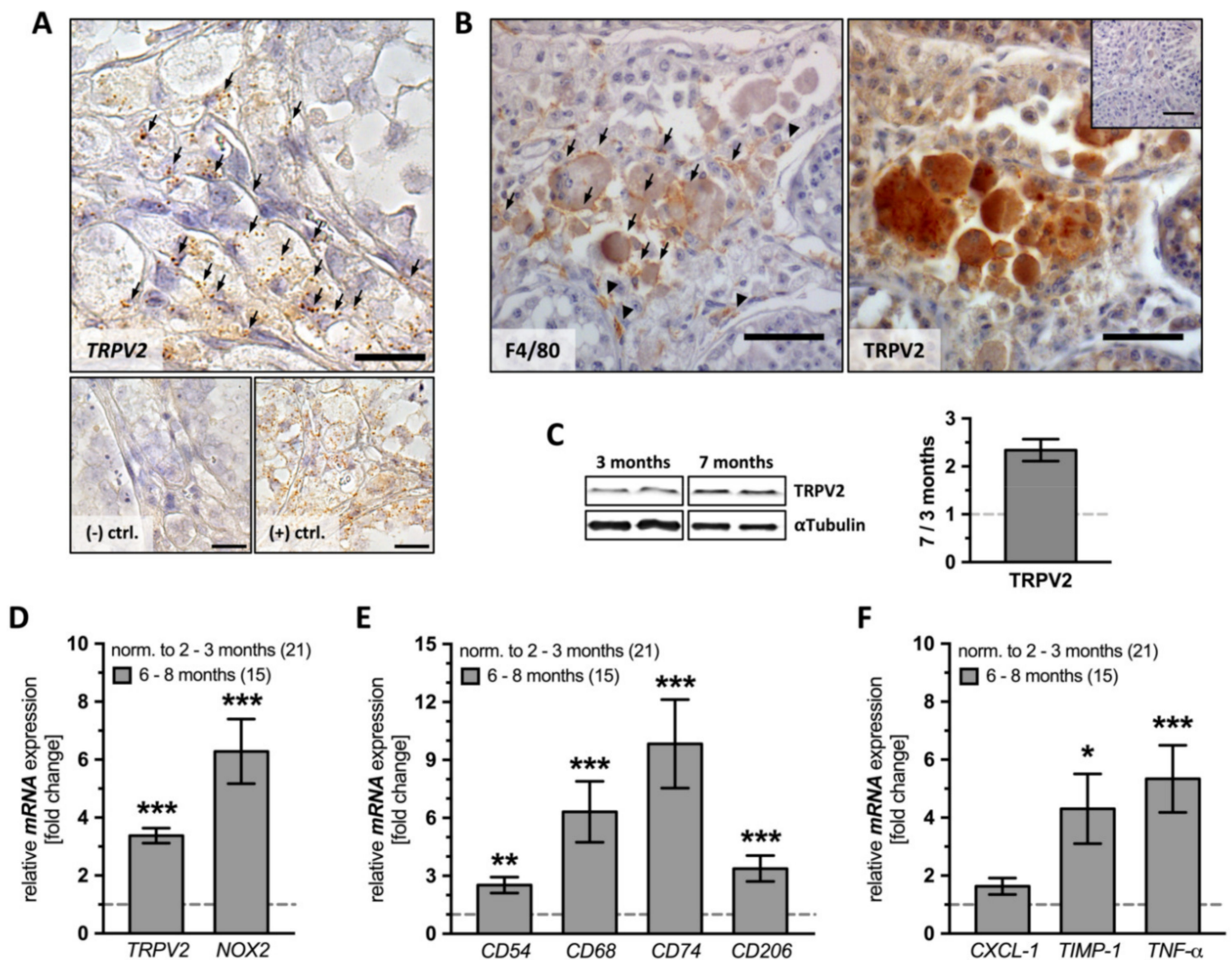


Figure 2. Expression profile of TRPV2, NOX2, macrophage and inflammation markers in AROM⁺ testes. (A) Testicular sections of 10 month-old AROM⁺ mice subjected to TRPV2 in situ hybridization (upper panel) revealed strong and punctuated staining mainly in the interstitial space (arrows). The negative control (lower left panel, (-) ctrl.) showed no signals, but the positive control (lower right panel, (+) ctrl.) did. Scale bar is 50 μ m. (B) Consecutive testicular sections of 10 month-old AROM⁺ animals subjected to immunohistochemistry using antibodies against the general murine macrophage marker F4/80 (left panel) and TRPV2 (right panel) revealed strong membrane-associated F4/80 staining in normal-sized and hyperplastic cells in the interstitial space (arrows), with some faint staining also within or close to the peritubular wall (arrow heads). TRPV2 showed a strong membrane-associated signal in the interstitial space, in both normal-sized and hyperplastic cells, whereas peritubular walls remained clear of any signal. The insert represents a negative control with the 1st antibody omitted. Scale bar is 50 μ m. (C) TRPV2 immunoblotting of whole testis lysates of young (3 months, $n = 2$) and old AROM⁺ animals (7 months, $n = 2$) showed that bands at the expected size and quantification confirmed increased expression levels on the protein level. α Tubulin was used as a loading control. (D–F) The mRNA of whole testis lysates from young and old AROM⁺ mice was subjected to quantitative RT-PCR to investigate the expression profile of (D) TRPV2 and NOX2, (E) macrophage and (F) inflammation markers revealing highly significant differences except for the inflammation marker CXCL-1 ($1.631 \pm 0.286, p = 0.1034$). The graphs represent the mean \pm SEM of old AROM⁺ mice (6–8 months, $n = 15$) normalized to young animals (2–3 months, $n = 21$); unpaired two-tailed t -test, $\alpha = 0.05$; * $p \leq 0.05$, ** $p \leq 0.01$, *** $p \leq 0.001$.

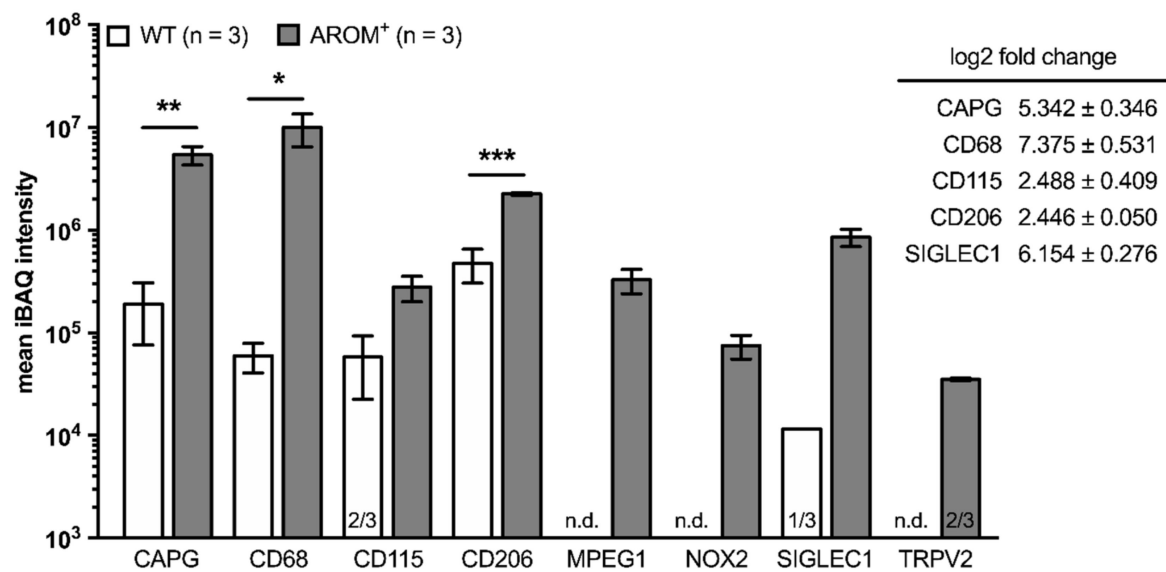


Figure 3. Mass spectrometry-based comparison of expression profiles in old WT and AROM⁺ testes. Extracted proteins from testicular tissue of 11 month-old WT and AROM⁺ animals ($n = 3$, each) were subjected to mass spectrometry. The graph presents iBAQ intensities (mean \pm SEM) of detected proteins and results of statistical analysis of a genotype-dependent comparison when proteins could be detected in all replicates using an unpaired two-tailed t -test with $\alpha = 0.05$; * $p \leq 0.05$, ** $p \leq 0.01$, *** $p \leq 0.001$. The numbers of positive replicates other than 3/3 are depicted at the bottom of each column (n.d.: not detected). The insert on the right depicts the mean differential expression of detected proteins (log₂ fold change) in testes from AROM⁺ animals compared to coeval WT animals, if calculable.

In terms of inflammation markers, already young AROM⁺ animals featured significantly higher *CXCL-1* (2.649 ± 0.319 , $p = 0.0012$), *TIMP-1* (4.787 ± 0.502 , $p \leq 0.0001$) and *TNF- α* expression levels (2.518 ± 0.375 , $p = 0.0057$) compared to coeval WT mice. An observation being even stronger in the old mice of the two genotypes (*CXCL-1*: 5.071 ± 0.889 , $p = 0.0007$; *TIMP-1*: 22.990 ± 6.436 , $p = 0.0002$; *TNF- α* : 9.102 ± 1.973 , $p \leq 0.0001$; Figure S3C), indicates the increasing severity of the inflammatory testicular phenotype with age.

In a recent study [3], proteomes from both WT and AROM⁺ testes of 11 month-old animals ($n = 3$, each) were studied by mass spectrometry and the datasets were screened for macrophage markers, inflammation markers, TRPV2 and ROS generating enzymes (Figure 3). The macrophage markers CAPG, CD68, and CD206 were readily found in all three animals of both genotypes with the mean iBAQ intensities being significantly higher in testes from AROM animals (CAPG: $p = 0.0097$; CD68: $p = 0.0484$; CD206: $p = 0.0007$). In addition, CD115, MPEG1, and SIGLEC1 could be detected in all three analyzed AROM⁺ mice, while in the WT animals CD115 was only present in two out of three animals, SIGLEC1 only in one and MPEG1 was even exclusively found in AROM⁺ mice.

Furthermore, next to MPEG1, both TRPV2 and NOX2, being the only ROS generating enzyme detected within these datasets, were exclusively found in AROM⁺ animals by this experimental approach.

2.4. Flow Cytometry Analysis of Testicular Macrophages from Young WT and AROM⁺ Mice

To obtain an in-depth insight into the true nature of the testicular macrophages being positive for TRPV2, whole testes of young WT and AROM⁺ mice (3 months, $n = 3$ each) were digested, and isolated cells were subjected to the flow cytometry (FACS) analysis. CD45⁺CD11b⁺F4/80⁺ macrophages were further subdivided into four subpopulations based on their CD206 and MHC II expression (CD206⁻MHC II⁻, CD206⁺MHC II⁻, CD206⁻MHC II⁺, CD206⁺MHC II⁺) and sorted (Figure 4A,C).

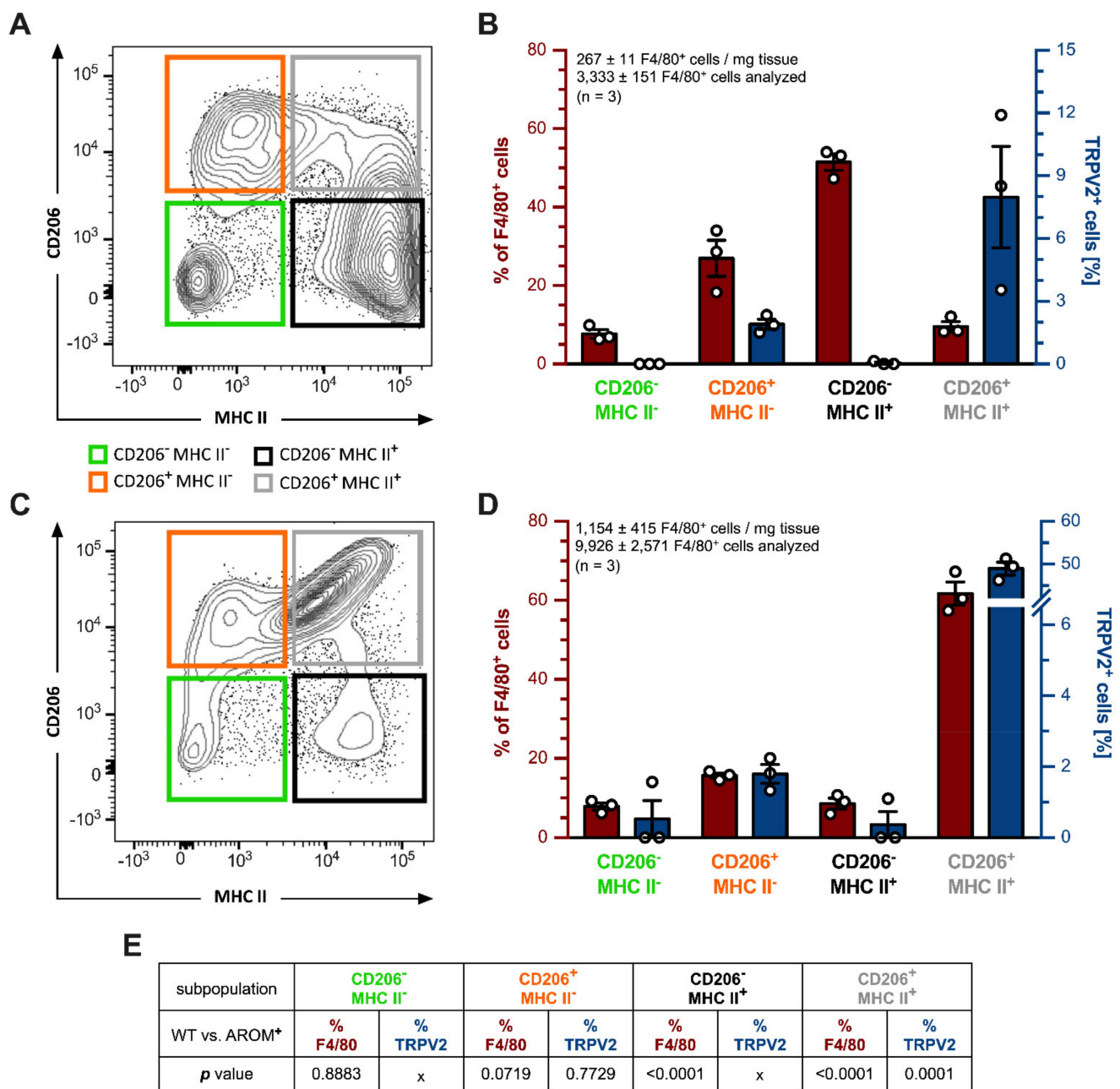


Figure 4. Flow cytometry analysis of testicular macrophage populations of young WT and AROM⁺ mice. Cells from 3 month-old WT and AROM⁺ testes ($n = 3$, each) were isolated, processed for FACS analysis and sorted for macrophage markers (CD45⁺CD11b⁺F4/80⁺), and further divided by CD206 and MHC II expression. TRPV2 expression was quantified within the resulting subpopulations. (A,C) Representative two-dimensional plots of a WT (A) and AROM⁺ animal (C), showing the four subpopulations depending on their CD206 and MHC II expression level (green—CD206⁻MHC II⁻, orange—CD206⁺MHC II⁻, black—CD206⁻MHC II⁺, gray—CD206⁺MHC II⁺). (B,D) Quantitative analyses of testicular macrophage subpopulations in WT and AROM⁺ mice. The percentages of total F4/80⁺ cells (red axis), and TRPV2⁺ cells within these particular subpopulations (blue axis) are shown. The graphs represent mean \pm SEM. (E) Results of statistical analysis (p values) of the particular subpopulations (% of F4/80⁺) and the corresponding percentage of TRPV2⁺ cells (TRPV2⁺ cells [%]) within these subpopulations of WT and AROM⁺ animals, using an unpaired two-tailed t -test, $\alpha = 0.05$, where Gaussian distribution is given and proteins could be detected in all replicates (3/3).

Testes from WT animals ($n = 3$) harbored a total of 267 ± 11 CD45⁺CD11b⁺F4/80⁺ cells per mg tissue and 3333 ± 151 of these cells were subjected to the flow cytometry analysis. The biggest fraction of these cells could be allotted to CD206⁻MHC II⁺ macrophages

($51.470 \pm 2.099\%$), followed by CD206⁺MHC II⁻ ($26.970 \pm 4.605\%$), CD206⁺MHC II⁺ ($9.583 \pm 1.260\%$), and CD206⁻MHC II⁻ ones ($7.677 \pm 1.107\%$; Figure 4B, plotted on the left red axis). Amongst these macrophage subpopulations, the double-positive group of CD206⁺MHC II⁺ macrophages had the highest percentage of TRPV2⁺ cells with $7.893 \pm 2.424\%$ (3/3). CD206⁺MHC II⁻ macrophages harbored $1.903 \pm 0.241\%$ TRPV2⁺ cells (3/3), whereas only in one animal (1/3) 0.140% of CD206⁻MHC II⁺ macrophages were also positive for TRPV2, giving further support to the findings made on mRNA expression levels from sorted macrophages (Figure 1F). The double negative CD206⁻MHC II⁻ subpopulation was bare of any TRPV2⁺ cells (0/0) (Figure 4B, plotted on the right blue axis).

In contrast, testes from AROM⁺ animals ($n = 3$) contained substantially more CD45⁺CD11b⁺F4/80⁺ cells with 1154 ± 415 cells per mg tissue and 9926 ± 2571 cells were subjected to the flow cytometry analysis revealing a drastically shifted distribution of macrophage subpopulations towards the double-positive CD206⁺MHC II⁺ subpopulation with $61.730 \pm 2.924\%$ of all F4/80⁺ cells (Figure 4C), and $48.970 \pm 1.488\%$ of those being also TRPV2⁺ (3/3). The double negative CD206⁻MHC II⁻ subpopulation represented only $7.890 \pm 0.900\%$ of all F4/80⁺ cells with 1.570% being also TRPV2⁺ (1/3). CD206⁺MHC II⁻ macrophages summed up to $15.670 \pm 0.639\%$ and CD206⁻MHC II⁺ subpopulations came to $8.593 \pm 1.375\%$ of total F4/80⁺ cells. Moreover, applying also for AROM⁺ mice, CD206⁺MHC II⁻ macrophages showed more TRPV2⁺ cells with $1.793 \pm 0.263\%$ (3/3) than those macrophages being CD206⁻MHC II⁺ with only 1.100% (1/3), respectively (Figure 4D).

For a comparison between the results obtained from these CD45⁺CD11b⁺F4/80⁺ cells derived from WT and AROM⁺ mice, datasets were statistically analyzed using a two-tailed unpaired *t*-test where Gaussian distribution was given and the corresponding protein could be detected in all three replicates of each group (Figure 4E). In terms of macrophage subpopulation composition (% of F4/80⁺ cells), there was no significant difference in the amount of CD206⁻MHC II⁻ ($p = 0.8883$) and CD206⁺MHC II⁻ ($p = 0.0719$) cells between the two genotypes. However, in AROM⁺ animals there were significantly fewer CD206⁻MHC II⁺ macrophages ($p \leq 0.0001$), but the percentage of the double-positive subpopulation of CD206⁺MHC II⁺ cells was significantly higher in these mice ($p \leq 0.0001$).

Expression of TRPV2 within these macrophage subpopulations (TRPV2⁺ cells [%]) could only be statistically investigated for CD206⁺MHC II⁻ and CD206⁺MHC II⁺ cells, since TRPV2 could be found in all the animals examined. For CD206⁺MHC II⁻ macrophages, there was no significant difference in TRPV2⁺ cells between the two genotypes ($p = 0.7729$), while in AROM⁺ animals the double-positive CD206⁺MHC II⁺ cells included significantly more TRPV2⁺ macrophages ($p = 0.0001$) compared to coeval WT mice.

2.5. TRPV2 in Rescue Experiments of AROM⁺ Mice

In previous studies [6,42], the altered endocrine phenotype of AROM⁺ testis was rescued by administration of an aromatase inhibitor or by cross-breeding with estrogen receptor α knock-out (ER α KO) animals. We examined whether under these conditions elevated TRPV2 and NOX2 but also macrophage and inflammation markers are reverted.

Briefly, 1 month-old WT and AROM⁺ animals were exposed to an aromatase inhibitor (finrozole) or corresponding placebo control (carboxymethyl-cellulose) for 6 weeks and mRNA was isolated from whole testis lysates after sacrifice of the animals for further analysis.

The data revealed that administration of the aromatase inhibitor caused only slight, but partially statistically significant changes in WT animals ($n = 7$), i.e., a slight increase in CD206 mRNA expression (1.825 ± 0.183 , $p = 0.0153$), whereas none of the other investigated markers showed significant changes compared to the placebo-treated WT animals ($n = 7$).

The analysis of placebo-treated AROM⁺ animals ($n = 7$) revealed expected results with significantly increased expression levels of TRPV2 and NOX2, as well as the majority of the macrophage and inflammation markers (TRPV2: 1.692 ± 0.094 , $p = 0.0369$; NOX2: 3.094 ± 0.532 , $p = 0.0078$; CD54: 3.940 ± 0.602 , $p = 0.0211$; CD68: 2.562 ± 0.244 , $p \leq 0.0001$; CD206: 2.113 ± 0.219 , $p = 0.0060$; TIMP-1: 1.722 ± 0.150 , $p = 0.0004$; TNF- α : 4.026 ± 0.841 , $p = 0.0014$). However, CD74 (0.533 ± 0.069 , $p = 0.0323$) was significantly decreased

and *CXCL-1* was indistinguishable from the placebo-treated WT animals (2.185 ± 0.333 , $p = 0.1204$).

The inhibitor treatment had a strong impact on *AROM*⁺ animals ($n = 6$) and, except for *CD206* (1.350 ± 0.172 , $p = 0.0491$), levels of all markers were significantly indistinguishable from the ones of placebo-treated WT (*TRPV2*: 0.867 ± 0.181 , $p = 0.3956$; *NOX2*: 1.731 ± 0.329 , $p = 0.2692$; *CD54*: 2.160 ± 0.332 , $p = 0.1934$; *CD68*: 0.778 ± 0.055 , $p = 0.9942$; *CD74*: 0.863 ± 0.143 , $p = 0.2712$; *CXCL-1*: 0.700 ± 0.122 , $p = 0.3389$; *TIMP-1*: 0.963 ± 0.148 , $p = 0.7161$; *TNF- α* : 1.453 ± 0.402 , $p = 0.6045$; Figure 5A–C).

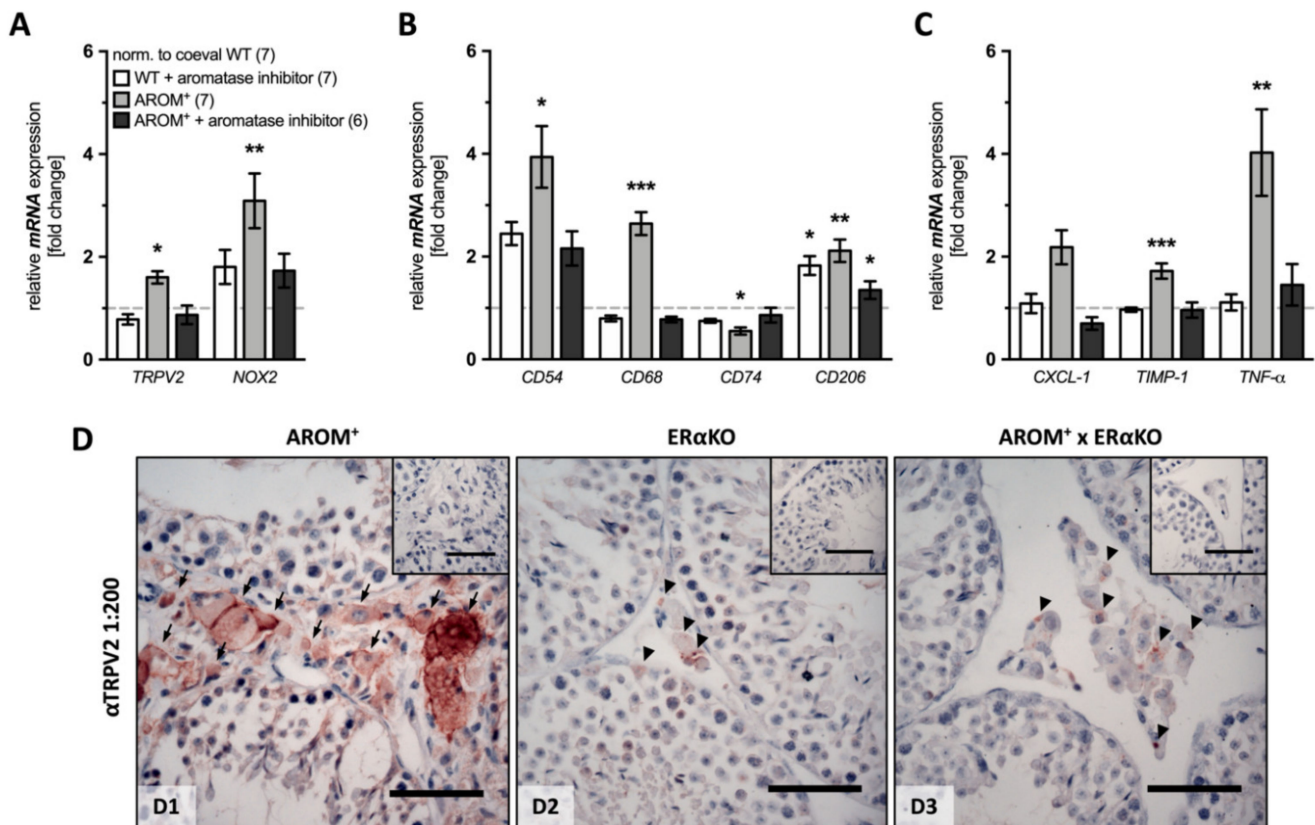


Figure 5. Rescue experiments of *AROM*⁺ mice prevent TRPV2 increases. (A–C) One month-old WT and *AROM*⁺ mice were treated with an aromatase inhibitor or with corresponding placebo for 6 weeks and whole testes were analyzed for their mRNA expression profile of (A) *TRPV2* and *NOX2*, (B) macrophage and (C) inflammation markers. The graphs represent mean \pm SEM of inhibitor-treated WT ($n = 7$, white bars) and *AROM*⁺ mice treated with either placebo ($n = 7$, light grey bars) or aromatase inhibitor ($n = 6$, dark grey bars) compared to coeval placebo-treated WT animals ($n = 7$); unpaired two-tailed t -test, $\alpha = 0.05$; * $p \leq 0.05$, ** $p \leq 0.01$, *** $p \leq 0.001$. (D) Immunohistochemistry for TRPV2 performed on testicular sections from 9 month-old *AROM*⁺ (D1), ER α KO (D2) and *AROM*⁺ mice crossbred with ER α KO mice (D3) revealed strong positive signals in the interstitial space of *AROM*⁺ mice mainly membranous in normal-sized and hyperplastic cells (arrows), but only very weak and faint staining within the interstitial space of ER α KO and in *AROM*⁺ mice crossbred with ER α KO animals, with a rather punctuated pattern (arrow heads). The inserts depict corresponding controls with the omitted 1st antibody. Scale bar is 50 μ m.

As shown before, crossbreeding of *AROM*⁺ mice with mice lacking estrogen receptor α recovered the normal histological appearance of testicular sections without hyperplastic cells in the interstitial space and normal spermatogenesis. In this study, the strong TRPV2-immunoreactive staining in the interstitial space localized to the cellular membrane in 9 month-old *AROM*⁺ animals (Figure 5D-D1), turned to only a weak and punctuated staining in the interstitial space of *AROM*⁺ mice crossed with ER α KO mice (Figure 5D-D3), similar to that observed in ER α KO animals (Figure 5D-D2).

2.6. TRPV2 in Adrenals and Brain

When we explored mRNA levels of *TRPV2* in the adrenal, another steroid-producing organ, from young and old WT and AROM⁺ animals ($n = 3$, each), we found that its levels slightly but not significantly increase with age in both WT (2.597 ± 0.618 , $p = 0.0613$) and in AROM⁺ mice (2.997 ± 1.014 , $p = 0.1203$) compared to the corresponding coeval animals. Expression levels of *TRPV2* in the immune-privileged organ brain, while readily detectable, did not change with age, neither in WT (1.210 ± 0.079 , $p = 0.0573$), nor in AROM⁺ animals (1.277 ± 0.150 , $p = 0.1365$). Taken together, the significantly increased expression levels of TRPV2 in the testis of old AROM⁺ mice (3.141 ± 0.538 , $p = 0.0163$) compared to young ones, in contrast to WT animals showing no changes (1.310 ± 0.241 , $p = 0.2687$), further confirm the testis-specificity of this observation (Figure S5).

3. Discussion

This study describes, for the first time, the expression pattern of the mysterious cation channel TRPV2 in murine testis with special regard to macrophages in the case of WT and the well-established model for male infertility AROM⁺, taking into account age-related changes. The results indicate that although TRPV2 is expressed by testicular macrophages in the WT mouse testis, expression levels are low and hence this channel likely is not to be considered a major factor involved in the regulation of testicular function during adult life and aging. However, the results of the analysis of testes from AROM⁺ animals imply that the population of TRPV2⁺ testicular macrophages massively increases with age induced by a misbalance of estrogen/androgen levels. It is likely that the testicular TRPV2⁺ macrophages are part of an inflammatory cascade in the testes of AROM⁺ and thereby are involved in the development of infertility.

TRPV2 could be detected and localized to interstitial cells of WT mice. However, the levels of TRPV2 were low, and the nature of the positive cells could not be readily identified by in situ hybridization studies. However, FACS isolation and subsequent RT-PCR showed that the TRPV2⁺ cells are mainly interstitial CD206⁺ macrophages rather than peritubular MHC II⁺ macrophages.

Pilot studies, namely the evaluation of organotypic incubations of mouse testes, indicated that in the presence of CB1 and CB2 blockers activation of testicular TRPV2 by CBD caused a detectable pro-inflammatory response, e.g., elevation of CXCL-1. The lack of more specific pharmacological tools, which would allow one to activate or block TRPV2 selectively, prevented us from further studies.

The magnitudes of the expression levels of TRPV2 and all analyzed macrophage or inflammation markers were not statistically significantly different in older WT animals. Of note, expression levels of the superoxide-producing enzyme *NOX2* increased, albeit only numerically with age. It may be a source of ROS, which have recently been described as natural activators and sensitizers of TRPV2 [28]. The role of *NOX2* (and *NOX1*) was also reported to be critical for the differentiation of monocytes to macrophages and the polarization of M2 type but not M1 type macrophages [43]. In immune cells, including macrophages [44], such a mechanism of activation is very likely responsible for the regulation of macrophage functionality. Thus, the macrophage number may increase in the aged rodent testis [17], and their phenotype may undergo alteration, yet an active role of TRPV2 in the testes of old mice requires further investigation.

AROM⁺ testes are characterized, amongst other changes, by increased numbers of macrophages [1]. They have not yet been fully examined but the expression of CD68 and high TNF- α implicate a polarization towards M1 macrophages [15]. The high phagocytotic activity can be concluded from the observation that the macrophages engulf other cells, including Leydig cells [42]. We extended previous studies on this topic. We found that TRPV2 was readily detected in testes of AROM⁺ mice already at young adult ages. A FACS analysis performed with young mice revealed the unique nature of these cells. They constitute a group of CD206⁺MHC II⁺ cells, which is almost absent in normal WT mouse testis. Hence, the hormonal imbalances in the testes of these mice likely had initiated changes

in the macrophage populations, resulting in the acquisition of this unique population. Whether the changes involve recruitment of a new macrophage population, as recently suggested to occur after radiation or infection [19] and whether or to which degree the factors of the local environment contribute to these changes [15], remain to be investigated.

The expression of TRPV2 and NOX2 in the AROM⁺ testes further increased with age. As mentioned, NOX2 is reported to be critical for the differentiation of monocytes to macrophages [43], but it is also a source of ROS and could thereby activate and sensitize TRPV2. The analysis of expression profile of AROM⁺ testes gave hints of both, higher NOX2 expression levels and more pro-inflammatory macrophages (evidenced, e.g., by higher inflammatory factors). The FACS analysis could not be readily performed in older animals, due to the altered and overall remodeled structure of the testes. Still, the evaluation of proteomic data of old animals indicated that several other macrophage markers increase in AROM⁺ animals (i.e., CAPG, CD68, CD206, MPEG1, and SIGLEC1). Furthermore, TRPV2 and NOX2 were exclusively found in AROM⁺ animals by this experimental approach, arguing against a role in normal aging in WT (see above) and for a role in AROM⁺.

Changes in testicular morphology and macrophage accumulation are initiated by hormonal imbalances and estrogen receptor α action, although the exact chain of events is unknown. It is assumed that increased estradiol levels stimulate Leydig cells to produce growth arrest-specific 6 (GAS6), which mediates phagocytosis of apoptotic cells by bridging cells with surface-exposed phosphatidylserine (PS) to macrophage receptors [45]. In general agreement with this assumption, we found that both the aromatase inhibitor treatment, as well as crossings of AROM⁺ with ER α KO, not only, as expected, rescued the infertile phenotype [6,42] and reverted macrophage and inflammation markers, but also reduced TRPV2 and NOX2 levels.

AROM⁺ mice have been studied for several years and changes in prostate, spleen, and testes were described. Higher plasma immunoglobulin levels in AROM⁺ mice are due to distinct changes in the spleen [4] and may indicate a generally altered immunological situation. Prostatitis and prostatic pre-malignancy occur in an age-dependent manner. Next to F4/80⁺ macrophages several other immune cell types were described in prostate. Increased macrophage numbers were first observed in the prostate of AROM⁺ mice at the age of 30 weeks and then increased with the advanced lifespan. In comparison, in AROM⁺ animals, testicular macrophages and testicular alterations are detectable at about 2 months of age, i.e., much earlier. Together with the other changes mentioned, this suggests organ-specific changes. We further monitored TRPV2 levels in adrenals and brains of male AROM⁺ and WT animals (see Supplementary Materials, Figure S5). We chose the brain since similar to the testis, it is an immune-privileged organ. However, we did not find any changes in TRPV2 expression in AROM⁺ compared to WT and no evidence for age-associated alterations either. In contrast, in steroid-producing adrenals, TRPV2 increased with age but in a similar fashion in both, WT and AROM⁺ mice. The results indicate that in the adrenal, which is similar to the testis produces steroids, age is the major factor in the induction of TRPV2. The results require additional studies, but taken together, the distinct changes in the mentioned organs indicate that changes in TRPV2 and macrophages occur in a highly organ-specific way.

In summary, our study further defines the phenotypes of testicular macrophages in the mouse. TRPV2⁺ macrophages normally reside in the mouse testis, yet are of limited number and do not change significantly with age. Hormonal imbalances, however, initiate a chain of events, in which the number of TRPV2⁺ macrophages increases. This situation causes the appearance of a CD206⁺MHC II⁺ subpopulation of TRPV2⁺ macrophages, which appear to be part of the inflammatory events in AROM⁺ animals and may play roles in testicular dysfunction and infertility.

4. Materials and Methods

4.1. Animals

For this study, animals of the well-established mouse model AROM⁺ (human P450arom transgene expressed under the ubiquitin C promotor) with the corresponding WT littermates were used and age-grouped for different approaches. Moreover, 1 month-old WT and AROM⁺ animals either treated with placebo (5 mg/mL carboxymethyl-cellulose in deionized water, Tamro Ltd., Vantaa, Finland) or 10 mg/kg aromatase inhibitor, finrozole (MPV-2213ad, Hormos Medical Ltd., Turku, Finland) for 6 weeks were included into this study. Further, estrogen receptor α knock-out mice, ER α KO, and ER α KO crossbred with AROM⁺ animals were histologically investigated. In addition to the phenotypic control (cryptorchidism, smaller and brownish testes), the expression of the hP450 transgene (*hCYP19A1*) in AROM⁺ mice was verified by means of PCR. The generation and treatment of these genetically modified mice has been described in detail elsewhere [1,2,6,7,41,42,46]. The animals had free access to soy-free food pellets (SDS; Witham, Essex, England) and tap water and were handled in accordance with the institutional animal care policies of the University of Turku (Turku, Finland).

4.2. Immunohistochemistry and In Situ Hybridization of Testicular Sections

After antigen retrieval using 10 mM citrate buffer at pH 6, sections from Bouin's solution-fixed and paraffin embedded mouse testicular samples of all the above-mentioned genotypes—AROM⁺, ER α KO, crossbreeding of these and corresponding WT animals, respectively—were immunohistochemically investigated for the presence of TRPV2 using a polyclonal antibody produced in rabbit (1: 400; HPA044993; Sigma-Aldrich, St. Louis, MO, USA). Additionally, consecutive testicular sections of AROM⁺ and the corresponding WT animals were scanned for the murine macrophage marker F4/80 (monoclonal antibody produced in rat; 1: 50; MCA497; AbD Serotec, Puchheim, Germany). Accordingly, biotinylated goat- α -rabbit (1: 2500; BA-1000; Vector Laboratories, Inc., Burlingame, CA, USA) and goat- α -rat (1: 1000; AB_2338179; Jackson Immuno Research Laboratories, Inc., Ely, Cambridgeshire, UK) secondary antibodies were used, followed by application of an avidin-biotin-complex peroxidase (ABC, Vector Laboratories, Inc. Burlingame, CA, USA) and DAB (Sigma-Aldrich, St. Louis, MO, USA). Primary antibodies omitted, non-immune serum or pre-adsorbed antibody (1: 100; APrEST83822, Sigma-Aldrich, St. Louis, MO, USA) served as negative controls. TRPV2 in situ hybridization was performed on PFA-fixed (10%) and paraffin embedded testicular sections from 2 and 10 month-old AROM⁺ and corresponding WT littermates using the RNAscope 2.5 HD-Brown Assay (ACD, Inc., Newark, NJ, USA) with probes against murine TRPV2 (Cat No. 522811), bacterial *DapB* as negative control [(-) ctrl.] and *PP1B* as positive control [(+) ctrl.] in accordance to the user manual. Sections from both immunohistochemistry and in situ hybridization were slightly counterstained with hematoxylin.

4.3. Western Blot

Protein was isolated from bisected testes of young (3 months, $n = 2$) and old AROM⁺ animals (7 months, $n = 2$) and the corresponding WT littermates ($n = 2$, each) by disruption of the tissue using lysing tubes containing ceramic beads (Lysing Matrix D; MP BiomedicalsTM; Irvine, CA, USA) and RIPA buffer supplemented with protease and phosphatase inhibitors (A32959; Thermo Fisher Scientific Inc., Waltham, MA, USA) in adequate volumes in a tissue homogenizer (FastPrep-24TM 5G; MP BiomedicalsTM; Irvine, CA, USA) with 2–3 cycles at 6.0 m/s speed for 120 s with pauses of 2 min on ice, followed by sonification and centrifugation at 13,000 rpm for 15 min. The sample concentration was measured by Lowry assay (DCTM Protein Assay; Bio-Rad Laboratories, Inc., Hercules, CA, USA), and equal amounts of protein (10 μ g/lane) were loaded. The membrane was incubated with a polyclonal TRPV2 antibody (1: 600; HPA044993; Atlas Antibodies, Stockholm, Sweden) at 4 °C over-night and a monoclonal α Tubulin antibody (1: 10,000; ab52866; Abcam, Cambridge, UK) for 1 h at room temperature, both produced in rabbit. An IRDye

800CW secondary antibody donkey- α -rabbit (1: 10,000; 926-32213; Li-COR Biosciences, Lincoln, NE, USA) was used and bands were detected with the Odyssey CLx imaging system (Li-COR Biosciences, Lincoln, NE, USA). Intensities were measured, background subtracted and normalized to α Tubulin.

4.4. Quantitative RT-PCR

Disruption of testicular, adrenal, and brain tissue, followed by isolation of mRNA, was done using the RNeasy Plus Universal Mini Kit (Qiagen, Hilden, Germany) following the manufacturer's protocol. The quantity of mRNA was measured using a spectrophotometrical approach (NanoDrop 2000c, Thermo Fisher Scientific Inc.) and the purity of isolated RNA was monitored by the 260/280 ratio. After that, mRNA was subjected to reverse transcription (SuperScriptTM II Reverse Transcriptase; Invitrogen, Carlsbad, CA, USA). Then, 4–10 ng cDNA were used for quantitative RT-PCR (LightCycler 96[®] System, Roche Diagnostics, Penzberg, Germany) using the QuantiFast SYBR Green PCR kit (Qiagen, Hilden, Germany). Ribosomal protein L19 (L19) served as an internal control and was used for normalization. The statistical analysis was performed on the Δ Cq values of each animal of treatment (for further details, see Section 4.9) and data are presented as changes in gene expression relative to the corresponding control group according to the $2^{-\Delta\Delta Cq}$ method, as described elsewhere [47]. PCR products were loaded on a 2% agarose gel supplemented with Midori Green Advance DNA stain (Nippon Genetics Europe, Dürren, Germany) for visualization, then separated, eluted, and sent for sequencing to verify their identity (GATC, Konstanz, Germany). Nucleotide sequences of the utilized primers and the size of the corresponding PCR products are given in Table 1.

Table 1. Oligonucleotide primer sequences and corresponding amplicon sizes.

Gene	Reference ID	Nucleotide Sequence	Amplicon Size (bp)
<i>hCYP19A1</i>	NM_000103	5'-GCT ACC CAG TGA AAA AGG GGA-3' 5'-GCC AAA TGG CTG AAA GTA CCT AT-3'	140
<i>L19</i>	NM_009078.2	5'-AGG CAT ATG GGC ATA GGG AA-3' 5'-CC ATG AGG ATG CGC TTG TTT-3'	199
<i>CD54</i>	NM_010493.3	5'-TGG AGA CGC AGA GGA CCT TA-3' 5'-CAG TGT GAA TTG GAC CTG CG-3'	182
<i>CD68</i>	NM_009853.1	5'-CCA GCT GTT CAC CTT GAC CT-3' 5'-AGA GGG GCT GGT AGG TTG AT-3'	208
<i>CD74</i>	NM_001042605.1	5'-GCC ACC ACT GCT TAC TTC CT-3' 5'-GTT CTT CAC AGG CCC AAG GA-3'	198
<i>CD206</i>	NM_008625.2	5'-GAG CCC ACA ACA ACT CCT GA-3' 5'-TCG CCA GCT CTC CAC CTA TA-3'	157
<i>COX2</i>	NM_011198.4	5'-CTT CGG GAG CAC AAC AGA GT-3' 5'-TTC AGA GGC AAT GCG GTT CT-3'	225
<i>CXCL-1</i>	NM_008176.3	5'-AGT TCC AGC ACT CCA GAC TC-3' 5'-AGT GTG GCT ATG ACT TCG GT-3'	246
<i>CXCL-2</i>	NM_009140.2	5'-TCA ATG CCT GAA GAC CCT GC-3' 5'-TTT GAC CGC CCT TGA GAG TG-3'	119
<i>IL-1β</i>	NM_008361.3	5'-TGA AGT TGA CGG ACC CCA AA-3' 5'-TGA TGT GCT GCT GCG AGA TT-3'	101
<i>IL-6</i>	NM_031168.2	5'-TTG GGA CTG ATG CTG GTG AC-3' 5'-CAG GTC TGT TGG GAG TGG TAT-3'	91
<i>MCP-1</i>	NM_011333.3	5'-GGC TCA GCC AGA TGC AGT TAA-3' 5'-CCA GCC TAC TCA TTG GGA TCA-3'	80
<i>TIMP-1</i>	NM_001044384.1	5'-TTC TTG GTT CCC TGG CGT AC-3' 5'-GCA AAG TGA CGG CTC TGG TA-3'	191
<i>TNF-α</i>	NM_013693.3	5'-CAC AGA AAG CAT GAT CCG CG-3' 5'-TGA TGA GAG GGA GGC CAT TTG-3'	209
<i>TRPV2</i>	NM_011706.2	5'-CGA TGA GTT CTA CCG AGG CC-3' 5'-TCA CCA CAT CCC ACT GCT TG-3'	206
<i>NOX2</i>	NM_007807.5	5'-GAG GTT GGT TCG GTT TTG GC-3' 5'-CAG GAG CAG AGG TCA GTG TG-3'	191

4.5. Mass Spectrometry

4.5.1. Sample Preparation

Approximately 1 mg of tissue was incised from 11 month-old WT and AROM⁺ mice testis ($n = 3$, each). The tissues were homogenized manually using Micro-homogenizers, PP (Carl Roth GmbH+Co. KG, Karlsruhe, Germany) and proteins were extracted using the iST Sample Preparation Kit (PreOmics, Martinsried, Germany) using the manufacturer's protocol. Briefly, tissues were lysed and subsequently sheared to get rid of DNA and other interfering molecules followed by incubation with Trypsin at 37 °C for 2.5 h. The resulting peptides were subsequently desalted, purified, and re-dissolved in 10 µL 'Load' solution after drying completely in a speed vac.

4.5.2. Mass Spectrometry Measurements

Reversed phase HPLC separation of peptides was performed on an Ultimate 3000 nanoLC system (Thermo Fisher Scientific Inc., Waltham, MA, USA). In addition, 5 µL of the solution was loaded onto the analytical column (120 × 0.075 mm, in the house packed with ReprosilC18-AQ, 2.4 µm, Dr. Maisch GmbH, Ammerbuch-Entringen, Germany), washed for 5 min with 3% ACN containing 0.1% FA at 300 nl/min, and subsequently separated applying a linear gradient from 3% ACN to 40% ACN over 50 min. Peptides eluted were ionized in a nanoESI source and on line detected on a QExactive HF mass spectrometer (Thermo Fisher Scientific Inc., Waltham, MA, USA). The instrument was operated in a TOP10 method in a positive ionization mode, detecting eluting peptide ions in the m/z range from 375 to 1600 and performing MS/MS analysis of up to 10 precursor ions. Peptide ion masses were acquired at a resolution of 60,000 (at 200 m/z). High-energy collision-induced dissociation (HCD) MS/MS spectra were acquired at a resolution of 15,000 (at 200 m/z). All mass spectra were internally calibrated to lock masses from ambient siloxanes. Precursors were selected based on their intensity from all signals with a charge state from +2 to +5, isolated in a 2 m/z window and fragmented using a normalized collision energy of 27%. To prevent repeated fragmentation of the same peptide ion, the dynamic exclusion was set to 20 s.

4.5.3. Data Analysis

Protein identification was performed by the MaxQuant 1.6.0.16 software package. Parent ion and fragment mass tolerances were 8 ppm and 0.7 Da, respectively and two missed cleavages were allowed. The mouse canonical protein database from Uniprot (release June, 2018), filtered to retain only the reviewed entries was used for the searches. Regular MaxQuant conditions were the following: Peptide FDR, 0.01; Protein FDR, 0.01; Min. peptide Length, 5; Variable modifications, Oxidation (M); Acetyl (Protein N-term); Acetyl (K); Dimethyl (KR); Fixed modifications, Carbamidomethyl (C); Peptides for protein quantitation, razor and unique; Min. peptides, 2; Min. ratio count, 2. Proteins were validated on the basis of at least 1 unique peptide detected.

4.6. Cell Sorting with Flow Cytometry

Mice were euthanized at the age of 2 or 7–8 months by CO₂ asphyxiation following cervical dislocation or cardiac puncture. Testes were removed, minced and digested with 50 µg/mL DNase 1 and 1 mg/mL Collagenase D in Hanks' solution at 37 °C for 45 min. The isolated cells were washed and suspended in PBS, and the cell suspension was filtered through a silk cloth (pore size 77 µm). Cells were incubated with unconjugated CD16/32 antibody (clone 2.4G2; Bio X Cell, Lebanon, NH, USA) to block the unspecific binding to low-affinity Fc-receptors and then stained for 30 min at 4 °C with the following antibodies: Anti-CD45-PerCP-Cy5,5 (clone 30-F11; BD, Franklin Lakes, NJ, USA), anti-F4/80-A488 (clone BM8; eBioscience, San Diego, CA, USA), anti-CD11b-BV786 (clone M1/70; BD, Franklin Lakes, NJ, USA), anti-CD206-BV650 (clone C068C2; BioLegend, San Diego, CA, USA), anti-MHC II-PE (clone M5/114.15.2; BD, Franklin Lakes, NJ, USA), anti-CD11c-BV711 (clone HL3; BD, Franklin Lakes, NJ, USA), anti-Ly6C-BV421 (clone AL-21; BD,

Franklin Lakes, NJ, USA), anti-TRPV2 (HPA044993; Sigma-Aldrich, St. Louis, MO, USA) conjugated with a secondary α -Rb A647 (A27040, Invitrogen, Carlsbad, CA, USA), diluted to the FACS-buffer. Cells were washed and fixed with 1% formaldehyde in PBS. Samples were acquired with the LSRFortessa flow cytometer (BD, Franklin Lakes, NJ, USA), and data were analyzed with the FlowJo software (FlowJo LLC, Ashland, OR, USA).

For subsequent quantitative RT-PCR analysis, wild-type CD45⁺CD11b⁺F4/80⁺ cells were sorted for either CD206⁺MHC II⁻ or CD206⁻MHC II⁺ using a Sony SH800 cell sorter (100 μ m nozzle, Sony Biotechnology Inc., San Jose, CA, USA). The purity of the isolated populations was >95%. The gating strategies for flow cytometric analyses are shown in Figure S4.

4.7. Organotypic Testicular Tissue Incubation

Freshly isolated testes from young WT animals (2–3 months, $n = 7$) were decapsulated, divided into four equally sized tissue pieces, placed into individual wells of a 24-well plate containing DMEM/F12 (Gibco, Paisley, UK) and incubated with CB1 (AM251, 80 nM; Tocris Bioscience, Bristol, UK) and CB2 blockers (AM630, 800 nM; Tocris Bioscience, Bristol, UK), respectively, for 1 h at 37 °C, 5% CO₂, and 95% humidity on a rocking platform. After this pre-incubation, CBD (Tocris Bioscience, Bristol, UK) was added at a final concentration of 30 μ M, with EtOH in equal volume as the solvent control and the tissue pieces were incubated for another 6 h. Afterwards, tissue pieces were frozen in liquid nitrogen, stored at –80 °C for RNA isolation. Supernatants were collected, frozen, and stored for further analysis in a proteome profiler.

4.8. Proteome Profiler

For this Proteome Profiler Mouse Cytokine Array Panel A (R&D Systems, Minneapolis, MN, USA) supernatants of incubated testicular tissues treated with 30 μ M CBD or the EtOH solvent control of one 2.5 month-old wild-type animal were used following the manufacturer's instructions. Briefly, membranes were blocked and incubated with a mixture consisting of supernatant and corresponding buffer overnight. On the next day, the membrane was incubated with Detection Antibody Cocktail followed by streptavidin-horseradish-peroxidase for 1 h each. Finally, a Chemi Reagent Mix was added to measure chemiluminescence with an exposure time of 5 min. The average spot signal density was measured, background subtracted, and normalized to the mRNA amount.

4.9. Data Analysis and Statistics

The testicular section of the above-listed animals subjected either to TRPV2 in situ hybridization or immunohistochemistry against F4/80 and TRPV2 were visualized using a Zeiss Axioplan microscope equipped with a Plan-Neofluar 40x/0.75 objective (Carl Zeiss Microscopy, Jena, Germany) and a Jenoptik camera (PROGRES GRYPHAX Arktur; Jenoptik, Jena, Germany) with the corresponding software (PROGRES GRYPHAX[®], Version 1.1.8.159 for Macintosh, 2017, Jenoptik Optical Systems GmbH, Jena, Germany). Microscopic images were further white-balanced and brightness was adjusted using Fiji (open source image processing package for ImageJ).

Quantitative RT-PCR datasets were analyzed using Microsoft Excel (2018, Microsoft, Redmond, WA, USA) and the statistical analysis was performed on the Δ Cq values of each animal/treated tissue using Prism 7 (GraphPad, San Diego, CA, USA). After outlier exclusion (ROUT method, $Q = 1\%$), datasets were checked for Gaussian distribution using the Shapiro-Wilk normality test ($\alpha = 0.05$) and were subjected either to an unpaired (animals with different age, genotype and treatment, unpaired conditions) or paired (organotypic testicular tissue incubation, paired conditions) two-tailed t-tests. Datasets of wild-type macrophages sorted for their CD206 and MHC II expression and further subjected to quantitative RT-PCR looking for TRPV2 (Figure 1F) were not statistically investigated due to the low n in this approach (2 months, $n = 1$, pool of three animals; 7–8 months, $n = 2$, pool of three animals each).

For analysis of mass spectrometry datasets, the measured iBAQ intensities were checked for Gaussian distribution using the Shapiro-Wilk normality test ($\alpha = 0.05$) followed by an unpaired two-tailed *t*-test, for those proteins detected in all three biological replicates of each group (3/3). The differential protein expression between the two genotypes is expressed as fold change based on the mean WT log₂ iBAQ intensity.

For analysis of the FACS datasets, calculated percentages of the corresponding macrophage subpopulations were checked for Gaussian distribution using the Shapiro-Wilk normality test ($\alpha = 0.05$), and were further subjected to an unpaired two-tailed *t*-test when all three biological replicates of each group (3/3) showed values greater than 0.

For all the tests, α was set to 0.05 (* $p \leq 0.05$, ** $p \leq 0.01$, *** $p \leq 0.001$), and data are depicted as mean \pm SEM.

Signal densities of Western Blot bands and Proteome Profiler spots were measured using Fiji and further quantifications were done with Excel and Prism 7. Due to the low *n* in both approaches (Western Blots: *n* = 2 for each group; proteome profiler: *n* = 1), no statistical analysis was performed.

Supplementary Materials: The following are available online at <https://www.mdpi.com/article/10.3390/ijms22094727/s1>.

Author Contributions: K.E. and A.M. (Artur Mayerhofer) conceived of and designed the experiments; K.E. performed the majority of the experiments, corresponding analysis, and interpretation; P.R. performed the FACS experiments and analysis; K.E., H.G., A.M. (Annika Missel), N.S., and L.W. generated testicular samples; C.H. supported the in situ hybridization experiments; S.L. performed the MS experiments and analysis; S.L., A.I., P.R., L.S., M.P., and A.M. (Artur Mayerhofer) contributed reagents/materials/analysis tools; K.E. and A.M. (Artur Mayerhofer) drafted the paper and all authors contributed to the final version. All authors have read and agreed to the published version of the manuscript.

Funding: This study was supported partly in parts by grants from Deutsche Forschungsgemeinschaft (DFG), especially MA1080/27-1 and 31-1 (project number 456828204) and SFB1123 TP Z02, and by grants from Deutscher Akademischer Austauschdienst (DAAD) and the Academy of Finland.

Institutional Review Board Statement: The animals were handled in accordance with the institutional animal care policies of the University of Turku (Turku, Finland). The number for animal license is KEK/2018-0608-Strauss.

Informed Consent Statement: Not applicable.

Data Availability Statement: Not applicable.

Acknowledgments: We thank Etta-Liisa Väänänen, Laura Grönfors, Emmi Lokka, and Hanna Heikelä for expert technical help and the Cell Imaging and Cytometry Core facility (Turku Bioscience, University of Turku, Åbo Akademi University, and Biocenter Finland) is acknowledged for services, instrumentation, and expertise. We are very grateful to Astrid Tiefenbacher and Nicole Kreitmair, as well as Melanie Kaseder and Verena Kast for the excellent laboratory support. The authors also thank Ignasi Forne of the Protein Analysis Unit (ZfP) of BioMedical Center, LMU, for assistance in the MS measurements.

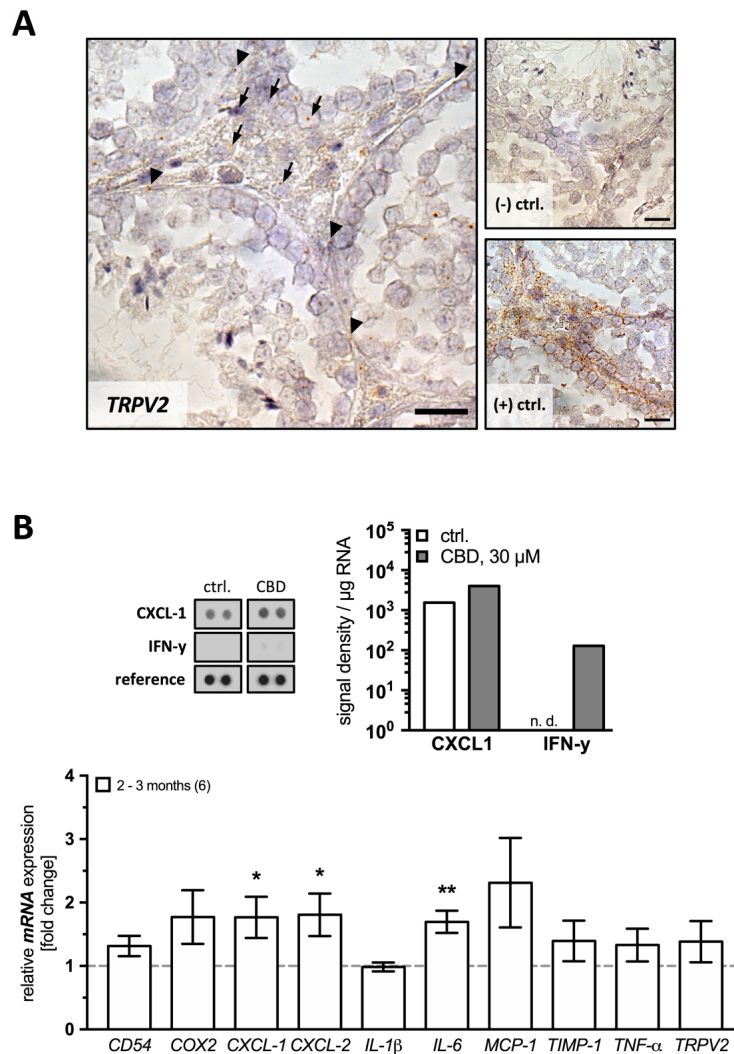
Conflicts of Interest: The authors declare no conflict of interest. The funding sponsors had no role in the design of the study, in the collection, analysis, or interpretation of data, in the writing of the manuscript, and in the decision to publish the results. This work was done in partial fulfillment of the requirements of a doctoral thesis of K.E. at LMU, Munich.

References

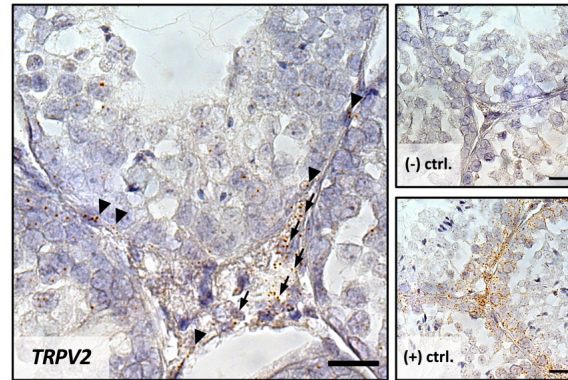
1. Li, X.; Nokkala, E.; Yan, W.; Streng, T.; Saarinen, N.; Wärrri, A.; Huhtaniemi, I.; Santti, R.; Mäkelä, S.; Poutanen, M. Altered structure and function of reproductive organs in transgenic male mice overexpressing human aromatase. *Endocrinology* **2001**, *142*, 2435–2442. [[CrossRef](#)] [[PubMed](#)]
2. Li, X.; Mäkelä, S.; Streng, T.; Santti, R.; Poutanen, M. Phenotype characteristics of transgenic male mice expressing human aromatase under ubiquitin C promoter. *J. Steroid Biochem. Mol. Biol.* **2003**, *86*, 469–476. [[CrossRef](#)]
3. Lahiri, S.; Walenta, L.; Aftab, W.; Strauss, L.; Poutanen, M.; Mayerhofer, A.; Imhof, A. Imaging mass spectrometry and shotgun proteomics reveal dysregulated pathways in hormone induced male infertility. *bioRxiv* **2020**. [[CrossRef](#)]

4. Aguilar-Pimentel, J.A.; Cho, Y.L.; Gerlini, R.; Calzada-Wack, J.; Wimmer, M.; Mayer-Kuckuk, P.; Adler, T.; Schmidt-Weber, C.B.; Busch, D.H.; Fuchs, H.; et al. Increased estrogen to androgen ratio enhances immunoglobulin levels and impairs B cell function in male mice. *Sci. Rep.* **2020**, *10*, 18334. [[CrossRef](#)]
5. Ellem, S.J.; Wang, H.; Poutanen, M.; Risbridger, G.P. Increased endogenous estrogen synthesis leads to the sequential induction of prostatic inflammation (prostatitis) and prostatic pre-malignancy. *Am. J. Pathol.* **2009**, *175*, 1187–1199. [[CrossRef](#)] [[PubMed](#)]
6. Li, X.; Strauss, L.; Mäkelä, S.; Streng, T.; Huhtaniemi, I.; Santti, R.; Poutanen, M. Multiple structural and functional abnormalities in the p450 aromatase expressing transgenic male mice are ameliorated by a p450 aromatase inhibitor. *Am. J. Pathol.* **2004**, *164*, 1039–1048. [[CrossRef](#)]
7. Li, X.; Strauss, L.; Kaatrasalo, A.; Mayerhofer, A.; Huhtaniemi, I.; Santti, R.; Mäkelä, S.; Poutanen, M. Transgenic mice expressing p450 aromatase as a model for male infertility associated with chronic inflammation in the testis. *Endocrinology* **2006**, *147*, 1271–1277. [[CrossRef](#)]
8. Frungieri, M.B.; Calandra, R.S.; Lustig, L.; Meineke, V.; Köhn, F.M.; Vogt, H.J.; Mayerhofer, A. Number, distribution pattern, and identification of macrophages in the testes of infertile men. *Fertil. Steril.* **2002**, *78*, 298–306. [[CrossRef](#)]
9. Adam, M.; Urbanski, H.F.; Garyfallou, V.T.; Welsch, U.; Köhn, F.M.; Ullrich Schwarzer, J.; Strauss, L.; Poutanen, M.; Mayerhofer, A. High levels of the extracellular matrix proteoglycan decorin are associated with inhibition of testicular function. *Int. J. Androl.* **2012**, *35*, 550–561. [[CrossRef](#)] [[PubMed](#)]
10. DeFalco, T.; Bhattacharya, I.; Williams, A.V.; Sams, D.M.; Capel, B. Yolk-sac-derived macrophages regulate fetal testis vascularization and morphogenesis. *Proc. Natl. Acad. Sci. USA* **2014**, *111*, E2384–E2393. [[CrossRef](#)]
11. Gaytan, F.; Bellido, C.; Aguilar, E.; van Rooijen, N. Requirement for testicular macrophages in Leydig cell proliferation and differentiation during prepubertal development in rats. *J. Reprod. Fertil.* **1994**, *102*, 393–399. [[CrossRef](#)] [[PubMed](#)]
12. DeFalco, T.; Potter, S.J.; Williams, A.V.; Waller, B.; Kan, M.J.; Capel, B. Macrophages Contribute to the Spermatogonial Niche in the Adult Testis. *Cell Rep.* **2015**, *12*, 1107–1119. [[CrossRef](#)]
13. Fijak, M.; Meinhardt, A. The testis in immune privilege. *Immunol. Rev.* **2006**, *213*, 66–81. [[CrossRef](#)] [[PubMed](#)]
14. Wang, L.L.; Li, Z.H.; Hu, X.H.; Muyayalo, K.P.; Zhang, Y.H.; Liao, A.H. The roles of the PD-1/PD-L1 pathway at immunologically privileged sites. *Am. J. Reprod. Immunol.* **2017**, *78*, e12710. [[CrossRef](#)] [[PubMed](#)]
15. Wang, M.; Fijak, M.; Hossain, H.; Markmann, M.; Nüsing, R.M.; Lochnit, G.; Hartmann, M.F.; Wudy, S.A.; Zhang, L.; Gu, H.; et al. Characterization of the Micro-Environment of the Testis that Shapes the Phenotype and Function of Testicular Macrophages. *J. Immunol.* **2017**, *198*, 4327–4340. [[CrossRef](#)]
16. Meinhardt, A.; Wang, M.; Schulz, C.; Bhushan, S. Microenvironmental signals govern the cellular identity of testicular macrophages. *J. Leukoc. Biol.* **2018**, *104*, 757–766. [[CrossRef](#)]
17. Matzkin, M.E.; Valchi, P.; Riviere, E.; Rossi, S.P.; Tavalieri, Y.E.; Muñoz de Toro, M.M.; Mayerhofer, A.; Bartke, A.; Calandra, R.S.; Frungieri, M.B. Aging in the Syrian hamster testis: Inflammatory-oxidative status and the impact of photoperiod. *Exp. Gerontol.* **2019**, *124*, 110649. [[CrossRef](#)]
18. Lokka, E.; Lintukorpi, L.; Cisneros-Montalvo, S.; Mäkelä, J.A.; Tyystjärvi, S.; Ojasalo, V.; Gerke, H.; Toppari, J.; Rantakari, P.; Salmi, M. Generation, localization and functions of macrophages during the development of testis. *Nat. Commun.* **2020**, *11*, 4375. [[CrossRef](#)]
19. Wang, M.; Yang, Y.; Cansever, D.; Wang, Y.; Kantores, C.; Messiaen, S.; Moison, D.; Livera, G.; Chakarov, S.; Weinberger, T.; et al. Two populations of self-maintaining monocyte-independent macrophages exist in adult epididymis and testis. *Proc. Natl. Acad. Sci. USA* **2021**, *118*, e2013686117. [[CrossRef](#)]
20. Perálvarez-Marín, A.; Doñate-Macian, P.; Gaudet, R. What do we know about the transient receptor potential vanilloid 2 (TRPV2) ion channel? *FEBS J.* **2013**, *280*, 5471–5487. [[CrossRef](#)]
21. Caterina, M.J.; Rosen, T.A.; Tominaga, M.; Brake, A.J.; Julius, D. A capsaicin-receptor homologue with a high threshold for noxious heat. *Nature* **1999**, *398*, 436–441. [[CrossRef](#)]
22. Park, U.; Vastani, N.; Guan, Y.; Raja, S.N.; Koltzenburg, M.; Caterina, M.J. TRP vanilloid 2 knock-out mice are susceptible to perinatal lethality but display normal thermal and mechanical nociception. *J. Neurosci.* **2011**, *31*, 11425–11436. [[CrossRef](#)]
23. Neeper, M.P.; Liu, Y.; Hutchinson, T.L.; Wang, Y.; Flores, C.M.; Qin, N. Activation properties of heterologously expressed mammalian TRPV2: Evidence for species dependence. *J. Biol. Chem.* **2007**, *282*, 15894–15902. [[CrossRef](#)]
24. Hu, H.Z.; Gu, Q.; Wang, C.; Colton, C.K.; Tang, J.; Kinoshita-Kawada, M.; Lee, L.Y.; Wood, J.D.; Zhu, M.X. 2-aminoethoxydiphenyl borate is a common activator of TRPV1, TRPV2, and TRPV3. *J. Biol. Chem.* **2004**, *279*, 35741–35748. [[CrossRef](#)] [[PubMed](#)]
25. Qin, N.; Neeper, M.P.; Liu, Y.; Hutchinson, T.L.; Lubin, M.L.; Flores, C.M. TRPV2 is activated by cannabidiol and mediates CGRP release in cultured rat dorsal root ganglion neurons. *J. Neurosci.* **2008**, *28*, 6231–6238. [[CrossRef](#)] [[PubMed](#)]
26. Maggi, C.A.; Santicioli, P.; Geppetti, P.; Parlani, M.; Astolfi, M.; Pradelles, P.; Patacchini, R.; Meli, A. The antagonism induced by ruthenium red of the actions of capsaicin on the peripheral terminals of sensory neurons: Further studies. *Eur. J. Pharmacol.* **1988**, *154*, 1–10. [[CrossRef](#)]
27. Nie, L.; Oishi, Y.; Doi, I.; Shibata, H.; Kojima, I. Inhibition of proliferation of MCF-7 breast cancer cells by a blocker of Ca²⁺-permeable channel. *Cell Calcium* **1997**, *22*, 75–82. [[CrossRef](#)]
28. Fricke, T.C.; Echtermeyer, F.; Zielke, J.; de la Roche, J.; Filipovic, M.R.; Claverol, S.; Herzog, C.; Tominaga, M.; Pumroy, R.A.; Moiseenkova-Bell, V.Y.; et al. Oxidation of methionine residues activates the high-threshold heat-sensitive ion channel TRPV2. *Proc. Natl. Acad. Sci. USA* **2019**, *116*, 24359–24365. [[CrossRef](#)]

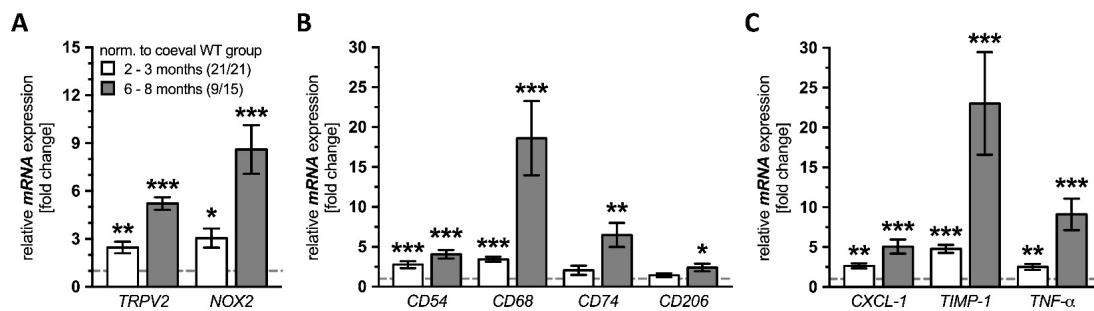
29. Shibasaki, K.; Murayama, N.; Ono, K.; Ishizaki, Y.; Tominaga, M. TRPV2 enhances axon outgrowth through its activation by membrane stretch in developing sensory and motor neurons. *J. Neurosci.* **2010**, *30*, 4601–4612. [[CrossRef](#)] [[PubMed](#)]
30. Hisanaga, E.; Nagasawa, M.; Ueki, K.; Kulkarni, R.N.; Mori, M.; Kojima, I. Regulation of calcium-permeable TRPV2 channel by insulin in pancreatic beta-cells. *Diabetes* **2009**, *58*, 174–184. [[CrossRef](#)]
31. Park, K.S.; Kim, Y.; Lee, Y.H.; Earm, Y.E.; Ho, W.K. Mechanosensitive cation channels in arterial smooth muscle cells are activated by diacylglycerol and inhibited by phospholipase C inhibitor. *Circ. Res.* **2003**, *93*, 557–564. [[CrossRef](#)]
32. Jang, Y.; Lee, Y.; Kim, S.M.; Yang, Y.D.; Jung, J.; Oh, U. Quantitative analysis of TRP channel genes in mouse organs. *Arch. Pharm. Res.* **2012**, *35*, 1823–1830. [[CrossRef](#)]
33. Stokes, A.J.; Shimoda, L.M.; Koblan-Huberson, M.; Adra, C.N.; Turner, H. A TRPV2-PKA signaling module for transduction of physical stimuli in mast cells. *J. Exp. Med.* **2004**, *200*, 137–147. [[CrossRef](#)] [[PubMed](#)]
34. Nagasawa, M.; Nakagawa, Y.; Tanaka, S.; Kojima, I. Chemotactic peptide fMetLeuPhe induces translocation of the TRPV2 channel in macrophages. *J. Cell Physiol.* **2007**, *210*, 692–702. [[CrossRef](#)] [[PubMed](#)]
35. Link, T.M.; Park, U.; Vonakis, B.M.; Raben, D.M.; Soloski, M.J.; Caterina, M.J. TRPV2 has a pivotal role in macrophage particle binding and phagocytosis. *Nat. Immunol.* **2010**, *11*, 232–239. [[CrossRef](#)]
36. Zhang, D.; Spielmann, A.; Wang, L.; Ding, G.; Huang, F.; Gu, Q.; Schwarz, W. Mast-cell degranulation induced by physical stimuli involves the activation of transient-receptor-potential channel TRPV2. *Physiol. Res.* **2012**, *61*, 113–124. [[CrossRef](#)] [[PubMed](#)]
37. Kajiji, H.; Okamoto, F.; Nemoto, T.; Kimachi, K.; Toh-Goto, K.; Nakayana, S.; Okabe, K. RANKL-induced TRPV2 expression regulates osteoclastogenesis via calcium oscillations. *Cell Calcium* **2010**, *48*, 260–269. [[CrossRef](#)] [[PubMed](#)]
38. Yamashiro, K.; Sasano, T.; Tojo, K.; Namekata, I.; Kurokawa, J.; Sawada, N.; Suganami, T.; Kamei, Y.; Tanaka, H.; Tajima, N.; et al. Role of transient receptor potential vanilloid 2 in LPS-induced cytokine production in macrophages. *Biochem. Biophys. Res. Commun.* **2010**, *398*, 284–289. [[CrossRef](#)] [[PubMed](#)]
39. Kanzaki, M.; Zhang, Y.Q.; Mashima, H.; Li, L.; Shibata, H.; Kojima, I. Translocation of a calcium-permeable cation channel induced by insulin-like growth factor-I. *Nat. Cell Biol.* **1999**, *1*, 165–170. [[CrossRef](#)]
40. Kowase, T.; Nakazato, Y.; Yoko, O.H.; Morikawa, A.; Kojima, I. Immunohistochemical localization of growth factor-regulated channel (GRC) in human tissues. *Endocr. J.* **2002**, *49*, 349–355. [[CrossRef](#)] [[PubMed](#)]
41. Lubahn, D.B.; Moyer, J.S.; Golding, T.S.; Couse, J.F.; Korach, K.S.; Smithies, O. Alteration of reproductive function but not prenatal sexual development after insertional disruption of the mouse estrogen receptor gene. *Proc. Natl. Acad. Sci. USA* **1993**, *90*, 11162–11166. [[CrossRef](#)]
42. Strauss, L.; Kallio, J.; Desai, N.; Pakarinen, P.; Miettinen, T.; Gylling, H.; Albrecht, M.; Mäkelä, S.; Mayerhofer, A.; Poutanen, M. Increased exposure to estrogens disturbs maturation, steroidogenesis, and cholesterol homeostasis via estrogen receptor alpha in adult mouse Leydig cells. *Endocrinology* **2009**, *150*, 2865–2872. [[CrossRef](#)]
43. Xu, Q.; Choksi, S.; Qu, J.; Jang, J.; Choe, M.; Banfi, B.; Engelhardt, J.F.; Liu, Z.G. NADPH Oxidases Are Essential for Macrophage Differentiation. *J. Biol. Chem.* **2016**, *291*, 20030–20041. [[CrossRef](#)] [[PubMed](#)]
44. Singel, K.L.; Segal, B.H. NOX2-dependent regulation of inflammation. *Clin. Sci.* **2016**, *130*, 479–490. [[CrossRef](#)] [[PubMed](#)]
45. Yu, W.; Zheng, H.; Lin, W.; Tajima, A.; Zhang, Y.; Zhang, X.; Zhang, H.; Wu, J.; Han, D.; Rahman, N.A.; et al. Estrogen promotes Leydig cell engulfment by macrophages in male infertility. *J. Clin. Investig.* **2014**, *124*, 2709–2721. [[CrossRef](#)]
46. Krege, J.H.; Hodgin, J.B.; Couse, J.F.; Enmark, E.; Warner, M.; Mahler, J.F.; Sar, M.; Korach, K.S.; Gustafsson, J.A.; Smithies, O. Generation and reproductive phenotypes of mice lacking estrogen receptor beta. *Proc. Natl. Acad. Sci. USA* **1998**, *95*, 15677–15682. [[CrossRef](#)] [[PubMed](#)]
47. Pfaffl, M.W. A new mathematical model for relative quantification in real-time RT-PCR. *Nucleic Acids Res.* **2001**, *29*, e45. [[CrossRef](#)] [[PubMed](#)]



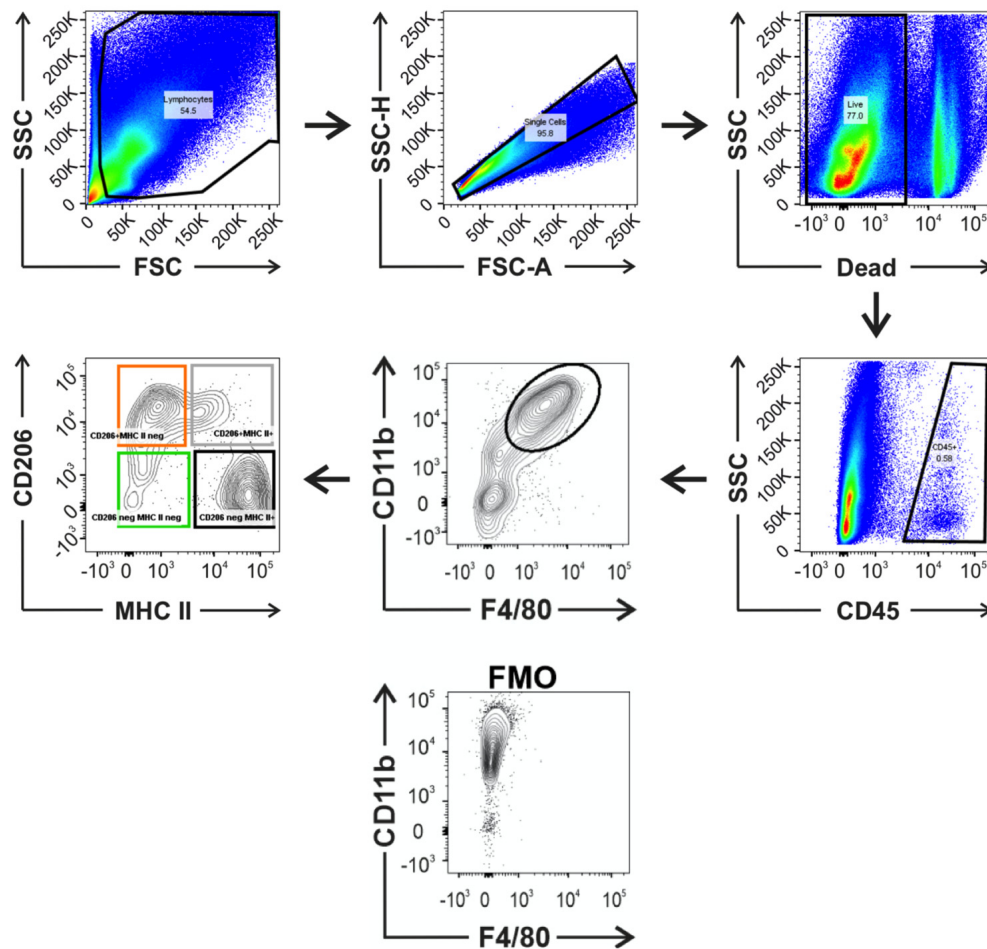
Supplementary Figure S1. TRPV2 in testicular sections from young and old WT mice and effects of CBD in testicular tissue incubation experiments. (A) 2 months-old WT mice subjected to *TRPV2* in situ hybridization (left panel) revealed punctuated staining both in the interstitial space (arrows) and within or in close proximity to the peritubular wall (arrow heads). Negative control (upper right panel, (-) ctrl.) showed no signals, but the positive control (lower right panel, (+) ctrl.) did. Scale bar 50 μm . (B) Testicular tissue from young WT mice incubated with 30 μM CBD together with CB1 and 2 blockers (AM251 and AM630, respectively) for 6 h showed higher CXCL-1 and IFN- γ levels in the supernatant, analyzed by a cytokine profiler (upper panel). mRNA levels of *CXCL-1* (1.767 ± 0.326 ; $p = 0.0493$) and 2 (1.807 ± 0.334 ; $p = 0.0018$), as well as *IL-6* (1.697 ± 0.174 ; $p = 0.0066$) increased significantly, whereas *CD54* (1.315 ± 0.159 ; $p = 0.0968$), *COX2* (1.772 ± 0.425 ; $p = 0.0919$), *IL-1 β* (0.985 ± 0.070 ; $p = 0.7045$), *MCP-1* (2.313 ± 0.705 ; $p = 0.0527$), *TIMP-1* (1.395 ± 0.320 ; $p = 0.4632$), *TNF- α* (1.330 ± 0.258 ; $p = 0.3588$) and *TRPV2* (1.383 ± 0.325 ; $p = 0.4549$) remained unchanged at the same time (n = 6). Graphs represent mean \pm SEM compared to solvent (EtOH) treated testicular tissue; paired two-tailed t-test, $\alpha = 0.05$.



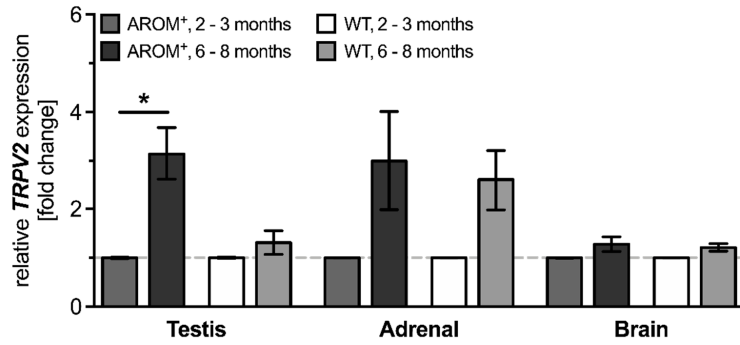
Supplementary Figure S2. TRPV2 in situ hybridization of young, 2 months-old AROM⁺ mice. Testicular sections of 2 months-old AROM⁺ mice subjected to TRPV2 in situ hybridization (left panel) revealed strong and punctuated staining mainly in the interstitial space (arrows), but also revealed TRPV2 signals within or in close proximity to the peritubular wall (arrow heads). Negative control (upper right panel, (-) ctrl.) showed no signals, but the positive control (lower right panel, (+) ctrl.) did. Scale bar 50 μ m.



Supplementary Figure S3. Genotypic comparison of expression profiles in young and old WT and AROM⁺ testes. (A-C) Genotype-dependent comparison of mRNA expression levels of (A) TRPV2 and NOX2, (B) macrophage and (C) inflammation markers in whole testis from young and old AROM⁺ mice (n = 9 and 15, respectively) compared to coeval WT animals (n = 21, each). mRNA expression levels were always significantly higher in AROM⁺ animals, except for CD74 (2.061 \pm 0.582, p = 0.7800) and CD206 (1.431 \pm 0.229; p = 0.4744) in the young animals. Graphs represent mean \pm SEM; unpaired two-tailed t-test, α = 0.05.



Supplementary Figure S4. Gating strategies for flow cytometry of testicular macrophages. FACS gating strategy with representative two-dimensional plots for murine testicular macrophages and fluorescence minus one (FMO) control. Living cells were gated for CD45⁺ F4/80⁺CD11b⁺ events before downstream analysis and were further sorted for MHC II and CD206, resulting in four macrophage subpopulations: CD206⁻MHC II⁻ (green gate), CD206⁺MHC II⁻ (orange gate), CD206⁻MHC II⁺ (black gate) and CD206⁺MHC II⁺ (gray gate).



Supplementary Figure S5. TRPV2 expression in testis, adrenal and brain of young and old WT and AROM⁺ mice. mRNA extracted from testis, adrenal and brain of young (2 - 3 months) and old (6 - 8 months) WT and AROM⁺ mice (n = 3, each) was subjected to quantitative RT-PCR revealing significantly higher TRPV2 expression levels in testicular tissue from old AROM⁺ animals compared to the young ones (3.141 ± 0.538 , $p = 0.0163$), but not in tissue from WT mice (1.310 ± 0.241 , $p = 0.2687$). TRPV2 expression levels were also numerically elevated in adrenal from old WT (2.597 ± 0.618 , $p = 0.0610$) and AROM⁺ (2.997 ± 1.014 , $p = 0.1203$) compared to the corresponding young animals, but did not reach significance. In brain, also immune privileged, TRPV2 expression was unchanged (WT: 1.210 ± 0.079 , $p = 0.0573$; AROM⁺: 1.277 ± 0.150 , $p = 0.1365$). Graphs represent mean \pm SEM; unpaired two-tailed t-test, $\alpha = 0.05$.

3.3 Publication III

A rapid and robust method for the cryopreservation of human granulosa cells.

Sarah Beschta*, Katja Eubler*, Nancy Bohne, Ignasi Forné, Dieter Berg, Ulrike Berg & Artur Mayerhofer

* joint first authors

Histochemistry and Cell Biology, July 2021

doi: 10.1007/s00418-021-02019-3

Human primary granulosa cells (GCs) derived from women undergoing oocyte retrieval can be cultured and are a cellular model for the study of human ovarian functions. *In vitro* they change rapidly, resembling initially cells of the preovulatory follicle and then cells of the corpus luteum. They are derived from individual patients and their different medical history, lifestyle and age lead to heterogeneity. Thus, cells can rarely be ideally matched for cellular experiments or, if available, only in small quantities. We reasoned that cryopreservation of human GCs may be helpful to improve this situation. Previous studies indicated feasibility of such an approach, but low survival of human GCs was reported and consequences on human GCs functionality were only partially evaluated. We tested a slow freezing protocol (employing FCS and DMSO) of human GCs upon isolation from follicular fluid. We compared cryopreserved and subsequently thawed cells with fresh, not cryopreserved ones, from the same patients. About 80 % of human GCs survived freezing/thawing. Neither morphology, survival rate in culture, nor levels of mitochondrial (*COX4*, *OPA1*, *TOMM20*), steroidogenic (*CYP11A1*, *CYP19A1*) and cell-cell contact genes (*GJA1*) were different between the two groups in cells cultured for 1-5 days. A proteomic analysis revealed no statistical significance in the abundance of a total of 5962 proteins. Both groups produced comparable basal levels of progesterone and responded similarly to hCG with elevation of progesterone. Taken together, we describe a rapid and readily available method for the cryopreservation of human GCs. We anticipate that it will allow future large-scale experiments and may thereby improve cellular studies with human ovarian cells.



A rapid and robust method for the cryopreservation of human granulosa cells

Sarah Beschta^{1,2} · Katja Eubler¹ · Nancy Bohne² · Ignasi Forne³ · Dieter Berg² · Ulrike Berg² · Artur Mayerhofer¹ 

Accepted: 14 July 2021 / Published online: 27 July 2021
© The Author(s) 2021

Abstract

Human primary granulosa cells (GCs) derived from women undergoing oocyte retrieval can be cultured and used as a cellular model for the study of human ovarian function. In vitro, they change rapidly, initially resembling cells of the preovulatory follicle and then cells of the corpus luteum. They are derived from individual patients, whose different medical history, lifestyle and age lead to heterogeneity. Thus, cells can rarely be ideally matched for cellular experiments or, if available, only in small quantities. We reasoned that cryopreservation of human GCs may be helpful to improve this situation. Previous studies indicated the feasibility of such an approach, but low survival of human GCs was reported, and effects on human GC functionality were only partially evaluated. We tested a slow freezing protocol (employing FCS and DMSO) for human GCs upon isolation from follicular fluid. We compared cryopreserved and subsequently thawed cells with fresh, non-cryopreserved cells from the same patients. About 80% of human GCs survived freezing/thawing. No differences were found in cell morphology, survival rate in culture, or transcript levels of mitochondrial (*COX4*, *OPA1*, *TOMM20*), steroidogenic (*CYP11A1*, *CYP19A1*) or cell–cell contact genes (*GJA1*) between the two groups in cells cultured for 1–5 days. A proteomic analysis revealed no statistically significant change in the abundance of a total of 5962 proteins. The two groups produced comparable basal levels of progesterone and responded similarly to hCG with elevation of progesterone. Taken together, our results show this to be a rapid and readily available method for the cryopreservation of human GCs. We anticipate that it will allow future large-scale experiments and may thereby improve cellular studies with human ovarian cells.

Keywords Cryopreservation · IVF · Ovarian cells · Cell culture · Mass spectrometry · Progesterone

Introduction

The development and widespread use of assisted reproductive technology (ART) has opened a unique possibility for the study of the human ovary, namely follicular fluid and granulosa cells. Human granulosa cells (GCs) are the

by-product of follicular aspiration performed on women undergoing medical procedures like in vitro fertilization (IVF), intracytoplasmic sperm injection (ICSI) or cryopreservation of their oocytes. They are therefore readily available and represent, in general, mural cells, which are in the process of luteinization (luteinizing GCs). They can be isolated from the follicular fluid, cultured in vitro and then studied (Blohberger et al. 2016; Bulling et al. 2000; Saller et al. 2014). As GCs fulfill an essential role in the follicle, form the environment for the oocyte and produce steroids, the study of cultured human GCs provides a unique window into the human ovary. A previous study employing a proteomic comparison revealed that IVF-derived human GCs in culture resemble initially luteinizing cells of the ovulatory follicle, but then are more comparable to the large luteinized granulosa cells of the corpus luteum (CL) (Bagnjuk and Mayerhofer 2019). During the culture period, human GCs further undergo striking changes and at later time points they are alike the cells of the regressing CL (Bagnjuk and

Sarah Beschta and Katja Eubler are joint first authors.

✉ Artur Mayerhofer
Mayerhofer@bmc.med.lmu.de

¹ Cell Biology, Anatomy III, Faculty of Medicine, Biomedical Center Munich (BMC), Ludwig-Maximilian-University (LMU), 82152 Martinsried, Germany

² Fertility Centre A.R.T. Bogenhausen, 81675 Munich, Germany

³ Protein Analysis Unit, Faculty of Medicine, Biomedical Center Munich (BMC), Ludwig-Maximilian-University (LMU), 82152 Martinsried, Germany

Mayerhofer 2019). Thus, cultured human GCs are highly dynamic and provide insight into different situations of the human ovary.

Indeed, the changes are rapid and occur within a few days; hence human GCs rarely can be ideally matched for cellular experiments. The cells stem from humans and due to patients' age, lifestyle and their medical history, human GCs are notoriously heterogeneous, a situation aggravated in conditions such as polycystic ovarian syndrome (PCOS). We reasoned that upon cryopreservation of human GCs, sufficient numbers of comparable cells may become available to improve cellular studies.

There are several studies demonstrating cryopreservation of ovarian tissues and cells in various species, including human and bovine (Amorim et al. 2011; Baufeld and Vanselow 2018; Bouillon et al. 2020; Kokotsaki et al. 2018; Pietrowski et al. 2020; Rivas Leonel et al. 2019; Santana et al. 2012; Shi et al. 2017; Sluss et al. 1994; Youm et al. 2014; Zheng et al. 2019). They indicate that freezing/thawing is, in general, possible, yet the survival rate of cells is rather low (45–58%; see Bouillon et al. 2020). Furthermore, the consequences of such procedures for GCs are not fully evaluated, especially for IVF-derived human GCs (Bouillon et al. 2020; Sluss et al. 1994).

Here we report a method for cryopreservation and later use of human GCs and show by employing different approaches, including a proteomic analysis, that the cryopreserved cells do not differ from their fresh counterparts.

Materials and methods

Human GC isolation and cell culture

For the isolation of human GCs, follicular fluid was used from patients undergoing medical procedures including in vitro fertilization (IVF), intracytoplasmic sperm injection (ICSI) or cryopreservation of oocytes primarily to address infertility. Patients with polycystic ovary syndrome (PCOS) were excluded from this study. By written consent, patients agreed to the scientific use of biological material, as part of ongoing projects within the framework of a German Research Foundation (DFG)-funded project (456828204). The use of human cells was approved by the Ethics Committee of LMU (Project number 20-697). Follicular fluid from two to six patients (average 3.2 ± 0.3 punctures) was pooled for this study, and human GCs were isolated using a cell strainer, as described previously (Bloherberger et al. 2016). After centrifugation of the cell suspension for 3 min at 800 rpm, isolated cells were mixed with trypan blue (Lonza, Basel, Switzerland) and counted using a Neubauer chamber.

The resulting number of cells was equally divided and one half was used for cryopreservation and the other half was seeded ($1-1.25 \times 10^5$ cells/dish) onto p35 cell culture dishes (Sarstedt, Leicester, UK) containing Dulbecco's modified Eagle medium/Ham's F-12 nutrient mixture (DMEM/F12; Gibco, Paisley, UK) supplemented with 1% penicillin/streptomycin (P/S; BioChrom, Berlin, Germany) and 10% fetal calf serum (FCS; Capricorn Scientific, Ebsdorfergrund, Germany) and kept at 37 °C, 5% CO₂ and 95% humidity until experimental use. On the first day of culture, human GCs were washed thoroughly with pure DMEM/F12 to get rid of remaining blood cells and tissue fragments and fresh supplemented culture medium (DMEM/F12 with 1% P/S and 10% FCS) was added. Cells were cultured up to 5 days for this study and medium was changed every other day.

Cryopreservation and thawing

For cryopreservation, half of the freshly isolated cells ($422,375 \pm 57,910$ cells, $n = 16$) were resuspended in 1 ml DMEM/F12 containing 1% P/S, 10% FCS and 10% dimethyl sulfoxide (DMSO; Sigma-Aldrich, St. Louis, MO, USA) and were transferred to a cryotube (Thermo Fisher Scientific, Waltham, MA, USA). Cells were cooled to -80 °C at a rate of -1 °C/min using an alcohol-free cell freezing container (BioCision CoolCell 1 ml FX, Brooks Life Sciences GmbH, Griesheim, Germany) and were transferred to liquid nitrogen the following day. Cells tested in this study were stored for up to 14 days in a liquid nitrogen tank. On the day of use, cells were rapidly thawed in a water bath at 37 °C and transferred to a falcon tube with about 7 ml DMEM/F12 supplemented with 1% P/S and 10% FCS. The suspension was then centrifuged for 3 min at 800 rpm and the pellet was resuspended in fresh supplemented culture medium. To determine the survival rate after this freeze/thaw process, cells were mixed with trypan blue and recounted using a Neubauer chamber. Cells, in identical numbers to those of freshly isolated human GCs, were plated on p35 cell culture dishes, washed thoroughly with pure DMEM/F12 on culture day 1 and kept at 37 °C, 5% CO₂ and 95% humidity until experimental use. Cells were cultured up to 5 days for this study, and the medium was changed every other day.

RNA isolation and reverse transcriptase quantitative PCR (RT-qPCR)

Cultured human GCs were washed thoroughly with 1 ml phosphate-buffered saline (PBS; Thermo Fisher Scientific) and RNA was isolated using the RNeasy Plus Micro Kit (Qiagen, Hilden, Germany) following the manufacturer's instructions. Depending on the amount of RNA, reverse transcription was performed with 400 ng to 1 µg RNA using random 15-mer primers (Metabion, Planegg, Germany)

and SuperScript II (Invitrogen, Carlsbad, CA, USA). Water within the reaction instead of enzyme served as a non-reverse transcription control, RT-qPCR was performed with 4 ng cDNA in the reaction, and RNA instead of cDNA was used as negative control using the QuantiFast SYBR Green PCR Kit (Qiagen). The mRNA levels of the investigated genes were set in relation to the housekeeper *RPL19* [ratio: $C_q(RPL19) / C_q(\text{gene of interest})$], compared between the coherent fresh and frozen/thawed samples [ratio (frozen/thawed) / ratio (fresh)], and are expressed as the difference between the thawed and fresh samples [Δ : 1 – ratio (frozen/thawed) / ratio (fresh)]. Detailed information about the oligonucleotide primers is depicted in Table 1.

Proteomics

Proteomic analysis was performed on culture day 3 with fresh and frozen/thawed human GCs from three individual batches. In brief, human GCs (1×10^5) were detached from the plate using Trypsin–EDTA solution (L2143, Biochrom GmbH, Berlin, Germany), and the reaction was stopped with 1.5 ml DMEM/F12 supplemented with 1% P/S and 10% FCS. The cells were washed three times with 1 ml PBS, and after the third washing step the excess liquid was removed and the cell pellet was frozen at -80°C . Samples were processed using the PreOmics iST sample preparation kit (PreOmics GmbH, Planegg/Martinsried, Germany) as recommended by the manufacturer.

For liquid chromatography–mass spectrometry (LC–MS) purposes, desalted peptides were injected in a nanoElute system (Bruker, Billerica, MA, USA) and separated in a 25-cm analytical column (75 μm ID, 1.6 μm C18, IonOpticks) with a 100-min gradient from 2 to 37% acetonitrile in 0.1%

formic acid. The effluent from the high-performance (HP)LC was directly electrosprayed into a hybrid trapped ion mobility-quadrupole time-of-flight mass spectrometer (timsTOF Pro, Bruker Daltonics, Bremen, Germany) using the nano-electrospray ion source at 1.4 kV (CaptiveSpray, Bruker Daltonics). The timsTOF was operated at 100% duty cycle in data-dependent mode to automatically switch between one full TIMS-MS scan and ten PASEF [parallel accumulation–serial fragmentation] MS/MS scans in a range from 100 to 1700 m/z in positive electrospray mode with an overall acquisition cycle of 1.23 s. The ion mobility was scanned from 0.6 to 1.60 Vs/cm^2 with TIMS ion charge control set to $5e4$, RF potential of 300 Vpp. The TIMS dimension was calibrated linearly using four selected ions from the Agilent ESI LC/MS tuning mix [m/z , 1/KO: (322.0481, 0.7318 Vs/cm^2), (622.0289, 0.9848 Vs/cm^2), (922.0097, 1.1895 Vs/cm^2), (1221.9906, 1.3820 Vs/cm^2)] (Agilent Technologies, Inc., Santa Clara, CA, USA). MaxQuant 1.6.10.43 was used for protein identification and label-free quantitation (LFQ) with the following parameters: Database, Uniprot_AUP000005640_Hsapiens_20200120.fasta; MS tol, 10 ppm; MS/MS tol, 20 ppm Da; Peptide false discovery rate (FDR), 0.1; Protein FDR, 0.01 Min. peptide length, 7; Variable modifications, oxidation (M); Fixed modifications, carbamidomethyl (C); Peptides for protein quantitation, razor and unique; Min. peptides, 1; Min. ratio count, 2. Identified proteins were considered as differential if their \log_2 fold change (LFQ) values were higher than \log_2 . The list of all proteins detected is provided in the supplementary data (S1). The data were analyzed with Perseus software (Computation Systems Biochemistry, Martinsried, Germany). The mass spectrometry proteomics data were deposited to the ProteomeXchange Consortium via the PRIDE (Proteomics

Table 1 Oligonucleotide primer sequences, annealing temperatures, amplicon sizes and references

Gene	Sequence	Annealing temperature ($^\circ\text{C}$)	Amplicon size (bp)	GenBank ID
<i>COX4</i>	5'-AGC GAG CAA TTT CCA CCT CT-3' 5'-TCA CGC CGA TCC ATA TAA GCT-3'	59	90	NM_001318797.1
<i>CYP11A1</i>	5'-TCG GCA GCC TGG AAG AAA GAC C-3' 5'-GGC GCT CCC CAA AAA TGA CG-3'	59	226	NM_001099773.2
<i>CYP19A1</i>	5'-GCT ACC CAG TGA AAA AGG GGA-3' 5'-GCC AAA TGG CTG AAA GTA CCT AT-3'	59	140	NM_000103
<i>GJA1</i>	5'-CAA TCA CTT GGC GTG ACT TC-3' 5'-CCT CCA GCA GTT GAG TAG GC-3'	60	120	NM_000165
<i>OPA1</i>	5'-CTC TGC AGG CTC GTC TCA AG-3' 5'-CAC ACT GTT CTT GGG TCC GA-3'	60	108	NM_130831.2
<i>RPL19</i>	5'-AGG CAC ATG GGC ATA GGT AA-3' 5'-CCA TGA GAA TCC GCT TGT TT-3'	59	199	NM_000981.3
<i>StAR</i>	5'-ACG TGG ATT AAC CAG GTT CG-3' 5'-CAG CCC TCT TGG TTG CTA AG-3'	58	149	NM_000349
<i>TOMM20</i>	5'-CCC CAA CTT CAA GAA CAG GC-3' 5'-GAT GGT CTA CGC CCT TCT CA-3'	60	185	NM_014765.3

Identifications Database) partner repository with the dataset identifier PXD025632.

Progesterone measurements

On culture day 3, fresh and frozen/thawed human GCs ($n=5$ each) were starved for 2 h in colorless DMEM/F12 without any supplements and then treated with 10 IU/ml human chorionic gonadotropin (hCG; Sigma-Aldrich) or corresponding solvent control (0.01 M NaH_2PO_4 , Sigma-Aldrich), respectively, for 24 h in the same medium. Supernatant was collected and stored at -20°C for measurement of progesterone content using the IMMULITE 2000 XPi immunoassay system (Siemens Healthineers, Erlangen, Germany). The quality of the measurement is being assessed regularly, as this system is used for routine clinical measurements. The inter-assay and intra-assay coefficients of variation are 0.059 and 0.036, respectively.

Cells were washed with cold PBS and protein was isolated using RIPA buffer supplemented with protease and phosphatase inhibitors (Thermo Fisher Scientific). Total protein amount was determined via the Lowry assay (DCTM Protein Assay; Bio-Rad Laboratories, Inc., Hercules, CA, USA) by measuring the absorbance values at 690 nm (FLU-Ostar OPTIMA, BMG LABTECH GmbH, Ortenberg, Germany) and interpolating the individual samples to a defined standard curve of bovine serum albumin (BSA, GE Healthcare, Solingen, Germany) dissolved in RIPA buffer ranging from 0 to 1.5 $\mu\text{g}/\mu\text{l}$, as described before (Blohberger et al. 2016). Protein values were used for normalization of measured progesterone levels.

Data analysis and statistics

Microscopical images were captured using a Leica DM IL LED microscope (Leica Microsystems GmbH, Wetzlar, Germany), equipped with a $\times 10$ objective (HI Plan CY $\times 10/0.25$ dry, Leica Microsystems) and a monochrome camera (DFC3000 G, Leica Microsystems) with the corresponding software (Leica Applications Suite X, version 3.7.0.20979, Leica Microsystems). Pictures were brightness and contrast adjusted using Fiji (open source image processing package for imageJ).

RT-qPCR data sets and progesterone measurements were analyzed using Microsoft Excel (2018, Microsoft, Redmond, WA, USA), and statistical analysis was performed with GraphPad Prism 7 software (GraphPad Software, San Diego, CA, USA). Normal distribution was assessed (Shapiro–Wilk normality test, $\alpha=0.05$), and one-way analysis of variance (ANOVA) was used for comparison of relative mRNA expression levels of fresh and frozen/thawed human GCs. A paired two-tailed t -test was used for comparison of progesterone levels and cell survival rates after 3 days in

culture of fresh and frozen/thawed human GCs. α was set to 0.05 ($*p<0.05$, $**p<0.01$, $***p<0.001$), and data are depicted as mean \pm SEM.

Results

Cell survival rate and gene expression

To examine, whether human GCs tolerate the freezing/thawing procedure, we counted the cells both directly after the isolation and after cryopreservation and thawing. The mean cell number directly after isolation amounted to $422,375 \pm 57,910$ counted cells and after cryopreservation and following thawing, a total of $339,688 \pm 54,460$ cells could be counted ($n=16$ each). The results indicate that $77.8 \pm 3.2\%$ ($n=16$) of human GCs survived the procedure of cryopreservation and thawing (Fig. 1a). Inspection by light microscopy indicated that the freezing and thawing process had no discernable influence on the general morphology (shape and size) of the cells. Both the fresh (left) and the frozen/thawed cells (right) showed typical clustering (Fig. 1b). To further investigate to which degree human GCs tolerate cryopreservation, corresponding fresh and frozen/thawed cells were counted after 3 days in culture (Fig. 1c). Freshly isolated and seeded human GCs exhibited a survival rate of $89.6 \pm 3.3\%$ after 3 days in culture, which is statistically indistinguishable from the survival rate of cryopreserved cells, at $93.0 \pm 1.4\%$ ($p=0.4885$, $n=4$).

Next we isolated mRNA from freshly isolated and seeded human GCs and their frozen/thawed counterparts at different cell culture days (days 1–5) to examine key markers by RT-qPCR. We focused on gap junctional cell–cell contact mitochondrial and steroidogenic markers (Fig. 2). For both the analyzed cell–cell contact marker *GJAI*, essential for gap junction formation, and all investigated mitochondrial markers—i.e. *COX4*, an important component of the mitochondrial electron transport chain; *OPA1*, essential for mitochondrial fusion process; and *TOMM20*, required for recognition and translocation of mitochondrial pre-proteins across the outer mitochondrial membrane—slight variability could be observed, which did not reach statistical significance independently of the cell culture day studied. Regarding mRNA levels of three important steroidogenic genes—i.e. *CYP11A1*, catalyzing the cholesterol cleavage to pregnenolone; *CYP19A1*, catalyzing for conversion of androgens to estrogens; and *StAR*, essential for steroid hormone synthesis—the strongest differences were found in terms of reduced expression levels in the frozen/thawed human GCs. However, only the mRNA level of *StAR* at cell culture day 5 was slightly, yet statistically significantly, lower (-0.084 ± 0.03 , $p=0.026$) compared to corresponding coeval freshly isolated and seeded cells.

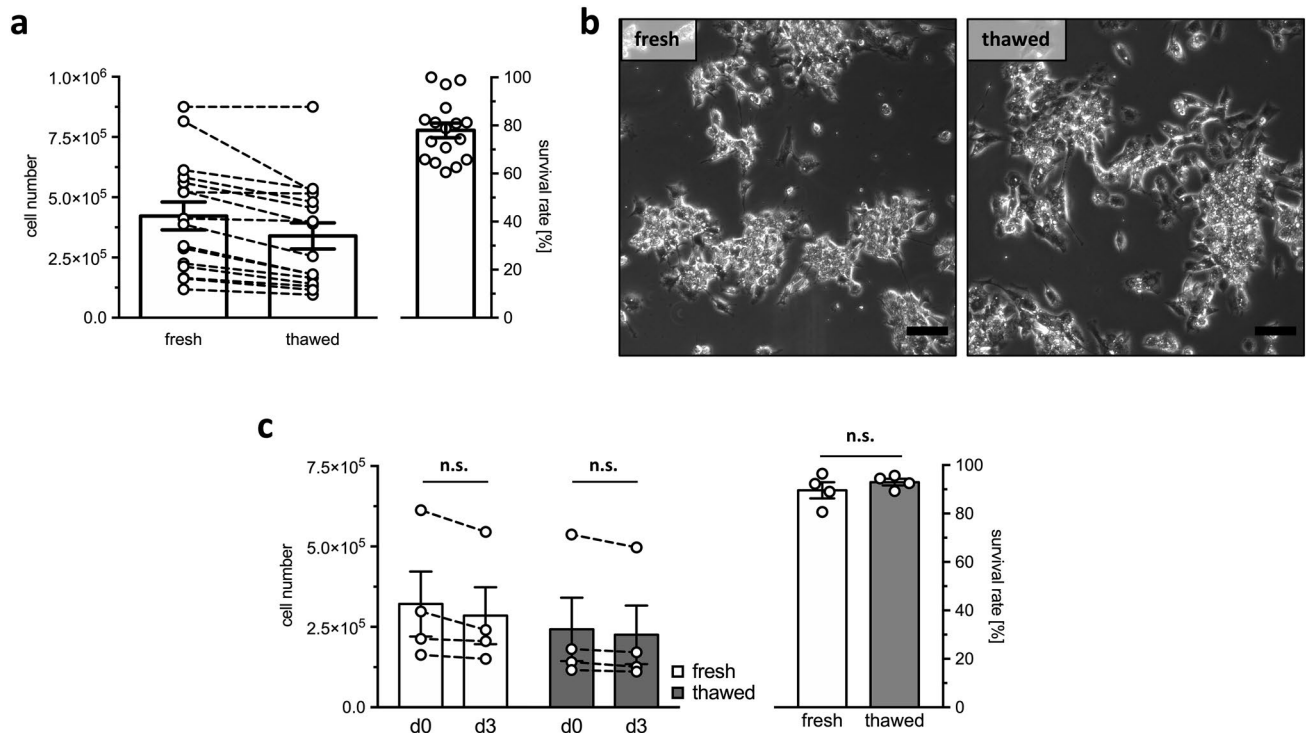


Fig. 1 Cell numbers, survival rate and morphological appearance of fresh and frozen/thawed human GCs. **a** Cell numbers of fresh and frozen/thawed cells (left panel) and survival rate (%) of human GCs after freezing and thawing (right panel), depicted as mean \pm SEM ($n=16$ each). **b** Phase-contrast images of fresh (left) and frozen/thawed (right) human GCs on culture day 3. No difference in morphological appearance of the cells was observed and both fresh and frozen/thawed cells showed typical clustering. Scale bar 100 μm . **c** Cell numbers of fresh (white bars) and frozen/thawed cells (grey

bars) on culture days 0 and 3, depicted as mean \pm SEM ($n=4$ each), and values of individual batches, with dashed lines representing coherent counts (left panel). Survival rate (%) of fresh (white bar) and frozen/thawed human GCs after 3 days in culture (right panel), depicted as mean \pm SEM ($n=4$ each). Upon given normal distribution of data sets (Shapiro–Wilk normality test, $\alpha=0.05$), both cell numbers and survival rates were statistically analyzed using a paired two-tailed t -test, $\alpha=0.05$; *n.s.* not significant

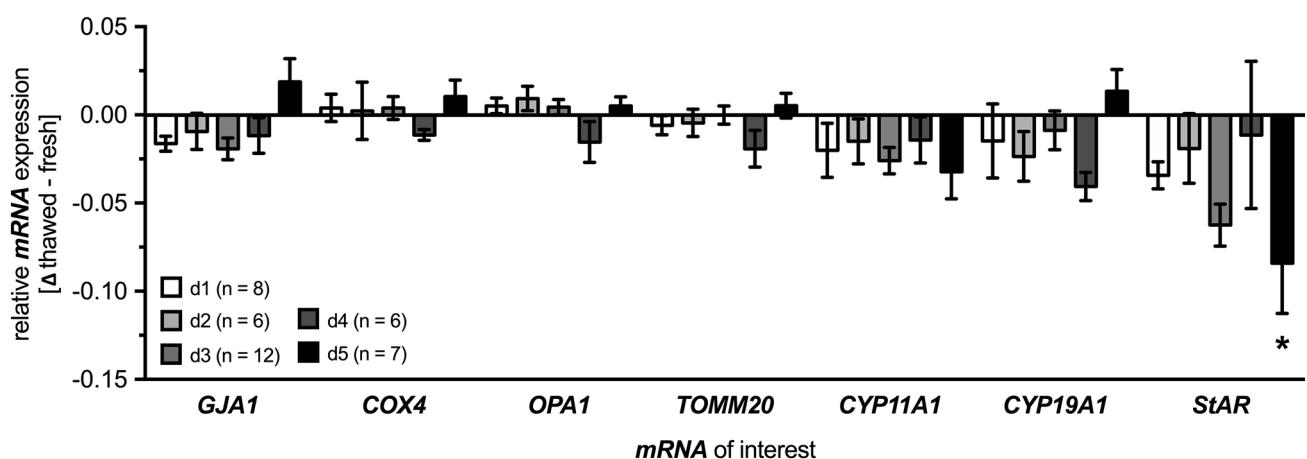


Fig. 2 Relative mRNA expression levels in frozen/thawed human GCs. mRNA expression levels of marker genes for cell–cell contact (*GJA1*) and mitochondrial (*COX4*, *OPA1*, *TOMM20*) and steroidogenic function (*CYP11A1*, *CYP19A1*, *StAR*) in frozen/thawed human

GCs compared to their coherent freshly isolated and seeded cells, harvested on cell culture days 1–5 (d1–5); mean \pm SEM ($n=6$ –12). One-way ANOVA, $\alpha=0.05$; * $p < 0.05$

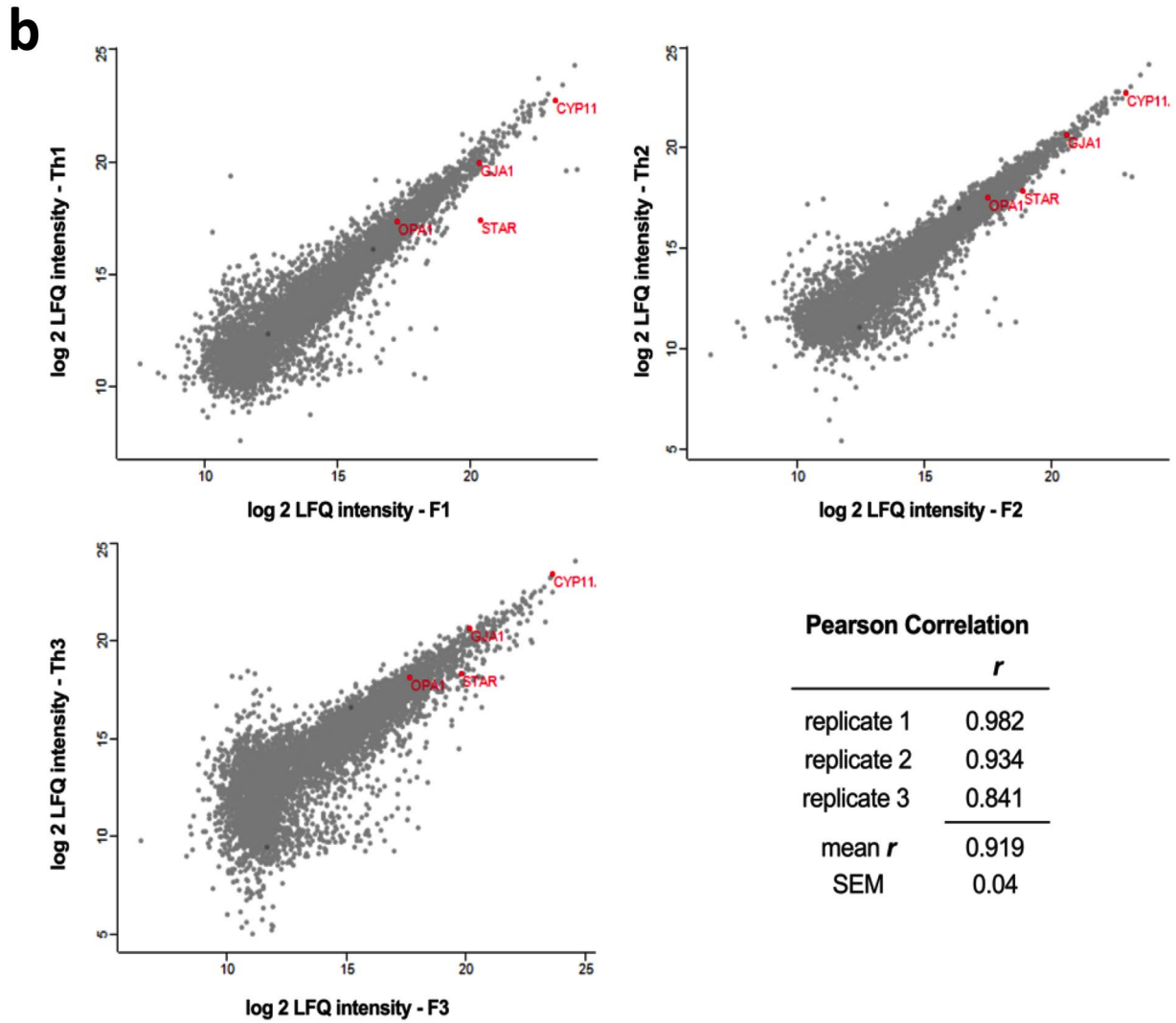
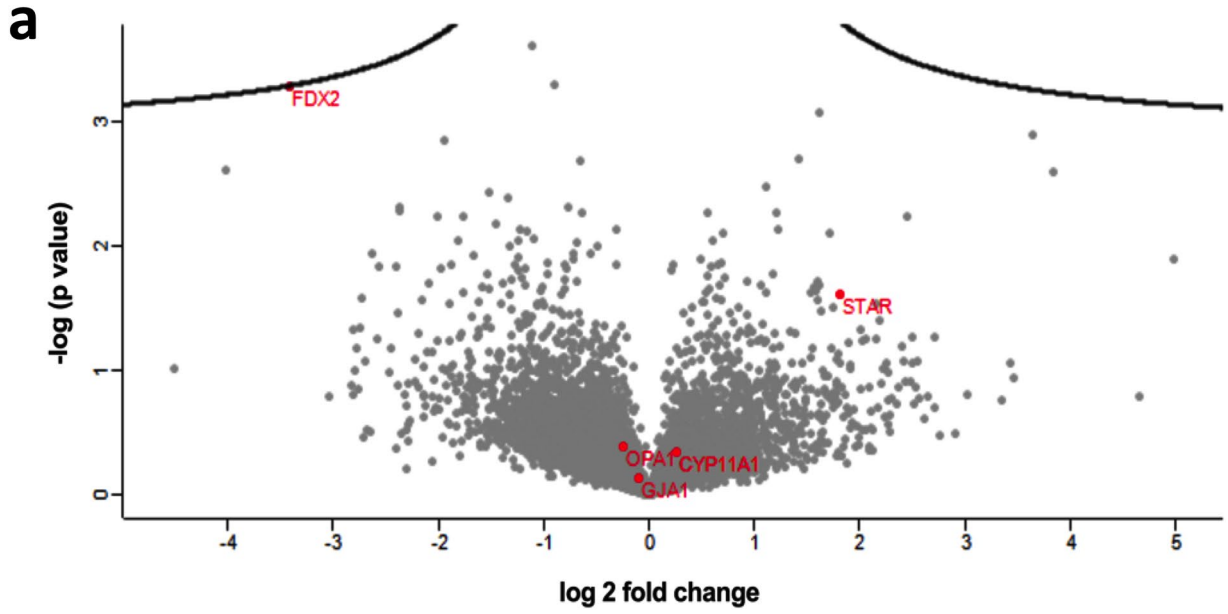


Fig. 3 Proteomics data of freshly isolated and seeded human GCs and the corresponding frozen/thawed cells. **a** Volcano Plot of differentially regulated proteins in response to freezing and thawing. Fresh and frozen/thawed human GCs from culture day 3 were harvested and proteins were quantified by mass spectrometry. Proteins were plotted by difference (log twofold change) and significance ($-\log_{10} p$ -value) using a false discovery rate (FDR) of 0.45 and a minimal fold change (s_0) of 0.1. No significant up- or downregulation was observed for the 5962 analyzed proteins using Perseus software. **b** Scatter Plots of relative protein amount in response to freezing and thawing from the three biological replicates. Log₂ LFQ intensities of fresh (F) and frozen/thawed (Th) human GCs are compared, and the corresponding Pearson correlation coefficients are depicted, indicating a strong linear relation of the protein amount. Genes also analyzed by RT-qPCR are indicated in red, and the position of the FDX2 is given

Proteomics data analysis

To explore differences that may exist between freshly isolated human GCs and cryopreserved and subsequently thawed cells, a proteomics data analysis was performed. To this end, fresh and frozen/thawed cells of three biological replicates were harvested on cell culture day 3 and analyzed by means of mass spectrometry. In total, 5962 proteins were detected (see Supplementary data), and differences in protein levels between the fresh and frozen/thawed human GCs were visualized in a volcano plot (Fig. 3a). Even at very generous conditions, with a false discovery rate (FDR) of 0.45 and a minimal fold change (s_0) of 0.1, no significant up- or downregulation was observed. Even ferredoxin 2 (FDX2), essential for heme A and iron-sulfur protein biosynthesis, which showed the largest aberrance, was within this range.

Furthermore, the individual biological replicates show very strong positive correlations, with a mean Pearson correlation coefficient r of 0.919 ± 0.04 , distinguishable by the scatter plots shown in Fig. 3b.

Progesterone levels

To further examine the potential influence of freezing and thawing on the ability to produce progesterone, we studied this point on cell culture day 3. Both freshly isolated and seeded human GCs and frozen/thawed GCs ($n = 5$ each) were treated with 10 IU/ml hCG or corresponding solvent control for 24 h, and supernatants were examined for their progesterone content (Fig. 4).

Under control conditions, supernatants of freshly isolated and seeded human GCs contained 408.6 ± 123.0 ng/ml progesterone, statistically indistinguishable from the levels of supernatants from frozen/thawed cells with 260.5 ± 95.2 ng/ml progesterone under these conditions ($p = 0.0901$). Upon administration of hCG, the level of progesterone increased significantly in the supernatants from both groups (fresh: 836.9 ± 196.1 ng/ml, $p = 0.007$; frozen/thawed: 985.2 ± 290.2 ng/ml, $p = 0.0228$), compared to the

corresponding control supernatants. The levels of progesterone in supernatants from freshly isolated and seeded human GCs and frozen/thawed cells upon hCG administration were similar ($p = 0.4799$).

Discussion and conclusion

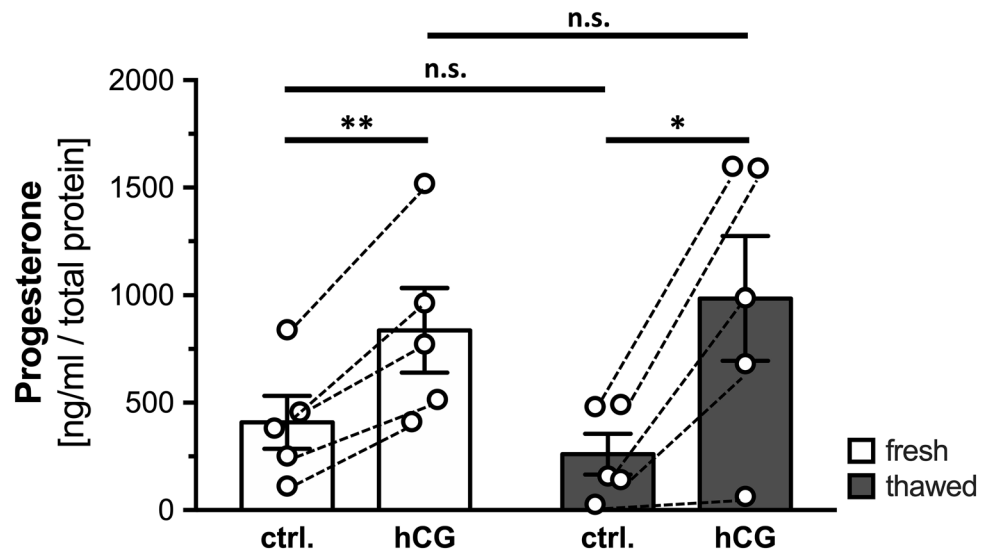
The research with primary, patient-derived human GCs holds promise for human-focused research, especially because human GCs in vitro are an apt model for the ovulatory follicle and the corpus luteum (Bagnjuk and Mayerhofer 2019). In practical terms, work with human GCs has limitations, particularly with respect to daily availability of comparable cells, given the source (i.e., individual patients) and the rapidly changing phenotype of cultured human GCs.

We reasoned that cryopreservation of human GCs may allow the collection of comparable cells over time, and thus may foster more precise, as well as large-scale experiments. We therefore tested whether a routine freezing method, used for cell lines in our laboratory, is also suitable for human GCs. We initially observed that human GCs tolerate the freezing/thawing procedure rather well and thus we performed a thorough investigation to examine consequences on cell composition and function.

Several freezing methods have been tested for ovarian tissue and its cells (Bouillon et al. 2020; Kokotsaki et al. 2018; Pietrowski et al. 2020; Rivas Leonel et al. 2019; Santana et al. 2012; Sluss et al. 1994), including human GCs and the human granulosa tumor cell line KGN. Cryopreservation by slowly freezing using a cryoprotectant and ultra-fast freezing by vitrification were tested, employing DMSO or ethylene glycol solutions (Kokotsaki et al. 2018). In these studies, usually only a few cell parameters were evaluated, with a focus on cell survival or cell death, respectively (Kokotsaki et al. 2018).

Sluss et al. and Bouillon et al. studied human GCs. In the more recent study (Bouillon et al. 2020), employing human GCs, two different freezing protocols were compared. The authors report that GCs tolerate both procedures, albeit with a rather poor survival rate of 45–58%, while survival of only about 32% was described in the older study by Sluss et al. (1994). The surviving cells remained responsive to follicle-stimulating hormone (FSH) stimulation after freezing/thawing, although FSH efficacy was decreased (Bouillon et al. 2020). The study compared freezing of cell pellets directly derived from follicular fluids, without further purification steps and freezing of cells after a Percoll purification step to remove red blood cells. In both cases, a solution containing 90% FCS and 10% DMSO and a concentration of 1×10^6 cells/ml and vial were used. A detailed description of the actual freezing method is, however, not provided. Our present study tried to find a simple, readily available

Fig. 4 Progesterone levels in the supernatants from freshly isolated and seeded human GCs and the corresponding frozen/thawed cells. Progesterone levels in the supernatants from freshly isolated and seeded human GCs (white bars) and frozen/thawed cells (grey bars) after administration of 10 IU/ml hCG (hCG) and corresponding solvent control (ctrl.) for 24 h on cell culture day 3. Values are mean \pm SEM ($n=5$ each), coherent measurements are depicted by dashed lines. Paired two-tailed t -test, $\alpha=0.05$; * $p<0.05$, ** $p<0.01$, n.s. not significant



freezing method also involving FCS and DMSO, and hence we adopted a method used in our laboratory for cell lines, including KGN cells. The results indicated a loss of about 20% of the cells, which may be partly related to the cytotoxic effect of DMSO (Santos et al. 2003). The survival rate of about 80% is, however, tolerable from a practical point of view. It is comparable to the one reported for the human GC line KGN (Kokotsaki et al. 2018; Pietrowski et al. 2020), in which related slow freezing methods were employed, and it is much higher than the low survival rate reported by a recent study of human GCs (Bouillon et al. 2020).

Furthermore, we found that when cells were cultured for 3 days, the survival rate of freshly plated human GCs did not differ from that of their frozen/thawed counterparts.

To thoroughly examine further consequences of the method, we first performed RT-qPCR screening of key markers of human GCs, namely the major gap junction gene *GJA1*, mitochondrial and steroidogenic genes, along with mass spectrometry analysis. The RT-qPCR results revealed no significant differences in transcript levels of selected genes between the groups of fresh and frozen/thawed cells, except for *StAR*, which was slightly reduced in frozen/thawed cells, albeit only < 10% and only on culture day 5. Most likely this small change in mRNA abundance is not of biological relevance.

A thorough analysis of three batches of cells was performed on culture day 3, employing mass spectrometry. With this approach, we monitored almost 6000 proteins, and none of them differed in abundance between the two groups.

Further, we examined the ability of fresh and frozen/thawed cells to produce progesterone, the major steroid of the corpus luteum. No difference was found in either basal or hCG-stimulated production of this hormone. Hence, the frozen/thawed and the fresh cells are virtually indistinguishable from each other. Sluss et al. also measured steroids, i.e.

basal production of estradiol and progesterone (Sluss et al. 1994). For cryopreserved cells, basal sex steroid secretion was reduced after cryopreservation (20% for estradiol and approximately 50% for progesterone), while aromatase activity was not different. While we did not examine estradiol syntheses directly, unchanged aromatase levels in the proteome analysis indicate that this function is fully retained. Furthermore, basal and stimulated progesterone production indicate that neither LH receptor signaling nor steroid machinery suffer from freezing/thawing.

In summary, we describe a simple, readily available method, which allows cryopreservation of human GCs upon isolation from follicular fluid. The human GCs retained their integrity and functionality. Furthermore, only 20% of the cells did not survive the procedure. The surviving 80% were functionally indistinguishable from fresh, non-cryopreserved human GCs. We anticipate that this method, which is superior to previously described methods, may facilitate future studies.

Supplementary Information The online version contains supplementary material available at <https://doi.org/10.1007/s00418-021-02019-3>.

Acknowledgements We thank Carola Herrmann, Kim-Gwendolyn Dietrich and Nicole Kreitmair for expert technical assistance, and Karin Metzrath for editorial help.

Author contributions SB and KE performed the cellular studies and evaluated the data. NB performed progesterone measurements, IF conducted and analyzed the mass spectrometry examination, DB and UB provided access to human GCs and conceptual input. AM conceived of the study and supervised the work. Together with KE and SB, he drafted the paper. All authors contributed to the final version and approved it.

Funding Open Access funding enabled and organized by Projekt DEAL. This study was supported in part by the Deutsche Forschungsgemeinschaft (DFG), project number 456828204.

Data availability The mass spectrometry proteomics data have been deposited to the ProteomeXchange Consortium (<https://www.ebi.ac.uk/pride/>) via the PRIDE [1] partner repository with the dataset identifier PXD025632.

Declarations

Conflict of interest The authors declare no conflict of interest.

Ethical approval The use of human cells was approved by the Ethics Committee of LMU (Project number 20-697).

Consent to participate By written consent, patients agreed to the scientific use of biological material, as part of ongoing projects within the framework of a DFG-funded project (project 456828204).

Open Access This article is licensed under a Creative Commons Attribution 4.0 International License, which permits use, sharing, adaptation, distribution and reproduction in any medium or format, as long as you give appropriate credit to the original author(s) and the source, provide a link to the Creative Commons licence, and indicate if changes were made. The images or other third party material in this article are included in the article's Creative Commons licence, unless indicated otherwise in a credit line to the material. If material is not included in the article's Creative Commons licence and your intended use is not permitted by statutory regulation or exceeds the permitted use, you will need to obtain permission directly from the copyright holder. To view a copy of this licence, visit <http://creativecommons.org/licenses/by/4.0/>.

References

- Amorim CA, Curaba M, Van Langendonck A, Dolmans MM, Donnez J (2011) Vitrification as an alternative means of cryopreserving ovarian tissue. *Reprod Biomed Online* 23:160–186. <https://doi.org/10.1016/j.rbmo.2011.04.005>
- Bagnjuk K, Mayerhofer A (2019) Human luteinized granulosa cells—a cellular model for the human corpus luteum. *Front Endocrinol (lausanne)* 10:452. <https://doi.org/10.3389/fendo.2019.00452>
- Baufeld A, Vanselow J (2018) A tissue culture model of estrogen-producing primary bovine granulosa cells. *J vis Exp*. <https://doi.org/10.3791/58208>
- Blohberger J, Buck T, Berg D, Berg U, Kunz L, Mayerhofer A (2016) L-DOPA in the human ovarian follicular fluid acts as an antioxidant factor on granulosa cells. *J Ovarian Res* 9:62. <https://doi.org/10.1186/s13048-016-0269-0>
- Bouillon C, Guérif F, Monget P, Maurel MC, Kara E (2020) Effect of cryopreservation on human granulosa cell viability and responsiveness to gonadotropin. *Cell Tissue Res* 379:635–645. <https://doi.org/10.1007/s00441-019-03123-6>
- Bulling A et al (2000) Identification of an ovarian voltage-activated Na⁺-channel type: hints to involvement in luteolysis. *Mol Endocrinol* 14:1064–1074. <https://doi.org/10.1210/mend.14.7.0481>
- Kokotsaki M, Mairhofer M, Schneeberger C, Marschalek J, Pietrowski D (2018) Impact of vitrification on granulosa cell survival and gene expression. *Cryobiology* 85:73–78. <https://doi.org/10.1016/j.cryobiol.2018.09.006>
- Pietrowski D, Mladek R, Frank M, Erber J, Marschalek J, Schneeberger C (2020) Analyses of human granulosa cell vitality by fluorescence activated cell sorting after rapid cooling. *Hum Fertil (Camb)*. <https://doi.org/10.1080/14647273.2020.1817578>
- Rivas Leonel EC, Lucci CM, Amorim CA (2019) Cryopreservation of human ovarian tissue: a review. *Transfus Med Hemotherapy* 46:173–181. <https://doi.org/10.1159/000499054>
- Saller S et al (2014) Dopamine in human follicular fluid is associated with cellular uptake and metabolism-dependent generation of reactive oxygen species in granulosa cells: implications for physiology and pathology. *Hum Reprod* 29:555–567. <https://doi.org/10.1093/humrep/det422>
- Santana LN, Van den Hurk R, Oskam IC, Brito AB, Brito DC, Domingues SF, Santos RR (2012) Vitrification of ovarian tissue from primates and domestic ruminants: an overview. *Biopreserv Biobank* 10:288–294. <https://doi.org/10.1089/bio.2011.0048>
- Santos NC, Figueira-Coelho J, Martins-Silva J, Saldanha C (2003) Multidisciplinary utilization of dimethyl sulfoxide: pharmacological, cellular, and molecular aspects. *Biochem Pharmacol* 65:1035–1041. [https://doi.org/10.1016/s0006-2952\(03\)00002-9](https://doi.org/10.1016/s0006-2952(03)00002-9)
- Shi Q, Xie Y, Wang Y, Li S (2017) Vitrification versus slow freezing for human ovarian tissue cryopreservation: a systematic review and meta-analysis. *Sci Rep* 7:8538. <https://doi.org/10.1038/s41598-017-09005-7>
- Sluss PM, Lee K, Mattox JH, Smith PC, Graham MC, Partridge AB (1994) Estradiol and progesterone production by cultured granulosa cells cryopreserved from in vitro fertilization patients. *Eur J Endocrinol* 130:259–264. <https://doi.org/10.1530/eje.0.1300259>
- Youm HW, Lee JR, Lee J, Jee BC, Suh CS, Kim SH (2014) Optimal vitrification protocol for mouse ovarian tissue cryopreservation: effect of cryoprotective agents and in vitro culture on vitrified-warmed ovarian tissue survival. *Hum Reprod* 29:720–730. <https://doi.org/10.1093/humrep/det449>
- Zheng YX, Ma LZ, Liu SJ, Zhang CT, Meng R, Chen YZ, Jiang ZL (2019) Protective effects of trehalose on frozen-thawed ovarian granulosa cells of cattle. *Anim Reprod Sci* 200:14–21. <https://doi.org/10.1016/j.anireprosci.2018.11.005>

Publisher's Note Springer Nature remains neutral with regard to jurisdictional claims in published maps and institutional affiliations.

4 Discussion

Membrane proteins resemble gateways within the otherwise unbreachable barrier embodied by the biological membrane and amount to approximately one third of the whole human proteome. This group of proteins also includes ion channels (Ahram et al., 2006; Alexander et al., 2011). Profound knowledge about a tissue's channelome and the associated functional roles of the distinct ion channels is essential. Once established, it can assist to distinguish, understand and potentially also manipulate the impact of ion channels upon tissue function, both in health and disease.

The 'mysterious' and non-selective cation channel TRPV2, clustering a huge clutch of secrets and controversies around itself since its first description in 1999, was recently demonstrated to be expressed in the human ovary and the human testis. Moreover, it can also be found in murine testicular tissue (Perálvarez-Marín et al., 2013; Flenkenthaler et al., 2014; Guo et al., 2018; Zhang et al., 2018b; Fan et al., 2019). Since gonadal TRPV2 expression has been completely unknown, this fact encouraged us to examine the cellular distribution and the functional scope of this ion channel. In addition, a method for cryopreservation of IVF patients-derived primary human granulosa cells (hGCs) was introduced to provide a basis for prospective cellular experiments, also with regard to functional examination of ovarian TRPV2.

4.1 TRPV2 - a new Player within the Gonadal Channelome

In the human testis, TRPV2 expression turned out to be mainly but not exclusively located in the myoid peritubular cells, HTPCs. In these cells, channel functionality was demonstrated upon short-term application of the known activator CBD using Ca^{2+} imaging experiments. Long-term exposure to CBD induced increased transcriptional expression and secretion of several cytokines. Especially the pro-inflammatory and pro-angiogenic chemokine interleukin 8 (IL-8), and other inflammatory factors, such as the chemokine *monocyte chemoattractant protein-1 (MCP-1)* and *osteopontin*, acting as chemotactic protein, amongst others, were elevated. Transfection with siRNA targeted against TRPV2 prevented these observations.

Of note, HTPCs remain the only human testicular cells, which can be isolated and cultured and thus are accessible to examination. Consequently, roles of TRPV2 in other testicular cells that also express TRPV2 cannot be readily evaluated. Channel expression was also found in Sertoli cells and cells of the interstitial space, presumably including macrophages. However, further studies are required to identify and characterize these TRPV2-positive cells of the human testis (Eubler et al., 2018).

In the human ovary, TRPV2 was identified in various cell types, including typical ovarian cells, i.e. theca and granulosa cells, and immune cells, for instance NK cells and T-lymphocytes (Zhang et al., 2018b; Fan et al., 2019; Bagnjuk et al., 2019a). In granulosa cells, TRPV2 expression increased during follicular development, emphasizing its potential importance in the physiology of the female reproduction (Zhang et al., 2018b). Yet the examination of such roles are hampered by the limited availability and quantity of IVF patients-derived primary human granulosa cells, hGCs. Our recently published rapid and robust method for cryopreservation of hGCs could help to improve this situation (Beschta et al, 2021).

The laboratory mouse is a standard model organism and was examined for gonadal TRPV2 expression. Male wild-type mice exhibit a testicular TRPV2 expression pattern comparable to the human, in general, with expression detected within the peritubular wall and the interstitial space. The cells expressing TRPV2 are peritubular cells and macrophages. Murine peritubular cells transferred to in vitro cell culture conditions retained TRPV2 expression. A detailed investigation of macrophages derived from testicular tissue lysates revealed stronger TRPV2 expression in the peritubular located, CD206 positive population, compared to the interstitially situated, MHC II positive one. Tissue incubation experiments with CBD generated elevated transcriptional levels of several chemo- and cytokines, i.e. *C-X-C motif chemokine ligand 1* and *2* and *IL-6*. In addition, testicular samples derived from the transgenic mouse line AROM⁺, generally accepted as animal model for male infertility associated with sterile inflammation, feature a strong infiltration of macrophages that aggravates with age. These macrophages give rise to a new and unusual subpopulation and thus introduce higher expression levels of TRPV2 within the testis (Eubler et al., 2021).

Furthermore, a preliminary survey with gonadal tissue from female animals detected TRPV2 expression predominantly in granulosa cells associated with growing follicles and in yet not further identified cells within the ovarian connective tissue (unpublished data). However, channel functionality in any of these cells still awaits respective and profound examination.

4.2 Gonadal TRPV2 - strong Evidence for Immunological Importance

In summary, the newly acquired insights in the gonadal expression patterns of TRPV2 in human and mouse and the functional results provide evidence for the involvement of this channel in immunological processes of the gonads, involving both somatic cells and immune cells.

i. Somatic Cells

Proven functional expression of TRPV2 by the smooth-muscle-like HTPCs resulted in increased transcript levels of several cytokines and chemokines, such as *IL-6*, *IL-8* and *MCP-1*, and secretion of IL-8 (Eubler et al., 2018). Similar observations have been made in human primary periodontal ligament cells that express functional TRPV2. Channel activation upon thermal stress or application of 2-APB induced increased intracellular Ca^{2+} concentrations followed by transcriptional elevation of both *IL-6* and *IL-8* that could be reduced in presence of a Ca^{2+} chelator. The authors conclude that the inflammatory response upon thermal stress depends on the expression of thermosensitive TRPs, i.e. V1-4, M8 and A1, by these cells (Son et al., 2015). Moreover, TRP channels have been demonstrated to be of essential importance for functionality and survival of vascular smooth muscle cells of rabbit, mouse, rat and human (Fantozzi et al., 2003; Park et al., 2003; Beech, 2005; Peng et al., 2010). Vascular smooth muscle TRPs, involving besides TRPV2 also C1, C3-6, P1, P2, M4 and M7, are suggested to be involved in the proliferation, in the modulation of cell contractility, in the regulation of changes in intracellular Ca^{2+} concentrations and in the detection of osmotic stress, thus influencing the myogenic tone and phenotype of these cells (Muraki et al., 2003; Beech, 2005; Perálvarez-Marín et al., 2013). As HTPCs represent smooth-muscle-like cells, it seems conceivable that TRPV2-mediated Ca^{2+} conductance may be involved in contractility and proliferation of these testicular cells, being essential for the pulsatile contractions along the

seminiferous tubules to transport immotile sperm. However, these possibilities remain to be studied.

Besides peritubular cells, also Sertoli cells stained positive for TRPV2 expression as seen upon immunohistological examination of human testicular sections. This somatic cell is essential for hormone secretion, nourishment of the developing germ cells, proper spermatogenesis, but also for the establishment and maintenance of the belt-like blood-testis-barrier and the spermatogonial stem cell niche. Beyond that, Sertoli cells function as phagocytes and as such engulf dead spermatocytes and residual sperm cytoplasm (Griswold, 1998; Peterson & Soder, 2006; Johnson et al., 2008; Meroni et al., 2019). The process of phagocytosis crucially depends on ionic fluxes and thus hinges upon ion channels (Edberg et al., 1998; Uribe-Querol & Rosales, 2020). In 2010, Link and colleagues demonstrated that TRPV2 plays a central and pivotal role in phagocytotic capacity of macrophages (Link et al., 2010) and consequently, it might be possible that TRPV2 is also of special importance for phagocytotic activity of Sertoli cells.

In the human ovary, TRPV2 expression was detected in granulosa cells, i.e. the major somatic cell type of the follicle, and showed developmental increases during follicle maturation (Zhang et al., 2018b; Bagnjuk et al., 2019a). Functional examination is still missing, but it appears conceivable that the intraovarian bio-mechanic situation, e.g. changes in pressure due to follicle growth associated with increasing amount of follicular fluid, could be sensed by TRPV2, as demonstrated for Chinese hamster ovary cells over-expressing TRPV2 (Muraki et al., 2003; McGohan et al., 2016). Thus, channel activation could be involved in the transformation of granulosa cells to luteinizing/luteinized granulosa cells (Bagnjuk & Mayerhofer, 2019). Further, Assuming comparable reactions downstream of channel activation result as seen in HTPCs, it appears conceivable that TRPV2 is involved in ovarian angiogenesis and thus in the formation of the *corpus rubrum*. With increased secretion of the pro-angiogenic factor IL-8 by granulosa and their developmental successor cells, i.e. large luteal cells, the perifollicular hyperaemia with the associated vascular development and angiogenesis in *corpus rubrum* and *corpus luteum* could be mediated (Xu et al., 2022).

Moreover, Buck and colleagues demonstrated that cultured hGCs produce ROS under basal conditions (Buck et al., 2019), which have been described to sensitize TRPV2, thus leading to channel activation at lower temperatures (Fricke et al., 2019).

ii. Immune Cells

Presence of TRPV2 in immune cells was recognized already during its first description and more details unravelled in the following decades (Caterina et al., 1999). TRPV2 expression was demonstrated in hematopoietic stem cells that give rise to all blood cell types, i.e. myeloid (thrombocytes, erythrocytes, granulocytes, monocytes) and lymphoid (T-lymphocytes, B-lymphocytes, NK cells) lineages. In these cells, TRPV2 plays essential roles in distinct cellular functions such as differentiation, migration, phagocytosis, cytokine production, degranulation and several signalling pathways (Park et al., 2011b; Santoni et al., 2013).

In the murine testis TRPV2 expression was proven in resident and infiltrating macrophage populations (Eubler et al., 2021). Further, TRPV2 emerged as the sole representative of the TRPV family in murine macrophages (Yamashiro et al., 2010), and moreover, TRPV2 was also detected in human macrophages (Kowase et al., 2002). In macrophages, induced channel translocation to the plasma membrane followed by elevated intracellular Ca^{2+} concentrations appeared to be essential for directed cell migration, but is also pivotal for membrane depolarization of the nascent phagosome and thus for particle binding and early phagocytosis (Lévêque et al., 2018; Link et al., 2010; Nagasawa & Kojima, 2012). Consequently, TRPV2-deficient animals suffer from higher pathogen load and exhibit higher mortality (Nagasawa et al., 2007; Link et al., 2010). Besides LPS-induced and TRPV2-mediated changes in intracellular Ca^{2+} concentrations, this cation channel is involved in nuclear factor kappa-B (NF- κ B) signaling leading to expression and production of TNF- α and IL-6 (Yamashiro et al., 2010; Link et al., 2010; Lévêque et al., 2018).

Although not yet proven for gonadal mast cells, TRPV2 is known to be expressed by this cell type, i.e. a *“highly engineered cell with multiple critical biological functions”* (Metcalf et al., 1997) involved in allergic and chronic inflammation, innate immunity, host defense mechanisms and immune-modulation in a tissue-dependent manner.

Channel activation upon stimulation with red laser light, mechanical or thermal stress and subsequent Ca^{2+} fluxes lead to degranulation and thus to the release of inflammatory factors (Stokes et al., 2004; Freichel et al., 2012; Zhang et al. 2012). Of note, this multifaceted cell type represents the major immune effector cell of the human testis (Nistal et al., 1986). Furthermore, male infertility has been associated with increased numbers and a shifted distribution of testicular mast cells that are also involved in fibrotic changes, often seen in testis from infertile men (Meineke et al., 2000; Yamanaka et al., 2000). Interestingly, the antiallergic drug and mast cell blocker tranilast, initially developed for treatment of asthma, has been successfully used on patients suffering from severe oligospermia causing significantly increased sperm counts and pregnancy rates (Schill et al., 1986; Yamamoto et al., 1994 & 1995). At the same time, this agent has been used as TRPV2-specific antagonist in several studies, although direct action on this channel is still unknown (Nie et al., 1997; Hisanaga et al., 2009; Mihara et al., 2010; Perálvarez-Marín et al., 2013). These findings and our observation of TRPV2 expression in human testicular mast cells (Mayerhofer et al, 2018) suggest that testicular mast cell actions leading to inflammatory processes or even infertility might involve TRPV2 channel activation.

4.2 Gonadal TRPV2 - Potential Impact on other Gonadal Channels

“ Ca^{2+} signaling affects every aspect of a cell's life and death. The most tightly regulated ion within all membrane-bound organisms, Ca^{2+} binds to thousands of proteins to effect changes in localization, association, and function” (Clapham, 2007b). However, TRP channel conductance is not exclusively composed of Ca^{2+} fluxes but also includes a big fraction of other cations. With a Ca^{2+} fraction of 5-24 %, the impact of other conducted cations needs to be considered, especially in terms of membrane depolarization (Gees et al., 2010). As TRPV2 is a non-selective cation channel mostly permeable for Ca^{2+} ($P_{\text{Ca}^{2+}}/P_{\text{Na}^+} = 2.94$; Venkatachalam & Montell, 2007), potential impact on other known gonadal channels or processes involved in Ca^{2+} signaling and membrane depolarization needs to be considered.

In excitable cells, TRP channel gating leads to depolarization of the cell membrane and thus regulates and triggers gating of voltage-dependent channels permeable for Ca^{2+} , K^+ and Na^+ (Gees et al., 2010).

Such regulative mechanisms have been shown for the brain, where TRPC3-5, TRPC7 and TRPV1 are present and interact with voltage-gated Ca^{2+} channels (Ramsey et al., 2006; Shibasaki et al., 2007; Li et al., 2010), but also for cardiac muscle and ileal smooth muscle cells, here in a TRPC-dependent manner (Ju & Allen, 2007; Tsvilovskyy et al., 2009). In the human gonads, excitable cells are represented by sperm and the smooth muscle-like testicular peritubular cells. In these cells, weak to moderate transcript expression levels of two voltage-dependent potassium ($\text{K}_v2.1$, $\text{K}_v11.1$) and calcium channels ($\text{Ca}_v1.3$, $\text{Ca}_v3.2$) were found, respectively (Guo et al., 2018), that consequently could be regulated by TRPV2. Contractive actions of adenosine triphosphate on murine and human peritubular cells upon local extracellular application were proven to involve purinergic receptors (Fleck et al., 2021). Assuming that TRPV2-mediated Ca^{2+} influx is sufficient to activate the expressed voltage-dependent channels listed above and thus to elicit cell contraction, it appears conceivable that this mechano-sensitive channel could be involved in propagation of the resulting contractive wave.

In non-excitabile cells, TRP channels are involved in fine-tuning of Ca^{2+} entry by regulating the driving forces for this divalent cation, which was described for TRPC1, TRPC6, TRPM4 and TRPM5 (Nilius & Vennekens, 2006; Vennekens et al., 2007). This fine-tuning encompasses depolarization and hyperpolarization mediated by the interplay of TRP channels and Ca^{2+} -activated K^+ channels, such as BK_{Ca} s, IKs and SKs, amongst others. Moreover, trafficking of BK_{Ca} was shown to be regulated by TRP channels in podocytes, i.e. TRPC3 and TRPC6, (Kim et al., 2008). Of note, expression of all three Ca^{2+} -activated K^+ channels, BK_{Ca} , IK and SK, by cultured human ovarian granulosa cells was demonstrated by Kunz and colleagues, who further linked these K^+ channels to steroidogenesis in these cells (Kunz et al., 2002; Traut et al., 2009). In this regard, it appears conceivable that TRPV2, which features increasing expression levels in parallel to follicle development, is involved in activation of these channels and thus also in production of progesterone. In this scenario, TRPV2 channel gating could happen upon changes in pressure within the growing follicle.

4.3 TRP Channels in the Human Gonads

By adding expressional and functional details about TRPV2, this thesis advanced the knowledge about the gonadal channelome. However, other members of the TRP superfamily are also encompassed that mostly still lack further investigation (Björkgren & Lishko, 2017). Based on the transcriptomic data sets of human testis and ovary made available in recent years, several TRP channels were found.

As such, TRPM7 expression is ubiquitously present in the testis. Also TRPA1, TRPC1, TRPM1-4 and TRPV6 were found in some cell types and in differing intensities (Guo et al., 2018). Surprisingly, TRPV4 was absent in this data set although Mundt and colleagues demonstrated that this thermo-sensitive ion channel is functionally expressed in human sperm. In these cells, TRPV4 gating leads to Na⁺-mediated membrane depolarization and thus facilitates the gating of CatSper which, in turn, is essential for sperm hyperactivation (Mundt et al., 2018). Also TRPC channels, especially TRPC1, TRPC3, TRPC4 and TRPC6, were found in the flagellum of human sperm and thus might be important for sperm motility (Castellano et al., 2003; Nilius et al., 2007). Moreover, functionality of thermo-sensitive TRPM8 was described for murine and human sperm (De Blas et al., 2009; Martínez-López et al., 2011), and yet is missing in the data set of Guo.

In the human ovary, TRPC4, TRPM4 and TRPM7 were present in theca cells and TRPC6 in stroma cells (Fen et al., 2019). In terms of follicular development, several TRP channels were found in oocytes from primordial to pre-ovulatory follicles including TRPA1, TRPC1, TRPC4, TRPC6, TRPC7, TRPM2, TRPM4, TRPM5, TRPM7, TRPV1, TRPV4 and TRPV6. However, no obvious regulative trends in expression levels become evident. Except for TRPV2, this also applies to the TRP channels found in granulosa cells from primordial to pre-ovulatory follicles, i.e. TRPC1, TRPC3, TRPC6, TRPM4, TRPM7 and TRPV1 (Zhang et al., 2018b). None of these TRP superfamily members were subjected to functional investigation yet.

4.4 Mouse is not Human - Species matters

With about 99 % sequence homology to the human genome, mouse is the most commonly used surrogate for biomedical research addressing basic human research needs with regard to genetics, physiology, pharmacology and pathology (Waterston et al., 2002). Since the 17th century, these little and fast reproducing creatures are in scientific and later also in laboratory use, there being beneficial due to convenient breeding and handling associated with low costs and, in addition, these rodents are easily genetically manipulated (Harvey, 1889; Hansen & Khanna, 2004; Hedrich, 2004; European Commission, 2010; Vandamme, 2014 & 2015).

However, bulk transcriptional datasets obtained from various organs and species including rodents and human revealed both conserved and differing gene expression. Thus, fundamental concerns have been raised in the last decades over the suitability of animal models and their transferability to the human (Lin et al., 2014; Monaco et al., 2015; Breschi et al., 2016 & 2017; Cardoso-Moreira et al., 2019; Blake et al., 2020). According to Gawrylewski *“the difficulties associated with using animal models [...] result from metabolic, anatomic, and cellular differences between humans and other creatures, but the problems go even deeper than that”* (Gawrylewski, 2007) and as per Kolata, going even a step further, *“years and billions of dollars have been wasted following false leads”* (Kolata, 2013). The differences become most apparent in animal models for human diseases, such as inflammation, Alzheimer’s and Parkinson’s disease, cancer and diabetes, and likely originate from existing immunological discrepancies (Seok et al., 2013; Cavanaugh et al., 2013; Garber, 2006).

Developmental, anatomical, functional and transcriptional differences certainly also exist between the gonads of murine and human beings. Based on the long time of intensive research on the mammalian testis, organogenesis as such showed to be well-conserved, whereas the spatio/temporal course differs between the species (Carmano et al., 2009). For the adult testis, species differences between mouse and human unfold in residing immune cells represented predominantly by mast cells in humans and by macrophages in rodents (Meineke et al., 2000; Yamanaka et al., 2000; Frungieri et al., 2002; Zhao et al., 2014; Mayerhofer et al., 2018; Hedger et al., 2002).

Further, the peritubular wall in the rodent testis consists of a single layer of peritubular cells, while several layers are present in the human testis (Mayerhofer, 2013; Knoblauch & True, 2011). Moreover, human Sertoli cells exhibited TRPV2 signals upon immunohistochemical examination, whereas murine Sertoli cells appeared devoid of any signal (Eubler et al., 2018 & 2021). In contrast to the testis, ovarian development and consequently the anatomical and functional organization of the mammalian ovary are more heterogenous (Mossman et al., 1973; Jiménez, 2009). The developmental differences root in the establishment and growth of sex cords in humans that are absent in mice (Kanai et al., 1989). The evident human medulla resulting in a regionalized ovary is poorly developed or inexistent in mice, and follicle maturation and ovulation differ substantially. In humans, only one follicle per cycle completely matures and ovulates, whereas in mice multiple mature follicles ovulate. Moreover, the distinctive cycle - oestrus cycle in mouse vs. menstrual cycle in human - resulting in different sexual activity and pregnancy maintenance either exclusively depends on the *corpus luteum* or in a later phase also on placenta (Pinkerton, 1961; McCracken et al., 1999; Jiménez, 2009; Rendi et al., 2011).

Consequently, the bottom line is that data obtained in gonadal tissues of rodent animal models may not be fully transferable to the human and generally should be regarded with caution.

4.5 Hunt for Physiological Activation Mechanisms of Gonadal TRPV2

The enigma of the “physiological activation mechanisms of gonadal TRPV2” still persists. As this cation channel is responsive to phytocannabinoids, amongst others including cannabinol (CBN), CBD, THC and THCV (Perálvarez-Marín et al., 2013), consumption of *Cannabis sativa* could result in channel activation in gonadal tissues. It may be followed by induction of inflammatory processes or even more severe events interfering with reproductive capacity. In this context, it has been shown that cannabinoids have an impact on male reproduction as they affect functionality of the pituitary gland and hence the levels of released gonadotropins. It is thought that this negatively influences sperm counts, motility and fertilizing ability (Wenger et al., 1987 & 1999; Hembree et al., 1978; Maccarrone et al., 2005; Rossato et al., 2005 & 2008).

Furthermore, it appears conceivable that the endocannabinoid system (ECS) of the gonadal organs is engaged in channel modulation, i.e. *“a definite network, including endocannabinoids, sex hormones, cytokines and leptin, that warrant a successful pregnancy in animals and humans”* (Battista et al., 2008). Endocannabinoids were shown to improve in vitro oocyte maturation (Totorikaguena et al., 2020) and to act as quiescent factors for sperm traveling through the female reproductive tract towards the egg (Schuel et al., 2002), emphasizing their importance for successful reproduction. The main ECS actors N-arachidonoyl-ethanolamine (AEA) and 2-arachidonoylglycerol (2-AG) operate at cannabinoid receptor 1 and 2 (CB1 & 2), representing the actual receptors of the ECS (Battista et al., 2007 & 2008). However, some ligands of CB1 and 2 also act on TRP channels, especially A1, V1, V2 and M8 (Devane et al., 1992; Mechoulam et al., 1995; Sugiura et al., 1995; De Petrocellis et al., 2010 & 2011). Consequently, it cannot be ruled out that TRPV2 represents a yet unknown player within the gonadal ECS.

Aside from that, changes in intragonadal pressure, relevant for both the testis and the ovary, possibly could be sensed by and impact TRPV2.

Additionally, infections and inflammatory processes could involve gonadal TRPV2 functionality, not only in immune cells as proven for mast cells and macrophages (Stokes et al., 2004; Nagasawa et al., 2007 & 2015; Link et al., 2010), but also in other gonadal cells.

5 Outlook & Future Perspectives

TRPV2 expressed by gonadal cells is emerging as an essential player in the interplay of immunological events. It might be activated by various stimuli originating from the unique characteristics of these organs. This thesis, while opening the door to this topic, only scratched the surface of the functional and expressional scope of gonadal TRPV2, still leaving numerous open questions to be answered in future studies.

First, a detailed translational, expressional and functional examination of the gonadal immunological repertoire focusing on TRPV2 itself, but also including structurally and pharmacologically related ion channels and interaction partners is required. The observed high abundance of this cation channel in testicular macrophages and the proven pivotal role of this channel for proper cell function demands attention. Therefore, functional examination of TRPV2 expressed by isolated murine and human gonadal macrophages is indicated. Complementary, expressional and functional investigation of mast cells could clarify if the observed tranilast-mediated improvement in sperm counts and motility, achieved in male patients suffering from severe oligospermia, depends on TRPV2.

Second, the relevance of TRPV2 for human Sertoli cells and their phagocytotic activity and thus for proper spermatogenesis needs to be assessed. However, there is no adequate human Sertoli cell culture system available, hampering such an attempt. Yet, a murine Sertoli cell line, i.e. TM4 (Mather, 1980), is available and despite the apparent discrepancies between murine and human Sertoli cells, it might be worthwhile to check for TRPV2 expression in this cell line.

Third, functional examination of ovarian TRPV2 is essential. Based on proven transcriptional expression in various somatic and immune cells, the newly available reliable method for cryopreservation of hGCs, offers a partial window into the human ovary. In these cells, channel expression features a developmental increase and thus suggest to have a say in the transformation of resting to finally luteinized granulosa cells, a process that may depend on pressure changes due to follicle maturation, for example.

Fourth, the potential role of TRPV2 within the gonadal ECS needs to be clarified. ECS-dependent channel activation, for instance in HTPCs, could be assessed by administration of the established ECS compounds AEA and 2-AG.

Finally, and of special interest, this still quite ‘mysterious’ cation channel was recently entitled as “*a cancer biomarker and potential therapeutic target*” [...] “*implicated in signalling pathways that mediate cell survival, proliferation, and metastasis*” (Siveen et al., 2020; Lehen’kyi & Prevarskaya, 2012; Perálvarez-Marín et al., 2013). Increased expression levels have so far been reported for liver, bladder, prostate, endometrial and glioma cancer (Vriens et al., 2004; Caprodossi et al., 2009; Liu et al., 2010; Yamada et al., 2010; Nabissi et al., 2010 & 2013; Monet et al., 2009 & 2010; Marinelli et al., 2020). In prostate cancer, endogenous LPS-induced translocation of TRPV2 resulted in Ca²⁺ uptake and increased cell migration (Monet et al., 2009 & 2010), and administration of tranilast inhibited IGF-1-dependant cell proliferation in human breast cancer cells (Nie et al., 1997). In human endometrial cancer, TRPV2 expression increases with tumor malignancy, correlates with short progression-free survival and CBD induced cell death, cell cycle arrest and autophagy (Marinelli et al., 2020). Furthermore, administration of CBD induced apoptotic cell death in human bladder cancer cells and glioblastoma cells (Monet et al., 2009; Yamada et al., 2010; Nabissi et al., 2013). Moreover, with respect to the gonads, expression of TRPV2 has also been found in the recently compiled proteome of the human granulosa-like tumor cell line KGN, derived from a patient suffering from an invasive ovarian granulosa cell carcinoma (Nishi et al., 2001; Schmid et al., 2021). In these cells, apoptotic cell death could be induced by hydrogen peroxide, either endogenously produced or exogenously added, and administration of the antioxidant Trolox or a TRPM2 blocker nullified this effect (Hack et al., 2019). These findings demonstrate vulnerability of human tumor lines to cell death using channelomics. Furthermore, as hydrogen peroxide is also known to sensitize and activate TRPV2, involvement of both TRP channels, TRPM2 and TRPV2, cannot be excluded and encourages more detailed and combinational examinations.

Taken together, these observations argue for a role of TRPV2 in cancer proliferation, invasiveness and metastasizing characteristics and moreover functional channel examination appears even more interesting and, hopefully, of clinical relevance in gonadal tumors.

6 References

- Abdul KL, Stacey M & Barrett-Jolley R. Emerging Roles of the Membrane Potential: Action Beyond the Action Potential. **2018**. *Frontiers in Physiology*. 9: 1661. doi: 10.3389/fphys.2018.01661.
- Agoston A, Kunz L, Krieger A, et al. Two types of calcium channels in human ovarian endocrine cells: involvement in steroidogenesis. **2004**. *Journal of Clinical Endocrinology and Metabolism*. 89 (9): 4503-12. doi: 10.1210/jc.2003-032219.
- Ahram M, Litou ZI, Fang R, et al. Estimation of membrane proteins in the human proteome. **2006**. *In Silico Bio*. 6 (5): 379-86. PMID: 17274767
- Alberts B, Bray D, Hopkin K, et al. *Molecular Biology of the Cell*. **2002**. 4th edition. ISBN: 978-0-8153-3218-3
- Alexander NB & Cotanch PH. The endocrine basis of infertility in women. **1980**. *Nursing Clinics of North America*. 15 (3): 511-24. PMID: 6777763
- Alexander SP, Mathie A & Peters JA. Ions Channels. **2011**. *British Journal of Pharmacology*. 164: 137-74. doi: 10.1111/j.1476-5381.2011.01649_5.x
- Almén MS, Nordström KJ, Frederiksson R, et al. Mapping the human membrane proteome: a majority of the human membrane proteins can be classified according to function and evolutionary origin. **2009**. *BMC Biology*. 7: 50. doi: 10.1186/1741-7007-7-50.
- Arai T, Kitahara S, Horiuchi S, et al. Relationship of testicular volume to semen profiles and serum hormone concentrations in infertile Japanese males. **1998**. *International Journal of Fertility and Women's Medicine*. 43 (1): 40-47. PMID: 9532468
- Araoye MO. Epidemiology of infertility: social problems of the infertile couples. **2003**. *West African Journal of Medicine*. 22 (2): 190-96. doi: 10.4314/wajm.v22i2.27946.
- Ashcroft FM. From molecule to malady. **2006**. *Nature*. 440: 440-47. doi: 10.1038/nature04707.
- Aumüller G, Engele J, Kirsch J, et al. *Duale Reihe Anatomie*. **2017**. 4th edition. ISBN: 978-3-1324-1752-6
- Bagnjuk K, Stöckl JB, Fröhlich T, et al. Necroptosis in primate luteolysis: a role for ceramide. **2019**. *Cell Death Discovery*. 5: 67. doi: 10.1038/s41420-019-0149-7.
- Bagnjuk K & Mayerhofer A. Human Luteinized Granulosa Cells - A Cellular Model for the Human Corpus Luteum. **2019**. *Frontiers in Endocrinology*. 10: 452. doi: 10.3389/fendo.2019.00452
- Bang S, Kim KY, Yoo S, et al. Transient receptor potential V2 expressed in sensory neurons is activated by probenecid. **2007**. *Neuroscience Letters*. 425 (2): 120-25. doi: 10.1016/j.neulet.2007.08.035.
- Barrett-Jolley R, Lewis R, Fallman R, et al. The emerging chondrocyte channelome. **2010**. *Frontiers in Membrane Physiology and Biophysics*. 1: 135. doi: 10.3389/fphys.2010.00135.
- Bar-Shavit R, Maoz M, Kancharla A, et al. G Protein-coupled Receptors in Cancer. **2016**. *International Journal of Molecular Sciences*. 17 (8): 1320. doi: 10.3390/ijms17081320.
- Battista N, Bari M, Rapino C, et al. Regulation of female fertility by the endocannabinoid system. **2007**. *Humun Fertility (Cambridge)*. 10 (4): 207-16. doi: 10.1080/14647270701429879.
- Battista N, Pasquariello N, Di Tommaso M, et al. Interplay between endocannabinoids, steroids and cytokines in the control of human reproduction. **2008**. *Journal of Neuroendocrinology*. 20 (Suppl 1): 82-89. doi: 10.1111/j.1365-2826.2008.01684.x.
- Beech DJ. Emerging functions of 10 types of TRP cationic channel in vascular smooth muscle. **2005**. *Clinical and Experimental Pharmacology and Physiology*. 32 (8): 597-603. doi: 10.1111/j.1440-1681.2005.04251.x.

- Beschta S, Eubler K, Bohne N, et al. A rapid and robust method for the cryopreservation of human granulosa cells. **2021**. *Histochemistry and Cell Biology*. 156 (5): 509-17.
doi: 10.1007/s00418-021-02019-3.
- Betts HC, Puttick MN, Clark JW, et al. Integrated genomic and fossil evidence illuminates life's early evolution and eukaryote origin. **2018**. *Nature Ecology and Evolution*. 2 (10): 1556-62.
doi: 10.1038/s41559-018-0644-x
- Bezanilla F & Armstrong CM. Negative conductance caused by entry of sodium and cesium ions into the potassium channels of squid axons. **1972**. *The Journal of General Physiology*. 60 (5): 588-608. doi: 10.1085/jgp.60.5.588.
- Björkgren I & Lishko PV. Fertility and TRP Channels. **2017**. *Neurobiology of TRP Channels*.
doi: 10.4324/9781315152837-11
- Blachly-Dyson E & Forte M. VDAC channels. **2001**. *International Union of Biochemistry and Molecular Biology Life*. 52 (3-5): 113-18. doi: 10.1080/15216540152845902.
- Blair NT, Carvacho I, Chaudhuri D, et al. Transient Receptor Potential channels in the IUPHAR/BPS Guide to Pharmacology Database. **2019**. *IUPHAR/PBS Guide to Pharmacology CITE*. 2019 (4).
doi: 10.2218/gtopdb/F78/2019.4.
- Blake LE, Roux J, Hernando-Herraez I, et al. A comparison of gene expression and DNA methylation patterns across tissues and species. **2020**. *Genome Research*. 30 (2): 250-62.
doi: 10.1101/gr.254904.119.
- Bodri D, Vernaeva V, Figueras F, et al. Oocyte donation in patients with Turner's syndrome: a successful technique but with an accompanying high risk of hypertensive disorders during pregnancy. **2006**. *Human Reproduction*. 21 (3): 829-32. doi: 10.1093/humrep/dei396.
- Boivin J, Bunting L, Collins JA, et al. International estimates of infertility prevalence and treatment-seeking: potential need and demand for infertility medical care. **2007**. *Human Reproduction*. 22 (6): 1506-12. doi: 10.1093/humrep/dem046.
- Breschi A, Djebali S, Gillis J, et al. Gene-specific patterns of expression variation across organs and species. **2016**. *Genome Biology*. 17 (1): 151. doi: 10.1186/s13059-016-1008-y.
- Breschi A, Gingeras TR & Guigó R. Comparative transcriptomics in human and mouse. **2017**. *Nature Reviews Genetics*. 18 (7): 425-40. doi: 10.1038/nrg.2017.19.
- Brown HM & Russel DL. Blood and lymphatic vasculature in the ovary: Development, function and disease. **2014**. *Human Reproduction Update*. 20 (1): 29-39. doi: 10.1093/humupd/dmt049.
- Brugh VM & Lipshultz LI. Male factor infertility. **2004**. *Medical Clinics of North America*. 88 (2): 367-85. doi: 10.1016/S0025-7125(03)00150-0.
- Buck T, Hack CT, Berg D, et al. The NADPH oxidase 4 is a major source of hydrogen peroxide in human granulosa-lutein and granulosa tumor cells. **2019**. *Scientific Reports*. 9 (1): 3585.
doi: 10.1038/s41598-019-40329-8.
- Bulletti C, Coccia ME, Battistoni S, et al. Endometriosis and infertility. **2010**. *Journal of Assisted Reproduction and Genetics*. 27 (8): 441-47. doi: 10.1007/s10815-010-9436-1.
- Bulling A, Berg FD, Berg U, et al. Identification of an ovarian voltage-activated Na⁺-channel type: hints to involvement in luteolysis. **2000**. *Molecular Endocrinology*. 14 (7): 1064-74.
doi: 10.1210/mend.14.7.0481.
- Bulmer D. The histochemistry of ovarian macrophages in the rat. **1964**. *Journal of Anatomy*. 98: 313-19. PMID: 14193191
- Camerino DC, Tricarico D & Desaphy JF. Ion channel pharmacology. **2007**. *Neurotherapeutics*. 4 (2): 184-98. doi: 10.1016/j.nurt.2007.01.013.

- Caprodossi S, Lucciarini R, Amantini C, et al. Transient Receptor Potential Vanilloid Type 2 (TRPV2) Expression in Normal Urothelium and in Urothelial Carcinoma of Human Bladder: Correlation with the Pathologic Stage. **2008**. *Eur Urol.* 54 (3): 612-20. doi: 10.1016/j.eururo.2007.10.016.
- Cardoso-Moreira M, Halbert J, Valloton D, et al. Gene expression across mammalian organ development. **2019**. *Nature.* 571 (7766): 505-09. doi: 10.1038/s41586-019-1338-5.
- Carlsen E, Giwercman A, Keiding N, et al. Evidence for decreasing quality of semen during past 50 years. **1992**. *British Medical Journal.* 305 (6854): 609-13. doi: 10.1136/bmj.305.6854.609.
- Carlson AE, Westenbroek RE, Quill T, et al. CatSper1 required for evoked Ca²⁺ entry and control of flagellar function in perm. **2003**. *Proceedings of the National Academy of Science of the USA.* 100 (25): 14864-68. doi: 10.1073/pnas.2536658100.
- Carmona FD, Lupiáñez DG, Martín JE, et al. The spatio-temporal pattern of testis organogenesis in mammals - insights from the mole. **2009**. *International Journal of Developmental Biology.* 53 (7): 1035-44 . doi: 10.1387/ijdb.072470fc.
- Casey PJ, Seabra MC. Protein prenyltransferase. **1996**. *The Journal of Biological Chemistry.* 271 (10): 5289-92. doi: 10.1074/jbc.271.10.5289.
- Castellano LE, Treviño CL, Rodríguez D, et al. Transient receptor potential (TRPC) channels in human sperm: expression, cellular localization and involvement in the regulation of flagellar motility. **2003**. *Federation of European Biochemical Societies Letters.* 541 (1-3): 69-74. doi: 10.1016/s0014-5793(03)00305-3.
- Caterina MJ, Schumacher MA, Tominaga M, et al. The capsaicin receptor: a heat-activated ion channel in the pain pathway. **1997**. *Nature.* 389 (6653): 816-24. doi: 10.1038/39807.
- Caterina MJ, Rosen TA, Tominaga M, et al. A capsaicin-receptor homologue with a high threshold for noxious heat. **1999**. *Nature.* 398 (6726): 436-41. doi: 10.1038/18906.
- Caterina MJ, Leffler A, Malmberg AB, et al. Impaired nociception and pain sensation in mice lacking the capsaicin receptor. **2000**. *Science.* 288 (5464): 306-13. doi: 10.1126/science.288.5464.306.
- Cavallini G. Male idiopathic oligoasthenoteratozoospermia. **2006**. *Asian Journal of Andrology.* 8 (2): 143-57. doi: 10.1111/j.1745-7262.2006.00123.x.
- Cavanaugh SE, Pippin JJ & Barnard ND. Animal models of Alzheimer disease: historical pitfalls and a path forward. **2014**. *Alternatives to Animal Experimentation.* 31 (3): 279-302. doi: 10.14573/altex.1310071.
- CDC (Centers for Disease control and Prevention). Assisted Reproductive Technology Fertility Clinic Success Rates Report. **2013**.
- CDC (Centers for Disease control and Prevention). Assisted Reproductive Technology National Summary Report. **2013**.
- CDC Centers for Disease control and Prevention). Assisted Reproductive Technology Fertility Clinic Success Rates Report. **2018**.
- Chai H, Cheng X, Zhou B, et al. Structure-Based Discovery of a Subtype-Selective Inhibitor Targeting Transient Receptor Potential Vanilloid Channel. **2019**. *Journal of Medical Chemistry.* 62 (3): 1373-84. doi: 10.1021/acs.jmedchem.8b01496.
- Chung JJ, Navarro B, Krapivinsky G, et al. A novel gene required for male fertility and functional CATSPER channel formation in spermatozoa. **2011**. *Nature Communications.* 2: 153. doi: 10.1038/ncomms1153.
- Clamp M, Fry B, Kamal M, et al. Distinguishing protein-coding and noncoding genes in the human genome. **2007**. *Proceedings of the National Academy of Science of the USA.* 104 (49): 19428-33. doi: 10.1073/pnas.0709013104.

- Clapham DE. TRP channels as cellular sensors. **2003**. *Nature*. 426 (6966): 517-24.
doi: 10.1038/nature02196.
- Clapham DE. Calcium signaling. **2007b**. *Cell*. 131 (6): 1047-58. doi: 10.1016/j.cell.2007.11.028.
- Clapham DE. Mammalian TRP Channels. **2007a**. *Cell*. 129 (1): 220. doi: 10.1016/j.cell.2007.03.034.
- Clapham DE, Julius D, Montell G, et al. International Union of Pharmacology. XLIX. Nomenclature and structure-function relationships of transient receptor potential channels. **2005**.
Pharmacological Reviews. 57 (4): 427-50. doi: 10.1124/pr.57.4.6.
- Clermont Y. Spermatogenesis in man. A study of the spermatogonial population. **1966**.
Fertility and Sterility. 17 (6): 705-21. PMID: 5920556.
- Colbert HA, Smith T & Bargmann CI. OSM-9, a novel protein with structural similarity to channels, is required for olfaction, mechanosensation, and olfactory adaption in *Ceanorhabditis elegans*. **1997**. *Journal of Neuroscience*. 17 (21): 8259-69. doi: 10.1523/JNEUROSCI.17-21-08259.1997.
- Collins AC, Salminen O, Marks MJ, et al. The road to discovery of neuronal nicotinic cholinergic receptor subtypes. **2009**. *Nicotine Pharmacology*. 192: 85-112. doi: 10.1007/978-3-540-69248-5_4.
- Cooke HJ & Saunders PTK. Mouse models of male infertility. **2002**. *Nature Reviews Genetics*.
3 (10): 790-801. doi: 10.1038/nrg911.
- Cooper GM. Structure of the Plasma Membrane. **2000**. *The Cell: A Molecular Approach*. 2nd edition.
ISBN: 978-0-87893-106-4
- Cosens DJ & Manning A. Abnormal electroretinogram from a *Drosophila* mutant. **1969**. *Nature*.
224 (5216): 285-87 doi: 10.1038/224285a0.
- Cui W. Mother of nothing: the agony of infertility. **2010**. *Bulletin of the World Health Organization*.
88 (12): 881-82. doi: 10.2471/BLT.10.011210.
- Cunningham GR & Rosen RC. Overview of male sexual dysfunction. **2018**. *UpToDate*.
- De Blas GA, Darszon A, Ocampo AY, et al. TRPM8, a versatile channel in human sperm. **2009**.
Public Library Of Science One. 4 (6): e6095. doi: 10.1371/journal.pone.0006095.
- De Petrocellis L & Di Marzo V. Non-CB1, non-CB2 receptors for endocannabinoids, plant cannabinoids, and synthetic cannabimimetics: focus on G-protein-coupled receptors and transient receptor potential channels. **2010**. *Journal of Neuroimmune Pharmacology*. 5 (1): 103-21.
doi: 10.1007/s11481-009-9177-z.
- De Petrocellis L, Ligresti A, Moriello AS, et al. Effect of cannabinoids and cannabinoid-enriched Cannabis extracts in TRP channels and endocannabinoid metabolic enzymes. **2011**.
British Journal of Pharmacology. 163 (7): 1479-94. doi: 10.1111/j.1476-5381.2010.01166.x.
- De Pinto V, Messina A, Lane D, et al. Voltage-dependant anion-selective channel (VDAC) in the plasma membrane. **2010**. *Federation of European Biochemical Societies Letters*. 584 (9): 1793-99.
doi: 10.1016/j.febslet.2010.02.049.
- Devane WA, Hanus L, Breuer A, et al. Isolation and structure of a brain constituent that binds to the cannabinoid receptor. **1992**. *Science*. 258 (5090): 1946-49. doi: 10.1126/science.1470919.
- Djokic T, Van Kranendonk MJ, Campbell KA, et al. Earliest signs of life on land preserved in ca. 3.5 Ga hot spring deposits. **2017**. *Nature Communications*. 8: 15263. doi: 10.1038/ncomms15263.
- Dodd MS, Papineau D, Grenne T, et al. Evidence for early life in Earth's oldest hydrothermal vent precipitates. **2017**. *Nature*. 543 (7643): 60-64. doi: 10.1038/nature21377.
- Doheny H, Houlihan DD, Ravikumar N, et al. Human Chorionic Gonadotrophin Relaxation of Human Pregnant Myometrium and Activation of the BK_{Ca} Channel. **2003**. *Journal of Clinical Endocrinology & Metabolism*. 88 (9): 4310-15. doi: 10.1210/jc.2003-030221.

- Doyle DA, Morais-Cabral J, Pfuetzner RA, et al. The structure of the potassium channel: molecular basis of K⁺ conduction and selectivity. **1998**. *Science*. 280: 69-77. doi: 10.1126/science.280.5360.69.
- Du C & Xie X. G protein-coupled receptors as therapeutic targets for multiple sclerosis. **2012**. *Cell Research*. 22 (7): 1108-28. doi: 10.1038/cr.2012.87.
- Edberg JC, Lin CT, Lau D, et al. The Ca²⁺ dependence of human Fc γ receptor-initiated phagocytosis. **1995**. *Journal of Biological Chemistry*. 270 (38): 22301-07. doi: 10.1074/jbc.270.38.22301
- Eubler K, Herrmann C, Tiefenbacher A, et al., Ca²⁺ Signaling and IL-8 Secretion in Human Testicular Peritubular Cells Involve the Cation Channel TRPV2. **2018**. *International Journal of Molecular Sciences*. 19 (9): 2829. doi: 10.3390/ijms19092829.
- Eubler K, Rantakari P, Gerke H, et al. Exploring the Ion Channel TRPV2 and Testicular Macrophages in Mouse Testis. **2021**. *International Journal of Molecular Sciences*. 22 (9): 4727. doi: 10.3390/ijms22094727.
- European Commission. Of mice and men - Are mice relevant models for human disease? Outcomes of the European Commission workshop. **2010**. London.
- Faddy MJ. Follicle dynamics during ovarian ageing. **2000**. *Molecular and Cellular Endocrinology*. 163 (1): 43-48. doi: 10.1016/s0303-7207(99)00238-5.
- Fan X, Bialecka M, Moustakas I, et al., Single-cell reconstruction of follicular remodelling in the human adult ovary. **2019**. *Nature Communications*. 10 (1): 3164. doi: 10.1038/s41467-019-11036-9.
- Fantozzi I, Zhang S, Platoshyn O, et al. Hypoxia increases AP-1 binding activity by enhancing capacitative Ca²⁺ entry in human pulmonary artery endothelial cells. **2003**. *American Journal of Physiology - Lung Cellular and Molecular Physiology*. 285 (6): L1233-45. doi: 10.1152/ajplung.00445.2002.
- Fausser BCJM, Diedrich K, Bouchard P, et al. Contemporary genetic technologies and female reproduction. **2011**. *Human Reproduction Update*. 17 (6): 829-47. doi: 10.1093/humupd/dmr033.
- Feng Q. Temperature sensing by thermal TRP channels: thermodynamic basis and molecular insights. **2014**. *Current Topics in Membranes*. 74: 19-50. doi: 10.1016/B978-0-12-800181-3.00002-6.
- Ferlin A, Arredi B & Foresta C. Genetic causes of male infertility. **2006**. *Reproductive Toxicology*. 22 (2): 133-41. doi: 10.1016/j.reprotox.2006.04.016.
- Fleck D, Kenzler L, Mundt N, et al. ATP activation of peritubular cells drives testicular sperm transport. **2021**. *eLife*. 10: e62885. doi: 10.7554/eLife.62885.
- Flenkenthaler F, Windschüttl S, Fröhlich T, et al. Secretome Analysis of Testicular Peritubular Cells: A Window into the Human Testicular Microenvironment and the Spermatogonial Stem Cell Niche in Man. **2014**. *Journal of Proteome Research*. 13 (3): 1259-69. doi: 10.1021/pr400769z.
- Fowler PW & Coveney PV. A Computational Protocol for the Integration of the Monotopic Protein Prostaglandin H₂ Synthase into a Phospholipid Bilayer. **2006**. *Biophysical Journal*. 91 (2): 401-10. doi: 10.1529/biophysj.105.077784.
- Freichel M, Almering J & Tsvilovskyy V. The role of TRP proteins in Mast cells. **2012**. *Frontiers in Immunology*. 3: 150. doi: 10.3389/fimmu.2012.00150.
- Fricke TC, Echtermeyer F, Zielke J, et al. Oxidation of methionine residues activates the high-threshold heat-sensitive ion channel TRPV2. **2019**. *Proceedings of the National Academy of Science of the USA*. 116 (48): 24359-65. doi: 10.1073/pnas.1904332116.
- Frungieri MB, Calandra RS, Lustig L, et al. Number, distribution pattern, and identification of macrophages in the testes of infertile men. **2002**. *Fertility and Sterility*. 78 (2): 298-306. doi: 10.1016/s0015-0282(02)03206-5.

- Fukumatsu Y, Katabuchi H, Naito M, et al. Effect of macrophages on proliferation of granulosa cells in the ovary in rats. **1992**. *Journal of Reproduction and Fertility*. 96 (1): 241-49. doi: 10.1530/jrf.0.0960241.
- Gabashvili IS, Sokolowski BHA, Morton CC, et al. Ion Channel Gene Expression in the Inner Ear. **2007**. *Journal of the Association for Research in Otolaryngology*. 8 (3): 305-28. doi: 10.1007/s10162-007-0082-y.
- Garber K. Realistic rodents? Debate grows over new mouse models of cancer. **2006**. *Journal of the National Cancer Institute*. 98 (17): 1176-78. doi: 10.1093/jnci/djj381.
- Gawrylewski A. "The Trouble With Animal Models". **2007**. *The Scientist*. Retrieved 6 August 2015.
- Gees M, Colsoul B & Nilius B. The role of transient receptor potential cation channels in Ca²⁺ signaling. **2010**. *Cold Spring Harbor Perspectives in Biology*. 2 (10): a003962. doi: 10.1101/cshperspect.a003962.
- Gerrits T. Social and cultural aspects of infertility in Mozambique. **1997**. *Patient Education and Counselling*. 31 (1): 39-48. doi: 10.1016/s0738-3991(97)01018-5.
- Gilbert SF. Oogenesis. **2000**. *Developmental Biology*, 6th edition. ISBN: 978-0-8789-3243-6
- Gleicher N, Weghofer A, Oktay K, et al. Do etiologies of premature ovarian aging (POA) mimic those of premature ovarian failure (POF)? **2009**. *Human Reproduction*. 24 (10): 2395-400. doi: 10.1093/humrep/dep256.
- Gore AC, Chappell VA, Fenton SE, et al. The Endocrine Society's Second Scientific Statement on Endocrine-Disrupting Chemicals. **2015**. *Endocrine Reviews*. 36 (6): E1-150. doi: 10.1210/er.2015-1010.
- Gotti C, Moretti M, Gaimarri A, et al. Heterogeneity and complexity of native brain nicotinic receptors. **2007**. *Biochemical Pharmacology*. 74 (8): 1102-11. doi: 10.1016/j.bcp.2007.05.023.
- Gould SB. Membranes and Evolution. **2018**. *Current Biology*. 28 (8): R381-85. doi: 10.1016/j.cub.2018.01.086.
- Griswold MD. The central role of Sertoli cells in spermatogenesis. **1998**. *Seminars in Cell and Developmental Biology*. 9 (4): 411-16. doi: 10.1006/scdb.1998.0203
- Guo J, Grow EJ, Mlcochova H, et al. The adult human testis transcriptional cell atlas. **2018**. *Cell Research*. 28 (12): 1141-57. doi: 10.1038/s41422-018-0099-2.
- Güven MA, Dilek U, Pata O, et al. Prevalence of Chlamydia trachomatis, Ureaplasma urealyticum and Mycoplasma hominis infections in the unexplained infertile woman. **2007**. *Archives of Gynecology & Obstetrics*. 276 (3): 219-23. doi: 10.1007/s00404-006-0279-z.
- Hack CT, Buck T, Bagnjuk K, et al. A Role for H₂O₂ and TRPM2 in the Induction of Cell Death: Studies in KGN Cells. **2019**. *Antioxidants (Basel)*. 8 (11): 518. doi: 10.3390/antiox8110518.
- Hansen K & Khanna C. Spontaneous and genetically engineered animal models; use in preclinical cancer drug development. **2004**. *European Journal of Cancer*. 40 (6): 858-80. doi: 10.1016/j.ejca.2003.11.031.
- Harada K, Kitaguchi T, Kamiya T, et al. Lysophosphatidylinositol-induced activation of the cation channel TRPV2 triggers glucagon-like peptide-1 secretion in enteroendocrine L cells. **2017**. *Journal of Biological Chemistry*. 292 (26): 10855-64. doi: 10.1074/jbc.M117.788653.
- Hardie RC & Minke B. The trp gene is essential for a light-activated Ca²⁺ channel in Drosophila photoreceptors. **1992**. *Neuron*. 8 (4): 643-51. doi: 10.1016/0896-6273(92)90086-s.
- Harvey W. On the Motion of the Heart and Blood in Animals. **1889**. George Bell & Sons
- Hauser AS, Attwood MM, Rask-Andersen M, et al. Trends in GPCR drug discovery: new agents, targets and indications. **2017**. *Nature Reviews Drug Discovery*. 16 (12): 829-42. doi: 10.1038/nrd.2017.178.

- Hedger MP. Macrophages and the immune responsiveness of the testis. **2002**. *Journal of Reproductive Immunology*; 57 (1-2): 19-34. doi: 10.1016/s0165-0378(02)00016-5.
- Hedrich H. The Laboratory Mouse - "The house mouse as a laboratory model: a historical perspective". **2004**. 1st edition. ISBN 9780080542539.
- Heiner I, Eisfeld J & Lückhoff A. Role and regulation of TRP channels in neutrophil granulocytes. **2003**. *Cell Calcium*. 33 (5-6): 533-40. doi: 10.1016/s0143-4160(03)00058-7.
- Hellwig N, Albrecht N, Harteneck C, et al. Homo- and heteromeric assembly of TRPV channel subunits. **2005**. *Journal of Cell Science*. 118 (5): 917-28. doi: 10.1242/jcs.01675.
- Hembree WC 3rd, Nahas GG, Zeidenberg P, et al. Changes in human spermatozoa associated with high dose marijuana smoking. **1978**. *Advances in Biosciences*. 2-233: 429-39. doi: 10.1016/b978-0-08-023759-6.50038-x.
- Hildebrand MS, Avenarius MR, Fellous M, et al. Genetic male infertility and mutation of CATSPER ion channels. **2010**. *European Journal of Human Genetics*. 18 (11): 1178-84. doi: 10.1038/ejhg.2010.108.
- Hille B. The permeability of the sodium channel to organic cations in myelinated nerve. **1971**. *The Journal of General Physiology*. 58 (6): 599-616. doi: 10.1085/jgp.58.6.599.
- Hille B. Potassium channels in myelinated nerve. Selective permeability to small cations. **1973**. *The Journal of General Physiology*. 61 (6): 669-86. doi: 10.1085/jgp.61.6.669.
- Hille B. Ionic selectivity, saturation, and block on sodium channels. A four-barrier model. **1975**. *The Journal of General Physiology*. 66 (5): 535-60. doi: 10.1085/jgp.66.5.535.
- Hille B. Ion Channels Of Excitable Membranes. **2001**. 3rd edition. ISBN: 978-0-8789-3321-1
- Hirsh A. Male subfertility. **2003**. *British Medical Journal*. 327 (7416): 669-72. doi: 10.1136/bmj.327.7416.669.
- Hisanaga E, Nagasawa M, Ueki K, et al. Regulation of calcium-permeable TRPV2 channel by insulin in pancreatic beta-cells. **2009**. *Diabetes*. 58 (1): 174-84. doi: 10.2337/db08-0862.
- Hoffmann BL & Williams JW. Williams Gynecology. **2012**. 2nd edition. ISBN: 978-0-0717-1672-7
- Hong TT & Shaw RM. Chapter 2: Ion Channel Trafficking. **2016**. *Ion Channels in Health and Disease*. ISBN: 978-0-1280-2002-9
- Hsueh AJ, Billig H & Tsafri A. Ovarian follicle atresia: a hormonally controlled apoptotic process. **1994**. *Endocrine Reviews*. 15 (6): 707-24. doi: 10.1210/edrv-15-6-707.
- Hu HZ, Gu Q, Wang C, et al. 2-aminoethoxydiphenyl borate is a common activator of TRPV1, TRPV2, and TRPV3. **2004**. *Journal of Biological Chemistry*. 279 (34): 35741-48. doi: 10.1074/jbc.M404164200.
- Imbrici P, Liantonio A, Camerino GM, et al. Therapeutic Approaches to Genetic Ion Channelopathies and Perspectives in Drug Discovery. **2016**. *Frontiers in Pharmacology*. 7: 121. doi: 10.3389/fphar.2016.00121.
- Inhorn MC. Global infertility and the globalization of new reproductive technologies: illustrations from Egypt. **2004**. *Social Science & Medicine*. 56 (9): 1837-51. doi: 10.1016/s0277-9536(02)00208-3.
- Inhorn MC & Wentzell EA. Embodying emergent masculinities: Men engaging with reproductive and sexual health technologies in Middle East and Mexico. **2011**. *American Ethnologist*. 38 (4): 801-25. doi: 10.1111/j.1548-1425.2011.01338.x
- Iwata Y, Katanosaka Y, Arai Y, et al. A novel mechanism of myocyte degeneration involving the Ca²⁺-permeable growth factor-regulated channel. **2003**. *Journal of Cellular Biology*. 161 (5): 957-67. doi: 10.1083/jcb.200301101.
- Jarow JP, Espeland MA & Lipshultz LI. Evaluation of azoospermic patient. **1989**. *Journal of Urology*. 142 (1): 62-65. doi: 10.1016/s0022-5347(17)38662-7.

- Jiménez R. Ovarian Organogenesis in Mammals: Mice Cannot Tell Us Everything. **2009**. *Sexual Development*. 3 (6): 291-301. doi: 10.1159/000280584
- Johnson L, Thompson DL Jr & Varner DD. Role of Sertoli cell number and function on regulation of spermatogenesis. **2008**. *Animal Reproduction Science*. 105 (1-2): 23-51. doi: 10.1016/j.anireprosci.2007.11.029.
- Ju YK & Allen DG. Store-operated Ca^{2+} entry and TRPC expression; possible roles in cardiac pacemaker tissue. **2007**. *Heart, Lung and Circulation*. 16 (5): 349-55. doi: 10.1016/j.hlc.2007.07.004.
- Juvin V, Penna A, Chemin J, et al. Pharmacological Characterization and Molecular Determinants of the Activation of Transient Receptor Potential V2 Channel Orthologs by 2-Aminoethoxydiphenyl Borate. **2007**. *Molecular Pharmacology*. 72 (5): 1258-68. doi: 10.1124/mol.107.037044.
- Kaipia A & Hsueh AJ. Regulation of ovarian follicle atresia. **1997**. *Annual Review of Physiology*. 59 (1): 349-63. doi: 10.1146/annurev.physiol.59.1.349.
- Kanai Y, Kurohmaru M, Hayashi Y, et al. Formation of male and female sex cords in gonadal development of C57BL/6 mouse. **1989**. *Nihon Juigaku Zasshi. Japanese Journal of Veterinary Science*. 51 (1): 7-16. doi: 10.1292/jvms1939.51.7.
- Kanzaki M, Zhang Y, Mashima H, et al. Translocation of a calcium-permeable cation channel induced by insulin-like growth factor-1. **1999**. *Nature Cell Biology*. 1 (3): 165-70. doi: 10.1038/11086.
- Karp G. Cell and Molecular Biology: Concepts and Experiments. **2009**. 4th edition. pp. 128. ISBN: 978-0-470-48337
- Kass RS. The channelopathies: novel insights into molecular and genetic mechanisms of human disease. **2005**. *Journal of Clinical Investigation*. 115: 1986-89. doi: 10.1172/JCI26011.
- Kavalali ET. SNARE interactions in membrane trafficking: a perspective from mammalian central synapses. **2002**. *BioEssays*. 24 (10): 926-36. doi: 10.1002/bies.10165.
- Kim EY, Alvarez-Baron CP & Dryer SE. Canonical transient receptor potential channel (TRPC)3 and TRPC6 associate with large-conductance Ca^{2+} -activated K^+ (BK_{Ca}) channels: role in BK_{Ca} trafficking to the surface of cultured podocytes. **2009**. *Molecular Pharmacology*. 75 (3): 466-77. doi: 10.1124/mol.108.051912
- Knoblauch S & True L. Comparative Anatomy and Histology: A Mouse and Human Atlas - Male Reproductive System. **2011**. 1st edition. ISBN: 978-0-12-381361-9
- Kolata G. "Mice Fall Short as Test Subjects for Some of Humans' Deadly Ills". **2013**. *New York Times*. Retrieved 6 August 2015.
- Kondratskyi A & Prevarskaya N. TRP Channels in Cancer. **2015**. *TRP Channels as Therapeutic Target*. ISBN: 978-0-1242-0024-1
- Kovacs GT & Norman R. Polycystic Ovary Syndrome. **2007**. 2nd edition. ISBN: 978-1-1394-6203-7
- Kowase T, Nakazato Y, Yoko-O H, et al. Immunohistochemical localization of growth factor-regulated channel (GRC) in human tissues. **2002**. *Endocrine Journal*. 49 (3): 349-55. doi: 10.1507/endocrj.49.349
- Krogh A, Larsson B, von Heijne G, et al. Predicting transmembrane protein topology with a hidden Markov model: application to complete genomes. **2001**. *Journal of Molecular Biology*. 305 (3): 567-80. doi: 10.1006/jmbi.2000.4315.
- Kunz L, Thalhammer A, Berg FD, et al. Ca^{2+} -activated, large conductance K^+ channel in the ovary: identification, characterization, and functional involvement in steroidogenesis. **2002**. *Journal of Clinical Endocrinology & Metabolism*. 87 (12): 5566-74. doi: 10.1210/jc.2002-020841.
- Kunz L, Rämisch R, Krieger A, et al. Voltage-dependent K^+ channel acts as sex steroid sensor in endocrine cells of the human ovary. **2006**. *Journal of Cellular Physiology*. 206 (1): 167-74. doi: 10.1002/jcp.20453

- Kupis L, Dobronski AP & Radziszewski P. Varicocele as a source of male infertility - current treatment techniques. **2015**. *Central European Journal of Urology*. 68 (3): 465-70. doi: 10.5173/ceju.2015.642.
- Lainez S, Schlingmann KP, van der Wijst J, et al. New TRPM6 missense mutations linked to hypomagnesemia with secondary hypocalcemia. **2014**. *European Journal of Human Genetics*. 22 (4): 497-504. doi: 10.1038/ejhg.2013.178.
- Lander ES, Linton LM, Birren B, et al. Initial sequencing and analysis of the human genome. **2001**. *Nature*. 409 (6822): 860-921. doi: 10.1038/35057062.
- Lappano R & Maggioloni M. G protein-coupled receptors: novel targets for drug discovery in cancer. **2011**. *Nat Rev Drug Discovery*. 10 (1): 47-60. doi: 10.1038/nrd3320.
- Leffler A, Linte RM, Nau C et al. A high-threshold heat-activated channel in cultured rat dorsal root ganglion neurons resembles TRPV2 and is blocked by gadolinium. **2007**. *European Journal of Neuroscience*. 26 (1): 12-22. doi: 10.1111/j.1460-9568.2007.05643.x.
- Lehen'kyi V & Prevarskaya N. TRPV2 (transient receptor potential cation channel, subfamily V, member 2). **2012**. *Atlas of Genetics and Cytogenetics in Oncology and Haematology*. 16: 563-67.
- Lehmann-Horn F & Jurkat-Rott K. Nanotechnology for neuronal ion channels. **2003**. *Journal of Neurology, Neurosurgery, and Psychiatry*. 74 (11): 1466-75. doi: 10.1136/jnnp.74.11.1466.
- Leslie SW, Siref LE & Khan MAB. Male Infertility. **2020**. *StatPearls*. PMID: 32965929
- Lévêque M, Penna A, Le Trionnaire S, et al. Phagocytosis depends on TRPV2-mediated calcium influx and requires TRPV2 in lipid rafts: alteration in macrophages from patients with cystic fibrosis. **2018**. *Scientific Reports*. 8 (1): 4310. doi: 10.1038/s41598-018-22558-5.
- Levine H, Jørgensen N, Martino-Andrade A, et al. Temporal trends in sperm count: a systemic review and meta-regression analysis. **2017**. *Human Reproduction Update*. 23 (6): 646-59. doi: 10.1093/humupd/dmx022.
- Li Y, Calfa G, Inoue T, et al. Activity-Dependent release of endogenous BDNF from mossy fibers evokes a TRPC3 current and Ca²⁺ elevations in Ca3 pyramidal neurons. **2010**. *Journal of Neurophysiology*. 103 (5): 2846-56. doi: 10.1152/jn.01140.2009.
- Lin S, Lin Y, Nery JR, et al. Comparison of the transcriptional landscapes between human and mouse tissues. **2014**. *Proceedings of the National Academy of Science of the USA*. 111 (48): 17224-29. doi: 10.1073/pnas.1413624111.
- Link TM, Park U, Vonakis BM, et al. TRPV2 plays a pivotal role in macrophage particle binding and phagocytosis. **2010**. *Nature Immunology*. 11 (3): 232-39. doi: 10.1038/ni.1842.
- Liu G, Xie C, Sun F, et al. Clinical significance of transient receptor potential vanilloid 2 expression in human hepatocellular carcinoma. **2010**. *Cancer Genetics and Cytogenetics*. 197 (1):54-59. doi: 10.1016/j.cancergencyto.2009.08.007.
- Lobley A, Pierron V, Reynolds L, et al. Identification of human and mouse CatSper3 and CatSper4 genes: characterisation of a common interaction domain and evidence for expression in testis. **2003**. *Reproductive Biology & Endocrinology*. 1: 53. doi: 10.1186/1477-7827-1-53.
- Lobo RA. Early ovarian ageing: a hypothesis. What is early ovarian ageing? **2003**. *Human Reproduction*. 18 (9): 1762-64. doi: 10.1093/humrep/deg377.
- Lodish H, Berk A, Zipursky SL, et al. Biomembranes: Structural Organization and Basic Functions. **2000**. *Molecular Cell Biology*. 4th edition. ISBN: 978-0-7167-3706-3
- Lodish H, Berk A, Kaiser CA, et al. Molecular Cell Biology. **2008**. 6th edition. ISBN: 978-1-4292-0314-2

- Lotti F & Maggi M. Ultrasound of the male genital tract in relation to male reproductive health. **2015**. *Human Reproduction Update*. 21 (1): 56-83. doi: 10.1093/humupd/dmu042.
- Maccarrone M, Barboni B, Paradisi A, et al. Characterization of the endocannabinoid system in boar spermatozoa and implications for sperm capacitation and acrosome reaction. **2005**. *Journal of Cell Science*. 118 (19): 4393-404. doi: 10.1242/jcs.02536.
- Marinelli O, Morelli MB, Annibali D, et al. The Effects of Cannabidiol and Prognostic Role of TRPV2 in Human Endometrial Cancer. **2020**. *International Journal of Molecular Sciences*. 21 (15): 5409. doi: 10.3390/ijms21155409.
- Martin J & Sawyer A. Elucidating the Structure of Membrane Proteins. **2019**. *Tech News. BioTechnique*. 66 (4): 167-70. doi: 10.2144/btn-2019-0030.
- Martínez-López P, Treviño CL, de la Vega-Beltrán JL, et al. TRPM8 in mouse sperm detects temperature changes and may influence the acrosome reaction. **2011**. *Journal of Cellular Physiology*. 226 (6): 1620-31. doi: 10.1002/jcp.22493.
- Mascarenhas MN, Flaxman SR, Boerma T, et al. National, regional, and global trends in infertility prevalence since 1990: a systematic analysis of 277 health surveys. **2012**. *Public Library of Science Medicine*. 9 (12): e1001356. doi: 10.1371/journal.pmed.1001356.
- Mather JP. Establishment and characterization of two distinct mouse testicular epithelial cell lines. **1980**. *Biology of Reproduction*. 23 (1): 243-52. doi: 10.1095/biolreprod23.1.243.
- Mayerhofer A. Human testicular peritubular cells: more than meets the eye. **2013**. *Reproduction*. 145 (5): R107-16. doi: 10.1530/REP-12-0497.
- Mayerhofer A & Kunz L. Ion channels of primate ovarian endocrine cells: identification and functional significance. **2006**. *Expert Review of Endocrinology and Metabolism*. 1 (4): 549-55. doi: 10.1586/17446651.1.4.549.
- Mayerhofer A, Walenta L, Mayer C, et al. Human testicular peritubular cells, mast cells and testicular inflammation. **2018**. *Andrologia*. 50 (11): e13055. doi: 10.1111/and.13055.
- McCracken JA, Custer EE & Lamsa JC. Luteolysis: a neuroendocrine-mediated event. **1999**. *Physiological Reviews*. 79 (2): 263-323. doi: 10.1152/physrev.1999.79.2.263.
- McGahon MK, Fernandez JA, Dash DP, et al. TRPV2 Channels Contribute to Stretch-Activated Cation Currents and Myogenic Constriction in Retinal Arterioles. **2016**. *Investigative Ophthalmology & Visual Science*. 57 (13): 5637–5647. doi: 10.1167/iovs.16-20279.
- McMohan MJ, Kofranek AM & Rubatzky VE. Plant Science: Growth, Development, and Utilization of Cultivated Plants. **2011**. 5th edition. ISBN: 978-0-1350-1407-3
- McKinley M & O’Loughlin VD. Human Anatomy. **2012**. 3rd edition. ISBN: 978-1-2602-5135-7
- McQuillan J, Greil AL, Whit L, et al. Frustrated Fertility: Infertility and Psychological Distress among Women. **2003**. *Journal of Marriage and Family*. 65 (4): 1007-18. doi: 10.1111/j.1741-3737.2003.01007.x
- Mechoulam R, Ben-Shabat S, Hanus L, et al. Identification of an endogenous 2-monoglyceride, present in canine gut, that binds to cannabinoid receptors. **1995**. *Biochemical Pharmacology*. 50 (1): 83-90. doi: 10.1016/0006-2952(95)00109-d.
- Meineke V, Frungieri MB, Jessberger B, et al. Human testicular mast cells contain tryptase: increased mast cell number and altered distribution in the testes of infertile men. **2000**. *Fertility and Sterility*. 74 (2): 239-44. doi: 10.1016/S0015-0282(00)00626-9
- Menkveld R, Van Zyl JA, Kotze TJW, et al. Possible Changes in Male Fertility Over a 15-Year Period. **1986**. *Archives of Andrology*. 17 (2): 143-44. doi: 10.3109/01485018608990186.

- Meroni SB, Galardo MN, Rindone Get al. Molecular Mechanisms and Signaling Pathways Involved in Sertoli Cell Proliferation. **2019**. *Frontiers in Endocrinology*. 10: 224.
doi: 10.3389/fendo.2019.00224
- Metcalf DD, Baram D & Mekori YA. Mast cells. **1997**. *Physiological Reviews*. 77 (4): 1033-79.
doi: 10.1152/physrev.1997.77.4.1033.
- Mihara H, Boudaka A, Shibasaki K, et al. Involvement of TRPV2 activation in intestinal movement through nitric oxide production in mice. **2010**. *Journal of Neuroscience*. 30 (49): 16536-44.
doi: 10.1523/JNEUROSCI.4426-10.2010.
- Miller JP, Moldenhauer HJ, Keros S, et al. An emerging spectrum of variants and clinical features in *KCNMA1*-linked channelopathies. **2021**. *Channels*. 15 (1): 447-64.
doi: 10.1080/19336950.2021.1938852.
- Miller WL & Auchus RJ. The molecular biology, biochemistry, and physiology of human steroidogenesis and its disorders. **2011**. *Endocrine Reviews*. 32 (1): 81-151. doi: 10.1210/er.2010-0013.
- Minke B, Wu C & Pak WL. Induction of photoreceptor voltage noise in the dark in *Drosophila* mutant. **1975**. *Nature*. 258 (5530): 84-87. doi: 10.1038/258084a0.
- Monaco G, van Dam S, Casal Novo Ribeiro JL, et al. A comparison of human and mouse gene co-expression networks reveals conservation and divergence at the tissue, pathway and disease levels. **2015**. *BMC Evolutionary Biology*. 15: 259. doi: 10.1186/s12862-015-0534-7.
- Monet M, Gkika D, Lehen'kyi V, et al. Lysophospholipids stimulate prostate cancer cell migration via TRPV2 channel activation. **2009**. *Biochimica et Biophysica Acta*. 1793 (3): 528-39.
doi: 10.1016/j.bbamcr.2009.01.003.
- Monet M, Lehen'kyi V, Gackiere F, et al. Role of cationic channel TRPV2 in promoting prostate cancer migration and progression to androgen resistance. **2010**. *Cancer Research*.; 70 (3): 1225-35.
doi: 10.1158/0008-5472.CAN-09-2205.
- Montague DK, Jarow JP, Broderick GA, et al. Chapter 1: The management of erectile dysfunction: an AUA update. **2015**. *Journal of Urology*. 174 (1): 230-39.
doi: 10.1097/01.ju.0000164463.19239.19.
- Monteith GR, McAndrew D, Faddy HM, et al. Calcium and cancer: targeting Ca²⁺ transport. **2007**. *Nature Reviews Cancer*. 7 (7): 519-30. doi: 10.1038/nrc2171.
- Montell C. The TRP superfamily of cation channels. **2005**. *Science's Signal Transduction Knowledge Environment*. 2005 (272): re3. doi: 10.1126/stke.2722005re3.
- Montell C, Birnbaumer L & Flockerzi V. The TRP channels, a remarkably functional family. **2002**. *Cell*. 108 (5): 595-98. doi: 10.1016/s0092-8674(02)00670-0.
- Montell C & Rubin GM. Molecular characterization of the *Drosophila* trp locus: a putative integral membrane protein required for phototransduction. **1989**. *Neuron*. 2 (4): 1313-23.
doi: 10.1016/0896-6273(89)90069-x.
- Moss SJ & Henley J. Receptor and Ion-Channel Trafficking: Cell Biology of Ligand-Gated and Voltage-Sensitive Ion Channels. **2002**. ISBN: 978-0-1926-3224-1
- Mossman HW & Duke KL: Comparative morphology of the mammalian ovary. **1973**.
The University of Wisconsin Press.
- Mukhopadhyay D, Varghese AC, Pal M, et al. Semen quality and age-specific changes: a study between two decades on 3,729 male partners of couples with normal sperm count and attending an andrology laboratory for infertility-related problems in an Indian city. **2010**. *Fertility and Sterility*. 93 (7): 2247-54. doi: 10.1016/j.fertnstert.2009.01.135.

- Mundt N, Spehr M, Lishko PV. TRPV4 is the temperature-sensitive ion channel of human sperm. **2018**. *eLife*. 7: e35853. doi: 10.7554/eLife.35853.
- Muraki K, Iwata Y, Katanosaka Y, et al. TRPV2 is a component of osmotically sensitive cation channels in murine aortic myocytes. **2003**. *Circulation Research*. 93 (9): 829-38. doi: 10.1161/01.RES.0000097263.10220.0C.
- Murature DA, Tang SY, Steinhardt G, et al. Phthalate esters and semen quality parameters. **1987**. *Biological Mass Spectrometry*. 14 (8): 473-77. doi: 10.1002/bms.1200140815.
- Nabissi M, Morelli MB, Amantini C, et al. TRPV2 channel negatively controls glioma cell proliferation and resistance to Fas-induced apoptosis in ERK-dependent manner. **2010**. *Carcinogenesis*. 31 (5): 794-803. doi: 10.1093/carcin/bgq019.
- Nabissi M, Morelli MB, Santoni M, et al. Triggering of the TRPV2 channel by cannabidiol sensitizes glioblastoma cells to cytotoxic chemotherapeutic agents. **2013**. *Carcinogenesis*. 34 (1): 48-57. doi: 10.1093/carcin/bgs328.
- Nagasawa M & Kojima I. Translocation of calcium-permeable TRPV2 channel to the podosome: Its role in the regulation of podosome assembly. **2012**. *Cell Calcium*. 51 (2): 186-93. doi: 10.1016/j.ceca.2011.12.012.
- Nagasawa M & Kojima I. Translocation of TRPV2 channel induced by focal administration of mechanical stress. **2015**. *Physiological Reports*. 3 (2): e12296. doi: 10.14814/phy2.12296.
- Nagasawa M, Nakagawa Y, Tanaka S, et al. Chemotactic peptide fMetLeuPhe induces translocation of the TRPV2 channel in macrophages. **2007**. *Journal of Cellular Physiology*. 210 (3): 692-702. doi: 10.1002/jcp.20883.
- Neeper MP, Liu Y, Hutchinson TL, et al. Activation properties of heterologously expressed mammalian TRPV2: evidence for species dependence. **2007**. *Journal of Biological Chemistry*. 282 (21): 15894-902. doi: 10.1074/jbc.M608287200.
- Nelson DL, Cox MM & Lehninger AL. Principles of Biochemistry. **2008**. 5th edition. ISBN: 978-1-4292-0892-5
- Nelson LM. Clinical practice. Primary ovarian insufficiency. **2009**. *The New England Journal of Medicine*. 360 (6): 606-14. doi: 10.1056/NEJMcp0808697.
- Nie L, Oishi Y, Doi I, et al. Inhibition of proliferation of MCF-7 breast cancer cells by a blocker of Ca(2+)-permeable channel. **1997**. *Cell Calcium*. 22 (2): 75-82. doi: 10.1016/s0143-4160(97)90107-x.
- Nieves-Cintrón M, Syed AU, Buonarati OR, et al. Impaired BK_{Ca} channel function in native vascular smooth muscle from humans with type 2 diabetes. **2017**. *Scientific Reports*. 7 (1): 14058. doi: 10.1038/s41598-017-14565-9.
- Nilius B & Owsianik G. Transient receptor potential channelopathies. **2010**. *Pflugers Archiv*. 460 (2): 437-50. doi: 10.1007/s00424-010-0788-2.
- Nilius B & Owsianki G. The transient receptor potential family of ion channels. **2011**. *Genome Biology*. 12 (3): 218. doi: 10.1186/gb-2011-12-3-218.
- Nilius B, Owsianik G, Voets T, et al. Transient receptor potential cation channels in disease. **2007**. *Physiological Reviews*. 87 (1): 165-217. doi: 10.1152/physrev.00021.2006.
- Nilius B & Voets T. The puzzle of TRPV4 channelopathies. **2013**. *European Molecular Biology Organization Reports*. 14 (2): 152-63. doi: 10.1038/embor.2012.219.
- Nilius B, Voets T & Peters T. TRP channels in disease. **2005**. *Science's Signal Transduction Knowledge Environment*. 2005 (295): re8. doi: 10.1126/stke.2952005re8.

- Nishi Y, Yanase T, Mu Y, et al. Establishment and characterization of a steroidogenic human granulosa-like tumor cell line, KGN, that expresses functional follicle-stimulating hormone receptor. **2001**. *Endocrinology*. 142 (1): 437-45. doi: 10.1210/endo.142.1.7862.
- Nishimura G, Lausch E, Savarirayan R, et al. TRPV4-associated skeletal dysplasias. **2012**. *American Journal of Medical Genetics, Part C: Seminars in Medical Genetics*. 160C (3): 190-204. doi: 10.1002/ajmg.c.31335.
- Nishimura K, Tanaka N, Ohshige A, et al. Effects of macrophage colony-stimulation factor on folliculogenesis in gonadotrophin-primed immature rats. **1995**. *Journal of Reproduction and Fertility*. 104: 325-30. doi: 10.1530/jrf.0.1040325.
- Nistal M, Santamaria L, Paniagua R, et al. Changes in the connective tissue and decrease in the number of mast cells in the testes of men with alcoholic and non-alcoholic cirrhosis. **1986**. *Acta Morphologica Hungarica*. 34 (1-2): 107-15. PMID: 3105254
- Oda M, Fujiwara Y, Ishizaki Y, et al. Oxidation sensitizes TRPV2 to chemical and heat stimuli, but not mechanical stimulation. **2021**. *Biochemistry and Biophysics Reports*. 28: 101173. doi: 10.1016/j.bbrep.2021.101173.
- O'Donnell L, Stanton P & de Kretser DM. Endocrinology of the Male Reproductive System and Spermatogenesis. **2017**. *Endotext*. PMID: 25905260
- Ong AC & Harris PC. A polycystin-centric view of cyst formation and disease: the polycystins revisited. **2015**. *Kidney Int*. 88 (4): 699-710. doi: 10.1038/ki.2015.207.
- Oparin AI. The Origin of Life. **1938**. *Phoenix Edition Series*. ISBN: 978-0-4864-9522-4
- Overington JP, Al-Lazikani B & Hopkins AL. How many drug targets are there? **2006**. *Nature Reviews Drug Discovery*. 5 (12): 993-36. doi: 10.1038/nrd2199.
- Pandruvada S, Royfman R, Shah TA, et al. Lack of trusted diagnostic tools for undetermined male infertility. **2021**. *Journal of Assisted Reproduction and Genetics*. 38 (2): 265-76. doi: 10.1007/s10815-020-02037-5.
- Park EH, Kim DR, Kim HY, et al. Panax ginseng induces the expression of CatSper genes and sperm hyperactivation. **2014**. *Asian Journal of Andrology*. 16 (6): 845-51. doi: 10.4103/1008-682X.129129.
- Park KS, Kim Y, Lee Y-H, et al. Mechanosensitive cation channels in arterial smooth muscle cells are activated by diacylglycerol and inhibited by phospholipase C inhibitor. **2003**. *Circulation Research*. 93 (6): 557-64. doi: 10.1161/01.RES.0000093204.25499.83.
- Park KS, Pang B, Park SJ, et al. Identification and functional characterization of ion channels in CD34(+) hematopoietic stem cells from human peripheral blood. **2011b**. *Molecules and Cells*. 32 (2): 181-88. doi: 10.1007/s10059-011-0068-9.
- Park U, Vastani N, Guan Y, et al. TRP vanilloid 2 knock-out mice are susceptible to perinatal lethality but display normal thermal and mechanical nociception. **2011a**. *Journal of Neuroscience*. 31 (32): 11425-36. doi: 10.1523/JNEUROSCI.1384-09.2011.
- Peng G, Lu W, Li X, et al. Expression of store-operated Ca²⁺ entry and transient receptor potential canonical and vanilloid-related proteins in rat distal pulmonary venous smooth muscle. **2010**. *American Journal of Physiology - Lung Cellular and Molecular Physiology*. 299 (5): L621-30. doi: 10.1152/ajplung.00176.2009.
- Penna A, Juvin V, Chemin J, et al. PI3-kinase promotes TRPV2 activity independently of channel translocation to the plasma membrane. **2006**. *Cell Calcium*. 39 (6): 495-507. doi: 10.1016/j.ceca.2006.01.009.

- Perálvarez-Marín A, Doñate-Macian P & Gaudet R. What do we know about the transient receptor potential vanilloid 2 (TRPV2) ion channel? **2013**. *The FEBS Journal*. 280 (21): 5471-87. doi: 10.1111/febs.12302.
- Peretó J. Controversies on the origin of life. **2005**. *International Microbiology*. 8 (1): 23-31. PMID: 15906258.
- Peterson C & Soder O. The Sertoli Cell - A Hormonal Target and 'Super' Nurse for Germ Cells That Determines Testicular Size. **2006**. *Hormone Research*. 66 (4): 153-61. doi: 10.1159/000094142
- Pinkerton JHM, McKay DG, Adams EC, et al. Development of the human ovary: A study using histochemical techniques. **1961**. *Obstetrics & Gynecology*. 18: 152-81. PMID: 13735859
- Plant TD. TRPs in mechanosensing and volume regulation. **2014**. *Handbook of Experimental Pharmacology*. 223: 743-66. doi: 10.1007/978-3-319-05161-1_2.
- Purves D, Augustine GJ, Fitzpatrick D, et al. Chapter 4: Channels and Transporters. **2001**. *Neuroscience*. 2nd edition. ISBN: 978-0-8789-3741-7
- Qi H, Moran MM, Navarro B, et al. All four CatSper ion channel proteins are required for male fertility and sperm cell hyperactivated motility. **2007**. *Proceedings of the National Academy of Science of the USA*. 104 (4): 1219-23. doi: 10.1073/pnas.0610286104.
- Quill TA, Ren D, Clapham DE, et al. A voltage-gated ion channel expressed specifically in spermatozoa. **2001**. *Proceedings of the National Academy of Science of the USA*. 98 (22): 12527-31. doi: 10.1073/pnas.221454998.
- Qin N, Neeper MP, Liu Y, et al. TRPV2 is activated by cannabidiol and mediates CGRP release in cultured dorsal root ganglion neurons. **2008**. *Journal of Neuroscience*. 28 (24): 6231-38. doi: 10.1523/JNEUROSCI.0504-08.2008.
- Qin Y, Jiao X, Simpson JL, et al. Genetics of primary ovarian insufficiency: new developments and opportunities. **2015**. *Human Reproduction Update*. 21 (6): 787-808. doi: 10.1093/humupd/dmv036.
- Raga F, Bauset C, Remohi J, et al. Reproductive impact of congenital Müllerian anomalies. **1997**. *Human Reproduction*. 12 (10): 2277-81. doi: 10.1093/humrep/12.10.2277.
- Ramsey IS, Delling M & Clapham DE. An introduction to TRP channels. **2006**. *Annual Review of Physiology*. 68: 619-47. doi: 10.1146/annurev.physiol.68.040204.100431.
- Rao K. Principles & Practice of Assisted Reproductive Technology. **2013**. 3rd volume. ISBN: 978-9-3509-0736-8
- Reichhart N, Keckeis S, Fried F, et al. Regulation of surface expression of TRPV2 channels in the retinal pigment epithelium. **2015**. *Graefe's Archive for Clinical and Experimental Ophthalmology*. 253 (6): 865-74. doi: 10.1007/s00417-014-2917-7.
- Ren D, Navarro B, Perez G, et al. A sperm ion channel required for sperm motility and male fertility. **2001**. *Nature*. 413 (6856): 603-09. doi: 10.1038/35098027.
- Rendi MH, Muehlenbachs A, Garcia RL, et al. Comparative Anatomy and Histology: A Mouse and Human Atlas - Female Reproductive System. **2011**. 1st edition. ISBN: 978-0-12-381361-9
- Restrepo B & Cardona-Maya W. Antisperm antibodies and fertility association. **2013**. *Actas Urológicas Españolas*. 37 (9): 571-78. doi: 10.1016/j.acuro.2012.11.003.
- Robbins N, Koch SE, Tranter M, et al. The History and Future of Probenecid. **2012**. *Cardiovascular Toxicology*. 12 (1): 1-9. doi: 10.1007/s12012-011-9145-8.
- Rohacs T & Nilius B. Regulation of transient receptor potential (TRP) channels by phosphoinositides. **2007**. *Pflugers Archiv*. 455 (1): 157-68. doi: 10.1007/s00424-007-0275-6.

- Rohacs T, Thyagarajan B & Lukacs V. Phospholipase C mediated modulation of TRPV1 channels. **2008**. *Molecular Neurobiology*. 37 (2-3): 153-63. doi: 10.1007/s12035-008-8027-y.
- Rolaki A, Drakakis P, Millingos S, et al. Novel trends in follicular development, atresia and corpus luteum regression: a role for apoptosis. **2005**. *Reproductive BioMedicine Online*. 11 (1): 93-103. doi: 10.1016/s1472-6483(10)61304-1.
- Rossato M, Ion Popa F, Ferigo M, et al. Human sperm express cannabinoid receptor Cb1, the activation of which inhibits motility, acrosome reaction, and mitochondrial function. **2005**. *Journal of Clinical Endocrinology & Metabolism*. 90 (2): 984-91. doi: 10.1210/jc.2004-1287.
- Rossato M, Pagano C & Vettor R. The Cannabinoid System and Male Reproductive Functions. **2008**. *Journal of Neuroendocrinology*. 20 (Suppl. 1): 90-93 doi: 10.1111/j.1365-2826.2008.01680.x
- Royle SJ & Murrel-Lagnado RD. Constitutive cycling: a general mechanism to regulate cell surface proteins. **2002**. *BioEssays*. 25 (1): 39-46. doi: 10.1002/bies.10200.
- Rutstein SO & Shah IH. Infecundity, infertility, and childlessness in developing countries. **2004**. Geneva: World Health Organization.
- Saladin K. Anatomy & Physiology: The unity of form and function. **2010**. 5th edition. ISBN: 978-1-2592-7772-6
- Santoni G, Farfariello V, Liberati S, et al. The role of transient receptor potential vanilloid type-2 ion channels in innate and adaptive immune responses. **2013**. *Frontiers in Immunology*. 4: 34. doi: 10.3389/fimmu.2013.00034.
- Schill W.B, Schneider J & Ring J. The use of ketotifen, a mast cell blocker, for treatment of oligo- and asthenozoospermia. **1986**. *Andrologia*. 18 (6): 570-73. doi: 10.1111/j.1439-0272.1986.tb01831.x.
- Schmid N, Dietrich KG, Forne I, et al. Sirtuin 1 and Sirtuin 3 in Granulosa Cell Tumors. **2021**. *International Journal of Molecular Sciences*. 22 (4): 2047. doi: 10.3390/ijms22042047.
- Schuel H, Burkman LJ, Lippes J, et al. N-Acylethanolamines in human reproductive fluids. **2002**. *Chemistry and Physics of Lipids*. 121 (1-2): 2112-27. doi: 10.1016/s0009-3084(02)00158-5.
- Segal TR & Giudice LC. Before the beginning: environmental exposures and reproductive and obstetrical outcomes. **2019**. 112 (4): 613-21. doi: 10.1016/j.fertnstert.2019.08.001.
- Sengupta P. Challenge of infertility: How protective the yoga therapy is? **2012**. *Ancient Science of Life*. 32 (1): 61-62. doi: 10.4103/0257-7941.113796.
- Seok J, Warren HS, Cuenca AG, et al. Inflammation and Host Response to Injury, Large Scale Collaborative Research Program. Genomic responses in mouse models poorly mimic human inflammatory diseases. **2013**. *Proceedings of the National Academy of Science of the USA*. 110 (9): 3507-12. doi: 10.1073/pnas.1222878110.
- Serour GI. Medical and socio-cultural aspects of infertility in the Middle East. **2008**. *European Society of Human Reproduction and Embryology Monographs*. 2008 (1): 34-41. doi: 10.1093/humrep/den143
- Shapovalov G, Lehen'kyi V, Skryma R, et al. TRP channels in cell survival and cell death in normal and transformed cells. **2011**. *Cell Calcium*. 50 (3): 295-302. doi: 10.1016/j.ceca.2011.05.006.
- Shibasaki K. Physiological significance of TRPV2 as a mechanosensor, thermosensor and lipid sensor. **2016**. *The Journal of Physiological Sciences*. 66 (5): 359-65. doi: 10.1007/s12576-016-0434-7.
- Shibasaki K, Suzuki M, Mizuno A, et al. Effects of body temperature on neural activity in the hippocampus: regulation of resting membrane potentials by transient receptor potential vanilloid 4. **2007**. *Journal of Neuroscience*. 27 (7): 1566-75. doi: 10.1523/JNEUROSCI.4284-06.2007.

- Shibasaki K, Murayama N, Ono K, et al. TRPV2 enhances axon outgrowth through its activation by membrane stretch in developing sensory and motor neurons. **2010**. *Journal of Neuroscience*. 30 (13): 4601-12. doi: 10.1523/JNEUROSCI.5830-09.2010.
- Singer SJ & Nicholson GL. The fluid mosaic model of the structure of cell membranes. **1972**. *Science*. 175 (4023): 720-31. doi: 10.1126/science.175.4023.720.
- Siveen KS, Nizamuddin PB, Uddin S, et al. TRPV2: A Cancer Biomarker and Potential Therapeutic Target. **2020**. *Disease Markers*. 2020: 8892312. doi: 10.1155/2020/8892312.
- Smith JF, Walsh TJ, Shindel AW, et al. Sexual, Marital, and Social Impact of a Man's Perceived Infertility Diagnosis. **2009**. *The Journal of Sexual Medicine*. 6 (9): 2505-15. doi: 10.1111/j.1743-6109.2009.01383.x.
- Smith LB & Walker WH. The regulation of spermatogenesis by androgens. **2014**. *Seminars in Cell & Developmental Biology*. 2-13. doi: 10.1016/j.semcd.2014.02.012.
- Son GY, Hong JH, Chang I, et al. Induction of IL-6 and IL-8 by activation of thermosensitive TRP channels in human PDL cells. **2015**. *Archives of Oral Biology*. 60 (4): 526-32. doi: 10.1016/j.archoralbio.2014.12.014.
- Stokes AJ, Shimoda LM, Koblan-Huberson M, et al. A TRPV2-PKA signaling module for transduction of physical stimuli in mast cells. **2004**. *Journal of Experimental Medicine*. 200 (2): 137-47. doi: 10.1084/jem.20032082
- Stotz SC, Vriens J, Martyn D, et al. Citral sensing by Transient [corrected] receptor potential channels in dorsal root ganglion neurons. **2008**. *Public Library Of Science One*. 3 (5): e2082. doi: 10.1371/journal.pone.0002082.
- Suginta W, Karoulias N, Aitken A, et al. Chloride intracellular channel protein CLIC4 (p64H1) binds directly to brain dynamin I in a complex containing actin, tubulin and 14-3-3-isoforms. **2001**. *Biochemical Journal*. 359 (Pt1): 55-64. doi: 10.1042/0264-6021:3590055.
- Sugio S, Nagasawa M, Kojima I, et al. Transient receptor potential vanilloid 2 activation by focal mechanical stimulation requires interaction with the actin cytoskeleton and enhances growth cone motility. **2017**. *Journal of the Federation of American Societies of Experimental Biology*. 31 (4): 1368-81. doi: 10.1096/fj.201600686RR
- Sugiura T, Kondo S, Sukagawa A, et al. 2-Arachidonoylglycerol: a possible endogenous cannabinoid receptor ligand in brain. **1995**. *Biochemical and Biophysical Research Communication*. 215 (1): 89-97. doi: 10.1006/bbrc.1995.2437.
- Sun X, Zhu Y, Wang L, et al. The Catsper channel and its roles in male fertility: a systematic review. **2017**. *Reproductive Biology & Endocrinology*. 15 (1): 65. doi: 10.1186/s12958-017-0281-2.
- Syrovatkina V, Alegre KO, Dey R, et al. Regulation, Signaling and Physiological Functions of G-Proteins. **2016**. *Journal of Molecular Biology*. 428 (19): 3850-68. doi: 10.1016/j.jmb.2016.08.002.
- Takahashi TA & Johnson KM. Menopause. **2015**. *The Medical Clinics of North America*. 99 (3): 521-34. doi: 10.1016/j.mcna.2015.01.006.
- Takida S & Wedegaertner PB. Exocytotic pathway-independent plasma membrane targeting of heterotrimeric G protein. **2004**. *Federation of European Biochemical Societies Letters*. 567 (2-3): 209-213. doi: 10.1016/j.febslet.2004.04.062.
- Tamura K, Tamura H, Kumasaka K, et al. Ovarian immune cells express granulocyte-macrophage colony-stimulating factor (GM-CSF) during follicular growth and luteinisation in gonadotropin-primed immature rodents. **1998**. *Molecular Cellular Endocrinology*. 142 (1-2): 153-63. doi: 10.1016/s0303-7207(98)00109-9.
- Tirard S. Abiogenesis. **2014**. *Encyclopedia of Astrobiology*. ISBN: 978-3-6422-7833-4

- Tóth BI & Nilius B. Transient Receptor Potential Dysfunctions in Hereditary Diseases: TRP Channelopathies and Beyond. **2015**. *TRP Channels as Therapeutic Target*. ISBN: 978-0-1242-0024-1
- Totorikaguena L, Olabarrieta E, Lolicato F, et al. The endocannabinoid system modulates the ovarian physiology and its activation can improve in vitro oocyte maturation. **2020**. *Journal of Cellular Physiology*. 235 (10): 7580-91. doi: 10.1002/jcp.29663.
- Traut MH, Berg D, Berg U, et al. Identification and characterization of Ca²⁺-activated K⁺ channels in granulosa cells of the human ovary. **2009**. *Reproductive Biology and Endocrinology*. 7: 28. doi: 10.1186/1477-7827-7-28.
- Tsvilovskyy VV, Zholos AV, Aberle T, et al. Deletion of TRPC4 and TRPC6 in mice impairs smooth muscle contraction and intestinal motility in vivo. **2009**. *Gastroenterology*. 137 (4): 1415-24. doi: 10.1053/j.gastro.2009.06.046.
- Uribe-Querol E & Rosales C. Phagocytosis: Our Current Understanding of a Universal Biological Process. **2020**. *Frontiers in Immunology*. 11: 1066. doi: 10.3389/fimmu.2020.01066.
- Valenzuela SM, Martin DK, Por SB, et al. Molecular cloning and expression of a chloride ion channel of cell nuclei. **1997**. *Journal of Biological Chemistry*. 272 (19): 12575-82. doi: 10.1074/jbc.272.19.12575.
- Vandamme TF. Use of rodents as models of human diseases. **2014**. *Journal of Pharmacy and Bioallied Sciences*. 6 (1): 2-9. doi:10.4103/0975-7406.124301.
- Vandamme TF. Rodent models for human diseases. **2015**. *European Journal of Pharmacology*. 759: 84-89. doi: 10.1016/j.ejphar.2015.03.046.
- Venkatachalam K & Montell C. TRP channels. **2007**. *Annual Review Biochemistry*. 76: 387-417. doi: 10.1146/annurev.biochem.75.103004.142819.
- Voet D, Voet JG & Pratt CW. Fundamentals of Biochemistry: Life at the Molecular Level. **2011**. 4th edition. p. 263. ISBN: 978-1-1183-4014-1
- von Heijne G. Membrane-protein topology. **2006**. *Nature Reviews Molecular Cell Biology*. 7 (12): 909-18. doi: 10.1038/nrm2063.
- Vriens J, Appendino G & Nilius B. Pharmacology of vanilloid transient receptor potential cation channels. **2009**. *Molecular Pharmacology*. 75 (6): 1262-79. doi: 10.1124/mol.109.055624.
- Vriens J, Janssens A, Prenen J, et al. TRPV channels and modulation by hepatocyte growth factor/scatter factor in human hepatoblastoma (HepG2) cells. **2004**. *Cell Calcium*. 36 (1): 19-28. doi: 10.1016/j.ceca.2003.11.006.
- Wallace WHB & Kelsey TW. Human Ovarian Reserve from Conception to the Menopause. **2010**. *Public Library Of Science ONE*. 5 (1): 8772. doi: 10.1371/journal.pone.0008772.
- Wallin E & von Heijne G. Genome-wide analysis of integral membrane proteins from eubacterial, archaean, and eukaryotic organisms. **1998**. *Protein Science*. 7 (4): 1029-38. doi: 10.1002/pro.5560070420.
- Wang J, Zhang W, Jiang H, et al. Mutations in HFM1 in recessive primary ovarian insufficiency. **2014**. *The New England Journal of Medicine*. 370 (10): 972-74. doi: 10.1056/NEJMc1310150.
- Waterston RH, Lindblad-Toh K, Birney E, et al. Initial sequencing and comparative analysis of the mouse genome. **2002**. *Nature*. 420 (6915): 520-62. doi: 10.1038/nature01262.
- Weinbauer GF, Luetjens CM, Simoni M, et al. Andrologie. **2009**. 3rd edition. p. 15-61. ISBN 978-3-540-92962-8

- Welsh M, Saunders PT, Atanassova N, et al. Androgen action via testicular peritubular myoid cells is essential for male fertility. **2009**. *Journal of the Federation of American Societies of Experimental Biology*. 23 (12): 4218-30. doi: 10.1096/fj.09-138347.
- Welsh M, Moffat L, Belling K, et al. Androgen receptor signalling in peritubular myoid cells is essential for normal differentiation and function of adult Leydig cells. **2012**. *International Journal of Andrology*. 35 (1): 25-40. doi: 10.1111/j.1365-2605.2011.01150.x.
- Wenger T, Fernández-Ruiz JJ & Ramos JA. Immunocytochemical demonstration of CB1 cannabinoid receptors in the anterior lobe of the pituitary gland. **1999**. *Journal of Neuroendocrinology*. 11 (11): 873-78. doi: 10.1046/j.1365-2826.1999.00402.x.
- Wenger T, Rettori V, Snyder GD, et al. Effects of delta-9-tetrahydrocannabinol on the hypothalamic-pituitary control of luteinizing hormone and follicle-stimulating hormone secretion in adult male rats. **1987**. *Neuroendocrinology*. 46 (6): 488-93. doi: 10.1159/000124870.
- Whiteford LM & Gonzalez L. Stigma: The Hidden Burden of Infertility. **1995**. *Social Science & Medicine*. 40 (1): 27-36. doi: 10.1016/0277-9536(94)00124-c.
- Witzany G. Crucial steps to life: From chemical reactions to code using agents. **2016**. *Biosystems*. 140: 49-57. doi: 10.1016/j.biosystems.2015.12.007.
- World Health Organization. International Classification of Diseases. **2018**. Geneva: World Health Organization. 11th Revision.
- Wosnitzer MS. Genetic evaluation of male infertility. **2014**. *Translational Andrology & Urology*. 3 (1): 17-26. doi: 10.3978/j.issn.2223-4683.2014.02.04.
- Wu LJ, Sweet TB & Clapham DE. International Union of Basic and Clinical Pharmacology. LXXVI. Current progress in the mammalian TRP ion channel family. **2010**. *Pharmacological Reviews*. 62 (3): 381-404. doi: 10.1124/pr.110.002725.
- Wu R, Van der Hoek KH, Ryan NK, et al. Macrophage contributions to ovarian function. **2004**. *Human Reproduction Update*. 10 (2): 119-33. doi: 10.1093/humupd/dmh011.
- Xiao R & Xu XS. *C. elegans* TRP channels. **2011**. *Advances in Experimental Medicine & Biology*. 704: 323-39. doi: 10.1007/978-94-007-0265-3_18.
- Xu X, Mu L, Li L, et al. Imaging and tracing the pattern of adult ovarian angiogenesis implies a strategy against female reproductive aging. **2022**. *Science Advances*. 8 (2): eabi8683. doi: 10.1126/sciadv.abi8683.
- Yamada T, Ueda T, Shibata Y, et al. TRPV2 activation induces apoptotic cell death in human T24 bladder cancer cells: a potential therapeutic target for bladder cancer. **2010**. *Urology*. 76 (2): 509.e1-7. doi: 10.1016/j.urology.2010.03.029.
- Yamamoto M, Hibi H & Miyake K. Appearance of spermatozoon after administration of mast cell blocker to a patient with azoospermia. **1994**. *Hinyokika Kyo. Acta Urologica Japonica*. 40 (6): 541-43. PMID: 7521117
- Yamamoto M, Hibi H & Miyake K. New treatment of idiopathic severe oligozoospermia with mast cell blocker. **1995**. *Fertility and Sterility*. 64 (6): 1221-23. doi: 10.1016/s0015-0282(16)57992-8.
- Yamanaka K, Fujisawa M, Tanaka H, et al. Significance of human testicular mast cells and their subtypes in male infertility. **2000**. *Human Reproduction*. 15 (7): 1543-47. doi: 10.1093/humrep/15.7.1543.
- Yamashiro K, Sasano T, Tojo K, et al. Role of transient receptor potential vanilloid 2 in LPS-induced cytokine production in macrophages. **2010**. *Biochemical and Biophysical Research Communications*. 398 (2): 284-89. doi: 10.1016/j.bbrc.2010.06.082.

- Zegers-Hochschild F, Adamson GC, de Mouzon J, et al. The International Committee for Monitoring Assisted Reproductive Technology (ICMART) and the World Health Organization (WHO) Revised Glossary on ART Terminology. **2009**. *Human Reproduction*. 24 (11): 2683-87. doi: 10.1093/humrep/dep343.
- Zhang AH, Sharma G, Undheim EA, et al. A complicated complex: Ion channels, voltage sensing, cell membranes and peptide inhibitors. **2018a**. *Neuroscience Letters*. 679: 35-47. doi: 10.1016/j.neulet.2018.04.030.
- Zhang D, Spielmann A, Wang L, et al. Mast-cell degranulation induced by physical stimuli involves the activation of transient-receptor-potential channel TRPV2. **2012**. *Physiological Research*. 61 (1): 113-24. doi: 10.33549/physiolres.932053.
- Zhang Y, Yan Z, Qin Q, et al. Transcriptome Landscape of Human Folliculogenesis reveals Oocyte and Granulosa Cell Interactions. **2018b**. *Molecular Cell*. 72 (6): 1021-34. doi: 10.1016/j.molcel.2018.10.029.
- Zhao S, Zhu W, Xue S, et al. Testicular defense systems: immune privilege and innate immunity. **2014**. *Cell Molecular Immunology*. 11 (5): 428-37. doi: 10.1038/cmi.2014.38.
- Zondervan KT, Becker CM & Missmer SA. Endometriosis. **2020**. *New England Journal of Medicine*. 382 (13): 1244-56. doi: 10.1056/NEJMra1810764.

Acknowledgements

The present work would not have been possible without all those helping hands and support of people around me.

First of all, sincere gratitude to Prof. Dr. med. Artur Mayerhofer who gave me the amazing chance to join his lab almost 7 years ago. You infected me with your great enthusiasm for reproductive sciences and never ending optimism (*“da simma im business”*), always seeing something (*“siagst’as, da is was”*). Besides always pushing me (*“des mach mer jetzt”*), you kind of made me do this PhD (*“Frau Eubler, Sie brauchen das”*) and finally also write (*“einfach locker von der Leber”*) and finish this thesis (*“des mach mer jetzt fertig”*). Thanks a ton. I am also especially grateful that you have always been empathetic no matter which topic came up, and always had an open ear for any concerns, ideas or wishes.

Special and sincere thanks to PD Lars Kunz for your tireless support in any concerns and your helpful input for writing, experimental settings and electrophysiological means (which we, to be honest, did not manage yet). You gave me the chance to keep my electrophysiological spirit and kept me in contact with my ‘scientific past’. I am really looking forward to reviving this spirit together with you.

Deep gratitude to PD Conny Kopp-Scheinflug for the nice discussions and the supportive feedback during the TAC meetings. Best thanks to Prof. Dr. Wolfgang Enard for readily taking over the task of second examiner, and also to Prof Dr. Laura Busse and Prof. Dr. Hans-Henning Kunz for spending their valuable time and joining the examining board.

Furthermore, I would like to express my deep gratitude to all my collaborators. Thanks to Prof. Dr. med. Johannes Ulrich Schwarzer, Prof. Dr. med Frank-Michael Köhn, Prof. Dr. med. Dieter Berg, Dr. Ulrike Berg and the laboratory team behind Andrologie Centrum München, Andrologicum München and Kinderwunschzentrum A.R.T. Bogenhausen for providing access to biological material and the corresponding information. In this regard, thanks also to Nancy Bohne for performing the progesterone measurements.

I am also very grateful to my collaboration partners in Turku, Finland, who not only shared their scientific know-how and experience with me, but also gave me the amazing chance to join their daily lab life in Turku. In particular, I would like to express my deep gratitude to Prof. Matti Poutanen, Prof. Leena Strauss and Prof. Pia Rantakari for granting me access to mouse samples, laboratory equipment and methods used in their teams. Moreover, special thanks to Dr. Hanna Heikelä, Dr. med. Michael Gabriel, Heidi Gerke, Emmi Lokka and Etta-Liisa Virtomaa for supporting me during my numerous stays, for making this amazing time unforgettable and also for staying in amicable contact afterwards.

Special thanks also to Dr. Shibojyoti Lahiri, Prof. Dr. Axel Imhoff, Dr. Thomas Fröhlich, Dr. Florian Flenkenthaler, Youli Stepanov and Karolina Caban for performing and analyzing the mass spectrometry. Prof. Dr. med. Doris Mayr also deserves special thanks for providing TMAs and corresponding information, but also her great experience and expertise.

Moreover, special and deep thanks to the whole AG Mayerhofer, the nice atmosphere in the team and the fun in the lab. In particular, I have to express my deep gratitude to Carola Herrmann and Verena Kast who always assisted me with their technical experience, endurance and patience. Without you I wouldn't have managed to get through the tough times and to drive this work that far, I really appreciate your friendship and support. Moreover, I would like to thank all former and current lab members - Daniel Aigner, Dr. Konstantin Bagnjuk, Sarah Beschta, Dr. Jan Blohberger, Dr. Theresa Buck, Fangfang Cheng, Kim Dietrich, Katharina Goetz, Theo Hack, Andreas Huber, Melanie Kaseder, Nicole Kreitmair, Benedikt Mach, Karin Metzrath, Annika Missel, Dr. Annette-Müllertaubenberger, Merit Müür, Moritz Offner, Dr. Veronica Rey Berrutti, Dr. Nina Schmid, Pia Seßenhausen, Jan Dominik Speidel, Astrid Teifenbacher, Dr. Lena Walenta, Dr. Harald Welter and Dr. Stefanie Windschüttl.

I also appreciate the BMC environment with all the nice barbecue sessions, the funny waffle session, retreats and other occasions. In this context, I would like to thank at least some of you - Ralf Bigiel, Giuliana Ciccopiedi, Renate Dombi, Johanna Frickel, Dr. Max Harner, Dr. Saskia Hutten, Prof. Dr. Jovica Ninkovic, Dr. Stefanie Ohlig, Daniela Rieger, Dr. Rico Schieweck, Julia Schneider, Katalin Vartas, Andrea Wilytsch and Serpil Yildirim.

Finally but most appreciated, I would like to express my deepest gratitude to my family and close friends for being my true and reliable backbone for everything. Without you, I wouldn't have got that far, thank you.

Additional Publications

Mitochondrial dynamics in ovarian granulosa cells during follicular growth and in human KGN cells.

Melanie Kaseder, Nina Schmid, **Katja Eubler**, Katharina Goetz, Annette Müller-Taubenberger, Dissen Gregory, Max Harner, Gerhard Wanner, Axel Imhoff, Ignasi Forne & Artur Mayerhofer.

submitted 21/03/2022. *Molecular Human Reproduction*,

Testicular adenosine acts as a pro-inflammatory molecule: role of testicular peritubular cells.

Annika Missel, Lena Walenta, **Katja Eubler**, Nadine Mundt, Ulrich Pickl, Mathias Trottmann, Bastian Popper, Matti Poutanen, Leena Strauss, Frank-Michael Köhn, Lars Kunz, Marc Spehr & Artur Mayerhofer. **2021.**

Molecular Human Reproduction. 27 (7): gaab037. doi: 10.1093/molehr/gaab037

Necrosulfonamide induces apoptosis in the human granulosa tumour cell line KGN.

Verena Kast, Konstantin Bagnjuk, **Katja Eubler**, Tosihiko Yanase, Alexander Burges, Doris Mayr & Artur Mayerhofer. **submitted 30/11/2020.** *Histochemistry and Cell Biology*

Filamin A Orchestrates Cytoskeletal Structure, Cell Migration and Stem Cell Characteristics in Human Seminoma TCam-2 Cells.

Harald Welter, Carola Herrmann, Thomas Fröhlich, Florian Flenkenthaler, **Katja Eubler**, Hubert Schorle, Daniel Nettersheim, Artur Mayerhofer & Annette Müller-Taubenberger. **2020.**

Cells. 9 (12): 2563. doi: 10.3390/cells912256

A Role for H₂O₂ and TRPM2 in the Induction of Cell Death: Studies in KGN Cells.

Carsten Theo Hack, Theresa Buck, Konstantin Bagnjuk, **Katja Eubler**, Lars Kunz, Doris Mayr & Artur Mayerhofer. **2019.**

Antioxidants. 8 (11): 518. doi: 10.3390/antiox8110518

Human testicular peritubular cells, mast cells and testicular inflammation.

Artur Mayerhofer, Lena Walenta, Christine Mayer, **Katja Eubler** & Harald Welter. **2018.**

Andrologia. 50 (11): e13055. doi: 10.1111/and.13055

Scientific Posters & Talks

Transient Receptor Potential V2 Channel in Murine Testis and Testicular Macrophages

Katja Eubler, Pia Rantakari, Heidi Gerke, Carola Herrmann, Annika Missel, Nina Schmid, Shibojyoti Lahiri, Axel Imhof, Leena Strauss, Matti Poutanen & Artur Mayerhofer
Virtual poster presentation, ASA 46th Annual Conference, virtual, 04/2021

Mouse testicular macrophages express transient receptor potential channel type V2 (TRPV2) - a cation channel involved in testicular inflammation in a mouse model for infertility (AROM⁺)

Katja Eubler, Melanie Kaseder, Annika Missel, Leena Strauss, Matti Poutanen & Artur Mayerhofer
Talk, 6th International Workshop Molecular Andrology, Gießen, Germany, 09/2019

Ca²⁺ signalling and IL-8 secretion in human testicular peritubular cells involve the cation channel TRPV2

Katja Eubler, Carola Herrmann, Astrid Tiefenbacher, Frank-Michael Köhn, Johannes Ulrich Schwarzer, Lars Kunz & Artur Mayerhofer
Talk, 20th European Testis Workshop, Óbidos, Portugal, 05/2018

Activation of TRPV2 induces IL-8 expression in human testicular peritubular cells

Katja Eubler, Carola Herrmann, Frank-Michael Köhn, Johannes Ulrich Schwarzer, Lars Kunz & Artur Mayerhofer
Poster, DVR meeting, Munich, Germany, 12/2017

TRPV2 - an ion channel of human testicular peritubular cells with a possible role in inflammation

Katja Eubler, Frank-Michael Köhn, Johannes Ulrich Schwarzer & Artur Mayerhofer
Flash talk & Poster, DGE meeting, Würzburg, Germany, 03/2017

TRPV2 ion channel in human testicular peritubular cells

Katja Eubler, Frank-Michael Köhn, Johannes Ulrich Schwarzer & Artur Mayerhofer
Talk, Februartagung, Munich, Germany, 02/2017

Curriculum Vitae

Katja Eubler
Katja.Eubler@bmc.med.lmu.de

Academic Studies

Ph.D. student, Ludwig-Maximilian-University Munich

BioMedical Center, Institute for Anatomy and Cell Biology, AG Mayerhofer *since 2018*

Scientific Assistant, Ludwig-Maximilian-University Munich

BioMedical Center, Institute for Anatomy and Cell Biology, AG Mayerhofer **2015 - 2018**

M.Sc. BioSciences, TU Kaiserslautern

Master Thesis: „Effects of ambient Glycine on the glycinergic Transmission of the MNTB-LSO-Synapse“ (Animal Physiology, TU Kaiserslautern, AG Friauf) **2011 - 2013**

B.Sc. BioSciences, TU Kaiserslautern

Bachelor Thesis: „Analysis of the spontaneous activity of LSO neurons in mice“ (Animal Physiology, TU Kaiserslautern, AG Friauf) **2008 - 2011**

Research experience

Collaborative research stays, University of Turku, Turku, Finland
(Poutanen & Rantakari lab) **2018 & 2019**

Collaborative research stay, RWTH Aachen University, Aachen, Germany
(Spehr lab) **2016**

Research Assistant, TU Kaiserslautern, Kaiserslautern, Germany (AG Friauf) **2011 - 2013**

Summer schools & Trainees

„Introduction to Cell Culture Under Flow, Shear Stress and Flow Patterns - Pump System Practical Course“, ibidi, Gräfelfing, Germany **2019**

„Life Cell Analysis by Impedance Measurements - ECIS Practical Course“, ibidi, Gräfelfing, Germany **2019**

„Basics and clinics of human reproduction – an interdisciplinary approach“, Centre of Reproductive Medicine and Andrology, Münster, Germany **2016**

„Chemotaxis Assays and Video Microscopy“, ibidi, Gräfelfing, Germany **2015**